

Fiscal Year 2017: Fourth Quarter

Progress Report
**Advanced Battery Materials
Research (BMR) Program**

Released December 2017
for the period of July – September 2017

Approved by

Tien Q. Duong, Advanced Battery Materials Research Program Manager
Vehicle Technologies Office, Energy Efficiency and Renewable Energy

TABLE OF CONTENTS

A Message from the Advanced Battery Materials Research Program Manager	xv
Task 1 – Advanced Electrode Architectures.....	1
Task 1.1 – Higher Energy Density via Inactive Components and Processing Conditions (Vincent Battaglia, Lawrence Berkeley National Laboratory).....	2
Task 1.2 – Prelithiation of Silicon Anode for High-Energy Lithium-Ion Batteries (Yi Cui, Stanford University)	4
Task 1.3 – Electrode Architecture-Assembly of Battery Materials and Electrodes (Karim Zaghib, Hydro-Quebec).....	7
Task 2 – Silicon Anode Research.....	9
Task 2.1 – High-Capacity and Long Cycle Life Silicon-Carbon Composite Materials and Electrodes (Gao Liu, Lawrence Berkeley National Laboratory)	10
Task 2.2 – Stable Operation of Silicon-Based Anode for Lithium-Ion Batteries (Ji-Guang Zhang and Jun Liu, Pacific Northwest National Laboratory; Prashant Kumta, University of Pittsburgh)	12
Task 3 – High-Energy-Density Cathodes for Advanced Lithium-Ion Batteries	15
Task 3.1 – Studies on High-Capacity Cathodes for Advanced Lithium-Ion Systems (Jagjit Nanda, Oak Ridge National Laboratory).....	16
Task 3.2 – High-Energy-Density Lithium Battery (Stanley Whittingham, Binghamton University, State University of New York).....	19
Task 3.3 – Development of High-Energy Cathode Materials (Ji-Guang Zhang and Jianming Zheng, Pacific Northwest National Laboratory).....	22
Task 3.4 – <i>In Situ</i> Solvothermal Synthesis of Novel High-Capacity Cathodes (Feng Wang and Jianming Bai, Brookhaven National Laboratory)	25
Task 3.5 – Novel Cathode Materials and Processing Methods (Michael M. Thackeray and Jason R. Croy, Argonne National Laboratory)	28
Task 3.6 – Advanced Cathode Materials for High-Energy Lithium-Ion Batteries (Marca Doeff, Lawrence Berkeley National Laboratory)	31
Task 3.7 – Discovery of High-Energy Lithium-Ion Battery Materials (Wei Tong, Lawrence Berkeley National Laboratory)	33
Task 3.8 – Exploiting Cobalt and Nickel Spinels in Structurally Integrated Composite Electrodes (Michael M. Thackeray and Jason R. Croy, Argonne National Laboratory)	36

Task 4 – Electrolytes	39
Task 4.1 – Understanding and Mitigating Interfacial Reactivity between Electrode and Electrolyte (Khalil Amine, Larry A. Curtiss, and Nenad Markovic, Argonne National Laboratory).....	41
Task 4.2 – Advanced Lithium-Ion Battery Technology: High-Voltage Electrolyte (Joe Sunstrom and Ron Hendershot, Daikin).....	43
Task 4.3 – Multi-Functional, Self-Healing Polyelectrolyte Gels for Long-Cycle-Life, High-Capacity Sulfur Cathodes in Lithium-Sulfur Batteries (Alex Jen and Jihui Yang, University of Washington).....	45
Task 4.4 – Development of Ion-Conducting Inorganic Nanofibers and Polymers (Nianqiang (Nick) Wu, West Virginia University; Xiangwu Zhang, North Carolina State University).....	49
Task 4.5 – High Conductivity and Flexible Hybrid Solid-State Electrolyte (Eric Wachsman, Liangbing Hu, and Yifei Mo, University of Maryland).....	52
Task 4.6 – Self-Forming Thin Interphases and Electrodes Enabling 3D Structured High-Energy-Density Batteries (Glenn Amatucci, Rutgers University).....	55
Task 4.7 – Dual Function Solid-State Battery with Self-Forming, Self-Healing Electrolyte and Separator (Esther Takeuchi, Stony Brook University).....	57
Task 5 – Diagnostics	60
Task 5.1 – Model System Diagnostics for High-Energy Cathode Development (Guoying Chen, Lawrence Berkeley National Laboratory).....	61
Task 5.2 – Interfacial Processes – Diagnostics (Robert Kostecki, Lawrence Berkeley National Laboratory).....	64
Task 5.3 – Advanced <i>In Situ</i> Diagnostic Techniques for Battery Materials (Xiao-Qing Yang and Seongmin Bak, Brookhaven National Laboratory).....	66
Task 5.4 – Nuclear Magnetic Resonance and Magnetic Resonance Imaging Studies of Solid Electrolyte Interphase, Dendrites, and Electrode Structures (Clare Grey, University of Cambridge).....	69
Task 5.5 – Advanced Microscopy and Spectroscopy for Probing and Optimizing Electrode-Electrolyte Interphases in High-Energy Lithium Batteries (Shirley Meng, University of California at San Diego).....	72
Task 5.6 – <i>In Situ</i> Diagnostics of Coupled Electrochemical-Mechanical Properties of Solid Electrolyte Interphases on Lithium-Metal Rechargeable Batteries (Xingcheng Xiao, General Motors; Brian W. Sheldon, Brown University; Yue Qi, Michigan State University; and Y. T. Cheng, University of Kentucky).....	76
Task 5.7 – Microscopy Investigation on the Fading Mechanism of Electrode Materials (Chongmin Wang, Pacific Northwest National Laboratory).....	80
Task 5.8 – Characterization and Computational Modeling of Structurally Integrated Electrodes (Michael M. Thackeray and Jason R. Croy, Argonne National Laboratory).....	83

Task 6 – Modeling Advanced Electrode Materials	86
Task 6.1 – Predicting and Understanding Novel Electrode Materials from First Principles (Kristin Persson, Lawrence Berkeley National Laboratory)	87
Task 6.2 – Addressing Heterogeneity in Electrode Fabrication Processes (Dean Wheeler and Brian Mazzeo, Brigham Young University)	89
Task 6.3 – Understanding and Strategies for Controlled Interfacial Phenomena in Lithium-Ion Batteries and Beyond (Perla Balbuena, Jorge Seminario, and Partha Mukherjee, Texas A&M University)	92
Task 6.4 – Electrode Materials Design and Failure Prediction (Venkat Srinivasan, Argonne National Laboratory)	95
Task 6.5 – First Principles Calculations of Existing and Novel Electrode Materials (Gerbrand Ceder, Lawrence Berkeley National Laboratory)	97
Task 6.6 – Dendrite Growth Morphology Modeling in Liquid and Solid Electrolytes (Yue Qi, Michigan State University)	99
Task 6.7 – First Principles Modeling and Design of Solid-State Interfaces for the Protection and Use of Li-Metal Anodes (Gerbrand Ceder, University of California at Berkeley).....	102
Task 7 – Metallic Lithium and Solid Electrolytes	104
Task 7.1 – Mechanical Properties at the Protected Lithium Interface (Nancy Dudney, Oak Ridge National Laboratory; Erik Herbert, Michigan Technological University; Jeff Sakamoto, University of Michigan).....	106
Task 7.2 – Solid Electrolytes for Solid-State and Lithium-Sulfur Batteries (Jeff Sakamoto, University of Michigan).....	108
Task 7.3 – Composite Electrolytes to Stabilize Metallic Lithium Anodes (Nancy Dudney and Frank Delnick, Oak Ridge National Laboratory)	111
Task 7.4 – Overcoming Interfacial Impedance in Solid-State Batteries (Eric Wachsman, Liangbing Hu, and Yifei Mo, University of Maryland)	113
Task 7.5 – Nanoscale Interfacial Engineering for Stable Lithium-Metal Anodes (Yi Cui, Stanford University)	116
Task 7.6 – Lithium Dendrite Prevention for Lithium-Ion Batteries (Wu Xu and Ji-Guang Zhang, Pacific Northwest National Laboratory)	119
Task 7.7 – Lithium Batteries with Higher Capacity and Voltage (John B. Goodenough, University of Texas at Austin).....	122
Task 7.8 – Advancing Solid State Interfaces in Lithium-Ion Batteries (Nenad Markovic and Larry A. Curtiss, Argonne National Laboratory)	124
Task 7.9 – Engineering Approaches to Dendrite-Free Lithium Anodes (Prashant Kumta, University of Pittsburgh)	126
Task 7.10 – Self-Assembling and Self-Healing Rechargeable Lithium Batteries (Yet-Ming Chiang, Massachusetts Institute of Technology; Venkat Viswanathan, Carnegie Mellon University).....	129

Task 8 – Lithium–Sulfur Batteries	132
Task 8.1 – New Lamination and Doping Concepts for Enhanced Lithium–Sulfur Battery Performance (Prashant N. Kumta, University of Pittsburgh).....	134
Task 8.2 – Simulations and X-Ray Spectroscopy of Lithium–Sulfur Chemistry (Nitash Balsara, Lawrence Berkeley National Laboratory)	137
Task 8.3 – Novel Chemistry: Lithium Selenium and Selenium Sulfur Couple (Khalil Amine, Argonne National Laboratory).....	139
Task 8.4 – Multi-Functional Cathode Additives for Lithium–Sulfur Battery Technology (Hong Gan, Brookhaven National Laboratory, and Co-PI Esther Takeuchi, Brookhaven National Laboratory and Stony Brook University).....	142
Task 8.5 – Development of High-Energy Lithium–Sulfur Batteries (Jun Liu and Dongping Lu, Pacific Northwest National Laboratory)	145
Task 8.6 – Nanostructured Design of Sulfur Cathodes for High-Energy Lithium–Sulfur Batteries (Yi Cui, Stanford University)	147
Task 8.7 – Addressing Internal “Shuttle” Effect: Electrolyte Design and Cathode Morphology Evolution in Lithium-Sulfur Batteries (Perla Balbuena, Texas A&M University).....	149
Task 8.8 – Investigation of Sulfur Reaction Mechanisms (Deyang Qu, University of Wisconsin at Milwaukee; Xiao-Qing Yang, Brookhaven National Laboratory)	152
Task 8.9 – Statically and Dynamically Stable Lithium–Sulfur Batteries (Arumugam Manthiram, University of Texas at Austin).....	155
Task 8.10 – Electrochemically Responsive, Self-Formed Lithium-Ion Conductors for High-Performance Lithium-Metal Anodes (Donghai Wang, Pennsylvania State University).....	158
Task 9 – Lithium–Air Batteries	161
Task 9.1 – Rechargeable Lithium–Air Batteries (Ji-Guang Zhang and Wu Xu, Pacific Northwest National Laboratory)	162
Task 9.2 – Efficient Rechargeable Li/O ₂ Batteries Utilizing Stable Inorganic Molten Salt Electrolytes (Vincent Giordani, Liox).....	165
Task 9.3 – Lithium–Air Batteries (Khalil Amine and Larry A. Curtiss, Argonne National Laboratory).....	167
Task 10 – Sodium-Ion Batteries	169
Task 10.1 – Exploratory Studies of Novel Sodium-Ion Battery Systems (Xiao-Qing Yang and Seongmin Bak, Brookhaven National Laboratory)	170

TABLE OF FIGURES

Figure 1. Characterizations of the $\text{Li}_x\text{Si}/\text{graphene}$ foil. (a) Photograph of large $\text{Li}_x\text{Si}/\text{graphene}$ foil with 8-cm width and 24-cm length. The right side of the foil is rolled around a thin tube to illustrate good flexibility. (b) Low-magnification transmission electron microscopy (TEM) image of the overlapped and interconnected graphene sheets. (c) TEM image shows a double-layer graphene sheet with the inter-layer distance of 0.334 nm. The inset is the atomic resolution image of the graphene sheet. (d) Uniaxial tensile test of the graphene foil (blue), bulky paper (black), Li-metal foil (orange), and $\text{Li}_x\text{Si}/\text{graphene}$ foil (red). (e) X-ray diffraction pattern reveals the highly crystalline nature of graphitic carbon and $\text{Li}_{22}\text{Si}_5$. (f) Top-view and (g) cross-sectional view of scanning electron microscopy images of the $\text{Li}_x\text{Si}/\text{graphene}$ foil.	5
Figure 2. Scanning electron microscopy image of (a) version 1 nano-Si/C composite made by electro spray process and (b) version 2.	8
Figure 3. Cell performance during cycling at C/6 rate between 1.5 V and 0.005 V at room temperature.	8
Figure 4. The Raman and X-ray diffraction spectra of pure SiO and SiO-PPy sintered at different temperature.	11
Figure 5. (a) The rate capabilities of pure SiO and SiO-PPy sintering at different temperature. (b) Cycling performance at C/10. (c) Cycling performance at C/3. (d) Coulombic efficiency for pure SiO and SiO-PPy samples.	11
Figure 6. Cycling stability of p-Si/C and nano-Si electrodes.	13
Figure 7. Cycling stability of Si/MWNT/C electrode.	13
Figure 8. Long-term cycling data of nano-Si conducting foam tested at 50 mA/g for initial 6 cycles followed by 0.5A/g in Li/Li+ system.	13
Figure 9. (a) Cross-sectional scanning electron microscopy image of a sputtered thin-film Li_2MoO_3 cathode. (b) X-ray diffraction pattern of a sputtered Li_2MoO_3 thin-film, Li_2MoO_3 powder, and the sputtering substrate (Pt on Al_2O_3). Galvanostatic charge/discharge curves for half-cells containing a (c) thin-film Li_2MoO_3 cathode and (d) slurry-cast Li_2MoO_3 cathode.	17
Figure 10. The cycling behaviors of $\text{Sn}_y\text{Fe}/\text{Li}_x\text{VOPO}_4$ full cells under different cycling conditions: (a-b) constant current cycling between 0.5 ~ 4.3V, (c-d) constant current and constant voltage cycling between 0.5 ~ 4.3V, and (e-f) constant capacity cycling.	20
Figure 11. (a) Cycling performance, (b) discharge mid-point voltage versus cycle number of Ni-rich $\text{LiNi}_{0.76}\text{Mn}_{0.14}\text{Co}_{0.10}\text{O}_2$ cathode in E-baseline and E-optimized electrolytes during cycling at C/3 (after 3 formation cycles at C/10) between 2.7~4.5 V. The corresponding charge/discharge voltage profile evolutions are shown in (c) E-baseline and (d) E-optimized.	23
Figure 12. High-angle annular dark field – scanning transmission electron microscopy (HAADF-STEM) images of Ni-rich $\text{LiNi}_{0.76}\text{Mn}_{0.14}\text{Co}_{0.10}\text{O}_2$ after 100 cycles at C/3 between 2.7~4.5 V in (a-b) E-baseline electrolyte and (c-d) E-optimized electrolyte.	23

Figure 13. Structural, chemical, and morphological evolution in the intermediates of NMC-71515 during heat treatment at 800°C, 850°C, and 900°C. (a) Evolution of the cationic disordering (that is, occupancy of nickel ions at 3b sites). (b) Thermogravimetric analysis curves of the precursors during holding at constant temperatures. (c) Evolution of crystallite size with holding time.	26
Figure 14. (a) Charge/discharge profiles. (b) Cycling performance of synthesized NMC-71515 at 800°C, 850°C, and 900°C.	26
Figure 15. Elemental mapping of layered-layered-spinel powder treated with 1 wt% Li_xCoPO_4 ($x = 1$) and annealed at 700°C.	29
Figure 16. (a) Cycle life of untreated and LCP-treated layered-layered-spinel (LLS) cathode materials. (b) Rate performance of untreated and Li_xPO_4 -treated ($x = 0.25, 0.5, 0.75, \text{ and } 1.0$) LLS. All charge cycles were carried out at 15 mA/g to 4.45 V after a first-cycle activation to 4.6 V. Discharge currents are labeled along the top of the figure. All electrochemical testing was carried out at 30°C versus Li-metal anodes. Electrode loadings were $\sim 6\text{ mg/cm}^2$	29
Figure 17. <i>In situ</i> hot stage X-ray diffraction patterns on a 50% delithiated NMC-622 sample (left) and a 100% delithiated sample (right).	32
Figure 18. X-ray diffraction Rietveld refinement of (a) LNMO, monoclinic C2/m, and LNRO, monoclinic C2/c. High-resolution transmission electron microscopy image of (c) LNMO, (e) LNRO with fast Fourier transformation of the selected area. Electron diffraction pattern of (d) LNMO and (f) LNRO.	34
Figure 19. O K-edge resonant inelastic X-ray scattering maps of (a) LNMO and (b) LNRO electrodes at various states of charge. The white arrow indicates the specific oxygen redox state that is absent in LNRO.	34
Figure 20. X-ray diffraction (XRD) of sol-gel LiCoO_2 (LCO) and $\text{LiCo}_{0.85}\text{Al}_{0.15}\text{O}_2$ (LCO-Al) samples fired at 400°C (low temperature) or 600°C (intermediate temperature). An XRD pattern of LCO, synthesized by solid-state reaction, is shown for comparison. Red circles indicate the peaks for Co_3O_4	37
Figure 21. (a, b) Initial voltage profiles and (c) normalized capacity of the sol-gel prepared samples.	37
Figure 22. <i>In situ</i> inductively coupled plasma mass spectrometry results of cobalt dissolution upon electro-chemical polarization using the stationary probe rotating disk electrode system. Working electrode: $\text{LiCoO}_2/\text{C}/\text{PVDF}$. Electrolyte: 1.2 M LiPF_6 in EC:EMC (3:7 by mass).	42
Figure 23. Total amount of cobalt dissolution upon electro-chemical polarization using as monitored by the stationary probe rotating disk electrode inductively coupled plasma mass spectrometry system. Same experimental conditions as in Figure 22.	42
Figure 24. Volume change as a function of cycle number as measured by the Archimedes method.	44
Figure 25. Self-healing behavior in PENDI- C_6/Py Linker blends is affected by both crosslink density and stoichiometry, which can be manipulated by adding “free” NDI or Py molecules to the blend.	46

Figure 26. Performance of thiol-modified mesoporous carbon cathodes depends strongly on the amount of modifier present, with 10 wt% representing an ideal combination of high capacity, improved retention, and low overpotential.	47
Figure 27. (A) Pure and Al-decorated $\text{Li}_{0.33}\text{La}_{0.56}\text{TiO}_3$ structures. (a-c) Side views of pure and most stable single-Al and double-Al decorated $\text{Li}_{0.33}\text{La}_{0.56}\text{TiO}_3$, respectively. (d) Top view of La-deficient layer of (b). Blue and green color blocks in (d) are used to represent two different regions in lithium atom transporting direction. (B) Transporting barriers for lithium atoms along transporting direction in pure, single-Al, and double-Al decorated $\text{Li}_{0.33}\text{La}_{0.56}\text{TiO}_3$ structure. The transporting trajectory is marked by dash line in inset.	50
Figure 28. (a) Li[PSTFSI-b-MPEGA-b-PSTFSI] triblock copolymer. (b) Room-temperature ionic conductivities of Li[PSTFSI-b-MPEGA-b-PSTFSI] triblock copolymer.....	51
Figure 29. Characterization of garnet fibrous membrane: (a) Powder X-ray diffraction patterns of the crushed garnet textile sintered at different temperatures; and (b) scanning electron microscopy image of the garnet textile converted from the precursor solution impregnated template.	53
Figure 30. <i>Mechanical characterization of garnet nanofibers</i> : (a) Atomic force microscopy scanning of the nano-indent points on garnet nanofiber; and (b) load-depth profile of garnet fiber. <i>Electrochemical characterization of hybrid composite polymer electrolyte</i> : (a) electrochemical impedance spectroscopy, Li-ion conductivity is 6.07×10^{-4} S/cm; and (b) cyclic voltammetry, stable up to 4.5 V.	53
Figure 31. Voltage profile of a cell utilizing hybridization of the transport pathways showing the <i>in situ</i> formation and first discharge.	56
Figure 32. Electrochemical impedance spectroscopy data: (a) pristine LiI solid electrolyte before and after charging, (b) pristine AgI solid electrolyte before and after charging, and (c) Composition I, a LiI-based electrolyte with AgI and polymer additive before and after charging.....	58
Figure 33. (a) Electrochemical impedance spectroscopy data of electrolyte Composition II before and after (inset) charging using four different interface conditions. (b) Step-wise charging of cells. (c) After step-wise charging, all cells maintained stable OCV.....	58
Figure 34. Differential electrochemical mass spectrometry analysis results obtained from a $\text{Li}_{1.3}\text{Nb}_{0.3}\text{Mn}_{0.4}\text{O}_2$ half-cell.....	62
Figure 35. (a-b) Total electron yield and fluorescence yield O <i>K</i> -edge soft X-ray absorption spectra. (c-d) Intensity ratio between pre-edge and post-edge peaks and intensity of the <i>p</i> -band as a function of lithium content in $\text{Li}_x\text{Nb}_{0.3}\text{Mn}_{0.4}\text{O}_2$	62
Figure 36. (a) Schematic diagram of metal organic compound formation from NMC cathode. (b) Capacity-cycling plot of NMC cathode / lithium anode cells electrolyte with/without 500 ppm Mn(III)(acac) ₃ . (Cells galvanostatically cycling between 2–4.7 V at 0.5C.)	65

Figure 37. Electrochemical performance of the Li/Li symmetrical cell with different electrolyte additives during subsequent charge/discharge cycling at 1 mA/cm ² current density with 1-h interval. (a) Development of overpotentials. (b) Nyquist plot measured at OCV. The yellow star marked in each curve is the impedance at 37 Hz. (c) Impedance at 37 Hz at selected cycle.	65
Figure 38. Three-dimensional electron tomography reconstructions of (a) pristine and (b) after 15 charge-discharge cycles of Li _{1.2} Ni _{0.15} Co _{0.1} Mn _{0.55} O ₂ material. The internal pore size distribution weighted by occurrence (upper) and by volume (lower) of (c) the pristine materials and (d) the sample after 15 cycles.	67
Figure 39. Experimental (black) electrochemistry of a Na-Sn cell cycled at C/20 between 2 and 0.001 V compared to theoretical (red/blue) predictions.	70
Figure 40. <i>Operando</i> (a) pair distribution functions and (b) ²³ Na nuclear magnetic resonance spectra for Na-Sn cells aligned with corresponding electrochemistry (c).	70
Figure 41. Left panel: (a) Structure of NaSn ₃ - <i>Pmmm</i> with sodium in yellow and tin in purple. (b) <i>Operando</i> X-ray diffraction patterns. (c) <i>Ex situ</i> ²³ Na and (d) ¹¹⁹ Sn 60 kHz magic angle spinning nuclear magnetic resonance at the end of process 1 and 1'. Right panel: (a) Structure of Na _{5-x} Sn ₂ . (b) Occupancy versus sodium site 3 versus time spent on process 3'. (c) Fit of the pair distribution function corresponding to the first frame in process 3'.	70
Figure 42. Neutron diffraction (ND) characterization of Li-rich layered oxide (LRLO) cycled electrode after heat treatment. (a) Refined ND patterns of the LRLO electrode after the initial cycle. (b-d) Refined ND patterns of the initially cycled electrode after heat treatment under 200, 250, and 300 °C, respectively. (e) Lithium occupancy in transition metal layer and (f) oxygen occupancy for different samples.	73
Figure 43. Diffraction data collected for Li-rich layered oxide electrode after the (a) first cycle and (b) fiftieth cycle. (c) Experimental schematic of the <i>in situ</i> Bragg Coherent Diffraction Imaging setup. Scale bar is 1e-8 1/Å.	74
Figure 44. Cryo-transmission electron microscopy (a) image and (b) its regional zoomed-in image with the bulk and surface fast Fourier transformation results of the electrochemically deposited lithium metal using conventional carbonate electrolyte.	74
Figure 45. The surface morphology of Li-metal electrode after first plating and stripping cycle. Current density 1mA/cm ² , and lithium capacity 4 mAh/cm ² . (a) Lithium electrode in carbonate-based electrolyte. (b) Lithium electrode in ether-based electrolyte. (c) Aluminum film coated lithium electrode in carbonate-based electrolyte.	77
Figure 46. Stress evolution of Li-metal electrodes in different electrolytes.	78
Figure 47. The band gap (HSE06) changes as a function of average anion distance, η	78
Figure 48. Scanning transmission electron microscopy – energy dispersive spectroscopy map showing the segregation of P and C on the surface of cathode particle of different composition following battery cycling. P and C are typical components from the electrolyte. This observation provides direct evidence on the reaction of cathode with the electrolyte.	81

Figure 49. (a) Calculated density functional theory formation energies of $\text{LiCo}_x\text{M}_{1-x}\text{O}_2$ ($M = \text{Mn}$ or Ni ; $0 \leq x \leq 1$) in both lithiated spinel (Fd-3m) and layered (R-3m) structures. The mixing energies of (b) $\text{LiCo}_x\text{Mn}_{1-x}\text{O}_2$ and (c) $\text{LiCo}_x\text{Ni}_{1-x}\text{O}_2$.	84
Figure 50. The relative surface oxygen release energy for the top 10 candidate dopants as compared to the pristine systems shown for representative (001) and (010) surface facets. A dark yellow color indicates stronger oxygen retention, while a purple color indicates less protection against oxygen release as compared to the pristine, undoped surface.	88
Figure 51. (a) Power spectral density for various battery films. Scanning laser doppler vibrometer results of various battery films with thicknesses of (b) 42 μm , (c) 38 μm , and (d) 26 μm .	90
Figure 52. SEI of two components with different activation barriers for lithium diffusion: purple (A, $E_a = 46.1$ KJ/mol) and white (B, $E_a = 65.3$ KJ/mol). SEI morphologies at B volume fractions of 5% in (a) and 33% in (b). (c) Total charging time and SEI thickness for the first charge with varying B volume fraction. (d) Concentration of active lithium traveling through the SEI interstitials (cc) with respect to the theoretical maximum (cM) for various B volume fractions.	93
Figure 53. (a) Impact of stress factor and current–distribution factor on the overall reaction current density. Electrolytes with shear modulus 20 times larger than that of lithium may prevent dendrite growth. (b) Phase map demonstrating the correlation between applied current density and electrolyte shear modulus on stabilization of lithium deposition.	96
Figure 54. (a) Effect of elastic-plastic deformation of both lithium metal and electrolyte on the overall suppression of the dendritic protrusion. (b) Increasing yield strength of the electrolyte may help to prevent dendrite growth even with present-day polymer electrolytes.	96
Figure 55. Energy dispersive spectroscopy mapping on one area of a LNF15 particle. Scale bars, red: 100 nm, blue: 25 nm.	98
Figure 56. ^{19}F spin echo nuclear magnetic resonance spectra obtained at 30 kHz magic angle spinning for LNF15 and LiF.	98
Figure 57. Differential electrochemical mass spectrometry (DEMS) study of LNF15 when charged to 4.8 V and discharged to 1.5 V at 20 mA g^{-1} , along with the DEMS results on O_2 (red circle) and CO_2 (blue triangle).	98
Figure 58. SEI properties – lithium dendrite morphology map from phase field simulation.	100
Figure 59. The excess electrons located on lanthanum atoms on LLZO surface.	100
Figure 60. Method adopted here to screen for promising electrolyte materials.	103
Figure 61. Scheme of the formation and propagation of lithium dendrites during electrochemical cycling of a solid-state battery.	103
Figure 62. (a) Cell layout and proposed Kirkendall effect. (b) Potential response to a constant 0.1 mA/cm^2 under a cyclic loading. (c) Representative impedance spectra at 2.4 and 1.2 MPa. (d) Measured interface impedance at each stack pressure during cycling loading.	107

Figure 63. The critical current density of an all solid-state Li-LLZO-Li cell exceeded 1 mA/cm ² . Red: current density; black: voltage.....	109
Figure 64. Results for trilayer cell polymer/ceramic/polymer electrolyte. (a-c) Electrochemical impedance spectroscopy (EIS) responses of ceramic plate, polymer electrolytes, and trilayer cells. All EIS responses are measured at 30°C. (Inset of c) Scanning electron microscopy of trilayer cell. (d) Arrhenius plot of interfacial resistance calculated from the trilayer cell data.	112
Figure 65. Arrhenius plot of composite containing LLZO, compared to that containing Ohara.	112
Figure 66. (left) Cycling data of NMC cathode/composite electrolyte/lithium cell on regular and expanded metal foils. (right) Galvanostatic cycling data showing the cycle stability between the 1st and 20th cycle.	112
Figure 67. Cycling performances of Li/NMC cells with garnet electrolytes. (a-b) Voltage profiles and cycling performance of Li/NMC cell with 13.5 mg/cm ² cathode at 0.1 C rate. Stable capacity at 175 mAh/g was achieved. (c) Cycling performance of Li/NMC cell with 13.5 mg/cm ² cathode at various rates. High Coulombic efficiency and capacity retention were achieved during 200 cycles. (d) Voltage profiles of Li/NMC cell with 32 mg/cm ² cathode at 0.05 C rate.	114
Figure 68. Cycling performances of Li/sulfur cell with garnet electrolytes. (a) Voltage profiles of the 1 st , 5 th , and 20 th cycles of the solid-state Li-S cell at 50 mA/g current density. 1200 mAh/g capacity and low capacity loss were achieved. (c) Cycling results of the solid-state Li-S cell. High capacity retention was achieved with near 100% Coulombic efficiency.	114
Figure 69. Schematics illustrating the fabrication process of the 3D lithium anode with flowable interphase for solid-state lithium battery. (A) 3D Li-rGO composite anode was first fabricated. (B) A flowable interphase for the 3D Li-rGO anode was created via thermal infiltration of liquid-like PEG-LiTFSI at a temperature of 150°C. (C) A composite polymer electrolyte (CPE) layer consisting of PEO, LiTFSI, and fumed silica or an LLZTO ceramic membrane was used as the middle layer; high-mass loading LFP cathode with the CPE as the binder was overlaid to construct the solid-state Li-LFP full cell.	117
Figure 70. Electrochemical performance of solid-state Li-LFP batteries.....	117
Figure 71. Scanning electron microscopy images of nano-seeds formed on copper substrate after linear sweep voltammetry to 0 V and held at 0 V for 1 min (left), after lithium deposition for 10 min (middle), and after lithium deposition for 15 h (right). The electrolyte is 1 M LiPF ₆ in PC, with 2% LiAsF ₆ and 2% VC. The current density is 0.1 mA cm ⁻²	120
Figure 72. Cycling stability of Coulombic efficiency of Li NMC-333 cells using three electrolytes of 1 M LiTFSI-LiBOB plus 0.05 M LiPF ₆ in EC-EMC with different solvent compositions and/or other additives (VC and FEC). The current density is 2.0 mA cm ⁻² . E-488 and E-580 have EC-EMC 4:6 by weight, while E-589 has EC-EMC 7:3 by weight. E-580 and E-589 also contain VC and FEC.....	120
Figure 73. Copper oxidation time and corresponding discharge capacity.....	123

Figure 74. Charge/discharge voltage curves of the copper cathode.	123
Figure 75. Lithium adsorbed on TiO ₂ -terminated (100) SrTiO ₃ surface, O ₂ -terminated (110) surface, and (3x1) reconstructed (110) surface. (bottom) Lithium binding energy as a function of oxygen stoichiometry.	125
Figure 76. X-ray photoelectron spectroscopy core-level spectra before (red) and after (blue) lithium deposition show (a) reduction of niobium in Nb:LLZO and (d) reduction of zirconium in Ta:LLZO. (b) Tantalum in Ta:LLZO and (c) zirconium in Nb:LLZO are all stable throughout the sputtering.	125
Figure 77. Scanning electron microscopy image of the high porosity (~ 85%) copper foams after sintering and removal of the sacrificial template.	127
Figure 78. Gen-2 copper foam electrodes demonstrate stable cycling region of 60 cycles at ~ 90% Coulombic efficiency.	127
Figure 79. Scanning electron microscopy images of the porous copper foam electrodes after cycling (~ 200 cycles). (a) Cross-section view. (b) Close up of lithium deposited within the foam structure. (c) Close up of lithium deposited on top of the foam surface following pore closure by competitive SEI formation in the foam structure.	127
Figure 80. Scanning electron microscopy (SEM) characterization of the morphology of the deposited lithium. (a/c) Top-view SEM images of lithium deposited in 1 M LiPF ₆ EC-DMC electrolyte. (b/d) Top-view SEM images of lithium deposited in 1 M LiPF ₆ -based electrolyte with a fluorine-containing additive. The scale bars in (a/b) are 5 μm. The scale bars in (c/d) are 2 μm. 3 mAh cm ⁻² of lithium is deposited at a current density of 0.6 mA cm ⁻²	130
Figure 81. Electrochemical cycling performance of the polysulfide-trapping-agent-coated directly doped sulfur architectures compared with commercial sulfur.	135
Figure 82. (a) UV – visible spectroscopy of polysulfide trapping agent (PTA)-coated directly doped sulfur architectures (DDSA) electrodes showing absence of polysulfide absorbance. (b) Comparison of X-ray photoelectron spectroscopy patterns of commercial sulfur and PTA - DDSA separators after 200 cycles.	135
Figure 83. <i>In situ</i> experiments on Li-S experiments. (a) X-ray tomography. (b) X-ray absorption spectroscopy: (left) early data with polysulfide dissolution and (right) new data with significantly less polysulfide dissolution.	138
Figure 84. Charge/discharge curve of Li/Se-S battery with 45 wt% Se-S loading in the composite at C/10 in LiTFSI/ANL-2.	140
Figure 85. Cycle performance of Li/Se-S battery with 45 wt% Se-S loading in the composite at C/10 in LiTFSI/ANL-2.	140
Figure 86. Cycle life test.	143
Figure 87. Discharge temperature effect.	143
Figure 88. Shelf-life; fully discharged.	143
Figure 89. Self-discharge rate.	143
Figure 90. Pouch cell rate capability.	143

Figure 91. (a) Component weight distribution of Li-S battery with energy density of 300 Wh/kg. (b) Photo image of single-layer pouch cell used in present study (electrode working area 19.4 cm ² , and sulfur mass loading 5.7 mg/cm ²). (c) Dependence of first discharge areal capacity and specific capacity on electrolyte/sulfur ratio (black symbol: pouch cell using pristine separator; red symbol: pouch cell using modified separator).	146
Figure 92. Li ₂ S ₆ polysulfide adsorption test. Inductively coupled plasma atomic emission spectroscopy data of (a) lithium intensity and (b) sulfur intensity with varying Li ₂ S ₆ concentrations without candidate materials, (c) calculated adsorption by candidate materials in 3mM Li ₂ S ₆ solution.	148
Figure 93. Molecular simulations reveal structural details of C-S composite.	150
Figure 94. Comparison of inhibition effect for nitrate additives, based on direct comparison of chromatographic distributions before and after contact with lithium metal.	153
Figure 95. Cycling performances of the cells fabricated with (a) LBL CNT#1, LBL CNT#2, and LBL CNT#3 separators with 5.4 mg cm ⁻² sulfur loading and (b) LBL CNT#3 separator with 5.4 and 7.5 mg cm ⁻² sulfur loadings. (c) Self-discharge rates of the cells fabricated with the three LBL CNT separators after storing for 360 days.	156
Figure 96. (a) Cycling performance and (b) self-discharge analysis of the cells fabricated with cotton-carbon cathodes with a sulfur loading of 30 mg cm ⁻² . (c) Cycling performance of a cotton-carbon cathode with even a higher sulfur loading of 60 mg cm ⁻²	156
Figure 97. X-ray photoelectron spectroscopy (XPS) spectra of C-SEI layer, S-SEI layer, and SCP-90-SEI layer. (a) S 2p XPS spectra. (b) C 1s XPS spectra. (c) F 1s XPS spectra.	159
Figure 98. Fourier transform infrared of C-SEI, S-SEI, and PST-90-SEI layer.	159
Figure 99. Indentation curves of the C-SEI layer (a), S-SEI layer (b), and PST-90-SEI layer (c).	159
Figure 100. Cycling performances of the cells using different electrolytes at a current density of 2 mA cm ⁻² with a deposition capacity of 1 mA h cm ⁻²	160
Figure 101. Comparison of cycle life of Li-O ₂ cells with and without pre-treatment. The cell cycling was conducted under the 1000 mAh g ⁻¹ capacity limited protocol at 0.1 mA cm ⁻² between 2.0 V and 4.5 V.	163
Figure 102. The AC-impedance spectra of the Li-O ₂ cells after pre-treatment at 4.3 V/10 min during 110 cycles (a), and pristine Li-O ₂ cells during 70 cycles (b). (c) Evolution of fitted resistance values of the above Li-O ₂ cells after pre-treatment at 4.3 V/10 min and pristine cells.	163
Figure 103. The schematic of the operation principle of beforehand protections for carbon nanotube air-electrode and Li-metal anode after <i>in situ</i> one-step electrochemical process.	163
Figure 104. Molten nitrate lithium cell voltage profile at 150°C using nano-porous nickel cathode (Ni:LiNO ₃ -KNO ₃ eutectic 50:50 wt%) at 0.2 mA/cm ₂ current density (mNi = mnitrate = 10 mg) and LLZO-protected Li-metal anode.	166

Figure 105. (a) Discharge/charge profile for 50 cycles. (b) The termination voltage of charge/discharge for 50 cycles.....	168
Figure 106. Charge compensation mechanism upon sodium deintercalation/intercalation in β -NaCu _{0.2} Mn _{0.8} O ₂ . (a) <i>In situ</i> X-ray absorption spectroscopy (XAS) spectra at manganese K-edge collected at different charge/discharge states. (b) <i>In situ</i> XAS spectra at copper K-edge collected at different charge/discharge states. (c) The load curve of β -NaCu _{0.2} Mn _{0.8} O ₂ during the first charge process for <i>in situ</i> XAS. (d) The enlarged XAS spectra at copper K-edge.	171

TABLE OF TABLES

Table 1. Five binders assessed for effect of binder molecular weight.	3
Table 2. Gas composition of LCO (red) and NMC-622 (yellow) cells determined by gas chromatography – mass spectroscopy/thermal conductivity detector as a function of FEC concentration.....	44
Table 3. Conductivity of ionogels based on solvate ionic liquid.....	46
Table 4. The ionic conductivities of Li[PSTFSI-b-MPEGA-b-PSTFSI] triblock copolymer.	51
Table 5. Conductivity of LiI with additives at 30°C.	58
Table 6. Measured and calculated properties of coated layer of battery films.....	90
Table 7. Additives tested in the project study using the unique high-performance liquid chromatography mass spectrometry method. (See references listed at the end of this section.).....	153

A MESSAGE FROM THE ADVANCED BATTERY MATERIALS RESEARCH PROGRAM MANAGER

This document summarizes the BMR investigators' activities performed during the period from August 1, 2017, through September 30, 2017. Selected highlights from the fourth quarter are summarized below:

- The Pacific Northwest National Laboratory Group headed by Zhang and Zheng demonstrated better capacity retention and improved interfacial stability in Ni-rich NMC using an electrolyte-optimized system that is a mixture of LiTFSI, LiBOB, and LiPF₆ in carbonates.
- Lawrence Berkeley National Laboratory (Kostecki's Group) investigated the effect of transition-metal dissolution and revealed the detrimental effect of manganese (III) acetylacetonate (Mn(III)(acac)₃) poisoning to the electrochemical performance of a Li-metal anode.
- The Group at Argonne National Laboratory (Amine, Curtiss, Markovic) demonstrated the first quantitative real-time analysis of cobalt dissolution that occurs during charging of LiCoO₂ in 1.2M LiPF₆ in EC:EMC 3:7 electrolyte. This unique capability for monitoring *in situ* dissolution of transition metals from battery cathodes can provide a deeper understanding of the fundamental processes responsible for performance degradation in Li-ion batteries.
- The University of Maryland Group headed by Eric Wachsman achieved a hybrid solid-state electrolyte with a high ionic conductivity ($\sim 0.5 \times 10^{-3}$ S/cm), high electrochemical stability (~ 4.5 V), and high mechanical property.
- Cambridge University (Grey's Group) investigated the phases formed during sodium insertion in high-capacity tin anodes, and obtained the first evidence for significant solid solution behavior and resulting metastability in the Na-Sn system.

This and prior quarterly reports have demonstrated the significant scientific contributions made by the BMR Investigators during FY 2017. In the next fiscal year, the BMR Program will continue to focus on the fundamental issues of materials and electrochemical interactions associated with beyond-lithium battery technologies as well as to explore novel diagnostic and modeling efforts to aid in this effort.

Sincerely,

Tien Q. Duong

Tien Q. Duong
Manager, Advanced Battery Materials Research (BMR) Program
Energy Storage R&D
Vehicle Technologies Office
Energy Efficiency and Renewable Energy
U.S. Department of Energy

TASK 1 – ADVANCED ELECTRODE ARCHITECTURES

Summary and Highlights

Energy density is a critical characterization parameter for batteries for electric vehicles (EVs), as there is only so much room for the battery and the vehicle needs to travel nearly 300 miles. The U.S. Department of Energy (DOE) targets are 500 Wh/L on a system basis and 750 Wh/L on a cell basis. Not only must the batteries have high energy density, they need to do so and still deliver 1000 Wh/L for 30 seconds at 80% of its accessible capacity. To meet these requirements not only entails finding new, high-energy-density electrochemical couples, but also highly efficient electrode structures that minimize inactive material content, allow for expansion and contraction for several thousand cycles, and allow full access to the active materials by the electrolyte during pulse discharges. In that vein, the DOE Vehicle Technologies Office (VTO) supports three projects in the Advanced Battery Materials Research (BMR) Program under Advanced Electrode Architectures: (1) Higher Energy Density via Modifications to the Inactive Components at Lawrence Berkeley National Laboratory (LBNL), (2) Electrode Architecture – Assembly of Battery Materials and Electrodes at Hydro-Quebec (HQ), and (3) Prelithiation of Silicon Anode for High-Energy Li-Ion Batteries at Stanford University.

The three tasks take three distinct approaches to improving energy density. The first task attempts to increase energy density by making thicker electrodes and reducing the amount of inactive components per cell. The second task attempts to improve the energy density of the anode through different processing conditions and binders of silicon composites. The third task attempts to increase the energy density of Li-ion cells with high capacity, prelithiated Si-based active materials.

The problem being addressed with the first approach is that as electrode thickness increases, the drying time can decrease, which allows additional time for segregation of electrode components. For a thicker electrode, winding leads to more hoop stress on the outer portion of the laminate. Both problems can result in delamination of the laminate from the current collector. The other problem with thicker electrodes is that they tend to not cycle as well as thinner electrodes and thus reach the end-of-life condition sooner, delivering fewer cycles.

The problem being addressed by the second approach is that silicon expands three times its original size when fully lithiated. To lessen the stress of this event, composites of silicon are often used. These researchers hope to discover the proper processing conditions and binders to allow a silicon material to be substituted into a Li-ion cell.

The problem being addressed by the third approach is that silicon does not immediately form a passivating coating during the first charge of lithium ions. This results in an imbalance of lithium in the two electrodes, reducing the cyclable capacity of the cell.

Task 1.1 – Higher Energy Density via Inactive Components and Processing Conditions (Vincent Battaglia, Lawrence Berkeley National Laboratory)

Project Objective. Thicker electrodes with small levels of inactive components that can still deliver most of their energy at C-rates of C/3 should result in batteries of higher energy density. In turn, higher energy density should translate to more miles per charge or smaller, less expensive batteries. Unfortunately, the limit to making thicker electrodes is not based on power capability but on mechanical capability; that is, the thicker electrodes delaminate from the current collector during calendaring or slicing. The objective of this research is to produce a high-energy-density electrode with typical Li-ion components that does not easily delaminate and still meets the EV power requirements through changes to the components and concomitant changes to processing conditions.

Project Impact. Today's batteries cost too much on a per kWh basis and have too low of an energy density to allow cars to be driven over 300 miles on a single charge. This research simultaneously addresses both problems. By developing thicker, higher-energy-density electrodes, the fraction of cost relegated to inactive components is reduced and the amount of energy that can be introduced to a small volume can be increased. Macroscopic modeling suggests that this could have as much as a 20% impact on both numbers.

Out-Year Goals. In outgoing years, the project will make changes to the binder molecular weight, conductive additive, and size distribution of the active material and will make whatever changes are necessitated by electrode processing conditions to increase the energy density while maintaining power capability. Changes in processing conditions can include the time of mixing, rate of casting, temperature of slurry during casting, drying conditions, and hot calendaring. Chemical modifications may include multiple binder molecular weights and changes in the conductive additive size and shape.

Collaborations. The project collaborates with several groups: Zaghbi's Group (HQ) for materials and cell testing; Wheeler's Group at Brigham Young University (BYU) for modeling analysis; Liu's group on polymer properties; Arkema for binders; and a commercial cathode material supplier.

Milestones

1. Fabricate "thick" laminates of NCM and establish the effect of calendaring at different temperatures. (Q1 – Completed December 2017)
2. Determine to what extent electrode performance can be improved through use of an active material of two particle size distributions. (Q2 – Delayed)
3. Determine the degree to which several updates in materials and processing are affecting cyclability. (Q3 – Delayed)
4. *Go/No-Go:* Determine if a binder of a mixture of molecular weights is worth pursuing to achieve thicker electrodes based on ease of processing and level of performance. If no, pursue a path of a single molecular weight binder. (Q4 – Delayed)

Progress Report

The fourth quarter milestone is delayed. This quarter, the project investigated the effect on electrode homogeneity and performance as a function of binder molecular weight. Next quarter, it will investigate the effect of mixing two binders of different molecular weight and compare the results to an electrode produced using a binder with the same average molecular weight.

The project has been investigating changes to electrode homogeneity and performance as a result of changes to the inactive components and to the processing conditions. This includes changes to the binder molecular weight, the slurry viscosity, the addition of carbon nanotubes, and impacts of calendaring at different temperatures. This quarter, the effort dove deeper into the effect of binder molecular weight by assessing five binders of different molecular weights (see Table 1). Next quarter, combinations of binders of different molecular weights will be investigated.

Table 1. Five binders assessed for effect of binder molecular weight.

PVDF Commercial Name	KF1100	Kynar 761	HSV 500	HSV800	HSV900
Molecular Weight	~ 280k	~ 400k	> 400k	< 1M	> 1M

The project's experience in fabricating thick laminates over the past few years clearly indicates that the viscosity of the laminate is critical to its final homogeneity, especially when allowed to dry via natural convection in a glovebox. As the molecular weight goes up, the viscosity of the laminate goes up. To compensate for this, more NMP is required of slurries consisting of higher molecular binders. Once the laminates are produced, they are cross sectioned and evaluated for their uniformity using techniques developed at LBNL. Other parts of the laminates are put through a bend test of rollers of ever reducing diameters, while still other portions of the laminate are cut into circular electrodes for coin cell testing. This assessment was not completed in time for this report; there are, however, preliminary results.

When these electrodes are allowed to dry overnight, the laminate with the lowest molecular weight binder ends up with a thin layer of binder and conductive carbon on the surface of the laminate. It is believed that when provided a long time to dry (hours), the dense, large active material particles can settle down to the current collector, while the lighter conductive agent and binder float to the top. A higher molecular weight binder appears to inhibit this separation.

The project also found that laminates with higher molecular weight binders can be bent around smaller mandrels. Thus, higher molecular weight binders are beneficial to making thick electrodes that are to be wound to form cylindrical cells.

Since electrodes in industry are typically dried in approximately three minutes (based on a coating speed of 30 m/min and a drying length of 100 m), the project believes it is imperative to perform studies on electrode uniformity and performance based on electrodes dried on the order of minutes, not hours. Development of these efforts has begun. Preliminary results indicate that electrodes with low molecular weight dry uniformly, but those of high molecular weight display large crevices where the current collector is clearly visible when looking down at the electrode. Unfortunately, thick laminates of low molecular weight binders do not possess the required properties to prevent delamination or adequate electrode bending. These results suggest that an optimization of the binder content and molecular weight may be important; thus, the project would like to assess electrodes made from a combination of binders of different molecular weights.

Task 1.2 – Prelithiation of Silicon Anode for High-Energy Lithium-Ion Batteries (Yi Cui, Stanford University)

Project Objective. Prelithiation of high-capacity electrode materials such as silicon is an important means to enable those materials in high-energy batteries. This study pursues two main directions: (1) developing facile and practical methods to increase first-cycle Coulombic efficiency (CE) of Li-ion batteries, and (2) synthesizing fully lithiated silicon and other lithium compounds for pre-storing lithium.

Project Impact. The first-cycle CE of Li-ion batteries will be increased dramatically via prelithiation. Prelithiation of high-capacity electrode materials will enable those materials in next generation, high-energy-density batteries. This project's success will make high-energy-density Li-ion batteries for EVs.

Out-Year Goals. Compounds containing a large quantity of lithium will be synthesized for pre-storing lithium ions inside batteries. First-cycle CE will be improved and optimized (over 95%) by prelithiation with the synthesized Li-rich compounds. The stability of prelithiation reagents in the air conditions and in solvents will be improved.

Collaborations. This project collaborates with BMR PIs, with Dr. Michael Toney at Stanford Linear Accelerator Center (SLAC) on *in situ* X-ray, and with Prof. Nix at Stanford University on mechanics.

Milestones

1. Synthesize Li_xSn nanoparticles and $\text{Li}_x\text{Sn-Li}_2\text{O}$ composites for anode prelithiation with improved air stability. (Q2 – Completed April 15, 2017)
2. Synthesize LiF-coated Li_xSi nanoparticles with improved stability in ambient air and polar solvents. (Q3 – Completed July 2017)
3. Fabricate air-stable and free-standing Li_xSi /graphene foil as an alternative to Li-metal anodes. (Q4 – Completion in November 2017)

Progress Report

Substantial improvements on energy density of Li-ion batteries require development of high-capacity electrodes. Alloy anodes, with much higher capacity, have been recognized as promising alternatives to graphites. Here, the project develops a Li-containing anode as an alternative to lithium metal, inheriting the desirable properties of alloy anodes and pure metal anodes. This large-scale, freestanding, Li_xSi /graphene foil consists of fine nanostructures of densely-packed Li_xSi nanoparticles (NPs) encapsulated by large graphene sheets. Li_xSi NPs were mixed with graphene sheets and polystyrene-butadiene rubber (SBR) (80:10:10 by weight) in toluene to form a slurry, which was then cast on a polyethylene terephthalate (PET) release film, where, upon drying, a freestanding film is formed. The photograph (Figure 1a) shows a large Li_xSi /graphene foil with 8-cm width and 24-cm length. The right side of the foil is rolled around a thin tube to illustrate its flexibility. The superior mechanical properties of the Li_xSi /graphene foil are further demonstrated by the uniaxial tensile test, which shows a similar trend to a Li-metal foil of much higher stress (Figure 1d). The graphene sheets were prepared by exfoliation of graphite with the assistance of a metal halide. A transmission electron microscopy (TEM) image with low magnification (Figure 1b) shows overlapped and interconnected graphene sheets with size up to several microns. A double-layer graphene sheet is clearly observed in Figure 1c, with an average inter-layer distance of 0.334 nm, as indicated by the inset. The X-ray diffraction (XRD) pattern (Figure 1e) of the Li_xSi /graphene foil contains peaks of $\text{Li}_{22}\text{Si}_5$ (PDF# 01-077-2882), graphitic carbon (PDF# 00-056-0159), and Li_2O (PDF# 04-008-3420). Li_xSi NPs are identifiable underneath the thin graphene sheet (Figure 1f). Li_xSi alloy is already in its fully-expanded state, so no void space is required to accommodate the volume expansion of the silicon. Accordingly, Li_xSi /graphene foil is ready to be thoroughly calendared without damaging its microstructure. After calendaring under a large stress of 40 MPa, Li_xSi NPs are in a densely-packed state, as illustrated in the cross-sectional view of the scanning electron microscopy (SEM) image (Figure 1g). With fully-expanded Li_xSi confined in the highly-conductive, chemically-stable graphene matrix, this foil maintains a stable structure and cyclability in half cells. The Li_xSi /graphene foil is successfully paired with high-capacity Li-free cathodes, such as V_2O_5 or sulfur, to achieve stable, full-cell cycling. The Li_xSi /graphene foil is stable in air because of its unique structure and the hydrophobicity and gas impermeability of graphene sheets.

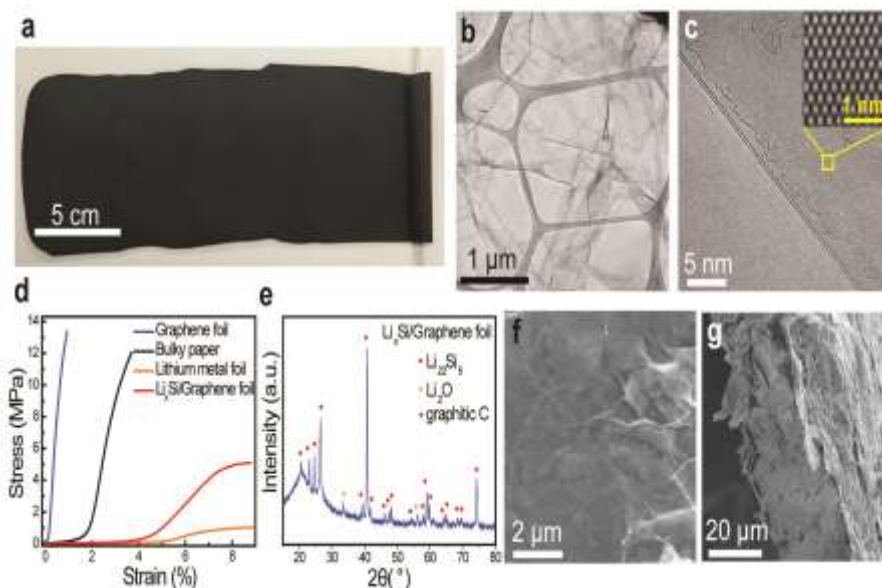


Figure 1. Characterizations of the Li_xSi /graphene foil. (a) Photograph of large Li_xSi /graphene foil with 8-cm width and 24-cm length. The right side of the foil is rolled around a thin tube to illustrate good flexibility. (b) Low-magnification transmission electron microscopy (TEM) image of the overlapped and interconnected graphene sheets. (c) TEM image shows a double-layer graphene sheet with the inter-layer distance of 0.334 nm. The inset is the atomic resolution image of the graphene sheet. (d) Uniaxial tensile test of the graphene foil (blue), bulky paper (black), Li-metal foil (orange), and Li_xSi /graphene foil (red). (e) X-ray diffraction pattern reveals the highly crystalline nature of graphitic carbon and $\text{Li}_{22}\text{Si}_5$. (f) Top-view and (g) cross-sectional view of scanning electron microscopy images of the Li_xSi /graphene foil.

Patents/Publications/Presentations

Publication

- Zhao, J., and G. Zhou, K. Yan, J. Xie, Y. Li, L. Liao, Y. Jin, K. Liu, P.-C. Hsu, J. Wang, H.-M. Cheng, and Y. Cui. “Air-Stable and Freestanding Lithium Alloy/Graphene Foil as an Alternative to Lithium Metal Anodes.” *Nat. Nanotech.* 12 (2017): 993.

Task 1.3 – Electrode Architecture-Assembly of Battery Materials and Electrodes (Karim Zaghib, Hydro-Quebec)

Project Objective. The project goal is to develop an electrode architecture based on nano-Si materials and to design a full cell having high energy density and long cycle life. To achieve the objective, this project investigates the structure of nano-Si materials that provide acceptable volume change to achieve long cycle life, while still maintaining the high-capacity performance of silicon. The project scope includes control of the particle size distribution of nano-Si materials, crystallinity, silicon composition, and the surface chemistry of nano-Si materials. The focus is to develop electrode formulations and electrode architectures based on nano-Si materials, which require optimized nano-Si/C composites and functional binders, as well as a controlled pore distribution in the electrode and the related process conditions to fabricate the electrode.

Project Impact. Silicon is a promising alternative anode material with a capacity of ~ 4200 mAh/g, which is more than a magnitude higher than that of graphite. However, many challenges remain unresolved, inhibiting commercialization of silicon; this is mainly due to the large volume variations of silicon during charge/discharge cycles that result in pulverization of the particle and poor cycling stability. Successful development of highly reversible silicon electrodes with acceptable cost will lead to higher-energy-density and lower-cost batteries that are in high demand, especially for expanding the market penetration for EVs.

Approach. The project approach will encompass the following:

- Explore synthesis methods for low-cost, nano-Si materials with controlled purity and particle morphology.
- Develop an appropriate silicon anode architecture that can tolerate volumetric expansion and provide an acceptable cycle life with low capacity fade.
- Identify a binder and electrode composition by investigating parameters that define the electrode structure, such as porosity, loading, and electrode density. The optimized Si-anode will be matched with a high-voltage NMC cathode to fabricate large-format Li-ion cells.
- Use *in situ* techniques such as SEM and impedance spectroscopy to monitor the particle and electrode environment changes during cycling.
- Achieve reduced cost by moving from silicon (> \$50/kg) to metallurgical silicon, projected to be \$3~\$5/kg.

Out-Year Goals. Conduct failure mode analysis of nano-Si anodes before and after cycling. Use dual-beam (electron + ion) microscopy and time-of-flight secondary ion mass spectrometry (TOF-SIMS) techniques to analyze residual lithium contents in the structure of delithiated anodes. This analysis will help in understanding the failure mode of the anode and help guide efforts to improve particle morphology and electrode architecture.

Collaborations. This project collaborates with BMR PIs: V. Battaglia and G. Liu (LBNL), C. Wong and Jason Zhang (Pacific Northwest National Laboratory, PNNL), and J. Goodenough (University of Texas, UT).

Milestones

1. Failure mode analysis of the nano-Si/C composite electrode before and after cycling. Improve the structure of the nano-Si/C composite based on the result of failure mode analysis. (Q1 – Completed December 2016)
2. Explore new binder system with nano-Si/C composite; make composite with electrospinning process. (Complete)
3. Optimize electrode composition with nano-Si/C composite; evaluate electrochemical performance. (Complete)
4. Verify performance in pouch-type full cell. *Deliverable:* 20g of nano-Si/C composite powder. (Deliverable completed; cell test is under way)

Progress Report

This quarter, Hydro-Quebec focused on optimizing the composition of a nano-Si/C composite electrode with different types of carbon additive. In previous efforts, the team produced micro-size nano-Si/C composites via an electrospray process. Based on these results, the project explored methods to make a more stable nano-Si/C composite.

The powder was produced by the same procedure, a water bath, as reported previously. In version 1, the composite electrode was composed of nano-Si, acetylene black, and a polyimide binder. In version 2, carbon fibers are added to the formulation. Figure 2a shows an SEM image of version 1; the powder is well mixed with carbon, but appears less compact and somewhat fractured. On the other hand, version 2 in Figure 1b appears strong and continuous.

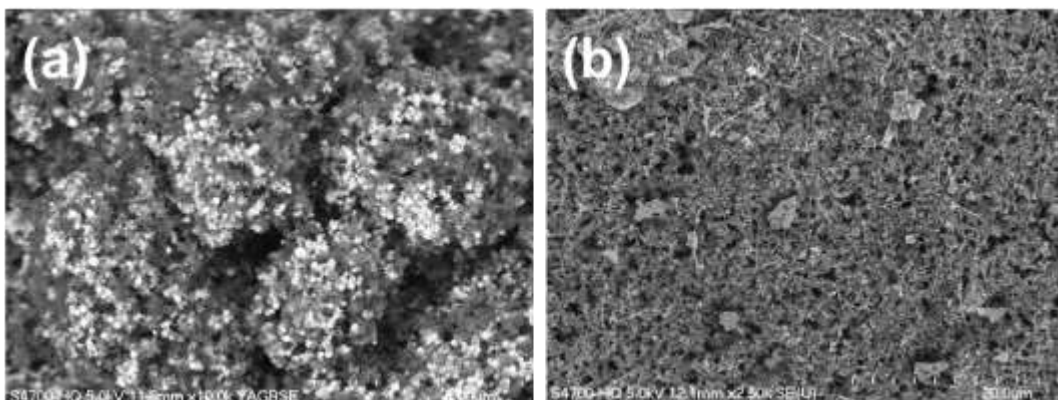


Figure 2. Scanning electron microscopy image of (a) version 1 nano-Si/C composite made by electrospray process and (b) version 2.

The electrochemical performance was tested with a coin-type half-cell with results provided in Figure 3. The total loading of the anode was around 1 mg/cm^2 (1 mAh/cm^2). The cells are cycled at a C/6 rate for charge and discharge. The composite version 2 that contains carbon fiber showed more stable capacity than that of version 1 after more than 100 cycles. In addition, the CE of the cell containing composite version 2 was higher. After *ca.* 50 cycles, the cell with composite version 1 showed decreasing efficiency, whereas the cell with composite version 2 continued to improve in efficiency. This behavior is attributed to the presence of the carbon fiber network in the anode material. The project will continue evaluating the full cell performance next quarter.

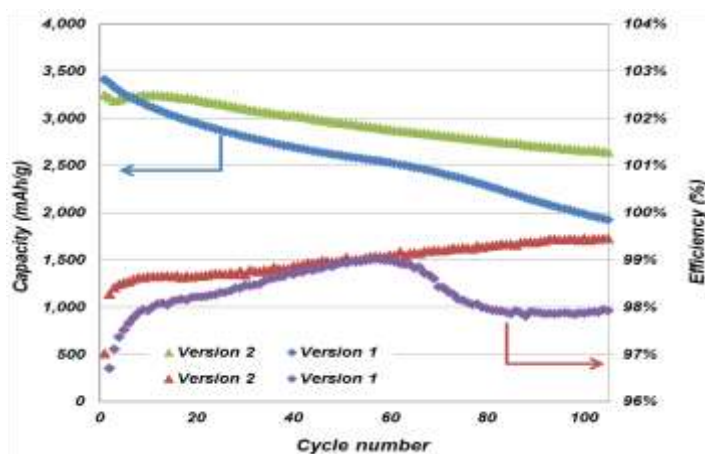


Figure 3. Cell performance during cycling at C/6 rate between 1.5 V and 0.005 V at room temperature.

Task 2 – Silicon Anode Research

Summary and Highlights

Most Li-ion batteries used in state-of-the-art EVs contain graphite as their anode material. Limited capacity of graphite (LiC_6 , 372 mAh/g) is one barrier that prevents the long-range operation of EVs required by the EV Everywhere Grand Challenge proposed by the DOE Office of Energy Efficiency & Renewable Energy (EERE). In this regard, silicon is one of the most promising candidates as an alternative anode for Li-ion battery applications. Silicon is environmentally benign and ubiquitous. The theoretical specific capacity of silicon is 4212 mAh/g ($\text{Li}_{21}\text{Si}_5$), which is 10 times greater than the specific capacity of graphite. However, the high specific capacity of silicon is associated with large volume changes (more than 300 percent) when alloyed with lithium. These extreme volume changes can cause severe cracking and disintegration of the electrode and can lead to significant capacity loss.

Substantial scientific research has been conducted to circumvent the deterioration of Si-based anode materials during cycling. Various strategies, such as reduction of particle size, generation of active/inactive composites, fabrication of Si-based thin films, use of alternative binders, and synthesis of one-dimensional silicon nanostructures, have been implemented by several research groups. Fundamental mechanistic research also has been performed to better understand the electrochemical lithiation and delithiation processes during cycling in terms of crystal structure, phase transitions, morphological changes, and reaction kinetics. Although significant progress has been made on developing Si-based anodes, many obstacles still prevent their practical application. Long-term cycling stability remains the foremost challenge for Si-based anode, especially for the high loading electrode ($> 3\text{mAh/cm}^2$) required for many practical applications. The cyclability of full cells using Si-based anodes is also complicated by multiple factors, such as diffusion-induced stress and fracture, loss of electrical contact among silicon particles and between silicon and current collector, and the breakdown of solid electrolyte interphase (SEI) layers during volume expansion/contraction processes. The design and engineering of a full cell with a Si-based anode still needs to be optimized. Critical research remaining in this area includes, but is not limited to, the following:

- Low-cost manufacturing processes must be found to produce nanostructured silicon with the desired properties.
- The effects of SEI formation and stability on the cyclability of Si-based anodes need to be further investigated. Electrolytes and additives that can produce a stable SEI layer need to be developed.
- A better binder and a conductive matrix need to be developed. They should provide flexible but stable electrical contacts among silicon particles and between particles and the current collector under repeated volume changes during charge/discharge processes.
- The performances of full cells using Si-based anode need to be investigated and optimized.

The main goal is to have a fundamental understanding on the failure mechanism on Si-based anode and improve its long-term stability, especially for thick electrode operated at full-cell conditions. Success of this project will enable Li-ion batteries with a specific energy of $> 350\text{ Wh/kg}$ (in cell level), 1000 deep-discharge cycles, 15-year calendar life, and less than 20% capacity fade over a 10-year period to meet the goal of the EV Everywhere Grand Challenge.

Task 2.1 –High-Capacity and Long Cycle Life Silicon-Carbon Composite Materials and Electrodes (Gao Liu, Lawrence Berkeley National Laboratory)

Project Objective. This project will synthesize Si/C anode composite materials at 1000 mAh/g capacity at a cost less than \$10/kg and fabricate a long-cycle-life electrode similar to a graphite electrode for high-energy-density Li-ion batteries.

Project Impact. Low energy density and limited lifetime are two major drawbacks of the automobile Li-ion batteries for EV and plug-in hybrid electric vehicle (PHEV) applications. The project will develop high-capacity and long-life Si/C composite anodes to prolong battery cycling and storage lifetime, and to provide an in-depth understanding of silicon electrode design strategies to stabilize silicon material volume change and to prevent surface side reactions. This research effort will generate new intellectual properties based on the fundamental discovery of novel materials and new synthesis processes, and will bridge the research and development (R&D) gaps between the fundamental research and the applied materials discovery, to pave the way for the successful commercialization of silicon materials in the United States.

Approach. This work combines novel materials design and innovative synthesis process to synthesize mechanically robust and dimensionally stable Si/C composite materials. In addition, it will use low-cost Si/C precursor materials and a scalable process to generate low-cost Si/C product.

Out-Year Goals. The work progresses toward study of the physical and chemical properties and of electrochemical properties of the low-cost precursor materials. Novel synthesis strategy will be developed and used to fabricate materials to tailor the morphology, structure, composite component, and electrochemical properties of the Si/C composite materials. The morphologic and structural features and electrochemical properties will be characterized for the as-prepared Si/C composited with functional binder during electrochemical testing. The goal is to achieve a high-capacity, long-life Li-ion battery using this Si/C composite anode.

Collaborations. This project is a single investigator project. However, the proposed work requires extensive collaboration with DOE user facilities at national laboratories and industries. These include the National Center for Electron Microscopy (NCEM) and the Advanced Light Sources (ALS) program at LBNL, *in situ* electrochemical TEM facilities at the Environmental Molecular Sciences Laboratory (EMSL), the national user facility at PNNL, HQ's Research Institute (IREQ), General Motors (GM) R&D Center, and LBNL BMR laboratories. The project will also involve collaboration with BMR participants at LBNL, including Dr. Marca Doeff's group and Dr. Vince Battaglia's group.

Milestones

1. Set up the silicon materials and carbon precursors library, and finish characterizing the starting materials. (Q1 – Completed December 2016)
2. Conduct preliminary tests to generate Si/C composite particles with the spray methods. (Q2 – Completed March 2017)
3. Electron microscopy image analyses of the Si/C samples, and development of functional binders based on Si/C composite structures. (Q3 – Completed June 2017)
4. Electrochemical analysis to demonstrate > 1000 mAh/g and > 3 mAh/cm² of the Si/C composite electrodes. (Q4 – Completed September 2017)

Progress Report

To obtain the structural information about the (SiO-Polypyrrole (PPy)-Temperature) composite, Raman spectroscopy is utilized. The two prominent peaks at 1340cm^{-1} and 1605cm^{-1} correspond to the D band and G band, respectively. The intensities of D and G band decrease with the increase of sintering temperature. The I_D/I_G ratios are 0.645, 0.580, and 0.561 for SiO-PPy-400, 500, and 600, respectively, indicating the graphitic degree increase with pyrolysis temperature of PPy polymer.

Galvanostatic charge–discharge curves of the SiO-PPy anode were obtained with the voltage window of 0.01 and 1.0 V versus Li/Li^+ (Figure 5). The first-cycle CE is around 65%. The irreversible capacity possibly attributed to the formation of SEI passivation film due to the irreversible reaction with electrolyte and chemical transformation of SiO. Figure 5a shows the rate performance. The SiO-PPy-500 delivers a capacity of 1127mAh g^{-1} at the rate of 0.1 C, and then gradually decreases to 649mAh g^{-1} at the rate of 0.5 C, to 487mAh g^{-1} at the rate of 1 C. The results show that the SiO-PPy-500 displays the most excellent rate performance with a stable cycling behavior at different current densities. The CE of SiO-PPy-500 is the best at both first cycles and subsequent cycles. The cycling performance of the anode measured at C/10 rate and C/3 rate are reported (Figure 5b-c). The specific capacity of the pure SiO electrode after 200 charge/discharge cycles is 534mAh g^{-1} with capacity retention of 65%. These results clearly show that SiO-PPy-500 has the best electrochemical performance and the sintering temperature plays an important role in affecting the structure of the coating layers. In Figure 5d, SiO-PPy-500 demonstrates a rapid increase of CE to 99.5% after only 5 cycles, including the first formation cycle, and stability in the rest cycles. The enhanced CE of SiO-PPy-500 samples is due to the graphitic carbon coatings from the PPy precursor.

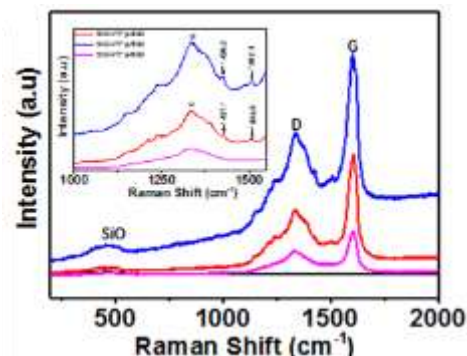


Figure 4. The Raman and X-ray diffraction spectra of pure SiO and SiO-PPy sintered at different temperature.

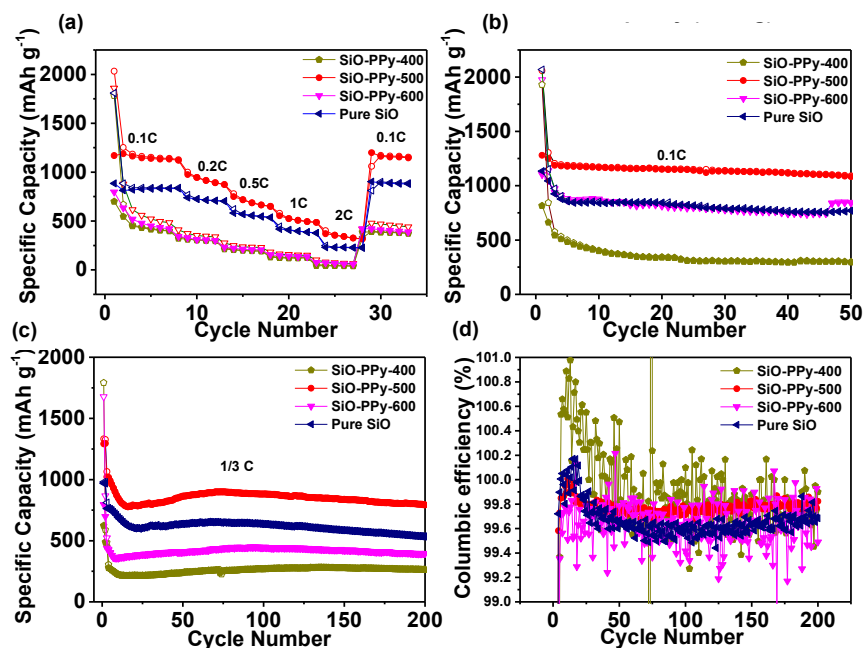


Figure 5. (a) The rate capabilities of pure SiO and SiO-PPy sintering at different temperature. (b) Cycling performance at C/10. (c) Cycling performance at C/3. (d) Coulombic efficiency for pure SiO and SiO-PPy samples.

Task 2.2 – Stable Operation of Silicon-Based Anode for Lithium-Ion Batteries (Ji-Guang Zhang and Jun Liu, Pacific Northwest National Laboratory; Prashant Kumta, University of Pittsburgh)

Project Objective. The project objective is to develop a low-cost approach to prepare high-capacity Si-carbon composite anodes with good cycle stability and rate capability to replace graphite anode used in Li-ion batteries. In one approach, low-cost Si-graphite-carbon composite will be developed to improve the long-term cycling performance while maintaining a reasonably high capacity. Si-based secondary particles with a nano-Si content of ~ 10 to 15 wt% will be embedded in the matrix of active graphite and inactive conductive carbon materials. Controlled void space will be pre-created to accommodate the volume change of silicon. A layer of highly graphitized carbon coating on the outside will be developed to minimize the contact between silicon and electrolyte and hence minimize the electrolyte decomposition. New electrolyte additives will be investigated to improve stability of the SEI layer. In another approach, nanoscale silicon and Li-ion conducting lithium oxide composites will be prepared by *in situ* chemical reduction methods. The stability of Si-based anode will be improved by generating the desired nanocomposites containing nanostructured amorphous or nanocrystalline silicon as well as amorphous or crystalline lithium oxide (Si+Li₂O) by the direct chemical reduction of a mixture and variety of silicon sub oxides (SiO and SiO_x) and/or dioxides. Different synthesis approaches comprising direct chemical reduction using solution, solid-state, and liquid-vapor phase methods will be utilized to generate the Si+Li₂O nanocomposites. The electrode structures will be modified to enable high utilization of thick electrode.

Project Impact. Si-based anodes have much larger specific capacities compared with conventional graphite anodes. However, the cyclability of Si-based anodes is limited because of the large volume expansion that is characteristic of these anodes. This work will develop a low-cost approach to extend the cycle life of high-capacity, Si-based anodes. The success of this work will further increase the energy density of Li-ion batteries and accelerate market acceptance of EVs, especially for PHEVs required by the EV Everywhere Grand Challenge.

Out-Year Goals. The main goal of the proposed work is to enable Li-ion batteries with a specific energy of > 200 Wh/kg (in cell level for PHEVs), 5000 deep-discharge cycles, 15-year calendar life, improved abuse tolerance, and less than 20% capacity fade over a 10-year period.

Collaborations. This project collaborates with Xingcheng Xiao (GM): *In situ* measurement of thickness swelling silicon anode.

Milestones

1. Synthesize micron-sized silicon with the desired porosity and *in situ* grown graphene coating. (Q1 – Completed December 2016)
2. Synthesize low-cost Si-based nanocomposite anode materials using high-energy mechanical milling (HEMM) and other economical template derived methods. (Q2 – Completed March 2017)
3. Identify new electrolyte additive to improve the stable operation of Si-based anode. (Q3 – Completed June 2017)
4. Fabricate and characterize Si-based anode with desired electrode capacity (~ 3 mAh/cm²). (Q4 – Completed September 2017)

Progress Report

This quarter, two types of micrometer-sized silicon anode materials were prepared and characterized, including porous Si/C from Mg-reduction of SiO₂ and the hierarchical structured Si/MWNT composite. In the case of porous Si/C anode, the preserved void space and the highly graphitic carbon enable good stability of the whole structure and low overall resistance, thus resulting in an enhanced cycle life and rate capability. High capacity (~ 1467 mAhg⁻¹ at 1C), long-term cycle life (200 cycles with 90% capacity retention), and high-rate capability (~ 650 mAh g⁻¹ at 5C) have been achieved. These results are much superior to nanometer-sized silicon, as shown in Figure 6. The areal capacity of the p-Si/C electrodes was ~ 1 mAh/cm².

For the hierarchical structured Si/MWNT composite anode, the unique structure and the MWNT backbone are expected to have appropriate designed void space to accommodate the volume expansion and to improve the electrical and mechanical property. As a result, the material provides the following: (1) enough void space to accommodate the volume change so that the swelling of the composite can be reduced to ~ 30%, which is only 1/10th of bulk silicon; (2) good mechanical structure and electronic conductivity; and (3) good electrochemical performance with a reversible capacity of 1290 mAh g⁻¹ at 1C and capacity retention of 87% after 300 cycles (Figure 7).

In another approach, silicon nanoparticles and nanocomposites (Si/carbon nanofiber, Si/metal oxide) have been synthesized using high throughput high energy mechanochemical reduction of SiO with different inorganic reducing agents. A commercial, water-soluble, template-based approach has been developed to incorporate silicon nanoparticles in a porous metallic conducting foam to maintain the electrical continuity and achieve high loading densities (5-10 mg/cm²) with the pores providing free space to counter the volume expansion of silicon electrode. The SEM image of the cross section of the nanocomposite foam shows completely interconnected porosity with pores replacing the sacrificial template upon dissolution from the pre-foamed compact. The porous nanocomposites were tested in anodes without any additives (binder, conductive C) in Li/Li⁺ coin cells at different current rates in 1M LiPF₆ EC:DEC:FEC (ethylene carbonate : diethyl carbonate : fluoroethylene carbonate) (45:45:10% Vol.) in the voltage window of 0.01–1.2 V. The electrodes show a first-cycle discharge and charge capacity of ~ 2970 mAh/g and ~ 1940 mAh/g, respectively, with a first-cycle irreversible (FIR) loss of ~ 30-45% (Figure 8) at a charge/discharge current rate of ~ 50 mA/g. The obtained porous nano-Si/conducting foam shows good capacity retention with a stable capacity of ~ 1025 mAh/g (~ 4 mAh/cm²) at the end of 55 cycles at 500 mA/g (Figure 8). The formation of the SEI layer on the nano-Si contributes to the FIR loss. Efforts are under way to incorporate nanoSi-carbon nanofibers (CNFs) as the active system. Furthermore, post cycling SEM analysis of these electrodes in lithiated/delithiated state is in progress to quantitatively analyze the overall volume changes of the electrode in Li/Li⁺ system.

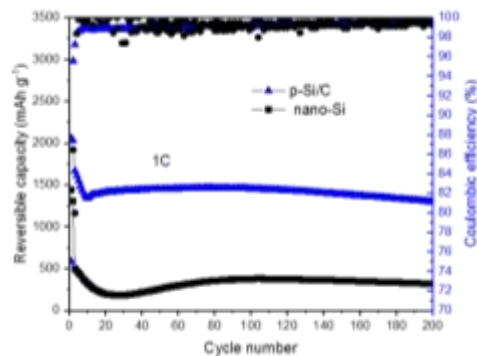


Figure 6. Cycling stability of p-Si/C and nano-Si electrodes.

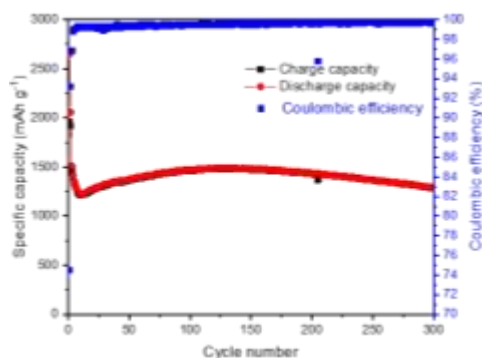


Figure 7. Cycling stability of Si/MWNT/C electrode.

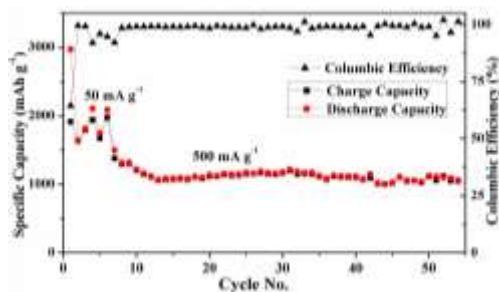


Figure 8. Long-term cycling data of nano-Si conducting foam tested at 50 mA/g for initial 6 cycles followed by 0.5A/g in Li/Li⁺ system.

Patents/Publications/Presentations

Publication

- Gattu, B., and P. H. Jampani, M. K. Datta, and P. N. Kumta. “Water-soluble Template Derived Nanoscale Silicon Nano-Flakes and Nano-Rods Morphologies: Stable Architectures for Lithium Ion Anodes.” *Nanoresearch* (2017).

Presentation

- 232nd Electrochemical Society (ECS) Meeting, National Harbor, Maryland (October 1–5, 2017): “CNT/Cu Electrodes: A Versatile Platform for High Performance Silicon and Sulfur Based Binder Free Electrodes in Li-Ion Battery”; B. Gattu, R. Kuruba, M. K. Datta, P. H. Jampani, P. Shanti, and P. N. Kumta.

TASK 3 – HIGH-ENERGY-DENSITY CATHODES FOR ADVANCED LITHIUM-ION BATTERIES

Summary and Highlights

Development of high-energy-density, low-cost, thermally stable, and environmentally safe electrode materials is a key enabler for advanced batteries for transportation. High energy density is synonymous with reducing cost per unit weight or volume. Currently, one major technical barrier toward development of high-energy-density Li-ion batteries is the lack of robust, high-capacity cathodes. As an example, the most commonly used anode material for Li-ion batteries is graphitic carbon, which has a specific capacity of 372 mAh/g, while even the most advanced cathodes such as NMC or NCA have a maximum capacity of ~ 180 mAh/g. This indicates an immediate need to develop high-capacity (and high-voltage) cathodes that have stable reversible capacities > 250 mAh/g. High volumetric energy density is also critical for transportation application. Alternative high-capacity cathodes such as those based on conversion compounds, Li-S, and metal-air chemistries still have fundamental issues that need to be addressed. Among oxide cathodes, Li-excess NMC and other cation disorder compositions provide a practical route toward high capacity at high redox voltage. Successful demonstration of practical high-energy cathodes will enable devices that meet or exceed the DOE cell level targets of 400 Wh/kg and 750 Wh/L with a system-level cost target of \$125/kWh.

During the last decade, many high-voltage cathode chemistries were developed under the BATT (now BMR) program including Li-rich NMC and Ni-Mn spinels. Current efforts are directed toward new synthesis methods and modifications for high-capacity, Ni-rich NMC to improve their structural and oxidative stability at higher voltage [Zhang, PNNL; Doeff & Tong, LBNL; Wang, Brookhaven National Laboratory (BNL)]. Thackeray and Croy's effort at Argonne National Laboratory (ANL) is focused on synthesis of composite layered-layered (LL) and layered-spinel (LS) high-voltage cathodes including Co- and Ni-based spinel phases. Nanda's effort at Oak Ridge National Laboratory (ORNL) is directed toward synthesis and stabilization of Li-excess disordered cathodes based on nickel, copper, molybdenum, chromium, and manganese. Whittingham's efforts at State University of New York (SUNY) at Binghamton are directed at high volumetric energy density Sn/Li_xVOPO₄ full cells and performance optimization.

Highlights. The highlights for this quarter are as follows:

- **Task 3.1.** Sputter deposited thin-film Li₂MoO₃ electrodes showed comparable electrochemical performance with respect to composite slurry Li₂MoO₃ synthesized from solid-state method.
- **Task 3.2.** Achieved CE of > 99% for Sn_yFe/Li_xVOPO₄ full cells by modifying the cycling protocol.
- **Task 3.3.** Improved interfacial stability of Ni-rich NMC cathode; that is, LiNi_{0.76}Mn_{0.14}Co_{0.10}O₂ has been further enhanced by using an optimized electrolyte composed of 0.6 M LiTFSI, 0.4 M LiBOB, and 0.05 M LiPF₆ in EC-EMC (ethyl methyl carbonate).
- **Task 3.4.** Optimized performance stoichiometric LiNi_{0.7}Mn_{0.15}Co_{0.15}O₂ with capacity up to 200 mAhg⁻¹ with excellent retention (> 84% for 50 cycles) based on *in situ/ex situ* synchrotron X-ray studies.
- **Task 3.5.** Developed wet chemical method to coat Li_xCoPO₄ on high-voltage layered-layered spinel (LLS) cathode.
- **Task 3.6.** Reported structural analysis of delithiated NMC-622 cathodes using *in situ* hot stage XRD.
- **Task 3.7.** Compared the oxygen redox participation for Li_{1.2}Ni_{0.2}Mn_{0.6}O₂ and Li_{1.2}Ni_{0.2}Ru_{0.6}O₂ cathodes using resonant inelastic X-ray scattering (RIXS).
- **Task 3.8.** Structural characterization of LCO and substituted LiCo_{1-x}Al_xO₂ (LCO-Al) samples synthesized by sol-gel reactions of metal acetates and glycolic acid at low (400°C) and intermediate temperature (600°C).

Task 3.1 – Studies on High-Capacity Cathodes for Advanced Lithium-Ion Systems (Jagjit Nanda, Oak Ridge National Laboratory)

Project Objective. The overall project goal is development of high-energy-density Li-ion battery electrodes for EV and PHEV applications that meet and/or exceed the DOE energy density and life cycle targets based on the USDRIVE/USABC roadmap. Specifically, this project aims to mitigate the technical barriers associated with high-voltage/high-capacity cathodes, including Li-rich transition metal (TM)-based oxides and multi-lithium compositions such as $\text{Li}_2\text{M}_x^{\text{I}}\text{M}_{1-x}^{\text{II}}\text{O}_2$ and $\text{Li}_2\text{M}_x^{\text{I}}\text{M}_{1-x}^{\text{II}}\text{O}_3$ where M^{I} and M^{II} are TMs that may or may not include nickel, copper, molybdenum, chromium, manganese, and/or cobalt. Major emphasis is placed on developing new materials modifications and synthetic approaches for stabilizing high-voltage cathodes to enable reversible capacities in the range of 250 mAh/g at an average nominal voltage > 3.7 V versus Li/Li⁺. Major technical barriers that will be addressed include: preventing the structural transitions during repeated electrochemical cycling; improving oxidative stability at higher redox potential by addressing interfacial stability; and reducing voltage hysteresis by improving kinetics and transport at the materials level. The cathode synthesis and optimization will utilize advanced characterization and diagnostic methods at the electrode and/or cell level for studying electrode and/or cell degradation under abuse conditions. The techniques include electrochemical impedance spectroscopy (EIS), micro-Raman spectroscopy; aberration corrected electron microscopy combined with electron energy loss spectroscopy (EELS), X-ray photoelectron spectroscopy (XPS), inductively coupled plasma (ICP) – atomic emission spectroscopy (AES), X-ray absorption near-edge spectroscopy (XANES), and X-ray and neutron diffraction.

Project Impact. Short-term and long-term deliverables are directed toward VTO Energy Storage 2015 and 2022 goals. Work involves advanced electrode couples that have cell-level energy density targets exceeding 400 Wh/kg and 700 Wh/l for 5000 cycles. Increasing energy density per unit mass or volume ultimately reduces the cost of battery packs consistent with the DOE 2022 EV Everywhere Grand Challenge goal of \$125/kWh.

Out-Year Goals. The goal is to develop new cathode materials that have high capacity, use low-cost materials, and meet the DOE road map in terms of safety and cycle life. The principal investigator (PI) has worked on improving cycle life and performance of high-capacity/high-voltage cathodes by utilizing new synthesis and interfacial approaches such as surface modification. The cathode chemistries include Li-Mn-rich NMC and multi-lithium TM oxides such as $\text{Li}_2\text{Ni}_x\text{Cu}_{1-x}\text{O}_2$ and Li_2MnO_3 . In coming years, the PI plans to improve the anionic (oxidative) stability of cathode compositions and develop new synthesis approaches to create disordered cathodes that avoid structural transformation and improve electrochemical stability. The tasks include collaborating with researchers at Stanford Synchrotron Research Laboratory (SSRL) and ALS to understand local changes in morphology, microstructure, and chemical composition under *in situ* and *ex situ* conditions.

Collaborations. This project collaborates with Johanna Weker at SSRL/SLAC on X-ray imaging and XANES; Pengfei Yan and Chongmin Wang at PNNL on electron microscopy; Feng Wang at BNL on X-ray synchrotron spectroscopy and microscopy; and Jason Croy at ANL.

Milestones

1. Synthesize Ni-rich $\text{Li}_2\text{Cu}_x\text{Ni}_{1-x}\text{O}_2$ cathodes with $x = 0.2$ and 0.3 and evaluate their high-voltage capacity and oxidative stability (> 225 mAh/g, 25 cycles). (Q1 – Completed December 2016)
2. Complete *in situ* and *ex situ* X-ray, neutron, and spectroscopic studies of Ni-rich $\text{Li}_2\text{Cu}_x\text{Ni}_{1-x}\text{O}_2$ and related high-voltage cathode compositions. (Q2 – Completed March 2017)
3. Synthesis of a particular class and composition of disordered cathodes such as Cr-substituted Li_2MoO_3 and Mo-doped NMC. (Q3 – No-go decision made)
4. Complete structural and electrochemical performance analysis of disordered cathodes— Li_2MoO_3 and Cr-substituted Li_2MoO_3 and Mo-doped NMC. (Q4 – On track)

Progress Report

Last quarter, synthesis of Cr-doped Li_2MoO_3 and Mo-doped NMC using solid-state method did not meet the expected outcome, which led to a no-go decision. The final product had impurity phases, and electrochemical performance and oxidative stability did not improve. Other synthesis routes will be carried out in fiscal year (FY) 2018 to stabilize these phases. This quarter, the project focused on preparing and characterizing Li_2MoO_3 thin-film cathodes for comparison with previous results obtained with traditional slurry-cast electrodes. Li_2MoO_3 films with thicknesses ranging from 1.0 – 1.2 μm were sputtered onto a Pt-coated Al_2O_3 substrate followed by heating at 675°C for 2 h under flowing Ar/H_2 (96/4). Figure 9a shows a cross-sectional SEM image of the resulting film, which was uniform and dense in appearance. The XRD patterns in Figure 9b demonstrate a phase-pure Li_2MoO_3 film with $R\bar{3}m$ symmetry produced; all diffraction peaks of this film could be assigned to either Li_2MoO_3 or the Pt-coated Al_2O_3 substrate.

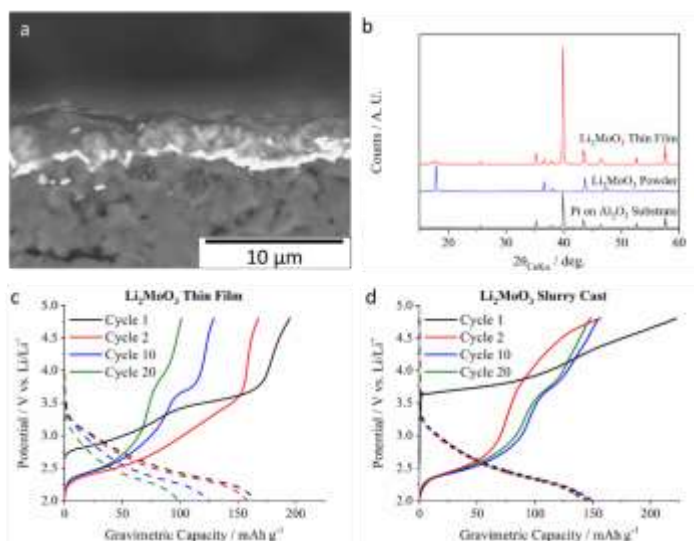


Figure 9. (a) Cross-sectional scanning electron microscopy image of a sputtered thin-film Li_2MoO_3 cathode. (b) X-ray diffraction pattern of a sputtered Li_2MoO_3 thin-film, Li_2MoO_3 powder, and the sputtering substrate (Pt on Al_2O_3). Galvanostatic charge/discharge curves for half-cells containing a (c) thin-film Li_2MoO_3 cathode and (d) slurry-cast Li_2MoO_3 cathode.

Galvanostatic charge/discharge experiments were conducted between 2.0 – 4.8 V for coin cells containing a Li_2MoO_3 thin-film cathode and a Li-metal anode. As shown in Figure 9c, the cathodes exhibited an initial charge capacity of 190 mAh/g and reversible capacity of 166 mAh/g . The voltage profile and initial capacities of the thin films are in reasonable agreement with the previous studies on slurry-cast Li_2MoO_3 cathodes (223 mAh/g and 147 mAh/g , respectively; see Figure 9d). However, while these slurry-cast electrodes demonstrated excellent cycling stability, the thin-film cathodes showed moderate capacity fade over 20 cycles. Future work on the thin-film Li_2MoO_3 cathodes will include additional synthesis and electrochemical characterization to understand the cause of this capacity fade. *In situ* Raman spectroscopy and mass spectrometry (MS) will also be performed to assess structural changes that occur during cycling, and these results will be compared with those obtained with traditional electrode structures.

Patents/Publications/Presentations

Publications

- Kan, W. H., and S. Kupan, C. Dhital, J. Nanda, A. Huq and G. Chen. “Crystal Chemistry and Electrochemistry of $\text{Li}_x\text{Mn}_{1.5}\text{Ni}_{0.5}\text{O}_4$ Solid Solution Cathode Materials.” *Chem. Mater.* 29 (2017): 6818.
- Ghadkolai, M. A., and S. Creager, J. Nanda, and R. Bordia. “Freeze Tape Cast Thick Mo-doped $\text{Li}_4\text{Ti}_5\text{O}_{12}$ Electrodes for Lithium-ion Batteries.” *J. Electrochem. Soc.* 164, no. 12 (2017): A2603.

Task 3.2 – High-Energy-Density Lithium Battery (Stanley Whittingham, SUNY Binghamton)

Project Objective. The project objective is to develop the anode and cathode materials for high-energy-density cells for use in PHEVs and EVs that offer substantially enhanced performance over current batteries used in PHEVs and with reduced cost. Specifically, the primary objectives are to:

- Increase the volumetric capacity of the anode by a factor of 1.5 over today’s carbons
 - Using a SnFeC composite conversion reaction anode.
- Increase the capacity of the cathode
 - Using a high-capacity conversion reaction cathode, CuF_2 , and/or
 - Using a high-capacity 2 lithium intercalation reaction cathode, VOPO_4 .
- Enable cells with an energy density exceeding 1 kWh/liter.

Project Impact. The volumetric energy density of today’s Li-ion batteries is limited primarily by the low volumetric capacity of the carbon anode. If the volume of the anode could be cut in half, and the capacity of the cathode to over 200 Ah/kg, then the cell energy density can be increased by over 50% to approach 1 kWh/liter (actual cell). This will increase the driving range of vehicles.

Moreover, smaller cells using lower cost manufacturing will lower the cost of tomorrow’s batteries.

Out-Year Goals. The long-term goal is to enable cells with an energy density of 1 kWh/liter. This will be accomplished by replacing both the present carbon used in Li-ion batteries with anodes that approach double the volumetric capacity of carbon, and the present intercalation cathodes with materials that significantly exceed 200 Ah/kg. By the end of this project, it is anticipated that cells will be available that can exceed the volumetric energy density of today’s Li-ion batteries by 50%.

Collaborations. The Advanced Photon Source (APS) at ANL and, when available, the National Synchrotron Light Source II (NSLS-II) at BNL will be used to determine the phases formed in both *ex situ* and *operando* electrochemical cells. The University of Colorado at Boulder and University of Michigan will provide some of the electrolytes to be used.

Milestones

1. Determine cyclability of $\text{Sn/Li}_x\text{VOPO}_4$. (Q1 – Completed December 2016)
2. Demonstrate cyclability of Sn/CuF_2 . (Q2 – Continuing)
3. Choose optimum couple. (Q3 – Completed June 2017)
4. Supply cells to the DOE. (Q4 – Continuing)

Progress Report

The project goal is to synthesize Sn-based anodes that have 1.5 times the volumetric capacity of the present carbons, and conversion and intercalation cathodes with capacities over 200 Ah/kg. The major efforts this fourth quarter were to optimize performance of the most promising $\text{Sn}_y\text{Fe}/\text{Li}_x\text{VOPO}_4$ electrochemical couple for full-cell evaluation

Milestone 3: “Choose optimum cell couple for optimization. The cells will be cycled until failure.”

$\text{Sn}_y\text{Fe}/\text{Li}_x\text{VOPO}_4$ was determined to be the most promising electrochemical couple for the full-cell study because either Li_xVOPO_4 cathode or Sn_yFe anode shows good cyclability and rate performance. The goal of 4 mAh for $\text{Sn}_y\text{Fe}/\text{Li}_x\text{VOPO}_4$ full cell has been achieved and shown in the last two quarterly reports. The main task this quarter was to optimize performance of the $\text{Sn}_y\text{Fe}/\text{Li}_x\text{VOPO}_4$ full cell.

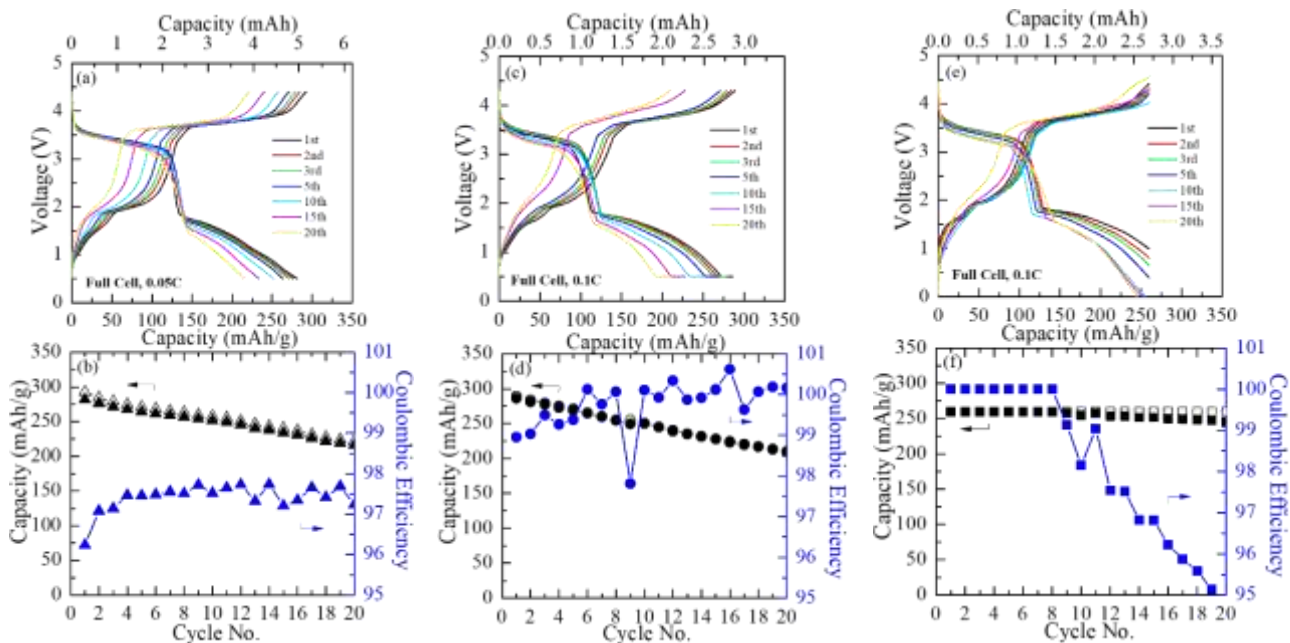


Figure 10. The cycling behaviors of $\text{Sn}_y\text{Fe}/\text{Li}_x\text{VOPO}_4$ full cells under different cycling conditions: (a-b) constant current cycling between 0.5 ~ 4.3V, (c-d) constant current and constant voltage cycling between 0.5 ~ 4.3V, and (e-f) constant capacity cycling.

With optimized Li_xVOPO_4 cathode and good capacity match of two electrodes (a little excess capacity of Sn_yFe anode), the cyclability of the $\text{Sn}_y\text{Fe}/\text{Li}_x\text{VOPO}_4$ full cell has been improved (Figure 10a-b); 80% capacity can be maintained up to 20 cycles. The observed capacity decay may be caused by the low CE of the full cell (~ 97%), which leads to a continuous lithium loss with cycling. To improve the CE, constant voltage discharge was added at the end of the constant current discharge process. This increased CE above 99% and close to 100% (Figure 10c-d). The cell was also tested using a fixed capacity. The first discharge capacity could only be maintained for a few cycles (Figure 10f) due to a voltage drift, and eventually the low voltage cut-off was reached (Figure 10e). This is in part due to both electrodes have sloping voltages. This issue will be addressed during the granted no-cost extension.

Patents/Publications/Presentations

Publication

- Zhou, Hui, and Yong Shi, Fengxia Xin, Fredrick Omenya, and M. Stanley Whittingham. “ ϵ - and β -LiVOPO₄: Phase Transformation and Electrochemistry.” *ACS Appl. Mater. & Interfaces* 9 (2017): 28537–28541. doi: 10.1021/acsami.7b07895.

Task 3.3 – Development of High-Energy Cathode Materials (Ji-Guang Zhang and Jianming Zheng, Pacific Northwest National Laboratory)

Project Objective. The project objective is to develop high-energy-density, low-cost, cathode materials with long cycle life. The previous investigation demonstrates that synthesis condition, synthesis approach, and surface modification have significant effects on performances of high-voltage spinel and LMR-NCM cathodes. These valuable understandings will be used to guide development of high-energy-density, enhanced long-term cycling stability of Ni-rich $\text{LiNi}_x\text{Mn}_y\text{Co}_z\text{O}_2$ (NMC) cathode materials that can deliver a high discharge capacity with long-term cycling stability.

Project Impact. Although state-of-the-art layered structure cathode materials, such as $\text{LiNi}_{1/3}\text{Mn}_{1/3}\text{Co}_{1/3}\text{O}_2$ and $\text{LiNi}_{0.4}\text{Mn}_{0.4}\text{Co}_{0.2}\text{O}_2$, have relatively good cycling stability at charge to 4.3 V, their energy densities need to be further improved to meet the requirements of EVs. This work focuses on the two closely integrated parts: (1) develop the high-energy-density NMC layered cathode materials for Li-ion batteries; and (2) characterize the structural properties of the NMC materials by various diagnostic techniques including scanning transmission electron microscopy (STEM)/EELS, energy-dispersive X-ray (EDX) mapping and SIMS, and then correlate with the first part. The success of this work will increase energy density of Li-ion batteries and accelerate market acceptance of EVs, especially for PHEVs required by the EV Everywhere Grand Challenge.

Approach. In FY 2016, the compositions of NMC cathode materials and the charge cutoff voltage were optimized. Ni-rich NMC cathode materials with initial discharge capacity higher than 200 mAh g^{-1} and capacity retention of 90% after 100 cycles were successfully achieved. However, the long-term cycling stability is still unsatisfactory and requires further improvement. In FY 2017, several strategies will be carried out to further enhance the long-term cycling stability as well as the thermal stability of NMC cathode materials, including (1) cationic/anionic lattice doping; (2) surface modification; and/or (3) introduction of effective electrolyte formulas/additives.

Out-Year Goals. The long-term goal of the proposed work is to enable Li-ion batteries with a specific energy of $> 96 \text{ Wh kg}^{-1}$ (for PHEVs), 5000 deep-discharge cycles, 15-year calendar life, improved abuse tolerance, and less than 20% capacity fade over a 10-year period.

Collaborations. This project engages with the following collaborators:

- Prof. Andy Sun (Western University) – atomic layer deposition (ALD) coating,
- Dr. Bryant Polzin (ANL) – NMC electrode supply,
- Dr. X. Q. Yang (BNL) – *in situ* XRD characterization during cycling, and
- Dr. Kang Xu (U.S. Army Research Laboratory, ARL) – new electrolyte.

Milestones

1. Complete lattice doping to enhance cycling stability of NMC at high charge cutoff voltages, and identify the effect of dopants in NMC during cycling using quantitative atomic level mapping. (Q1 – Completed December 2016)
2. Identify appropriate solvents for surface modification of NMC, and reveal the structural changes of different NMC materials after wash with water. (Q2 – Completed March 2017)
3. Complete surface modification to enhance the cycling stability of NMC at high charge cutoff voltages. (Q3 – Completed June 2017)
4. Achieve NMC performance improvement of 200 mAh g^{-1} and 80% capacity retention after 200 cycles. (Q4 – Completed September 2017)

Progress Report

This quarter's milestone was completed. The surface structural/interfacial stability of a Ni-rich NMC cathode, (that is, $\text{LiNi}_{0.76}\text{Mn}_{0.14}\text{Co}_{0.10}\text{O}_2$) has been further enhanced by using an optimized electrolyte (E-optimized) composed of 0.6 M LiTFSI, 0.4 M LiBOB, and 0.05 M LiPF₆ in EC-EMC carbonate mixtures, leading to significantly enhanced electrochemical performances.

The electrochemical performance data showed that, in E-optimized, the Ni-rich $\text{LiNi}_{0.76}\text{Mn}_{0.14}\text{Co}_{0.10}\text{O}_2$ was able to deliver an initial discharge capacity of 220 mAh g^{-1} and achieve 90.1% capacity retention after 200 cycles, much superior over those (213 mAh g^{-1} , 85% retention after 200 cycles) obtained in E-baseline (1M LiPF₆/EC-EMC); See Figure 11a. Meanwhile, the $\text{LiNi}_{0.76}\text{Mn}_{0.14}\text{Co}_{0.10}\text{O}_2$ retained a stable mid-point voltage during discharge, exhibiting only 0.019 V decay during the 200 cycles (Figure 11b). This value is much smaller than that (0.092 V) observed for Ni-rich NMC in E-baseline electrolyte. The advantage of using the E-optimized for Ni-rich NMC could be further evidenced by the much-improved stability of charge/discharge voltage profile as compared to that using E-baseline (Figure 11c-d).

The mechanism behind the enhanced the electrochemical performances of Ni-rich NMC using E-optimized electrolyte was systematically investigated

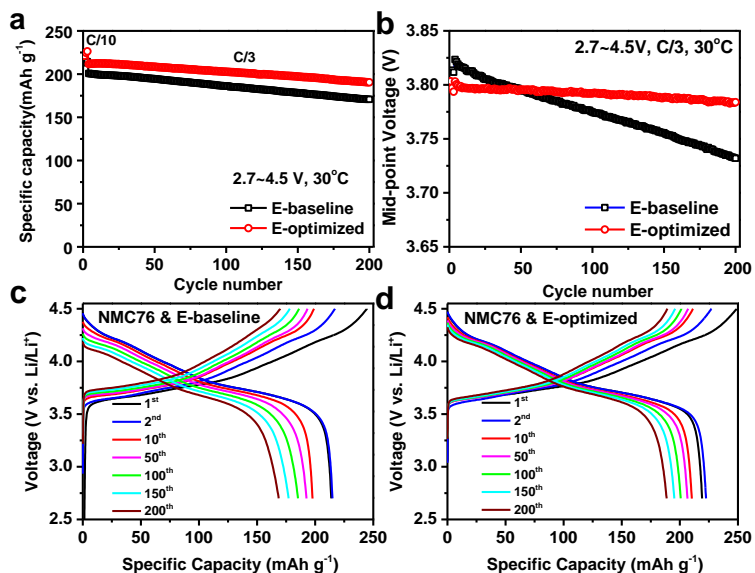


Figure 11. (a) Cycling performance, (b) discharge mid-point voltage versus cycle number of Ni-rich $\text{LiNi}_{0.76}\text{Mn}_{0.14}\text{Co}_{0.10}\text{O}_2$ cathode in E-baseline and E-optimized electrolytes during cycling at C/3 (after 3 formation cycles at C/10) between 2.7~4.5 V. The corresponding charge/discharge voltage profile evolutions are shown in (c) E-baseline and (d) E-optimized.

using SEM, TEM, XPS, EIS analysis, etc. On the one hand, the E-optimized has been proved to be stable with the Li-metal anode, thereby suppressing the capacity fade resulted from the anode side. On the other hand, the E-optimized was identified to greatly enhance the surface structural stability of $\text{LiNi}_{0.76}\text{Mn}_{0.14}\text{Co}_{0.10}\text{O}_2$. Although similar particle cracking was observed in the two electrolytes, reduced corrosion and much less structural transformation (from R-3m layered to Fm-3m rock salt) were detected at the particle surface of Ni-rich NMC cycled in E-optimized (Figure 12). This improvement can be ascribed to the absence of HF acidic species that could severely etch the cathode particle surface, resulting in the phase transformation from layered to disordered rock salt phase. The enhanced surface structural/interfacial stability is the primary reason accounting for the improved capacity retention and mitigated voltage decay of Ni-rich $\text{LiNi}_{0.76}\text{Mn}_{0.14}\text{Co}_{0.10}\text{O}_2$. The results highlight the importance of maintaining the particle surface structural/interfacial stability to enable the sustainable operation of Ni-rich cathode materials for high-energy-density Li-ion batteries.

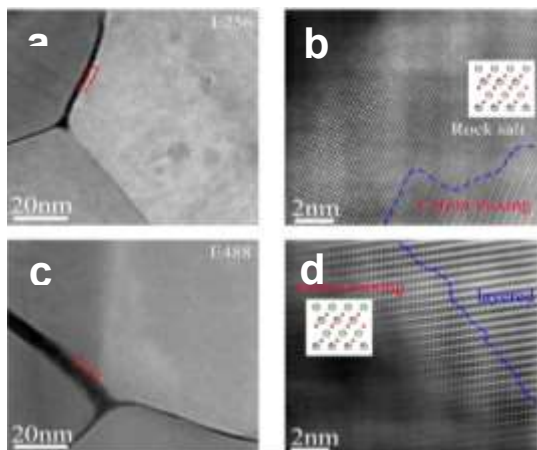


Figure 12. High-angle annular dark field – scanning transmission electron microscopy (HAADF-STEM) images of Ni-rich $\text{LiNi}_{0.76}\text{Mn}_{0.14}\text{Co}_{0.10}\text{O}_2$ after 100 cycles at C/3 between 2.7~4.5 V in (a-b) E-baseline electrolyte and (c-d) E-optimized electrolyte.

Patents/Publications/Presentations

Publication

- Zheng, Jianming, and Pengfei Yan, Jiandong Zhang, Mark Engelhard, Zihua Zhu, Bryant Polzin, Steve Trask, Jie Xiao, Chongmin Wang, and Ji-Guang Zhang. “Suppressed Oxygen Extraction and Degradation of $\text{LiNi}_x\text{Mn}_y\text{Co}_z\text{O}_2$ Cathodes at High Charge Cut-Off Voltages.” *Nano Research*. <https://doi.org/10.1007/s12274-017-1761-6>.

Task 3.4 – *In Situ* Solvothermal Synthesis of Novel High-Capacity Cathodes (Feng Wang and Jianming Bai, Brookhaven National Laboratory)

Project Objective. The goal is to develop novel high-capacity cathodes with precise control of the phase, stoichiometry, and morphology. Despite considerable interest in developing low-cost, high-energy cathodes for Li-ion batteries, designing and synthesizing new cathode materials with the desired phases and properties have proven difficult, due to complexity of the reactions involved in chemical synthesis. Building on established *in situ* capabilities/techniques for synthesizing and characterizing electrode materials, this project will undertake *in situ* studies of synthesis reactions under real conditions to identify the intermediates and to quantify the thermodynamic and kinetic parameters governing the reaction pathways. The results of such studies will enable strategies to “dial in” desired phases and properties, opening a new avenue for synthetic control of the phase, stoichiometry, and morphology during preparation of novel high-capacity cathodes.

Project Impact. Present-day Li-ion batteries are incapable of meeting the targeted miles of all-electric-range within the weight and volume constraints, as defined by the DOE in the EV Everywhere Grand Challenge. New cathodes with higher energy density are needed for Li-ion batteries so that they can be widely commercialized for plug-in electric vehicle (PEV) applications. The effort will focus on increasing energy density (while maintaining the other performance characteristics of current cathodes) using synthesis methods that have the potential to lower cost.

Out-Year Goals. This project is directed toward developing novel high-capacity cathodes, with a focus on Ni-rich layered oxides. Specifically, synthesis procedures will be developed for making LiNiO_2 and a series of Co/Mn substituted solid solutions, $\text{LiNi}_{1-x}\text{M}_x\text{O}_2$ ($\text{M} = \text{Co}, \text{Mn}$); through *in situ* studies, this project undertakes systematic investigations of the impact of synthesis conditions on the reaction pathways and cationic ordering processes toward the final layered phases. The structural and electrochemical properties of the synthesized materials will be characterized using scanning XRD, neutron scattering, TEM, EELS, and various electrochemical techniques. The primary goal is to develop a reversible cathode with an energy density of 660 Wh/kg or higher.

Collaborations. This project engages with the following collaborators: Lijun Wu and Yimei Zhu at BNL; Khalil Amine, Zonghai Chen, Yang Ren, and Chengjun Sun at ANL; Jagjit Nanda and Ashfia Huq at ORNL; Nitash Balsara, Wei Tong, and Gerbrand Ceder at LBNL; Peter Ko at Cornell High Energy Synchrotron Source; Scott Misture at Alfred University; Peter Khalifha at SUNY; and Kirsuk Kang at Seoul National University.

Milestones

1. Identify the synthesis reactions and involved structural ordering in both Ni-rich and Co-rich layered oxides through *in situ* synchrotron X-ray studies. (Q1 – Completed December 2016)
2. Develop neutron scattering-based techniques for *in situ* probing cation ordering in Ni-rich NMC layered oxides during synthesis under controlled atmosphere. (Q2 – Completed March 2017)
3. Identify synthesis procedures for kinetic control of the structural ordering in NMC layered oxides through combined *in situ/ex situ* synchrotron X-ray and neutron studies. (Q3 – Completed June 2017)
4. Complete the evaluation of synthesis conditions, specifically identifying the effect of temperature and time on the structural ordering and electrode performance of Ni-rich NMC layered cathodes. (Q4, September 2017 – Completed)

Progress Report

This quarter, the impact of synthesis conditions on the electrochemical performance of $\text{LiNi}_{0.7}\text{Mn}_{0.15}\text{Co}_{0.15}\text{O}_2$ (NMC-71515) was evaluated through *in situ* XRD, X-ray absorption spectroscopy (XAS), thermogravimetric analysis (TGA), and *ex situ* structural/electrochemical characterizations. Optimal conditions were identified and utilized to obtain stoichiometric NMC-71515 that exhibits high capacity (up to 200 mAhg^{-1}) with excellent retention ($> 84\%$ for 50 cycles).

The results from combined *in situ* XRD, XAS measurements (not shown here) and TGA analysis revealed a strong temperature dependence of the kinetics of cationic ordering in NMC-71515 because of thermal-driven oxidation of TMs and Li/O loss that concomitantly occurred during heat treatment (Figure 13a-b). In addition, particles grew quickly upon high-temperature treatment (Figure 13c). Kinetic control of the cationic ordering and morphology, via finely tuning heating temperature and holding time, was found to be crucial to optimizing the electrochemical performance of the final products.

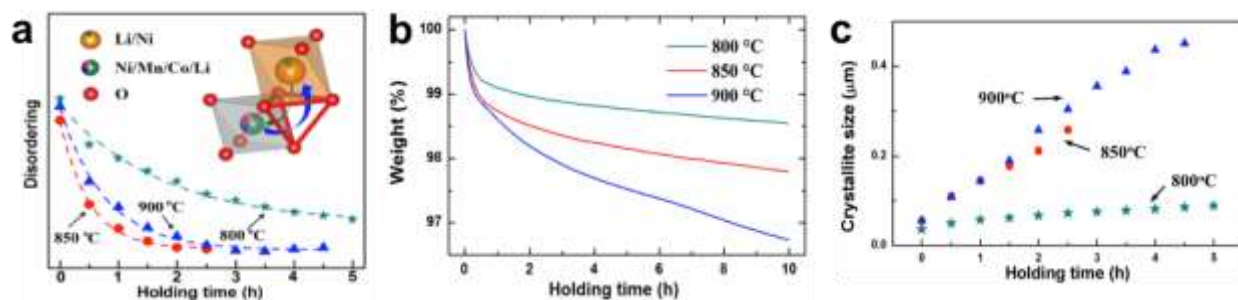


Figure 13. Structural, chemical, and morphological evolution in the intermediates of NMC-71515 during heat treatment at 800°C, 850°C, and 900°C. (a) Evolution of the cationic disordering (that is, occupancy of nickel ions at 3b sites). (b) Thermogravimetric analysis curves of the precursors during holding at constant temperatures. (c) Evolution of crystallite size with holding time.

The findings from this study enabled the project to identify optimal conditions for synthesizing NMC-71515 with low cationic disordering and high electrochemical activity. Figure 14a displays the representative charge/discharge voltage profiles of synthesized materials, indicating much higher discharge capacity in the sample synthesized at 850°C, 197 mAh g^{-1} , compared to that obtained at 800°C and 900°C, 162 and 174 mAhg^{-1} , respectively. In addition, a lower overpotential was obtained in the sample heated at 850°C. The measured electrochemical performance is in good agreement with structural analysis, that is, the sample heated at 850°C has low Li/Ni mixing at 3b sites, large lithium slab, and moderate crystallite size. Excellent capacity retention was obtained in the three samples obtained at 800, 850, and 900 °C, of 93.5%, 84.1%, and 84.5% after 50 cycles (Figure 14b). The extension of electrochemical windows to 4.5, 4.7 V led to greatly increased capacity, but at the cost of capacity retention. The findings from this study provide new insights into synthetic design of high-Ni layered oxide cathodes.^[1]

All FY 2017 milestones were completed on-time or ahead of schedule, and progress for this project exceeded the expected year-end status (as listed in the Out-Year Goals).

[1] Wang et al., *Adv. Mater.* doi: 10.1002/adma.201606715.

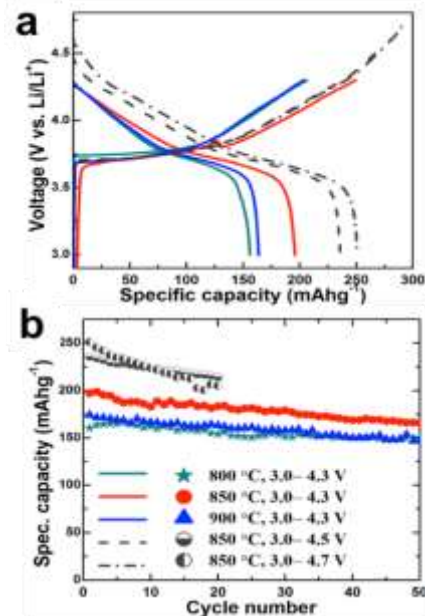


Figure 14. (a) Charge/discharge profiles. (b) Cycling performance of synthesized NMC-71515 at 800°C, 850°C, and 900°C.

Patents/Publications/Presentations

Publications

- Wang, D., and R. Kou, Y. Ren, C-J. Sun, H. Zhao, M-J. Zhang, Y. Li, A. Huq, J.Y.P. Ko, F. Pan, Y-K. Sun, Y. Yang, K. Amine, J. Bai, Z. Chen, and F. Wang. “Synthetic Control of Kinetic Reaction Pathway and Cationic Ordering in High-Ni-Rich Layered $\text{LiNi}_{0.7}\text{Co}_{0.15}\text{Mn}_{0.15}\text{O}_2$ Cathodes.” *Adv. Mater.* doi: 10.1002/adma.201606715.
- Park, Y-U., and J. Bai, L. Wang, G. Yoon, W. Zhang, H. Kim, S. Lee, S-W. Kim, J. P. Looney, K. Kang, and F. Wang. “*In Situ* Tracking Kinetic Pathways of Li^+/Na^+ Substitution during Ion-exchange Synthesis of $\text{Li}_x\text{Na}_{1.5-x}\text{VOPO}_4\text{F}_{0.5}$.” *J. Am. Chem. Soc.* 139 (2017): 12504.

Presentations

- American Chemical Society (ACS) Spring Meeting (April 17–21, 2017): “*In Situ* Structure-Tracking Aided Design in Synthesis of Energy-Storage Materials”; F. Wang and J. Bai.
- ACS Spring Meeting (April 17–21, 2017): “Synthetic Control of Structural and Electrochemical Properties of High-Ni Layered Oxide Cathodes for Next-Generation Li-Ion Batteries”; D. Wang, M-J. Zhang, J. Bai, and F. Wang.

Task 3.5 – Novel Cathode Materials and Processing Methods (Michael M. Thackeray and Jason R. Croy, Argonne National Laboratory)

Project Objective. The project goal is to develop low-cost, high-energy, and high-power Mn-oxide-based cathodes for Li-ion batteries that will meet the performance requirements of PHEVs and EVs. Improving the design, composition, and performance of advanced electrodes with stable architectures and surfaces, facilitated by an atomic-scale understanding of electrochemical and degradation processes, is a key objective.

Project Impact. Standard Li-ion battery technologies are unable to meet the demands of the next-generation EVs and PHEVs. Battery developers and scientists will take advantage of both the applied and fundamental knowledge generated from this project to advance the field. This knowledge should enable progress toward meeting DOE goals for 40-mile, all-electric range PHEVs.

Approach. Exploit the concept and optimize performance of structurally integrated “composite” electrode structures with a primary focus on “layered-layered-spinel” materials. Alternative processing routes will be investigated; ANL’s comprehensive characterization facilities will be used to explore novel surface and bulk structures by both *in situ* and *ex situ* techniques in pursuit of advancing properties of state-of-the-art cathode materials. A theoretical component will complement the project’s experimental work.

Out-Year Goals. The out-year goals are as follows:

- Identify high-capacity (LL and LS) composite electrode structures and compositions that are stable to electrochemical cycling at high potentials (~ 4.5 V).
- Identify and characterize surface chemistries and architectures that allow fast Li-ion transport and mitigate or eliminate TM dissolution.
- Use complementary theoretical approaches to further understanding of electrode structures and electrochemical processes to accelerate progress of materials development.
- Scale-up, evaluate, and verify promising cathode materials in conjunction with scale-up and cell fabrication facilities at ANL.

Collaborators. This project engages with the following collaborators: Eungje Lee, Roy Benedek, Arturo Gutierrez, and Meinan He in Chemical Sciences and Engineering (CSE) at ANL.

Milestones

1. Explore the energy content, and stabilization thereof, of moderate Li_2MnO_3 -content ($25\% < x < 50\%$) $y[\text{xLi}_2\text{MnO}_3 \cdot (1-x)\text{LiMO}_2] \cdot (1-y)\text{LiM}_2\text{O}_4$ ($M = \text{Mn, Ni, Co}$), LL and LLS electrodes; target capacity ≥ 220 mAh/g. (Q1 – Completed March 2017; Ongoing)
2. Identify surface-treatment strategies that enable LLS electrodes to maintain high capacities (≥ 220 mAh/g) and high rate performance (~ 200 mAh/g at 1C). (Q2 – Completed June 2017; Ongoing)
3. Demonstrate oxide energy densities ≥ 750 Wh/kg_{oxide} in full-cell testing of surface-modified, LLS electrodes. (Q3-4, September 2017 – In progress)

Progress Report

Surface reconstruction during first-cycle activation of composite cathode materials (that is, LL or LLS) is intimately related to surface-oxygen instabilities and can be detrimental to both cycle life and rate capability. Lithium-TM-phosphate materials (LiMPO_4 , where $M = \text{Fe, Mn, Co, or Ni}$), due to their strong covalent bonding within PO_4 polyanion groups and high voltage stabilities, are of interest as surface stabilizers for composite cathodes. However, LiMPO_4 materials generally suffer from notoriously slow lithium diffusion when compared to traditional cathode oxides. In this report, efforts to identify unique surface-treatment strategies that can enable stable cycling and high capacities ($\sim 200\text{mAh/g}$) at 1C, through the utilization of stabilizing LiMPO_4 materials, is reported. The data are preliminary findings based on an investigation of LLS, $\text{Li}_{1.18}\text{Mn}_{0.54}\text{Co}_{0.18}\text{Ni}_{0.28}\text{O}_2$ with $\sim 6\%$ spinel, modified by LiCoPO_4 (LCP) surface treatments.

Wet-chemical methods were employed to surface-treat the LLS powder with Li_xCoPO_4 ($0.25 \leq x \leq 1.0$), followed by heating at 700°C in air. Figure 15 shows a representative (energy dispersive spectroscopy (EDS) map of the surface-treated samples (here, $x = 1.0$) demonstrating an even distribution of phosphorus over the particles. Figure 16a shows the cycling performance of the untreated baseline and LCP-treated ($x = 1.0$) electrodes, cycled between 4.45–2.5 V at 15 mA/g and 30°C (1st cycle activation between 4.6–2.0 V). Results show that both samples delivered $\sim 210\text{mAh/g}$ with very similar cycle life. Figure 16b shows the rate performance of four, treated samples ($x = 0.25, 0.5, 0.75,$ and 1.0) compared to the untreated baseline. No improvement of the rate performance was seen for the sample treated with stoichiometric ($x = 1.0$, red circles) LCP, when compared to the baseline. However, as the initial lithium used for the surface treatments decreased below $x = 1.0$, the rate performance appeared to improve. Furthermore, as the initial lithium decreased to $x = 0.25$ the rate tests indicated a possible advantage at the highest currents tested (300 mA/g). The rate performance of the materials may be ranked as follows: $\text{Li}_{0.25}\text{CoPO}_4 > \text{Li}_{0.5}\text{CoPO}_4 = \text{Li}_{0.75}\text{CoPO}_4 > \text{LiCoPO}_4 = \text{untreated baseline}$. These data suggest that a path for improving lithium diffusion in LiMPO_4 -type materials might be possible via synthesis strategies and stoichiometric control. Future studies will focus on how the initial composition of surface treatments influences final surface structures and surface-to-bulk interfaces. Promising candidates will be chosen for further evaluation in full cells utilizing graphite electrodes.

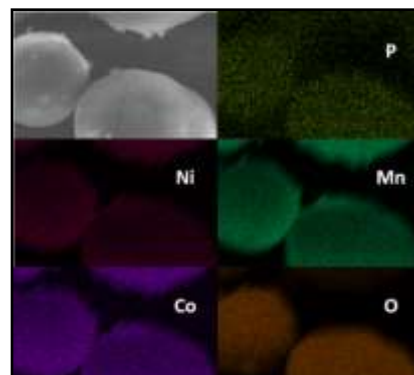


Figure 15. Elemental mapping of layered-layered-spinel powder treated with 1 wt% Li_xCoPO_4 ($x = 1$) and annealed at 700°C .

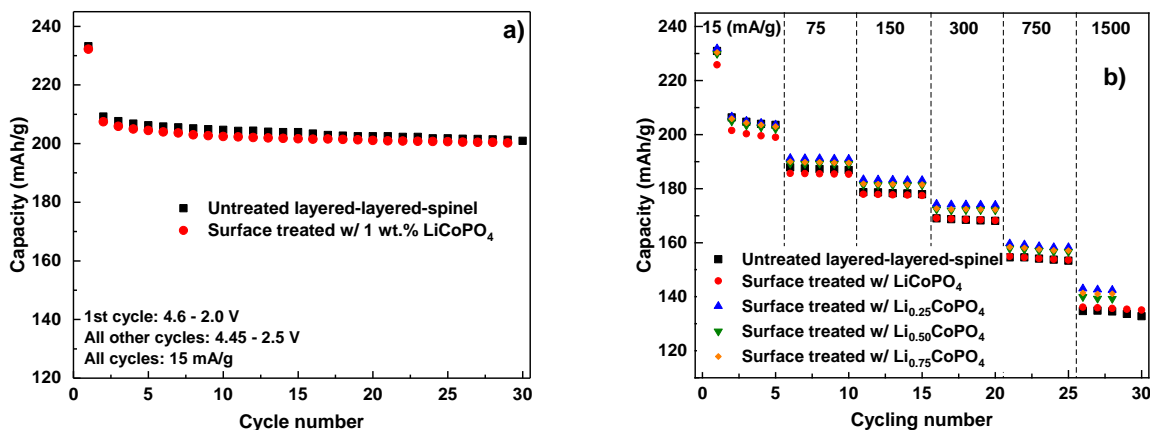


Figure 16. (a) Cycle life of untreated and LCP-treated layered-layered-spinel (LLS) cathode materials. (b) Rate performance of untreated and Li_xPO_4 -treated ($x = 0.25, 0.5, 0.75,$ and 1.0) LLS. All charge cycles were carried out at 15 mA/g to 4.45 V after a first-cycle activation to 4.6 V. Discharge currents are labeled along the top of the figure. All electrochemical testing was carried out at 30°C versus Li-metal anodes. Electrode loadings were $\sim 6\text{mg/cm}^2$.

Patents/Publications/Presentations

Presentation

- Summer Institute on Sustainability and Energy, ANL, Lemont, Illinois (August 10, 2017): “The Evolution of Energy Storage Demands and Argonne’s Role”; A. Gutierrez. Invited.

Task 3.6 – Advanced Cathode Materials for High-Energy Lithium-Ion Batteries (Marca Doeff, Lawrence Berkeley National Laboratory)

Project Objective. Microscopy and synchrotron X-ray absorption and photoemission techniques will be used to study the phenomenon of surface reconstruction to rock salt on NMC particle surfaces as a function of composition, synthesis method, surface chemistry, and electrochemical history. Because the surface reconstruction is implicated in capacity fading and impedance rise during high-voltage cycling, a thorough understanding of this phenomenon is expected to lead to principles that can be used to design robust, high-capacity NMC materials for Li-ion cells. The emphasis will be on stoichiometric NMCs with high nickel content such as 622 and 523 compositions.

Project Impact. To increase the energy density of Li-ion batteries, cathode materials with higher voltages and/or higher capacities are required, but safety and cycle life cannot be compromised. Ni-rich NMCs can provide higher capacities and lower cost in comparison with low nickel content NMCs, but surface reactivity is an issue. A systematic evaluation of the effects of synthesis method, composition, and cell history on the surface reconstruction phenomenon will lead to higher capacity, robust, and structurally stable positive electrode materials that result in higher-energy-density Li-ion cells than are currently available.

Out-Year Goals. The information generated by the in-depth characterization will be used to design robust NMC materials that can withstand cycling to high potentials and deliver > 200 mAh/g.

Collaborations. Transmission X-ray microscopy (TXM) is done in collaboration with Yijin Liu (SSRL). Synchrotron hard and soft XAS efforts are in collaboration with Dr. Dennis Nordlund, Dr. Yijin Liu, and Dr. Dimosthenis Sokaras (SSRL).

Milestones

1. Complete thermal characterization of Ni-rich NMC materials by TXM and X-ray Raman. (Q1 – Completed December 31, 2016)
2. Synthesize Ti-substituted Ni-rich NMCs by conventional and spray pyrolysis methods. (Q2 – Completed March 31, 2017)
3. Complete electrochemical characterization of Ti-substituted, Ni-rich NMCs. (Q3 – Completed June 30, 2017)
4. *Go/No-Go*: Core-shell composites made by infiltration and re-firing of spray-pyrolyzed hollow spherical particles. (September 30, 2016 – *No-Go* decision made)

Progress Report

Analysis of thermal data on chemically delithiated NMC-622 samples is in progress. In addition to synchrotron experiments done on samples examined at room temperature or after heating to 170°C or 350°C (discussed last quarter), hot stage XRD experiments were performed on several samples delithiated to different levels. Figure 17 shows some of these results (on 50% and 100% delithiated materials; 10%, 25%, and 75% delithiated samples were also examined).

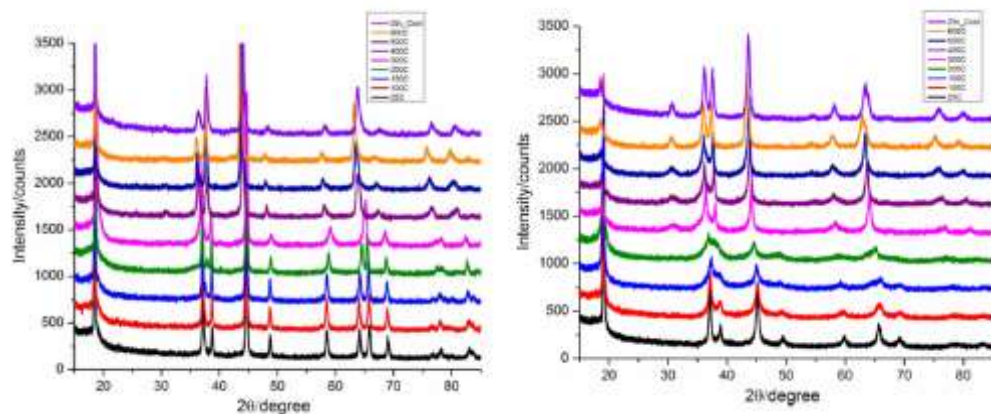


Figure 17. *In situ* hot stage X-ray diffraction patterns on a 50% delithiated NMC-622 sample (left) and a 100% delithiated sample (right).

In general, thermal stability decreases as the level of delithiation increases. Phase conversion is observed as low as 150–200°C for the 100% delithiated sample, compared to about 300°C for the 10% delithiated sample. The products of the thermal treatment are also dependent on degree of delithiation, progressing from a “splayed” (intermediate between spinel and layered) product for the 10% delithiated material, to LiMn_2O_4 -type spinel for the 25% delithiated sample, to M_3O_4 -type spinels and rock salt (MO) phases for the more highly delithiated samples. In other words, there is more oxygen release, and reduction of metals as lithium is progressively removed; this happens at lower temperatures.

Next quarter, the project will further analyze the thermal data and write a paper summarizing the results. It will also begin work on NMC-811.

Patents/Publications/Presentations

Publications

- Lin, Feng, and Yijin Liu, Xiqian Yu, Lei Cheng, Andrej Singer, Oleg G. Shpryko, Huolin Xin, Nobumichi Tamura, Chixia Tian, Tsu-Chien Weng, Xiao-Qing Yang, Ying Shirley Meng, Dennis Nordlund, Wanli Yang, and Marca Doeff. “Synchrotron X-Ray Techniques for Studying Materials Electrochemistry in Rechargeable Batteries.” *Chem. Rev.* (2017). doi: 10.1021/acs.chemrev.7b00007.
- Kan, Wang, and Saravanan Kuppan, Lei Cheng, Marca Doeff, Jagjit Nanda, Ashfia Huq, and Guoying Chen. “Crystal Chemistry and Electrochemistry of $\text{LiMn}_{1.5}\text{Ni}_{0.5}\text{O}_4$ Solid Solution Cathode Materials.” *Chem. Mater.* (2017). doi: 10.1021/acs.chemmater.7b01898.

Task 3.7 – Discovery of High-Energy Lithium-Ion Battery Materials (Wei Tong, Lawrence Berkeley National Laboratory)

Project Objective. This project aims to develop a cathode that can cycle > 200 mAh/g while exhibiting minimal capacity and voltage fade. The emphasis will be on oxides with high nickel contents. This task focuses on the compositions in the Li-Ni-O phase space, which will be explored using a combinatorial materials approach to search for new high-capacity cathodes. The specific objectives of this project are to: (1) investigate and understand the correlation between the synthesis and electrochemical performance of Ni-based compounds, and (2) design, synthesize, and evaluate the potential new high-capacity cathodes within Li-Ni-O composition space using the percolation theory as a guideline.

Project Impact. Energy density needs to be at least doubled to meet the performance requirements of EVs (300 to 400 mile). Although capacities approaching 300 mAh/g have been reported in Li-, Mn-rich layered oxide compounds, capacity decay and voltage fading in the long-term cycling are always observed. Therefore, new materials are urgently needed to make the breakthrough in Li-ion battery technology.

Approach. Recent discovery of high-capacity Li-excess cathodes provides new insights into material design principle. According to percolation theory, lithium excess is required to access 1 lithium exchange capacity in LiTmO_2 compounds. This seems to be independent of TM species and, therefore, could open a composition space for the search of new materials with high capacity. The interesting $\text{Ni}^{2+}/\text{Ni}^{4+}$ redox is selected as the electrochemically active component, and combinatorial materials design concept will be used to discover the potential cathode material candidates in the Li-Ni-O phase space.

Out-Year Goals. The long-term goal is to search new high-energy cathodes that can potentially meet the performance requirements of EVs with a 300- to 400-mile range in terms of cost, energy density, and performance. Work will progress from understanding of the known compounds, LiNiO_2 and Li_2NiO_2 , toward development of new Ni-based, high-energy cathode oxides.

Collaborations. The PI closely collaborates with M. Doeff (LBNL) on soft XAS, C. Ban (National Renewable Energy Laboratory, NREL) on ALD coating, B. McCloskey (LBNL) for differential electrochemical mass spectrometry (DEMS), and R. Kostecki (LBNL) for Raman spectroscopy. In addition, collaboration with other BMR PIs (X.-Q. Yang and F. Wang at BNL; K. Persson at LBNL) for crystal structure evolution upon cycling and material computation is in progress.

Milestones

1. Use Li-, Mn-rich oxide as the baseline material; develop synthesis that can be used to screen second TMs for Li-rich, Ni-based oxides. (Q1 – Completed December 2016)
2. Design Li-rich, Ni-based oxide compositions; perform synthesis of designed compositions. (Q2 – Completed March 2017)
3. Complete electrochemical tests on synthesized Li-rich, Ni-based oxides; down select one composition that shows promising electrochemical performance with an initial capacity > 200 mAh/g. (Q3 – Completed June 2017)
4. Complete structural characterization of selected composition; compare performance with Li-, Mn-rich oxide baseline. (Q4 – Completed September 2017)

Progress Report

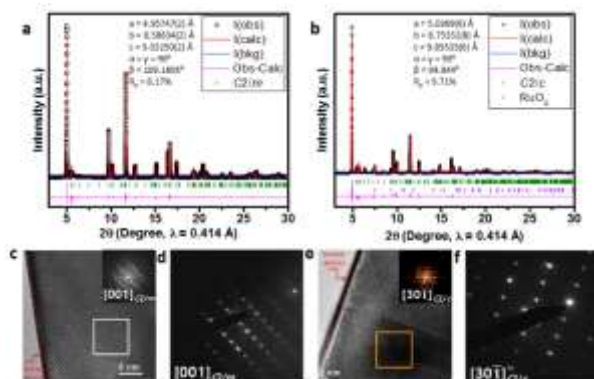


Figure 18. X-ray diffraction Rietveld refinement of (a) LNMO, monoclinic $C2/m$, and LNRO, monoclinic $C2/c$. High-resolution transmission electron microscopy image of (c) LNMO, (e) LNRO with fast Fourier transformation of the selected area. Electron diffraction pattern of (d) LNMO and (f) LNRO.

activity in both compounds by RIXS. In O K-edge RIXS maps (Figure 19), the RIXS intensity was plotted against the excitation energy (y axis) and emission energy (x axis). For LNMO electrodes (Figure 19a), one relatively large fluorescence feature was observed at an excitation of ~ 529.2 eV (t_{2g} orbitals) along with a relatively small feature at ~ 531.5 eV (e_g orbitals) in the pristine state. Upon charging, the 529.2 eV feature tended to grow due to its more covalent nature (corresponding to nickel oxidation). The most striking phenomenon was the appearance of an additional feature (marked by arrow) at an excitation energy, 530.9 eV, between the pre-edge peaks, but at slightly lower emission energy (~ 1 eV) in LNMO at 4.8 V charge. More importantly, this additional feature disappeared, and the other two pre-edge features reverted to their original states at 2 V discharge. In contrast, the main features of the LNRO spectra (Figure 19b) were similar to those of LNMO, except at slightly different excitation energies, 528.5 and 531.1 eV. However, at 4.8 V charge, the new feature at 530.9 eV excitation observed in LNMO was absent in LNRO. The hypothesis is that this additional feature that appears at 530.9 eV excitation and 523.2 eV emission energy is a direct evidence of the participation of electrons from anionic oxygen in the electrochemistry of LNMO. Therefore, the inference is that no electrons from anionic oxygen participate in the electrochemistry of LNRO; instead, nickel and ruthenium are electrochemically active. The sharp contrast between LNMO and LNRO of similar structure clearly demonstrates the critical role that TM plays in the anionic oxygen activity in Li-rich metal oxides.

This quarter, $\text{Li}_{1.2}\text{Ni}_{0.2}\text{Mn}_{0.6}\text{O}_2$ and $\text{Li}_{1.2}\text{Ni}_{0.2}\text{Ru}_{0.6}\text{O}_2$, denoted as LNMO and LNRO, respectively, were selected to study the oxygen activity in Li-rich metal oxides, given the sharp contrast in charge profile as reported last quarter. The similar crystal structure between LNMO and LNRO was further confirmed by Rietveld refinement and high-resolution transmission electron microscopy (HRTEM) analysis (Figure 18). Both LNMO and LNRO samples fit the structural model of monoclinic solid solution, and electron diffraction (ED) patterns and fast Fourier transformation (FFT) results along the $[001]$ and $[30\bar{1}]$ zone axis of $C2/m$ and $C2/c$ from LNMO and LNRO particle showed high structural consistency.

These two compounds demonstrated completely different gas evolution behavior, as revealed by *operando* DEMS. The project further investigated the anionic oxygen

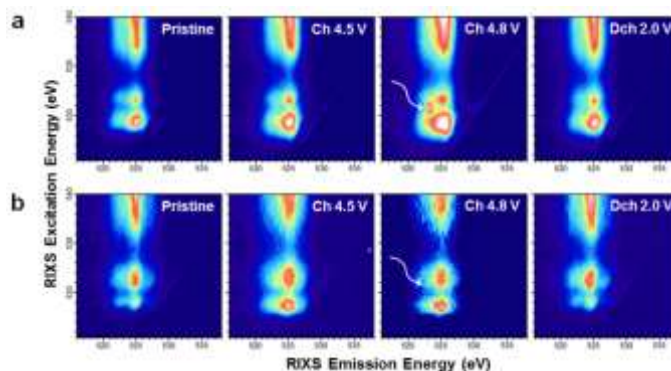


Figure 19. O K-edge resonant inelastic X-ray scattering maps of (a) LNMO and (b) LNRO electrodes at various states of charge. The white arrow indicates the specific oxygen redox state that is absent in LNRO.

Patents/Publications/Presentations

Publications

- Tong, W., and G. G. Amatucci. “Silver Copper Fluoride: A Novel Perovskite Cathode for Lithium Batteries.” *Journal of Power Sources* 362 (2017): 86–91.
- Xing, Z., and Y. Qi, Z. Tian, J. Xu, Y. Yuan, C. Bommier, J. Lu, W. Tong, D. Jiang, and X. Ji. “Identify the Removable Substructure in Carbon Activation.” *Chemistry of Materials* 29 (2017): 7288–7295.

Presentation

- Department of Chemical Engineering Colloquium, University of Waterloo (August 2017): “Exploring Anionic Oxygen Activity in Li-Rich Layered Oxide Cathodes”; W. Tong. Invited.

Task 3.8 – Exploiting Cobalt and Nickel Spinel in Structurally Integrated Composite Electrodes (Michael M. Thackeray and Jason R. Croy, Argonne National Laboratory)

Project Objective. The project goal is to stabilize high-capacity, composite ‘layered-layered’ electrode structures with lithium-cobalt-oxide and lithium-nickel-oxide spinel components (referred to as LCO-S and LNO-S, respectively), or solid solutions thereof (LCNO-S), which can accommodate lithium at approximately 3.5 V versus Li/Li⁺. This approach and the motivation to exploit the electrochemical and structural LCO-S and LNO-S spinel structures, about which relatively little is known, are unique.

Project Impact. State-of-the-art Li-ion batteries are currently unable to satisfy the performance goals for PHEVs and EVs. If successful, this project will impact the advance of energy storage for electrified transportation as well as other applications, such as portable electronic devices and the electrical grid.

Approach. This work will focus on the design and synthesis of new spinel compositions and structures that operate above 3 V and below 4 V and on determining their structural and electrochemical properties through advanced characterization. This information will be subsequently used to select the most promising spinel materials as stabilizers in high-capacity composite electrode structures.

Out-Year Goals. The electrochemical capacity of most high-potential, Li-metal oxide insertion electrodes is generally severely compromised by structural instability and surface reactivity with the electrolyte at low lithium loadings (that is, at highly charged states). Although progress has been made by cation substitution and structural modification, the practical capacity of these electrodes is still restricted to approximately 160-170 mAh/g. This project proposes a new structural and compositional approach with the goal of producing electrode materials that can provide 200-220 mAh/g without significant structural or voltage decay for 500 cycles. If successful, the materials processing technology will be transferred to the ANL Materials Engineering and Research Facility (MERF) for scale up and further evaluation.

Collaborations. This project collaborates with Eungje Lee, Arturo Gutierrez, Meinan He, Roy Benedek, and Fulya Dogan (CSE, ANL).

Milestones

1. Explore solution-based synthesis routes to optimize the structure and performance of Co-based spinel and structurally integrated LS electrodes. (Q1 – Complete/Ongoing)
2. Determine structure/electrochemical property relationships of Co-based spinel materials and when structurally integrated in composite layered-spinel electrodes. (Q2 – Complete/Ongoing).
3. Investigate bulk and surface modifications of Co-based spinel and LS electrodes. (Q3/Q4 – In progress)

Progress Report

Previous reports have discussed the synthesis, structure, and electrochemistry of lithiated-spinel, LiCoO_2 (LCO) materials when prepared by low-temperature (LT) solid-state synthesis^[1]. This quarter, a sol-gel method, which ensures better atomic-scale cation mixing than solid-state routes, was used to prepare LT-LCO structures and to investigate the effect of aluminum substitution on the electrochemical properties of these electrode materials. This approach was adopted because of the important role that aluminum substitution plays in fortifying the structure of several well-known Li-TM oxides, such as layered $\text{LiNi}_{0.8}\text{Co}_{0.15}\text{Al}_{0.05}\text{O}_2$ (NCA) and Li-Mn-oxide spinel materials. These LT-LCO materials hold promise for stabilizing layered-layered electrodes to combat voltage fade.

A series of LCO and substituted $\text{LiCo}_{1-x}\text{Al}_x\text{O}_2$ (LCO-Al) samples was synthesized by sol-gel reactions of metal acetates and glycolic acid. The resulting sol-gel precursors were subsequently fired in air at 400°C (LT) or at an intermediate temperature of 600°C (IT). Figure 20 shows the XRD patterns of LCO and substituted LCO-Al ($x = 0.15$) products prepared by this method. The LT-LCO sample could be indexed to a cubic spinel structure, consistent with products made by solid-state synthesis at 400°C ^[1]. LT-LCO particles prepared by the sol-gel method were observed to have a larger crystallite size, as determined by XRD, relative to solid-state LT-LCO. In addition, a Co_3O_4 impurity phase, also apparent in IT-LCO samples but in lower concentrations, was also found in the LT-LCO. The IT-LCO product prepared at 600°C has a well-defined layered structure, indicated by the split of (018) and (110) peaks at $\sim 66^\circ 2\theta$; unlike the materials prepared by solid-state reaction that require a higher synthesis temperature ($\geq 700^\circ\text{C}$) to produce well-ordered, layered structures^[1]. The LT and IT LCO-Al samples have similar structures as their LCO analogs, but do not contain Co_3O_4 impurities. The lower-firing temperature required to order the lithium and TM ions and the growth of larger crystallites in the final products suggest that, relative to solid-state reactions, the sol-gel method lowers the kinetic barriers to form well-defined LCO structures.

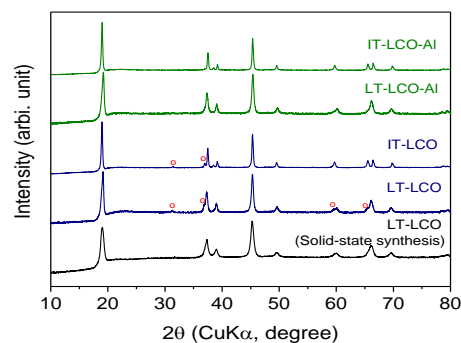


Figure 20. X-ray diffraction (XRD) of sol-gel LiCoO_2 (LCO) and $\text{LiCo}_{0.85}\text{Al}_{0.15}\text{O}_2$ (LCO-Al) samples fired at 400°C (low temperature) or 600°C (intermediate temperature). An XRD pattern of LCO, synthesized by solid-state reaction, is shown for comparison. Red circles indicate the peaks for Co_3O_4 .

Voltage profiles of lithium cells with LT-LCO and LT-LCO-Al cathodes show two voltage plateaus, corresponding to layered (3.9 V) and spinel (3.6 V) components (Figure 21a), whereas cells with IT-LCO and IT-LCO-Al electrodes exhibit only the 3.9 V plateau, corroborating the XRD data (Figure 21b). Al-substitution improves the cycling stability of both LT and IT electrodes (Figure 21c).

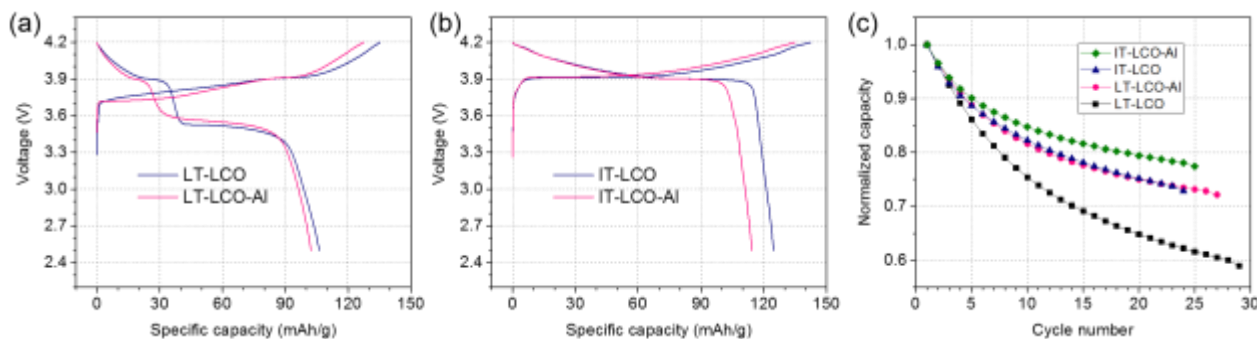


Figure 21. (a, b) Initial voltage profiles and (c) normalized capacity of the sol-gel prepared samples.

[1] E. Lee, J. R. Croy, M. M. Thackeray et al., *ACS Appl. Mater. & Interfaces* 8 (2016): 27720.

Patents/Publications/Presentations

Presentation

- 68th Annual Meeting of the International Society of Electrochemistry (ISE), Providence, Rhode Island, (August 27 – September 1, 2017): “Coherently Integrated Layered-Spinel Cathodes for Lithium-Ion Batteries”; Eungje Lee, Joong Sun Park, Hacksung Kim, Qianqian Li, Fernando C. Castro, Jinsong Wu, Vinayak P. Dravid, Soo Kim, Christopher Wolverton, Pengfei Yan, Chongmin Wang, Roy Benedek, Jason R. Croy, and Michael M. Thackeray.

TASK 4 – ELECTROLYTES

Summary and Highlights

The BMR Program goal is to develop long-life batteries superior to commercial Li-ion systems in terms of cost, vehicle range, and safety. The BMR Program addresses the fundamental problems of electrode chemical and mechanical instabilities that have slowed development of affordable, high performance, automotive batteries. The aim is to identify electrode/electrolyte materials that yield enhanced battery performance and lead to greater acceptance of EVs. Currently, the VTO supports seven projects in the BMR Program under the Electrolytes area. These projects can be categorized into three general topics:

- **Liquid.** The projects for liquid electrolyte aim to develop an atomic/molecular level understanding of the stability of electrochemical interfaces during charge-discharge cycling to stabilize solid/liquid interfaces in Li-ion batteries. In addition, electrolyte formulations, based on fluoro-chemistries, will be developed to achieve significantly improved operating voltage, increased durability, and increased energy density of Li-ion batteries at a reasonable cost.
- **Polymer.** The target of polymer electrolyte projects is mainly for use in Li-S batteries. Inorganic/polymer and polymer/gel hybrid electrolytes that have flexibility, mechanical strength, thermal stability, high ionic conductivity, stable interfaces against lithium metal, and polysulfide-trapping capability will be developed to enable energy densities twice that of the state-of-the-art Li-ion batteries, with comparable cycle life.
- **Self-Forming & Self-Healing.** The self-forming and self-healing electrolyte projects focus on developing and implementing Li-metal-based metal fluorite and metal iodide batteries, capable of energy densities > 400-500 Wh/kg and 1000 Wh/L.

Highlights

This quarter, the group at ANL has demonstrated first quantitative real-time analysis of cobalt dissolution that happens during charging of LiCoO₂ in 1.2M LiPF₆ in EC:EMC 3:7 electrolyte. This unique capability for monitoring *in situ* dissolution of TM from battery cathodes can provide deeper understanding on the fundamental processes responsible for performance degradation in Li-ion batteries.

At the Daikin group, data for gas kinetics based on cathode surface composition have been collected. Batteries cycled between 3.0 V and 4.6 V with LCO cathodes generated less gas than those with NMC-622 as the cathode. Of the cells that contain FEC, a larger percentage in the electrolyte suppressed gas evolution with increasing cycle number. Although not depicted, batteries cycled between 3.0 V and 4.2 V exhibited significantly less gassing with both LCO and NMC-622 as the cathode.

The University of Maryland (UMD) group has achieved hybrid solid-state electrolyte (SSE) with a high ionic conductivity ($\sim 0.5 \times 10^{-3}$ S/cm), high electrochemical stability (~ 4.5 V), and high mechanical property.

At the University of Washington, the group has synthesized several ionogels based on diluted solvate ionic liquids (SILs), termed diluted solvate ionogels (DSIGs), which despite being freestanding solids, are able to achieve high conductivities approaching 10^{-3} S/cm (as measured by EIS). In addition, self-healing behavior in PENDI-C6/Py Linker blends is shown to be affected by both crosslink density and stoichiometry, which can be manipulated by adding “free” NDI or Py molecules to the blend. Furthermore, 10 wt% thiol-modified mesoporous carbon cathodes have shown good capacity retention as well as minimal overpotentials.

The West Virginia University (WVU) successfully tested the temperature-dependence ionic conductivity of inorganic nanofibers including the bulk and grain-boundary conductivity; and synthesized the Al-doped LLZO and studied effects of aluminum on ionic conductivity as well as the thermal, mechanical, and electrochemical stability. Meanwhile, they have also synthesized the ion-conducting polymers and characterized their chemical compositions, the phase and the structure features, as well as the temperature-dependence ionic conductivity.

The Stony Brook University group has successfully achieved the goal set by the *Go/No-Go* of identifying two electrolyte compositions with conductivities $\geq 10^{-3}$ S/cm at 30°C. *Ex situ* measurements of the solid electrolyte demonstrated the importance of the electrolyte–substrate interface contribution to total measured resistance, and hence the cell performance.

At Rutgers, the team has transferred exclusively to the maskless, scalable manufacturing process for all R&D work, one year ahead of schedule. They have achieved approximately 570 Wh/L, an energy density value higher than the 500 Wh/L *Go/No-Go* goal. They have also increased the positive electrode utilization from 24% to over 30%. The group has shown that using the hybridization of the transport pathways, they were able to achieve a greater than an order of magnitude increase in the discharge current densities and also achieve C/10 rate capability. This has firmly established a viable pathway for them to achieve even higher rates moving into FY 2018.

Task 4.1 – Understanding and Mitigating Interfacial Reactivity between Electrode and Electrolyte (Khalil Amine, Larry A. Curtiss, and Nenad Markovic, Argonne National Laboratory)

Project Objective. This project aims to develop an understanding, at atomic/molecular levels, of the stability of electrochemical interfaces during charge-discharge cycling and to use the knowledge for stabilizing solid/liquid interfaces in Li-ion batteries. The goal is to improve stability of solid/liquid interfaces using insights into the atomic/molecular processes that limit stability during cycling. The core objective is to identify, rationalize, and understand the dynamics of the dissolution processes of 3D-TM cations in the cathode materials, stability of various commercial and highly purified electrolytes comprised of organic solvents, salts, and additives, and evolution of O₂ and other gaseous products formed from the electrode material or the electrolyte during the charging-discharging of the Li-ion battery.

Project Impact. The instability of the solid-liquid interfaces during cycling limits use of novel cathodes such as 6:2:2 and 8:1:1 NMC cathodes with higher voltage and higher power densities. Stabilization of solid/liquid interfaces in Li-ion batteries can lead to enhanced performance and increased safety.

Approach. This project follows an integrated program focused on solid-liquid interfaces in Li-ion batteries using state-of-the-art *in situ* characterization tools and computational modeling to understand and design interfaces with enhanced stability. The range of high-end analytical tools includes the following: (1) a three-electrode rotating disk electrode (RDE) setup; (2) ICP-MS; (3) gas chromatography (GC) with Triple Quadrupole MS (GC-QqQ) in Headspace sampling mode; and (4) DEMS. High-precision electrochemical measurements in combination with *in situ* measurements and characterization are highly suitable to investigate correlation of stability with various electrochemical, structural, and compositional properties of interfaces. Computational methods that provide reaction energies and barriers as well as structural information at the atomic level will be used to predict and test possible reactions that affect stability of solid-liquid interfaces.

Out-Year Goals. Work will progress toward more comprehensive *in situ* characterization and integrated modeling capabilities with applications to solid-liquid interfaces of electrolytes and 6:2:2 NMC cathodes. If the project can harness the complexity that governs interface instability, it should be able to move far beyond current state-of-the-art Li-ion systems and create new avenues to design and deploy cathode materials and electrolytes.

Collaborations. This project collaborates with Jun Liu at PNNL and X. He at Tsinghua University. At ANL, Zonghai Chen, Sanja Tepavcevic, Pietro Papa Lopes, and Peter Zapol contribute to the project.

Milestones

1. Perform first *ex situ* measurements of electrode/electrolyte decomposition products using ICP-MS and GC-MS. (Q1 – Complete)
2. Develop protocol for calculating electrochemical reactions at electrolyte-electrode interfaces. (Q1 – Complete)
3. Build a new 16-channel high-precision electrochemical measurement system dedicated to this project. (Q2 – Complete)
4. Benchmark the kinetics of direct electrochemical oxidation of baseline electrolyte at different potentials. (Q3 – Complete)
5. Couple ICP-MS with electrochemical cell for direct *in situ* investigation of metal dissolution from the cathode. (Q4 – Complete)

Progress Report

Previously, the project reported on first-of-its-kind experiments to measure *in situ* dissolution of cobalt from LiCoO₂ under charging as monitored by a stationary probe rotating disk electrode (SPRDE) ICP-MS setup. This methodology allows simultaneous monitoring of the charge/discharge process arising from lithium de-intercalation/intercalation in cathode material and the kinetics of TM dissolution as a function of time and potential. While the first experiments served to demonstrate the method, the new results shown in Figure 22

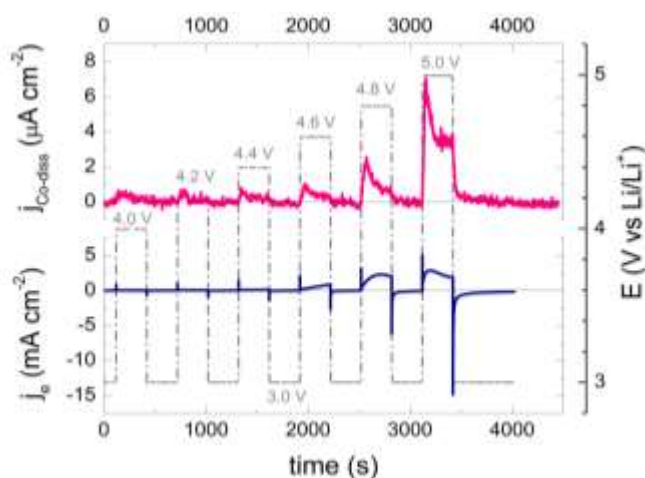


Figure 22. *In situ* inductively coupled plasma mass spectrometry results of cobalt dissolution upon electro-chemical polarization using the stationary probe rotating disk electrode system. Working electrode: LiCoO₂/C/PVDF. Electrolyte: 1.2 M LiPF₆ in EC:EMC (3:7 by mass).

provide the first quantitative real-time analysis of cobalt dissolution that happens during charging of LiCoO₂ in 1.2M LiPF₆ in EC:EMC 3:7 electrolyte. The project first explored the dynamics of cobalt dissolution during potential step transients from 3 V versus Li/Li⁺ to an upper potential limit (UPL) that lasted 300 seconds per step. At each consecutive step, the project increased the UPL from 4 V up to 5 V versus Li/Li⁺ in 0.2 V increments. As observed from Figure 22, the first potential step to 4 V was enough to trigger a very small transient of cobalt dissolution that quickly decayed to the same level of signal as in the background. Consecutive steps up to 4.2 and 4.4 showed only this transient behavior as well. However, for potential steps starting at 4.6 V and above, it becomes clear that the dissolution current is composed of the initial transient and additional continuous dissolution kinetics. While the charging current is of the order of 1 mAcm⁻² at 4.6 V, the respective cobalt dissolution current is 3 orders

of magnitude smaller, indicating that any degradation process that involves cobalt dissolution is only happening at the surface of the material and is not a bulk process as intercalation/de-intercalation.

Providing deeper insight on how much cobalt dissolved after the potential steps, Figure 23 shows the total amount of cobalt dissolution, obtained as the area under the dissolution curve shown in Figure 22, as a function of the UPL. While the trend of increasing dissolution with increasing UPL is clear, the amount of cobalt dissolved reveals the importance of surface processes in battery stability dynamics. Even though the cobalt dissolution transients that were observed at 4 V are small, the amount of cobalt loss represents a significant portion of the electrode surface (a few percent), which helps to understand why there would be a loss of electrical contact between different particles as their surfaces are evolving after multiple cycles. Therefore, the project's unique capability for monitoring *in situ* dissolution of TM from battery cathodes can provide deeper understanding on the fundamental processes responsible for performance degradation in Li-ion batteries.

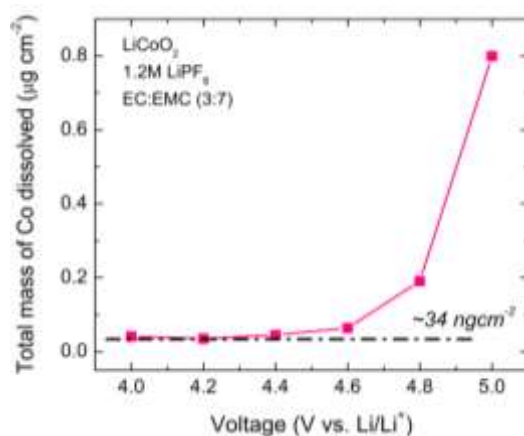


Figure 23. Total amount of cobalt dissolution upon electro-chemical polarization using as monitored by the stationary probe rotating disk electrode inductively coupled plasma mass spectrometry system. Same experimental conditions as in Figure 22.

Task 4.2 – Advanced Lithium-Ion Battery Technology: High-Voltage Electrolyte (Joe Sunstrom and Ron Hendershot, Daikin)

Project Objective. The overall project objective is to identify electrolyte formulations, based on fluoro-chemistries, that will allow significantly improved operating voltage, increased durability, and increased energy density of Li-ion batteries at a reasonable cost. The project objective is to understand the conditions under which the electrolyte degrades, the effect on battery performance, and solutions that can overcome current limitations of the electrolyte. Gassing in Li-ion batteries is one of the most common failure mechanisms, and poses the greatest safety risk in consumer devices. This project aims to investigate the gas composition as a function of cathode material, electrolyte formulation, and operating voltage, and proposes optimal cell compositions at decomposition voltages.

Project Impact. Developing an understanding of under what operating conditions gasses form in Li-ion batteries enables the project to propose optimized cell compositions, which operate at higher voltages for a longer period. Different fluorinated electrolyte components and additives may suppress and/or eliminate gas generation at or above hypothesized decomposition voltages. To investigate these topics, it is imperative that the project utilize multiple approaches, including, but not limited to: cathode material, electrolyte composition, operating voltage, and cycle number.

Approach. The evolving composition of the electrolyte in the battery will be examined by a variety of analytical instruments to study volatiles [GC-MS/thermal conductivity detector (TCD)], liquid [liquid chromatography MS (LC-MS)], and solid (TOF-SIMS, TGA-MS, XPS) electrolyte decomposition products during battery operation. In the first year, the team will address the gas composition and kinetics for both hydrocarbon and fluorocarbon as a function of several charge/discharge conditions, which include (but are not limited to) electrode composition, operational voltage and current, temperature, and cycle number.

Out-Year Goals. Work will progress toward formulating rough mass balances of both the fluorinated and hydrocarbon electrolytes under the performance parameters suggested. Specifically, analysis of the liquid and solid decomposition products will be pursued. Understanding how the mass balance and kinetics change will provide information on decomposition pathways and will suggest new electrolyte formulations to increase battery performance.

Milestones

1. Determination of gas composition. Gas composition as a function of voltage and cathode surface. (Q2 - Complete)
2. Gassing kinetics as a function of FEC concentration under different operating conditions. (Q3 – 75% complete)
3. Gas kinetics based on cathode surface composition. (Q4 – Complete)

Progress Report

The results from two long-term tests are shown in Figure 24 and Table 2. Both experiments were designed by varying the percent composition of nickel in the cathode material, while also changing the FEC concentration of fluorinated electrolyte under different operating conditions. As an example, Table 2 displays the qualitative gas composition of select LCO and NMC-622 batteries after an extended open circuit voltage (OCV) period at 55°C after formation and final charge to 4.6 V.

Table 2. Gas composition of LCO (red) and NMC-622 (yellow) cells determined by gas chromatography – mass spectroscopy/thermal conductivity detector as a function of FEC concentration.

[FEC]	CH ₄	C ₂ H ₂	C ₂ H ₄	C ₂ H ₆	C ₃ H ₆	C ₃ H ₈	C ₄ H ₁₀	CH ₃ F	C ₂ H ₅ F	CO	CO ₂	O ₂	H ₂	PF ₃
10%	X		X	X	X	X	X	X	X	X	X	X		X
20%	X	X		X		X	X	X	X	X	X	X		
10%	X		X	X				X	X	X	X	X	X	
20%	X	X		X				X	X	X	X	X	X	

Two different concentrations of FEC (v/v %) were tested, for the extended aging experiment. The LCO cathode cell with 10 % FEC exhibited the largest amount of gas produced, in addition to the only battery evolving larger hydrocarbon gases. In all batteries, CO₂ and cobalt are the largest components of the analyzed gas, with quantifiable amounts of methane, ethylene, and O₂ also being generated. The additional gases (PF₃, etc.) are present in trace but measurable quantities. Although the NMC-622 cells produce quantifiable amounts of H₂, the project cannot rule out the presence in LCO cells due to detection limits (> 8.5 v/v %) while using helium as the carrier gas in a GC-MS/TCD instrument. Quantitative gas analysis is ongoing on battery cells, with varying amounts of FEC in the electrolyte and nickel content in the cathode.

Figure 24 depicts the volume change of 200-mAh cells as a function of cycle number. The cells depicted were charged to 4.6 V, which is just beyond the failure voltage. LCO (0% nickel) cathode cells are depicted on the left, and NMC-622 (60% nickel) on the right. In addition to differing cathode materials, the project varied the concentration of FEC in the electrolyte from 0-20% (v/v) to investigate its contribution to cell gassing. This experiment is ongoing, and will cease after 200 charge/discharge cycles at a rate of 0.7 C.

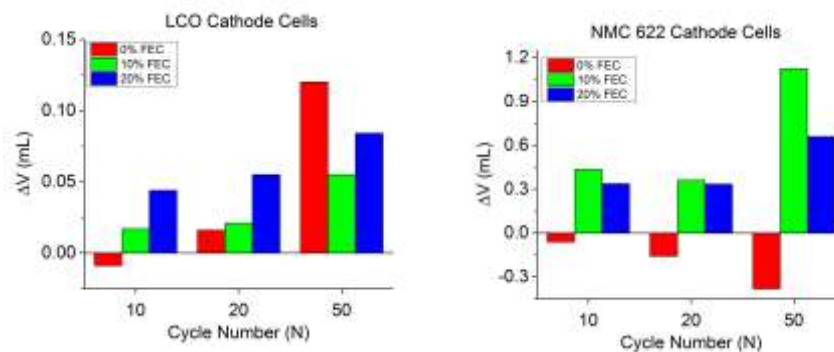


Figure 24. Volume change as a function of cycle number as measured by the Archimedes method.

Overall, batteries cycled between 3.0 V and 4.6 V with LCO cathodes generated less gas than those with NMC-622 as the cathode. Of the cells that contain FEC, a larger percentage in the electrolyte suppressed gas evolution with increasing cycle number. Although not depicted, batteries cycled between 3.0 V and 4.2 V exhibited significantly less gassing with both LCO and NMC-622 as the cathode. Two additional chemistries (NMC-111 and NMC-532) will be completed in the first quarter of 2018.

Task 4.3 – Multi-Functional, Self-Healing Polyelectrolyte Gels for Long-Cycle-Life, High-Capacity Sulfur Cathodes in Lithium-Sulfur Batteries (Alex Jen and Jihui Yang, University of Washington)

Project Objective. The project objective is to develop self-healing and polysulfide-trapping polyelectrolyte gels containing room-temperature ionic liquid (RTIL) for the Li-S battery system. The battery design will be able to achieve gravimetric and volumetric energy densities of ≥ 800 Wh/kg and ≥ 1000 Wh/L, respectively.

Project Impact. The Li-S battery system is currently hampered by poor capacity retention, primarily caused by dissolution of polysulfide reaction intermediates in typical organic electrolytes, as well as poor electrical contact between insulating sulfur and the conductive carbon matrix. This project aims to produce a high-capacity, long-cycle-life Li-S battery system by using rational molecular design strategies to address each capacity loss mechanism directly. A long-cycle-life Li-S battery system with the capability of doubling Li-ion energy density would enable production of lighter, longer range EVs at a cost that is affordable to the average U.S. household.

Approach. The team will develop Li-S coin cells that utilize self-healing, interpenetrated ionomer gel electrolytes in both the cathode and separator. The team will synthesize necessary starting materials and fabricate components of these gels while testing their relevant electrochemical and mechanical properties. All components will be combined into interpenetrating structures, which will be tested both alone and in cell configurations. Device performance data will be collected and used to further optimize designs of both material and cell, culminating in an optimized Li-S battery design capable of doubling the energy density of traditional Li-ion batteries. During the first year, the team is focusing on (1) synthesis of a variety of precursors for gel electrolytes, (2) fabrication and testing of both baseline materials and novel materials made from these precursors, and (3) iterative validation and improvement of design principles through both materials and device testing.

Out-Year Goals. Work will progress toward developing structure-property relationships for the self-healing, interpenetrated gel ionomer electrolyte and its individual components, as well as successful incorporation of such an electrolyte into a working Li-S cell. The team plans to demonstrate significant improvements in both capacity and retention when using the project's novel materials, as compared to state-of-the-art baseline systems.

Collaborations. This project funds work at the University of Washington. Dr. Alex Jen (PI) focuses on design, synthesis, and testing of novel materials, as well as device-based verification of design principles. Dr. Jihui Yang (Co-PI) focuses on optimization of device fabrication and testing, as well as investigation of failure mechanisms in devices using novel materials. PNNL facilities will be used for detailed study of device operation.

Milestones

1. Synthesize organic starting materials, and demonstrate both an ionomer gel electrolyte and a self-healing film based on these materials. (Q3 – Completed June 2017)
2. Integrate S/C composites into Li-S coin cells, and cycle them both with an organic electrolyte system and with several novel gel electrolyte systems. (Q4 – Completed September 2017)

Progress Report

Multifunctional Ionomer Gels. Gel fabrication processes were refined to create a protocol that repeatably produces high-quality gels based on ionic liquid and poly(ethylene glycol) (PEG) dimethacrylates. Notably, this process works exceedingly well with “solvate” or “pseudo” ionic liquids based on stoichiometric complexes of tetraglyme and LiTFSI. These complexes offer many of the same advantages of organic ionic liquids, such as high conductivity, low vapor pressure, low polysulfide solubility, and lithium dendrite suppression, while possessing a lithium transference number greater than 0.5, which significantly improves the current density achievable in cells. These SILs can also be diluted with small quantities of low-to-moderate-polarity organic solvent to boost conductivity while retaining the ionic-liquid-like properties relevant to cell performance. As such, the project has synthesized several ionogels based on diluted SILs, or DSIGs.

These DSIGs, despite being freestanding solids, are able to achieve astonishingly high conductivities approaching 10^{-3} S/cm (as measured by EIS). This is, to the team’s knowledge, a higher conductivity than has previously been reported for any gel electrolyte based on ionic liquid. The team is confident that further optimization of the formulas will result in ionomer gels that surpass the 10^{-3} S/cm barrier, with a lithium transference number well above 0.5. Several formulas under investigation and their corresponding conductivity data are summarized in Table 3.

Table 3. Conductivity of ionogels based on solvate ionic liquid.

PEGDMA (750Da)	Ionomer	Li(G4)TFSI	Ether Solvent	Conductivity ($\times 10^{-4}$ S/cm)
20%vol	0% vol	80% vol	+0% vol	2.79
20%vol	0% vol	80% vol	+50% vol	9.23
10%vol	20% vol	70% vol	+40% vol	3.70

Self-Healing Materials. The mechanism of self-healing in supramolecular polymer blends containing naphthalene diimide (NDI) and pyrene (Py) was investigated in detail. A combination of ultraviolet-visible (UV-Vis) and nuclear magnetic resonance (NMR) data indicated that both 2:1 and 1:1 stoichiometric complexes of NDI:Py are energetically favorable, and the prevalence of one versus the other depends strongly on NDI and Py concentrations available. The 2:1 complex was calculated to be roughly twice as energetically favorable in dilute dichloromethane solution as the 1:1 complex (-16.5 kJ/mol versus 8.2 kJ/mol).

These concentration-dependent differences in binding were explored as a way to influence self-healing behavior in the polymer composites. A series of three blends was prepared using PENDI-C₆ copolymer and Py Linker: a 1:1 molar ratio of NDI:Py (PP-1), a 2:1 molar ratio of NDI:Py prepared by adding a stoichiometric amount of dibutyl NDI to the control blend (PP-NDI), and a 1:1 molar ratio of NDI:Py prepared by adding a stoichiometric amount of Py to the control blend (PP-Py).

Dramatic differences in self-healing were observed between the three blends, summarized in Figure 25. The PP-NDI blend was unable to self-heal at temperatures below 70°C , while the

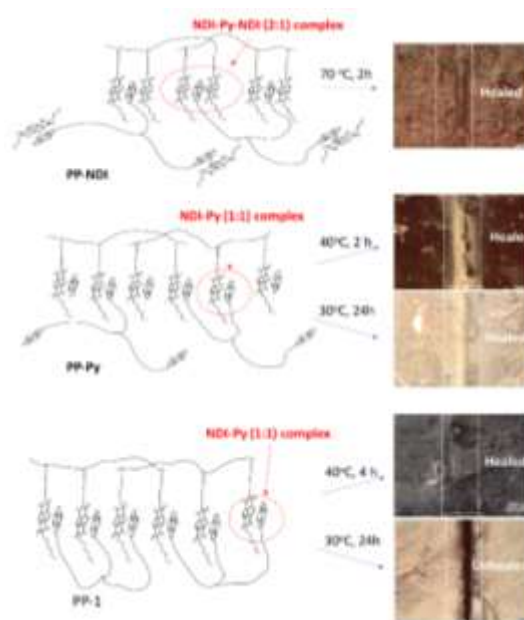


Figure 25. Self-healing behavior in PENDI-C₆/Py Linker blends is affected by both crosslink density and stoichiometry, which can be manipulated by adding “free” NDI or Py molecules to the blend.

PP-Py blend was able to self-heal at temperatures as low as 30°C, despite both blends possessing a theoretically identical density of supramolecular crosslinks. This is because the crosslinking in the PP-NDI blend consists primarily of the stronger 2:1 complex, which requires more energy to dissociate. The PP-1 blend required a slightly higher self-healing temperature of 40°C, theorized to be due to the increased density of (weaker 1:1) crosslinks. Notably, the *type* of crosslink appears to influence self-healing behavior more strongly than the concentration of crosslinks alone. The crosslinking behavior of these blends also exerts a predictable influence on their elastic moduli, which range from 53 MPa for PP-Py to 98 MPa for PP-NDI. Notably, the moduli of all blends are much higher than the vast majority of self-healing materials commonly reported in literature, which rarely exceed 10 MPa. Up to 77% of the original tensile modulus was recovered for PP-Py after 40°C, 12 h heat treatment. Finally, PENDI-C₆:Py Linker blends were doped with LiTFSI in a 20:1 [EO]:[Li⁺] ratio, and the resulting materials were demonstrated by EIS to have an ionic conductivity > 10⁻⁶ S/cm at 50°C, confirming that this self-healing materials system can transport lithium. The project is preparing a manuscript on these findings for submission to a peer-reviewed journal.

Mesoporous Carbon Functionalization. To investigate the origin of increased overpotential and reduced initial capacity in thiol-modified mesoporous carbon cathodes, the project studied a series of carbons with increasing weight percentage of thiol modifier, from 5% to 20%, controlled *via* reaction conditions. The project observed that cathodes with 10 wt% modifier carbon were able to increase capacity retention without significantly affecting the overpotentials observed during cell operation. Notably, modification beyond 15 wt% created a sloped initial voltage profile, while lower surface coverage cathodes retained plateau-like behavior (Figure 26a-d), potentially indicating a switch from two-phase to one-phase reaction. Brunauer–Emmett–Teller (BET) analysis revealed that surface modification up to 10 wt% induced only a modest decrease in specific surface area and pore volume, while coverage of 15 wt% above reduced both properties by ~ 50%.

Taken altogether, these results paint a picture of cell operation in which thiol surface modifiers form covalent bonds with polysulfides *in situ*. This achieves the desired effect of suppressing polysulfide escape into bulk electrolyte, which improves capacity retention; however, when the concentration of modifiers is too high, interior pore space is clogged, forcing electrochemical reactions to proceed via a solid-state mechanism, with associated overpotential increase. This sort of concentration-dependent surface modification behavior has yet to be extensively explored in literature, representing a unique contribution of this work.

The project is attempting to verify the hypothesis on modifier-polysulfide interaction by obtaining direct evidence of S-S bond formation through both XPS and Li⁷ NMR studies (in collaboration with PNNL). Collection of this data will be followed by publication of the combined results in a peer-reviewed journal.

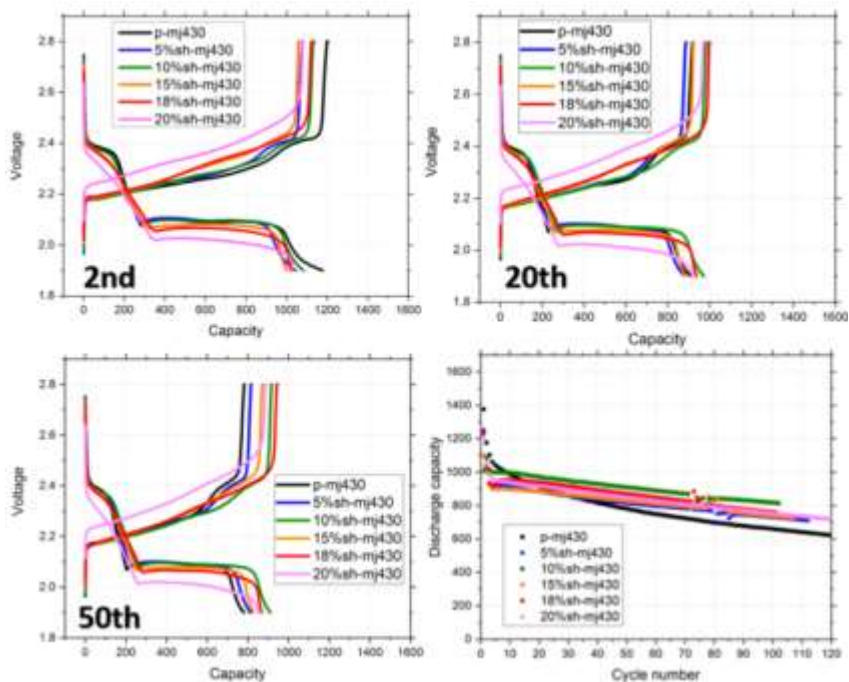


Figure 26. Performance of thiol-modified mesoporous carbon cathodes depends strongly on the amount of modifier present, with 10 wt% representing an ideal combination of high capacity, improved retention, and low overpotential.

Patents/Publications/Presentations

Publication

- Qin, J., and D. Hubble, F. Lin, J. Yang, and A. K.-Y. Jen. “Tunable Self-Healing Ability in a Rigid, Ion-Conductive Supramolecular Polymer.” In preparation.

Task 4.4 – Development of Ion-Conducting Inorganic Nanofibers and Polymers (Nianqiang (Nick) Wu, West Virginia University; Xiangwu Zhang, North Carolina State University)

Project Objective. The project objective is to develop SSEs based on the highly-conductive inorganic nanofibrous network in the polymer matrix for lithium batteries.

Project Impact. The research team will conduct R&D on solid-state inorganic nanofiber-polymer composite electrolytes that will not only provide higher ionic conductivity, improved mechanical strength, and better stability than the polyethylene oxide polymer electrolyte, but also exhibit better mechanical integrity, easier incorporation, and better compatibility with the Li-metal anode than the planar ceramic membrane counterparts. The proposed inorganic nanofiber-polymer composite electrolytes will enable practical use of high-energy-density, high-power-density Li-metal batteries, and Li-S batteries.

Approach. Integration of the highly Li⁺-conductive inorganic nanofiber network into the polymer matrix not only provides the continuous Li⁺ transport channels, but also kinetically inhibits the crystallization from the amorphous state of polymer electrolyte. The inorganic nanofibers will be fabricated with an electrospinning technique; and the ionic conductivity of inorganic nanofibers will be improved by chemical substitution or doping. Highly ionic-conductive polymers will be developed by cross-linking and/or creation of a block-copolymer structure; the composition and microstructure of the composite electrolyte will be designed to suppress the lithium dendrite formation.

Out-Year Goals. Work will progress toward synthesis of the inorganic nanofibers and the polymer matrix. The goal is to find the optimal synthetic route to achieve the desirable conductivity.

Collaborations. This project funds work at WVU and North Carolina State University (NCSU). Dr. Nianqiang (Nick) Wu at WVU serves as PI, and Dr. Xiangwu Zhang at NCSU acts as Co-PI. Sujan Kasani (Ph.D. student at WVU), Hui Yang (Postdoctoral Fellow at WVU), Botong Liu (Ph.D. student at WVU), Chaoyi Yan (Ph.D. student at NCSU) and Mahmut Dirican (Postdoctoral Fellow at NCSU) contributed to the project.

Milestones

1. **Subtask 1.1.4.** Test the temperature-dependence ionic conductivity of inorganic nanofibers, and the bulk and grain-boundary conductivity. (Q4 – Completed July 2017)
2. **Subtask 1.1.5.** Dope the lithium lanthanum zirconium oxide (LLZO) with aluminum, and study the effects of aluminum on the ionic conductivity as well as the thermal, mechanical, and electrochemical stability. (Q4 – Completed July 2017)
3. **Subtask 1.2.2.** Synthesize the ion-conducting polymers. (Q4 – Completed July 2017)
4. **Subtask 1.2.3.** Characterize the chemical composition, the phase, and the structure of ion-conducting polymers. (Q3 – April 2017; Completed, 80%)
5. **Subtask 1.2.4.** Test the temperature-dependence ionic conductivity of polymers and other properties. (Q4 – Completed July 2017)

Progress Report

Dr. Yang, a project collaborator, has completed the theory calculation of the aluminum doping of inorganic Perovskite-type lithium lanthanum titanate $\text{Li}_{0.33}\text{La}_{0.56}\text{TiO}_3$ (LLTO) nanofibers. After calculations, the project team found that the transporting barrier for pure, single-Al, and double-Al decorated structure is 0.365 eV, 0.165 eV, and 0.225 eV, respectively. For the polymer matrix, Li[PSTFSI-b-MPEGA-b-PSTFSI] triblock copolymer with different feed EO/Li⁺ ratios of 32, 24, and 16 was synthesized. Cross-linked polyethylene/poly(ethylene oxide) (PE/PEO) polymers were plasticized with 10~40 wt% (monomer amount) PEG. A composite electrolyte based on cross-linked polymer and poly(vinylidene fluoride-hexafluoropropylene) (PVdF-HFP) was fabricated and tested. The LLTO nanofibers were further modified with lithium phosphate.

Synthesis of Inorganic Nanofibers – Calculation of Al-Doped $\text{Li}_{0.33}\text{La}_{0.557}\text{TiO}_3$ (LLTO) Structures

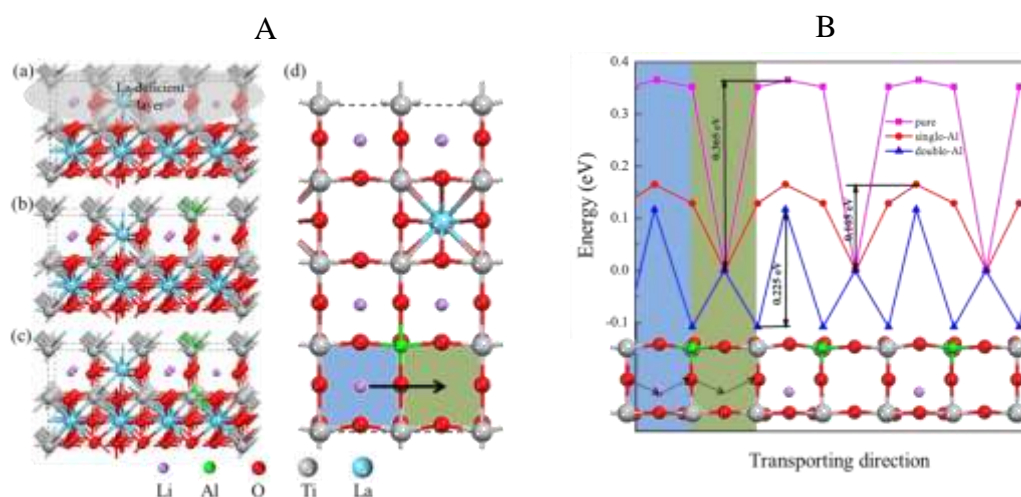


Figure 27. (A) Pure and Al-decorated $\text{Li}_{0.33}\text{La}_{0.56}\text{TiO}_3$ structures. (a-c) Side views of pure and most stable single-Al and double-Al decorated $\text{Li}_{0.33}\text{La}_{0.56}\text{TiO}_3$, respectively. (d) Top view of La-deficient layer of (b). Blue and green color blocks in (d) are used to represent two different regions in lithium atom transporting direction. (B) Transporting barriers for lithium atoms along transporting direction in pure, single-Al, and double-Al decorated $\text{Li}_{0.33}\text{La}_{0.56}\text{TiO}_3$ structure. The transporting trajectory is marked by dash line in inset.

To study the transporting behavior of lithium atoms in pure and Al-decorated $\text{Li}_{0.33}\text{La}_{0.56}\text{TiO}_3$ structures, the project has constructed the La-full and La-deficient layers along stuck direction in Figure 27. Figure 27A:d gives the ideal transporting direction to simplify this research. After calculations, the project found that the transporting barrier for pure, single-Al, and double-Al decorated structure is 0.365 eV, 0.165 eV, and 0.225 eV, respectively. This tendency is consistent with experiments. To explain this behavior, the project analyzed the Bader charge of those structures. Before Li-atom transporting across the door, the project found that the charge value on oxygen atoms in the door has the sequence as double-Al > single-Al > pure structure, which indicates that Coulomb potential between lithium with oxygen atoms becomes stronger as more titanium is decorated by aluminum. However, when two titanium atoms are decorated by aluminum atoms, the Coulomb potential is too strong, so that the most stable site for lithium then changes to the door, not in the cubic center (in Figure 27B). To obtain higher transporting efficiency for lithium atoms in $\text{Li}_{0.33}\text{La}_{0.56}\text{TiO}_3$ structure, the main aim is to control the Coulomb potential between lithium atom and oxygen atoms, reasonably.

Synthesis of Polymer Matrix

Li[PSTFSI-b-MPEGA-b-PSTFSI] Triblock Copolymer. The Li[PSTFSI-b-MPEGA-b-PSTFSI] block copolymer with different feed EO/Li⁺ ratios of 32, 24, and 16 was synthesized using (4-styrenesulfonyl) (trifluoromethanesulfonyl)imide (STFSI) and methoxy-polyethylene glycol acrylate (MPEGA) monomers through free radical polymerization and nitroxide-mediated polymerization (NMP) (Figure 28). This polymer exhibits ionic conductivity of 1.16×10^{-5} S/cm, 3.30×10^{-5} S/cm, and 8.90×10^{-6} S/cm, respectively (Table 4).

Table 4. The ionic conductivities of Li[PSTFSI-b-MPEGA-b-PSTFSI] triblock copolymer.

Samples	Feed EO/Li ⁺ Ratio	Ionic Conductivity (S/cm)
Triblock copolymer (Li[PSTFSI-b-MPEGA-b-PSTFSI])		
t-BCP1	32.00	1.16×10^{-5}
t-BCP2	24.00	3.30×10^{-5}
t-BCP 3	16.00	8.90×10^{-6}

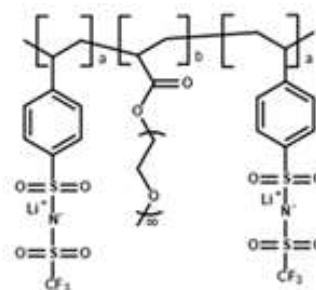


Figure 28. (a) Li[PSTFSI-b-MPEGA-b-PSTFSI] triblock copolymer. (b) Room-temperature ionic conductivities of Li[PSTFSI-b-MPEGA-b-PSTFSI] triblock copolymer.

Cross-Linked PE/PEO Polymer with LiTFSI Salt. 10~40 wt% (monomer content) PEG was introduced to the cross-linked PE/PEO polymers, which were synthesized using butyl acrylate (BA) as the PE monomer and poly(ethylene glycol) dimethacrylate (PEGDMA) as the cross-linker. PEG plasticization would help reduce the glass transition temperature of cross-linked polymer and also increase the ionic conductivity. 40 wt% (monomer content) PEG plasticized polymer shows the highest ionic conductivity of 1.65×10^{-4} S cm⁻¹ at room temperature.

Development of Inorganic Nanofibers-Polymer Composites

Inorganic Nanofibers/Cross-Linked Polymers with 40 wt% (monomer amount) PEG plasticized. Introducing the LLTO nanofibers in cross-linked polymer with 40 wt% PEG plasticizer resulted in the formation of a composite with ionic conductivity of 4.72×10^{-4} S/cm. Addition of 15 wt% LLAZO nanofiber into the cross-linked polymer with 40 wt% (monomer amount) PEG plasticizer formed composite electrolytes with ionic conductivity of 3.46×10^{-4} S/cm at room temperature.

Inorganic Nanofibers/PVDF-HFP/LiTFSI. The project has fabricated the composite electrolyte based on PVDF-HFP/LiTFSI and aluminum-doped ($\text{Li}_{0.33}\text{La}_{0.557}\text{Ti}_{1.005}\text{Al}_{0.005}\text{O}_3$) (LLATO) nanofiber. The LLATO nanofibers were further modified with lithium phosphate to form a continuous Li-ion-conducting channel on the fiber surface, improving the Li-ion mobility. The ionic conductivity of PVDF-HFP/LiTFSI/LLATO/Li₃PO₄ reached 5.1×10^{-4} S/cm.

Task 4.5 – High Conductivity and Flexible Hybrid Solid-State Electrolyte (Eric Wachsman, Liangbing Hu, and Yifei Mo, University of Maryland)

Project Objective. The project objective is to develop flexible hybrid electrolyte with garnet nanofibers to achieve the following: (1) flexible, with greater mechanical strength (~ 10 MPa) and thermal stability than polymer electrolytes; (2) high room-temperature ionic conductivity, ~ 0.5 mS/cm; (3) stable interface with lithium metal and effective blocking of lithium dendrites at current densities up to 3 mA/cm²; and (4) battery performance with Li-S chemistry with an energy density of ≥ 450 Wh/kg (and ≥ 1000 Wh/L) and maintaining $\geq 80\%$ of capacity up to 500 cycles.

Project Impact. Instability and/or high resistance at the interface of lithium metal with various solid electrolytes limit the use of the metallic anode for batteries with high energy density, such as Li-air and Li-S batteries. The critical impact of this endeavor will be focused on developing a new type of SSE that is highly conductive, highly flexible, and electrochemically stable. The new SSE will enable Li-metal anodes with excellent interfacial impedance and blocking of lithium dendrite formation.

Approach. The project will synthesize garnet nanofibers, fill the porous region with polymer electrolyte, and characterize the flexible hybrid membrane properties. The flexible hybrid SSE microstructure will be determined using focused ion beam (FIB)/SEM and integrated with electrochemical methods to investigate the properties and stability with Li-metal anode.

Out-Year Goals. The project will develop a fundamental understanding of the mechanism of Li-ionic diffusion in garnet nanofibers and their mechanical properties, as well as these properties for hybrid garnet-fiber/polymer hybrids. Work will progress toward the study of the electrode assembly during electrochemical cycling of the anode.

Collaborations. This project funds work at UMD, College Park. Dr. Eric D. Wachsman (PI) will focus on optimizing the garnet network to achieve high ionic conductivity and flexibility using FIB/SEM and EIS characterization. Dr. Liangbing Hu (Co-PI) focuses on synthesis of the hybrid electrolyte and test for Li-metal anode with the hybrid electrolyte. Dr. Yifei Mo (Co-PI) will lead efforts on computational modeling of the garnet nanofiber hybrid electrolytes for fundamental mechanistic understanding.

Milestones

1. Fabricate 4-cm by 4-cm garnet nanofiber membrane. (Q1 – Completed December 2016)
2. Synthesize ion-conductive polymers, synthesize ion-insulation polymers, and *in situ* synthesize polymer electrolyte coated garnet nanofibers. (Q2 – Completed March 2017)
3. Understand Li-ionic diffusion in garnet nanofibers and its response to mechanical deformation. (Q3 – Completed June 2017)
4. Achieve hybrid SSE with high ionic conductivity ($\sim 0.5 \times 10^{-3}$ S/cm), high electrochemical stability (~ 4.5 V), and high mechanical property. (Q4 – Completed September 2017)

Progress Report

Garnet-type $\text{Li}_{6.4}\text{La}_3\text{Zr}_2\text{Al}_{0.2}\text{O}_{12}$ (LLZO) nanofibers were prepared using cellulose textile templates. The templates were soaked in a 2.5 mol/L LLZO precursor solution for 24 h. Calcination of the precursor impregnated templates was conducted in oxygen at different temperatures to obtain garnet fibrous membrane. The crystalline phase of the LLZO was confirmed by XRD. The garnet nanofibers after sintering show cubic phase crystalline structure, which matches very well with the standard $\text{Li}_5\text{La}_3\text{Nb}_2\text{O}_{12}$ (JCPDS card 80-0457). The garnet fibers retained the characteristic physical features of the original template (Figure 29b).

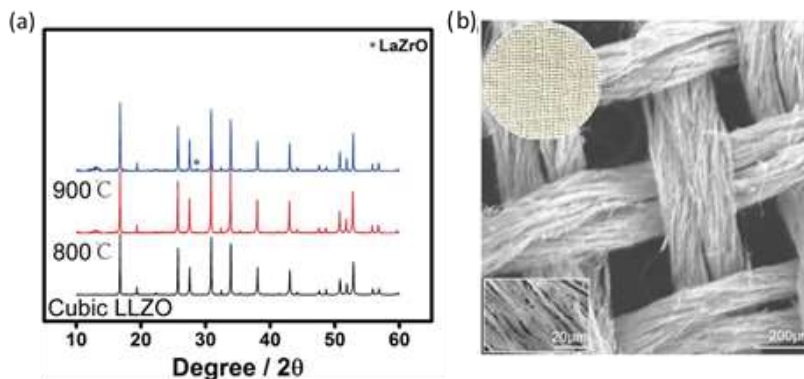


Figure 29. Characterization of garnet fibrous membrane: (a) Powder X-ray diffraction patterns of the crushed garnet textile sintered at different temperatures; and (b) scanning electron microscopy image of the garnet textile converted from the precursor solution impregnated template.

Nano-indentation is a technique widely used for determining mechanical properties of the near-surface region of materials. By combining the application of low loads, measuring the resulting displacement, and determining the contact area between the tip of the indenter and the sample, hardness (H) and elastic modulus (E) are able to be measured. The position of the center of the garnet nanofiber was evaluated with individual scans of the atomic force microscopy (AFM) image, and the location of the fiber was manually adjusted. As shown in Figure 30a-b, hardness and Young's modulus of garnet fiber are 0.28 ± 0.04 GPa and 6.3 ± 0.5 GPa, respectively.

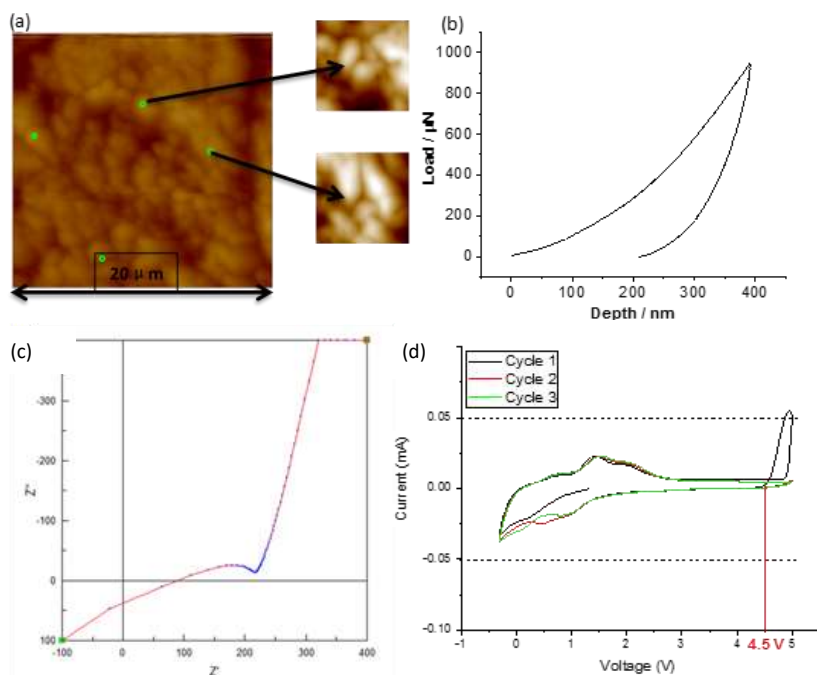


Figure 30. Mechanical characterization of garnet nanofibers: (a) Atomic force microscopy scanning of the nano-indent points on garnet nanofiber; and (b) load-depth profile of garnet fiber. Electrochemical characterization of hybrid composite polymer electrolyte: (a) electrochemical impedance spectroscopy, Li-ion conductivity is 6.07×10^{-4} S/cm; and (b) cyclic voltammetry, stable up to 4.5 V.

Hybrid composite polymer electrolyte was prepared by mixing the garnet fibers with polymer electrolyte (LiTFSI-PEO). The as-obtained hybrid SSE shows good flexibility. Figure 30c-d shows the EIS and cyclic voltammetry (CV) of the hybrid electrolyte based garnet fibers. The Li-ion conductivity is 6.07×10^{-4} S/cm measured at room temperature. According to the CV measurement of the hybrid SSE, its electrochemical voltage window is stable up to 4.5 V.

Patents/Publications/Presentations

Publication

- Gong, Y., and K. Fu, S. Xu, J. Dai, T. R. Hamann, L. Zhang, G. T. Hitz, X. Han, L. Hu, and E. D. Wachsman. “Lithium-Ion Conductive Ceramic Textile: A New Architecture for Flexible Solid-State Lithium Metal Batteries.” *Materials Today*. Minor revision.

Task 4.6 – Self-Forming Thin Interphases and Electrodes Enabling 3D Structured High-Energy-Density Batteries (Glenn Amatucci, Rutgers University)

Project Objective. The project objective is to develop and implement a novel *in situ* formed Li-metal-based metal fluoride battery that will enable packaged 10 mAh batteries of energy densities > 1000 Wh/L and > 400 Wh/kg at 12 V.

Approach. The project focuses on the coalescence of three main aspects of the baseline technology, corresponding to the three sub-tasks of the project: the self-forming chemistry comprised of electrodes and electrolyte, electrode and electrolyte fabrication, and cell design.

Impact. Successful realization of 3D batteries formed *in situ* with a practical approach to large-scale fabrication would address some of the DOE EV performance goals, including: (1) areal capacity increase, (2) improved rates, and (3) designs to enable high-voltage unit cells.

Out-Year Goals. Work will continue toward improvement of reactive current collectors and cell design to optimize electrochemical performance of the cell stack in terms of energy density both gravimetric and volumetric as well as capacity retention upon cycling. A secondary focus will be implementation of bipolar design within the cell structure.

Collaborations. All project tasks will be performed at Rutgers University.

Milestones

1. Establish cell-stack design to achieve the first *Go/No-Go* point with 50% utilization of the positive reactive current collector. (Q1 – Completed by December 2017)
2. Implement maskless scalable patterning technique for fabrication of solid-state cells demonstrating electrochemical activity upon *in situ* formation. (Q2 – Completed by March 2017)
3. Establish bi-ion solid-state conducting glass composition with ionic conductivity $> 1 \times 10^{-4}$ S/cm prior to *in situ* formation. (Q3 – Completed by December 2017)
4. Establish positive reactive current collector compositions that achieve 50% of the theoretical energy density. (Q4 – In progress).
5. *Go/No-Go*: Achieve self-formed cell-stack with > 500 Wh/L and 200 Wh/kg at a rate of C/10. (Q4 – In progress).

Progress Report

This quarter, the project continued developing the reactive positive current collector compositions and microstructure to further improve the utilization or degree of conversion into the initial amount of active metal fluoride during *in situ* formation. The project has been able to achieve consistent progress in the past year by improving the reactive positive current collector utilization from 24% in last quarter to over 30% this quarter. The project does not foresee any technical barriers that would prevent achievement of the 50% target of milestone 1.

The main focus has shifted toward improvement of the full-cell energy density at higher rates. As such, two major approaches were investigated for the cell design. The first consisted of evaluation of significant changes to the cell architecture, which allowed for overcoming barriers that were initially stunting further cell formation. The second approach involved hybridization of transport pathways. Each approach contributed in different ways to improving the cell design. It was concluded that changes to the architecture did not significantly contribute to a steep change in rate capability, but did show overall higher energy and utilization. Hybridization resulted in greater than an order of magnitude increase in discharge current densities and enabled the project to achieve C/10 rate capability. Figure 31 shows the voltage profile obtained with a full-cell design using hybridization, illustrating the cell *in situ* formation followed by a discharge segment at a 0.54C rate followed by relaxation step, then another discharge segment at a faster 0.27C rate. The project demonstrated a path to achieve over an order of magnitude improvement in current density leading to initial results achieving > C/10 discharge rates.

Through advancements in chemistry and architecture, the project surpassed the year-end goal of self-formed cell-stack energy density of 500 Wh/L to achieve 570 Wh/L. Through this methodology, consistent progress has been realized during the past year from 5% of the 500-Wh/L goal in the second quarter, to 70% in the third quarter, to 120% this quarter.

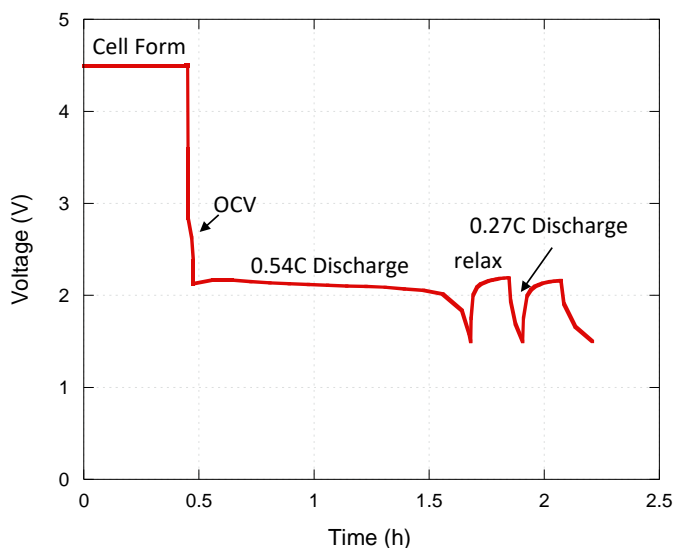


Figure 31. Voltage profile of a cell utilizing hybridization of the transport pathways showing the *in situ* formation and first discharge.

Task 4.7 – Dual Function Solid-State Battery with Self-Forming, Self-Healing Electrolyte and Separator (Esther Takeuchi, Stony Brook University)

Project Objective. The project objective is to demonstrate a solid-state rechargeable battery based on a Li-metal anode and iodine cathode with a self-forming, self-healing electrolyte and separator with high gravimetric and volumetric energy density.

Project Impact. This program will enable demonstration of the proposed rechargeable battery with improved power capability, high energy density, and a self-forming, self-healing SSE/separator. Technical insight will be gained regarding improved conductivity of the solid lithium iodide (LiI) based electrolyte, power capability of the proposed system, the self-healing nature of the LiI layer, the nature of the electrode-electrolyte interfaces, and feasibility of the system to reach the DOE targets.

Approach. The proposed concept is a dual function rechargeable solid-state battery utilizing LiI combined with silver iodide (AgI) as the electrolyte, with lithium metal (and small quantities of silver metal) as the anode and iodine as the cathode with a self-forming, self-healing separator/electrolyte. The battery will be assembled in the discharged state where the anode and cathode will be created during the first formation (charge) step. Initially, silver ion (Ag^+) will diffuse toward the negative electrode and be reduced to silver metal (Ag^0), and iodine ion (I^-) will be oxidized to elemental iodine (I_2) at the cathode side. As the formation of the battery continues, lithium ion (Li^+) will form a Li-metal layer at the anode, with generation of iodine at the cathode. LiI will remain and serve as both the separator and electrolyte.

Out-Year Goals. This is a multiyear program where the effort is divided into three major tasks.

- Year 1 involves electrolyte preparation and characterization including preparation of SSEs and conductivity measurements.
- Year 2 will focus on cell construction and testing including both *in situ* and *ex situ* analysis.
- Year 3 will focus on cell characterization. Under the program, cycle life, efficiency, energy density, and the functional capacity of cells will be determined.

Collaborations. This project collaborates with Amy Marschilok and Kenneth Takeuchi of Stony Brook University.

Milestones

1. Reagents procured; composition, purity, and water content verified. (Q1 – Complete)
2. Develop methodology for AC impedance measurement as a function of temperature. (Q2 – Complete)
3. Identify the four most conductive silver-containing LiI solid electrolytes for further study. (Q3 – Complete)
4. At least one electrolyte with conductivity $\geq 10^{-3}$ S/cm. (Q4 – Complete)

Progress Report

Identification of Electrolyte with Conductivity $\geq 10^{-3}$ S/cm. The fourth-quarter milestone (*Go/No-Go*) was the identification of at least one electrolyte with conductivity $\geq 10^{-3}$ S/cm. The project used its previously demonstrated method of measuring AC electrochemical impedance methodology of solid electrolytes to measure LiI-based solid electrolytes with varying compositions, including the polymeric additives poly-2-vinylpyridine and 3-hydroxypropionitrile. The team successfully achieved the goal by identifying two electrolyte compositions with conductivities $\geq 10^{-3}$ S/cm at 30°C (Table 5).

Table 5. Conductivity of LiI with additives at 30°C.

Sample	σ , 30° C (S/cm)
A. LiI + additives	1.0×10^{-3}
B. LiI + additives	1.1×10^{-3}

Feasibility Demonstration. Initial charging data demonstrates proof of concept for feasibility of *in situ* generation of anode, cathode, and solid electrolyte/separator, with notable decrease in EIS after charge (Figure 32a-b). Characterization demonstrated *in situ* generation of lithium or silver and iodine. A more highly conductive composite electrolyte (Composition I) containing LiI, AgI, and additives was also successfully charged (Figure 32c).

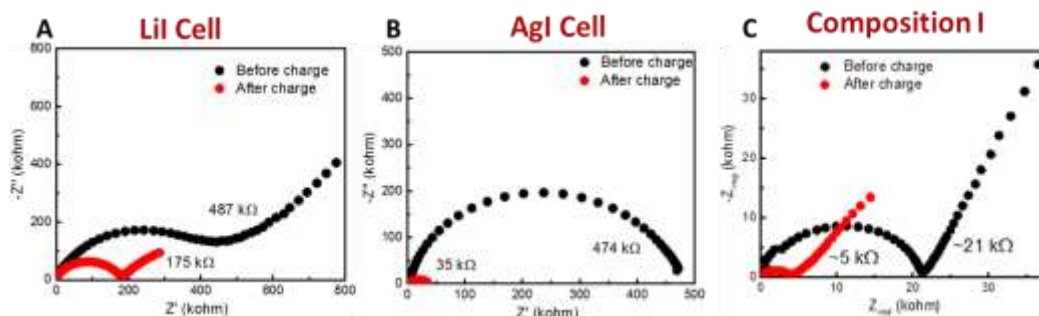


Figure 32. Electrochemical impedance spectroscopy data: (a) pristine LiI solid electrolyte before and after charging, (b) pristine AgI solid electrolyte before and after charging, and (c) Composition I, a LiI-based electrolyte with AgI and polymer additive before and after charging.

Role of Interface. *Ex situ* measurements of the solid electrolyte demonstrated the importance of the electrolyte-substrate interface contribution to total measured resistance. A LiI-based composite electrolyte (Composition II) was explored in cells using four different interfaces demonstrating the role of the interface. Figure 33a shows the resistance before and after charge (inset). Figure 33b illustrates step-wise charging of the cells with increasing currents made possible by impedance decrease on charge. Figure 33c shows OCV stability at 2.8 V for charged cells consistent with the Li/I₂ couple.

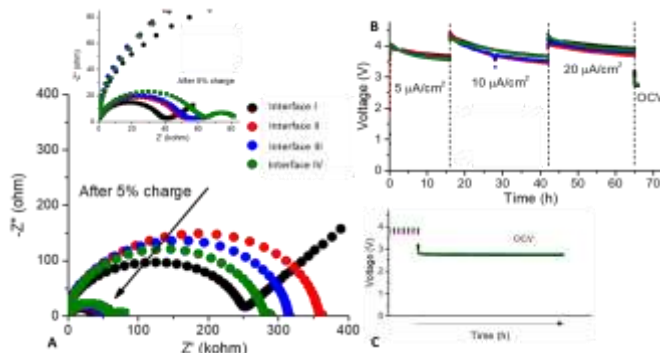


Figure 33. (a) Electrochemical impedance spectroscopy data of electrolyte Composition II before and after (inset) charging using four different interface conditions. (b) Step-wise charging of cells. (c) After step-wise charging, all cells maintained stable OCV.

Highlights of Year 1. The highlights of the first year are as follows:

- Identified LiI-based solid electrolytes with conductivities $\geq 10^{-3}$ S/cm.
- Modified electrolyte/substrate interface to reduce total measured resistance, a key feature in cell design.
- Demonstrated step-wise charging with increasing current levels that decreases total charge time.
- Demonstrated OCV stability for cells after charge, showing successful *in situ* formation of active Li/I₂ cell.

Patents/Publications/Presentations

Presentations

- BMR/ABR/Battery 500 Research Information Exchange, Berkeley, California (January 17–19, 2017): “Dual Function Solid State Battery with Self-Forming Self-Healing Electrolyte and Separator”; E. Takeuchi, A. Marschilok, and K. Takeuchi.
- Program Officer Site Visit, Stony Brook University, Stony Brook, New York (May 3, 2017): “Dual Function Solid State Battery with Self-Forming Self-Healing Electrolyte and Separator”; E. Takeuchi, A. Marschilok, and K. Takeuchi.
- DOE 2017 Annual Merit Review (AMR), Washington, D. C. (June 5–9, 2017): “Dual Function Solid State Battery with Self-Forming Self-Healing Electrolyte and Separator”; E. Takeuchi, A. Marschilok, and K. Takeuchi. Poster.

TASK 5 – DIAGNOSTICS

Summary and Highlights

To meet the goals of the VTO Multi-Year Program Plan and develop lower-cost, abuse-tolerant batteries with higher energy density, higher power, better low-temperature operation and longer lifetimes suitable for the next-generation of HEVs, PHEVs, and EVs, there is a strong need to identify and understand structure-property-electrochemical performance relationships in materials, life-limiting and performance-limiting processes, and various failure modes to guide battery development activities and scale-up efforts. In the pursuit of batteries with high energy density, both high cell operating voltages and demanding cycling requirements lead to unprecedented chemical and mechanical instabilities in cell components. Successful implementation of newer materials such as silicon anode and high-voltage cathodes also requires better understanding of fundamental processes, especially those at the solid/electrolyte interface of both anode and cathode.

This Task takes on these challenges by combining model system, *ex situ*, *in situ*, and *operando* approaches with an array of state-of-the-art analytical and computational tools. Four subtasks are tackling the chemical processes and reactions at the electrode/electrolyte interface. Researchers at LBNL use *in situ* and *ex situ* vibrational spectroscopy, far- and near-field scanning probe spectroscopy and laser-induced breakdown spectroscopy (LIBS) to understand the composition, structure, and formation/degradation mechanisms of the SEI at silicon anode and high-voltage cathodes. The University of California at San Diego (UCSD) combines STEM/EELS, XPS and *ab initio* computation for surface and interface characterization and identification of instability causes at both electrodes. At the University of Cambridge, NMR is being used to identify major SEI components, their spatial proximity, and how they change with cycling. Subtasks at BNL and PNNL focus on the understanding of fading mechanisms in electrode materials, with the help of synchrotron-based X-ray techniques (diffraction and hard/soft X-ray absorption) at BNL and HRTEM and spectroscopy techniques at PNNL. At LBNL, model systems of electrode materials with well-defined physical attributes are being developed and used for advanced diagnostic and mechanistic studies at both bulk and single-crystal levels. These controlled studies remove the ambiguity in correlating material's physical properties and reaction mechanisms to performance and stability, which is critical for further optimization. The final subtask takes advantage of the user facilities at ANL that bring together X-ray and neutron diffraction, X-ray absorption, emission and scattering, HRTEM, Raman spectroscopy, and theory to investigate the structural, electrochemical, and chemical mechanisms in the complex electrode/electrolyte systems. The diagnostics team not only produces a wealth of knowledge key to developing next-generation batteries, it also advances analytical techniques and instrumentation that have a far-reaching effect on material and device development in various fields.

Task 5.1 – Model System Diagnostics for High-Energy Cathode Development (Guoying Chen, Lawrence Berkeley National Laboratory)

Project Objective. This project will use a rational, non-empirical approach to design and synthesize next-generation high-energy, high-voltage cathode materials. Combining a suite of advanced diagnostic techniques with model cathode materials and model electrode/electrolyte interfaces, the project will perform systematic studies to achieve the following goals: (1) obtain new insights into solid-state chemistry, particularly cationic and/or anionic redox activities during charge and discharge of high-capacity Li-TM oxides, (2) gain fundamental understanding on cathode/electrolyte interfacial chemistry and charge transfer process as a function of operating voltage, (3) reveal performance- and stability-limiting properties and processes in high-energy, high-voltage cathodes, and (4) develop strategies to mitigate the structural and interfacial instabilities.

Project Impact. The project will improve the commercial viability of next-generation high-energy cathode materials. The findings will enable more stable high-voltage cycling of existing Li-TM oxides as well as development of novel high-capacity cathode materials for advanced Li-ion batteries.

Approach. Prepare crystal samples of Li-stoichiometric and Li-excess TM oxides with well-defined physical attributes. Perform advanced diagnostic and mechanistic studies at both bulk and single-crystal levels. Global properties and performance of the samples will be established from the bulk analyses, while the single-crystal-based studies will utilize time- and spatial-resolved analytical techniques to probe the material redox transformation process and failure mechanisms under battery operating conditions.

Out-Year Goals. Obtain fundamental knowledge on performance-limiting physical properties, phase transition mechanisms, parasitic reactions, and transport processes that prevent cathode materials from delivering higher capacities and achieving more stable cycling at high voltages. Develop approaches to mitigate cathode structural and interfacial instabilities during high-voltage operation. Design and synthesize optimized Li-TM oxide cathodes as well as novel high-energy electrode materials.

Collaborations. This project collaborates with the following: G. Ceder, K. Persson, M. Doeff, and P. Ross (LBNL); V. Srinivasan (ANL); Simon Mun (Gwangju Institute of Science and Technology, GIST); Y. Liu (SSRL); J. Guo (ALS); C. Wang (PNNL); C. Grey (Cambridge); and A. Huq and J. Nanda (ORNL).

Milestones

1. Synthesize model Li-TM oxide cathode materials with several different chemical compositions and/or morphologies. (Q1 – Completed December 2016)
2. Investigate the bulk activities of TM and oxygen redox centers in Li-TM oxides as a function of state of charge and temperature. (Q2 – Completed March 2017)
3. *Go/No-Go*: Investigate synthesis methods for preparing single crystals of Li-excess TM oxides with previously reported reversible oxygen redox activities. *No-Go* if high-quality crystals of the oxide cannot be made. (Q3 – Completed June 2017)
4. Determine the activities of lattice oxygen and TM on particle surface and the impact of cathode chemistry and surface facet. (Q4 – Completed September 2017)

Progress Report

In collaboration with B. McCloskey at University of California at Berkeley, *operando* DEMS was used to examine the process of extracting lattice O^{2-} in the form of evolved gas. Figure 34 shows the first two cycle results obtained from a $Li_{1.3}Nb_{0.3}Mn_{0.4}O_2$ half-cell cycled at a current density of 25 mA/g. Both CO_2 and O_2 evolution were detected in the first cycle. CO_2 evolution began around 3.8 V during the charge, and completed around the mid-discharge cycle (blue guidelines). There was an increase in intensity around the mid-plateau after the onset of O_2 evolution, and the peak CO_2 evolution was reached at the end of charge at 4.8 V. Oxygen gas was not detected until the mid-plateau region at about 4.5 V, which also peaked at the upper cut-off voltage of 4.8 V. Oxygen evolution completes at the beginning of first discharge (red guidelines), and no O_2 was detected in the following cycle.

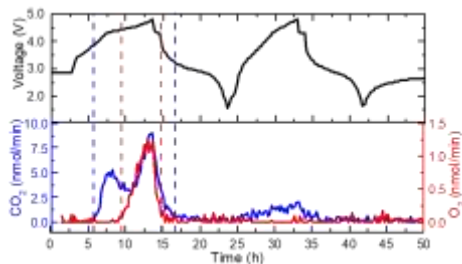


Figure 34. Differential electrochemical mass spectrometry analysis results obtained from a $Li_{1.3}Nb_{0.3}Mn_{0.4}O_2$ half-cell.

Evaluation on oxygen activities during first delithiation was then carried out by soft XAS measurements at SSRL. Depth profiling from surface to bulk was achieved by using two different detectors in total electron yield (TEY) and fluorescence yield modes that have a typical probing depth of 5 and 50 nm, respectively. Figure 35a-b shows the evolution of TEY and fluorescence yield O *K*-edge XAS spectra as a function of lithium content in $Li_xNb_{0.3}Mn_{0.4}O_2$. In both cases, the spectra can be separated into the pre-edge region and post-edge region at the black dashed line (533 eV). Features in the post-edge region are often attributed to $O1s \rightarrow O2p$ -TM4s4p hybridization, while those in the pre-edge region are attributed to $O1s \rightarrow O2p$ -TM3d hybridization. The

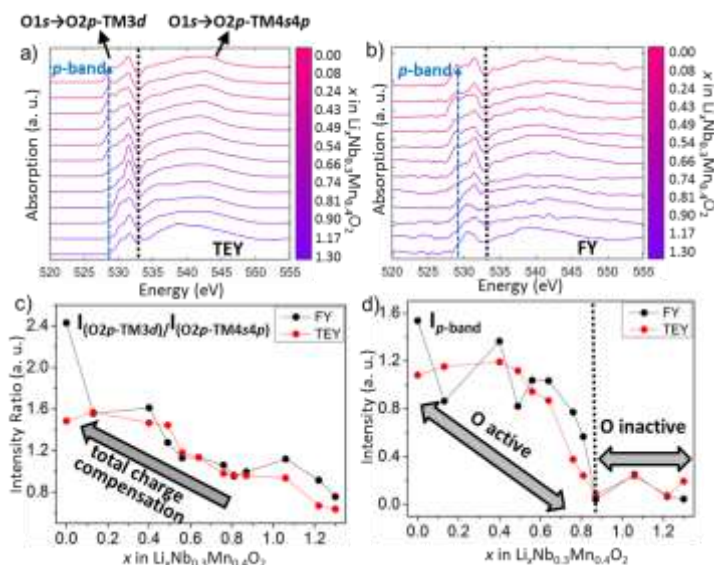


Figure 35. (a-b) Total electron yield and fluorescence yield O *K*-edge soft X-ray absorption spectra. (c-d) Intensity ratio between pre-edge and post-edge peaks and intensity of the *p*-band as a function of lithium content in $Li_xNb_{0.3}Mn_{0.4}O_2$.

this new hybridization arises from the interaction between oxygen anions as a result of oxygen redox activities. Further quantification shows that the initial *p*-band intensity in the pristine $Li_{1.3}Nb_{0.3}Mn_{0.4}O_2$ is extremely low, which remains nearly constant below lithium content of ~ 0.9 (Figure 35d), suggesting negligible interactions between oxygen anions or oxygen redox activities. As x decreases below 0.9, there is a rapid increase in the *p*-band intensity, and it continues to rise until full delithiation ($x = 0$). Results indicate an increase in oxygen valence states in this region and participation of oxygen redox for charge compensation. Note that the *p*-band intensity in the $x < 0.9$ region is generally higher in the fluorescence yield mode than in the TEY, consistent with a difference in oxygen activities mostly involving O^{2-} anion oxidation to O^{n-} ($0 < n < 2$) species in the bulk and lattice oxygen loss on the surface.

pre-edge region is therefore of most interest and may be used as a qualitative measure for holes generated from electron extraction, either from oxygen or TM at the $O2p$ -TM3d energy level. As expected, both TEY and fluorescence yield spectra exhibit significant increase in the pre-edge peak intensity with lithium extraction from $Li_{1.3}Nb_{0.3}Mn_{0.4}O_2$, which is demonstrated by the continuous increase in the ratio between the pre-edge peaks and post-edge absorption peaks (Figure 35c). A new low-energy shoulder peak at 529 eV also appeared and gradually grew along with delithiation, suggesting the involvement of additional O-TM hybridization (referred to as *p*-band) during the process. Due to the similarity between the *p* band and the pre-edge absorption peak observed in peroxide and super-peroxide species, the project speculates

Patents/Publications/Presentations

Publication

- Kan, W. H., and S. Kuppan, L. Cheng, M. Doeff, J. Nanda, A. Huq, and G. Chen. “Crystal Chemistry and Electrochemistry of $\text{Li}_x\text{Mn}_{1.5}\text{Ni}_{0.5}\text{O}_4$ Solid Solution Cathode Materials.” *Chemistry of Materials* 29, no. 16 (2017): 6818. doi: 10.1021/acs.chemmater.7b01898.

Task 5.2 – Interfacial Processes – Diagnostics (Robert Kostecki, Lawrence Berkeley National Laboratory)

Project Objective. This collaborative project involves developing and applying advanced experimental methodologies to study and understand the mechanism of operation and degradation of high-capacity NMC materials for Li-ion cells for PHEV and EV applications. The main objective is to apply *in situ* and *ex situ* far- and near-field optical multi-functional probes to obtain detailed insight into the active material structure and the physicochemical phenomena at electrode/electrolyte interfaces of stoichiometric NMCs with high nickel contents such as 622 and 523 composition materials at a spatial resolution that corresponds to the size of basic chemical or structural building blocks. The primary goal of these studies is to unveil the structure and reactivity at hidden or buried interfaces and interphases that determine material, composite electrode, and full-cell electrochemical performance and failure modes.

Project Impact. Instability and/or high resistance at the interface of high-voltage Li-ion cathodes limits electrochemical performance of high-energy density batteries. A better understanding of the underlying principles that govern these phenomena is inextricably linked with successful implementation of high-energy-density materials such as silicon and high-voltage cathodes in Li-ion cells for PHEVs and EVs. The proposed work constitutes an integral part of the concerted effort within the BMR Program, and it supports development of new cathode materials for high-energy Li-ion cells.

Approach. The pristine and cycled NMC powders and electrodes will be probed using a variety of surface- and bulk-sensitive techniques, including Fourier transform infrared (FTIR), attenuated total reflection (ATR)-FTIR, near-field infrared and Raman spectroscopy and microscopy, and scanning probe microscopy to identify and characterize changes in materials structure and composition. Novel *in situ/ex situ* far- and near-field optical multi-functional probes in combination with standard electrochemical and analytical techniques are developed to unveil the structure and reactivity at interfaces and interphases that determine materials electrochemical performance and failure modes.

Out-Year Goals. Determine the degradation mechanism(s) of high-voltage cathodes; propose and test effective remedies to intrinsic interfacial instability of these materials and composite electrodes.

Collaborations. NMC materials and composite electrodes tested under different cycling regimes by M. Doeff (LBNL) and C. Ban (NREL) will be studied. The diagnostic studies will be carried out in sync with DEMS analysis by B. McCloskey (LBNL) and other diagnosticians in the BMR program. This project will also work closely with V. Battaglia (LBNL) to obtain samples from full-cell cycling experiments.

Milestones

1. Determine relationship between surface reconstruction and aging/cycling of NMC powders/electrodes. (Q1– Completed December 2016)
2. Complete *in situ* AFM characterization of interfacial activity of the model NMC material in organic carbonate electrolytes. (Q3 – Completed June 2017)
3. Determine composition of surface film and its effect on electrochemical performance of NMC electrodes. (Q3 – Completed June 2017)
4. Determine relationship between surface reconstruction, film formation, and metal dissolution in NMC electrodes. (Q4 – Completed September 2017)

Progress Report

This quarter, the project studied the effect of TM dissolution from NMC cathodes on the electrochemical performance of lithium anode. The mechanism of electrolyte oxidation at NMC cathode surface during high-voltage operation, producing Me-organic coordination compounds is illustrated in Figure 36a.^[1] These compounds form a surface film and also dissolve into the electrolyte. To understand the effect of these dissolved compound on Li-metal anode performance, control coin cells NMC/Li/1M LiPF₆, EC/DEC (vol. 1:2) were assembled with or without 500 ppm of manganese(III) acetylacetonate (Mn(III)(acac)₃) additive, and their cycling performance was compared. As Figure 36b shows, capacity retention in both cells is similar during the 1st to 40th cycles. However, the cell with Mn(III)(acac)₃ experienced significant capacity fading compared to the control cell without the Mn(III)(acac)₃ additive during long-term cycling.

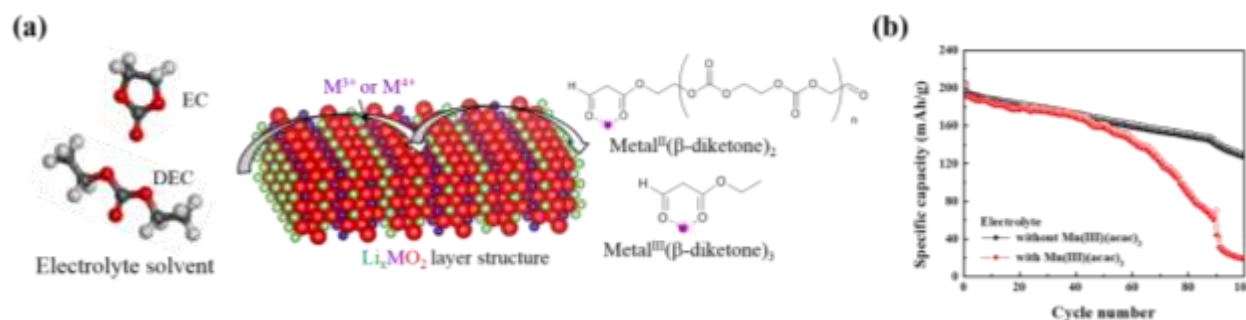


Figure 36. (a) Schematic diagram of metal organic compound formation from NMC cathode. (b) Capacity-cycling plot of NMC cathode / lithium anode cells electrolyte with/without 500 ppm Mn(III)(acac)₃. (Cells galvanostatically cycling between 2–4.7 V at 0.5C.)

To isolate the possible effect of Mn(III)(acac)₃ on the lithium anode, the cyclic performance of Li/Li/1M LiPF₆, EC/DEC (vol. 1:2) symmetric cells with or without Mn(III)(acac)₃ additive was compared. Figure 37a shows no voltage polarization in both cells during the first 30 cycles. However, prolonged cycling led to a significant polarization increase, which was more pronounced in the cell with Mn(III)(acac)₃. Cell impedance was measured at s10, 20, 30, 40, and 50 cycle and the corresponding Nyquist plots and the overall impedance at 37 Hz are shown in Figure 37b and 37c, respectively. Both cells show similar modest impedance increase during the initial 30 cycles. However, the impedance of the cell with Mn(III)(acac)₃ additive shows sharp increase during prolonged cycling (> 30). Such a significant raise of impedance of the lithium cell may explain the observed capacity fading of the NMC/lithium cell (Figure 36a) with Mn(III)(acac)₃ additive in the electrolyte. In summary, these results demonstrate that Mn(III)(acac)₃ poisoning is equally detrimental to Li-metal electrode as previously observed for graphite anodes and possibly other (inter)metallic electrodes such as tin and silicon.

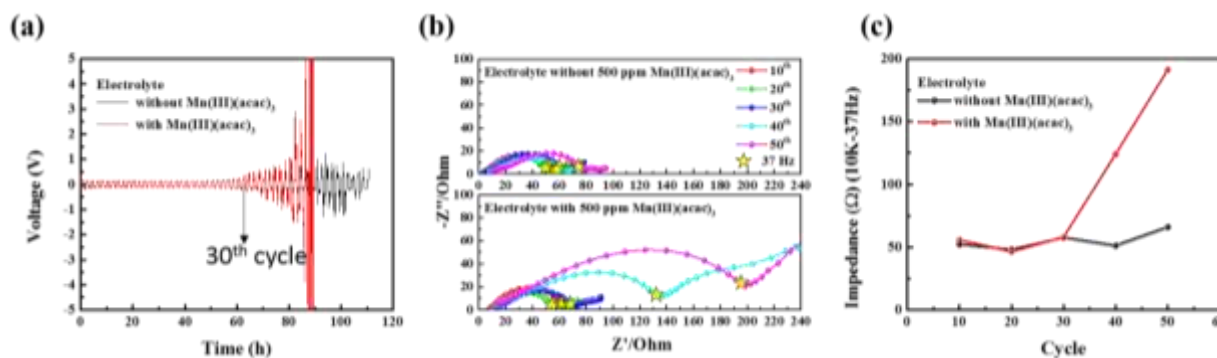


Figure 37. Electrochemical performance of the Li/Li symmetrical cell with different electrolyte additives during subsequent charge/discharge cycling at 1 mA/cm² current density with 1-h interval. (a) Development of overpotentials. (b) Nyquist plot measured at OCV. The yellow star marked in each curve is the impedance at 37 Hz. (c) Impedance at 37 Hz at selected cycle.

[1] Jarry, A., and S. Gottis, Y. S. Yu, J. Roque-Rosell, C. Kim, J. Cabana, J. Kerr, and R. Kostecki. *J. Am. Chem. Soc.* 137 (2015): 3533.

Task 5.3 – Advanced *In Situ* Diagnostic Techniques for Battery Materials (Xiao-Qing Yang and Seongmin Bak, Brookhaven National Laboratory)

Project Objective. The primary project objective is to develop new advanced *in situ* material characterization techniques and to apply these techniques to support development of new cathode and anode materials for the next generation of Li-ion batteries for PHEVs. To meet the challenges of powering the PHEV, Li-ion batteries with high energy and power density, low cost, good abuse tolerance, and long calendar and cycle life must be developed.

Project Impact. The VTO Multi-Year Program Plan describes the goals for battery: “Specifically, lower-cost, abuse-tolerant batteries with higher energy density, higher power, better low-temperature operation, and longer lifetimes are needed for development of the next-generation of HEVs, PHEVs, and EVs.” The knowledge gained from diagnostic studies through this project will help U.S. industries develop new materials and processes for new generation Li-ion batteries in the effort to reach these VTO goals.

Approach. This project will use the combined synchrotron-based *in situ* X-ray techniques (XRD, and hard and soft XAS) with other imaging and spectroscopic tools such as HRTEM and MS to study the mechanisms governing the performance of electrode materials.

Out-Year Goals. Complete the first-stage development of diagnostic technique to study effects of microstructural defects on performance fading of high-energy-density LMR cathode materials for Li-ion batteries using pair distribution function (PDF), XRD, and XAS combined with STEM imaging and TXM. Apply these techniques to study the structural changes of various new cathode materials.

Collaborations. The BNL team will work closely with material synthesis groups at ANL (Drs. Thackeray and Amine) for the high-energy composite; and at PNNL for the Si-based anode materials. The project will also collaborate with industrial partners at GM and Johnson Controls, as well as with international collaborators.

Milestones

1. Complete the structure studies of $\text{Li}_2\text{Ru}_{0.5}\text{Mn}_{0.5}\text{O}_3$, as a model compound for Li- and Mn- rich (LMR) high-energy-density cathode materials using PDF to correlate the voltage and capacity fading with microstructural defects in this type of material. (Q1 – Completed December 2016)
2. Complete the structure studies $\text{Li}_2\text{Ru}_{0.5}\text{Mn}_{0.5}\text{O}_3$, as a model compound for LMR high-energy-density cathode materials using STEM to correlate the voltage and capacity fading with microstructural defects in this type of material. (Q2 – Completed March 2017)
3. Complete the XRD and XAS studies of $\text{Li}_2\text{Ru}_{0.5}\text{Mn}_{0.5}\text{O}_3$ cathode material samples with different cycle history (charge and discharge limit and cycle numbers). (Q3 – Completed June 2017)
4. Complete the structure studies of $\text{Li}_{1.2}\text{Ni}_{0.15}\text{Co}_{0.1}\text{Mn}_{0.55}\text{O}_2$ for LMR high-energy-density cathode materials using STEM to correlate the voltage and capacity fading with microstructural defects in this type of material. (Q4 – Completed September 2017)

Progress Report

The fourth milestone for FY 2017 was completed. BNL has been focused on the structure studies of $\text{Li}_{1.2}\text{Ni}_{0.15}\text{Co}_{0.1}\text{Mn}_{0.55}\text{O}_2$ for Li- and Mn-rich (LMR) high-energy-density cathode materials using STEM to correlate the voltage and capacity fading with micro-structural defects in this type of materials. To pinpoint the structure nucleation and evolution, the project performed atomic-resolution annular dark-field scanning transmission electron microscopic (ADF-STEM) imaging, spatially resolved EELS, and ADF-STEM tomography. Using ADF-STEM tomography, the 3D internal structures of the cathode material before and after 15 charge-discharge cycles were reconstructed. The 3D-rendered reconstructions in Figure 38 qualitatively show that a new population of large pores had formed in the interior of the cycled particle after 15 cycles. By analyzing the pore size distributions (Figure 38c-d), it can be quantitatively concluded that the large pores observed in Figure 38b belong to a new modal that did not appear in the pristine samples. The volume weighted distribution shows that the large-pore modal contributes to the majority of porosity in the material. As formation of the large pores are correlated with charge cycles, they are likely formed by nucleating vacancies that had been left behind by oxygen loss, agreeing well with the “lattice densification” model.

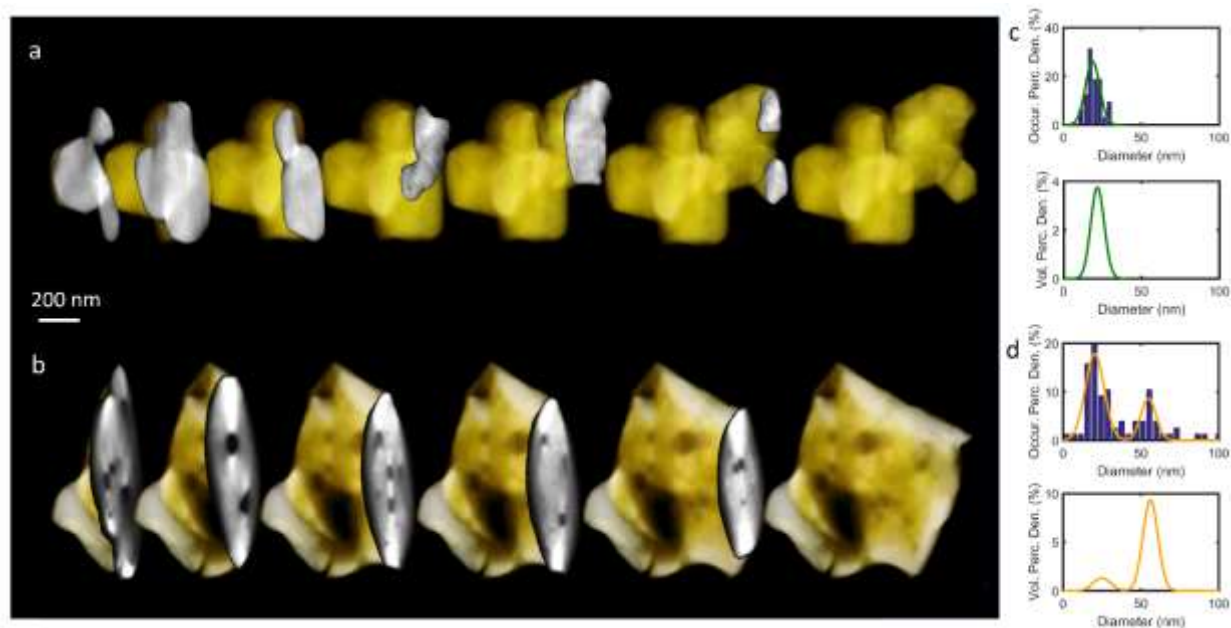


Figure 38. Three-dimensional electron tomography reconstructions of (a) pristine and (b) after 15 charge-discharge cycles of $\text{Li}_{1.2}\text{Ni}_{0.15}\text{Co}_{0.1}\text{Mn}_{0.55}\text{O}_2$ material. The internal pore size distribution weighted by occurrence (upper) and by volume (lower) of (c) the pristine materials and (d) the sample after 15 cycles.

Patents/Publications/Presentations

Publications

- Liu, Jue, and Pamela S. Whitfield, Michael R. Saccomanno, Shou-Hang Bo, Enyuan Hu, Xiqian Yu, Jianming Bai, Clare P. Grey, Xiao-Qing Yang, and Peter G. Khalifah. “*In Situ* Neutron Diffraction Studies of Ion Exchange Synthesis Mechanism of $\text{Li}_2\text{Mg}_2\text{P}_3\text{O}_9\text{N}$: Evidence for Hidden Phase Transition.” *J. Am. Chem. Soc.* (2017). Publication date: July 6, 2017; doi: 10.1021/jacs.7b02323.
- Lin, Feng, and Yijin Liu, Xiqian Yu, Lei Cheng, Andrej Singer, Oleg G. Shpyrko, Huolin L. Xin, Nobumichi Tamura, Chixia Tian, Tsu-Chien Weng, Xiao-Qing Yang, Ying Shirley Meng, Dennis Nordlund, Wanli Yang, and Marca M. Doeff. “Synchrotron X-ray Analytical Techniques for Studying Materials Electrochemistry in Rechargeable Batteries.” *Chemical Review*. Publication date (web): September 29, 2017; doi: 10.1021/acs.chemrev.7b00007.

Presentation

- 12th International Forum on Lithium Battery Technology & Industrial Development, Xinixiang, China, (September 19–21, 2017): “Characterizations of High Energy Density Cathode Materials Using Synchrotron Based XAS and Transmission X-ray Microscopy as Well as 3-Dimensional STEM Tomography”; Enyuan Hu, Xiao-Qing Yang, Seong-Min Bak, Ruoqian Lin, Zulipiya Shadike, Hung-Sui Lee, Xuelong Wang, Huolin Xin, Yijin Liu, Xiqian Yu, and Hong Li. Invited.

Task 5.4 – Nuclear Magnetic Resonance and Magnetic Resonance Imaging Studies of Solid Electrolyte Interphase, Dendrites, and Electrode Structure (Clare Grey, University of Cambridge)

Project Objective. The growth of a stable SEI on most electrode materials is key to long-term capacity retention of a working Li-ion battery. On anodes such as silicon, this is particularly critical because the continual expansion and contraction of this intermetallic upon alloying with lithium exposes fresh, reactive surfaces that result in further electrolyte decomposition and SEI growth. This project will perform a detailed multinuclear NMR study of the SEI that forms on silicon, where thick SEIs typically grow and where SEI stability is a key aspect hindering commercialization of this technology. The focus will be to determine how additives (for example, FEC) and charging parameters (for example, voltage) influence the composition and stability of the SEI. Fundamental studies of SEI structure *in operando* will be complemented by a synthetic program aimed at preparing new silicon coatings based on phosphazene (P-N) elastomeric polymers to increase CE. Further, the nature of the SEI is one factor that appears to control the type of lithium microstructures that form on lithium metal during cycling. To test this hypothesis, the project will use MRI to investigate lithium dendrite versus moss formation in different electrolytes as a function of salt concentration and with different additives. Finally, it will compare lithium and sodium metal anode chemistries to determine the composition, morphology, and stability of local structures that form on sodiating anodes such as tin and hard carbons.

Project Impact. The first impact of this project will be a molecular-level understanding of how factors such as applied voltage and electrolyte additives modify the SEI that forms on silicon anodes. The insight gained from these studies will guide the design of new P-N coatings for silicon. A rationally designed surface coating has the potential to improve SEI stability, and thus increase CE for silicon and beyond. A description of how SEI composition influences lithium microstructures will provide the foundation to mitigate dendrite formation during cycling that currently limits the safety of many promising electrode materials. These approaches will be extended to study Na-ion battery electrodes to provide an understanding of how to chemically manipulate both electrodes as well as the electrolyte to avoid adverse failure mechanisms in next-generation batteries.

Out-Year Goals. The project goals are as follows: (a) determine the effect of voltage and additives (for example, FEC) on the composition of the silicon SEI; (b) synthesize and test new inorganic coatings to increase the CE seen on cycling silicon; (c) identify correlations between SEI structure and thickness and Li-metal dendrite formation; and (d) determine the local and long-range structures formed on cycling sodium anode materials and compare with lithium. To facilitate these goals, the project will prepare ^{13}C -enriched FEC for ^{13}C NMR multinuclear studies to investigate the SEI that forms on silicon during cycling. It will synthesize new P-N polymers for coating silicon nanoparticles and probe changes in performance in the presence of these coatings. In addition, the project will use MRI to correlate lithium dendrite formation with the nature of the SEI. Finally, it will apply the methods developed to study lithium chemistries to investigate sodium electrodes.

Collaborations. This project collaborates with B. Lucht (University of Rhode Island); J. Cabana, (University of Illinois – Chicago); Y. Shirley Meng (UCSD), S. Whittingham (SUNY – Binghamton); P. Bruce (St. Andrews); S. Hoffman and A. Morris (Cambridge); and P. Shearing (University College London).

Milestones

1. Synthesis of ^{13}C FEC. (Q1 – Complete)
2. Prepare P-N coatings on silicon (Q2 – Complete); Develop *in situ* ^{19}F NMR studies of FEC. (Q2 – Ongoing)
3. Multinuclear NMR studies of SEI coatings on silicon with FEC. (Q3 – Complete; first manuscript published, and second manuscript in preparation)
4. Test P-N coatings (Ongoing); MRI/dendrite studies of 2 ionic liquids. (Q4 – Ongoing; focus on additives)

Progress Report

The overarching goal of this study was to understand the phases formed during sodium insertion in high capacity tin anodes for Na-ion batteries. *Ab initio* random structure searching (AIRSS) and high-throughput screening using a species-swap method allowed the project to explore the phase chemistry of the Na-Sn system and predict new structures. These structures were linked to experiments using *operando* PDF analysis, XRD, ^{23}Na solid-state nuclear magnetic resonance (ssNMR), and *ex situ* ^{119}Sn ssNMR. Here, the project identified: (1) the number and nature of the crystalline phases formed during the first electrochemical process; (2) the structural features of the amorphous phase formed during the second electrochemical process; and (3) the phase formed during the third process.

Figure 39 shows electrochemistry data for a Na-Sn cell compared to theoretical predictions. From *operando* PDF and ssNMR (Figure 40), XRD measurements, and theoretical calculations, the project proposed the following discharge mechanism for the Na-Sn system:

- Process 1: $\text{Sn} \rightarrow \text{NaSn}_3$
- Process 1': $\text{Sn}, \text{NaSn}_3 \rightarrow \text{NaSn}_2$
- Process 2: $\text{NaSn}_2 \rightarrow a\text{-Na}_{1.2}\text{Sn}$
- Process 2': $a\text{-Na}_{1.2}\text{Sn} + \text{NaSn}_2 \rightarrow a\text{-Na}_{1.2}\text{Sn} + \text{expanded Na}_{1+x}\text{Sn}_2$ (solid solution)
- Process 3: $a\text{-Na}_{1.2}\text{Sn} + \text{expanded Na}_{1+x}\text{Sn}_2 \rightarrow \text{Na}_{4.4}\text{Sn}_2$
- Process 3': $\text{Na}_{4.4}\text{Sn}_2 \rightarrow \text{Na}_{4.75}\text{Sn}_2$ (solid solution)
- Process 4: $\text{Na}_{4.75}\text{Sn}_2 \rightarrow \text{Na}_{15}\text{Sn}_4$
- Process 4': $\text{Na}_{15}\text{Sn}_4 \rightarrow \text{Na}_{15+x}\text{Sn}_4$

The first electrochemical process of sodium insertion into tin results in the conversion of crystalline tin into a layered structure consisting of mixed Na/Sn occupancy sites intercalated between planar hexagonal layers of tin atoms (NaSn_3 ; Figure 41, left panel). Following this, NaSn_2 , which is predicted to be thermodynamically stable, forms NaSn_2 containing hexagonal layers closely related to NaSn_3 , but has no tin atoms between the layers. In Process 2, NaSn_2 is broken down into an amorphous phase of approximate composition $\text{Na}_{1.2}\text{Sn}$, which is predicted to exhibit tin chains. *Operando* ssNMR and PDF refinements show evidence that further reaction with sodium results in the formation of structures containing Sn-Sn dumbbells, which interconvert through a solid-solution mechanism in Process 3'. These structures are based upon $\text{Na}_{5-x}\text{Sn}_2$, with increasing occupancy of one of its sodium sites commensurate with the amount of sodium added (Figure 41b, right panel). Finally, ssNMR results indicate that the final product, $\text{Na}_{15}\text{Sn}_4$, can store additional sodium atoms as an off-stoichiometry compound, $\text{Na}_{15+x}\text{Sn}_4$, analogous to previous observations in the Li-Si

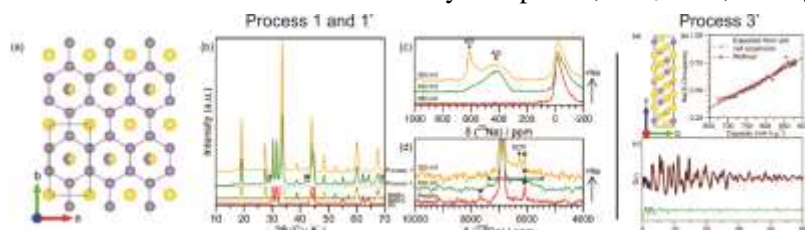


Figure 41. Left panel: (a) Structure of NaSn_3 -*Pmmn* with sodium in yellow and tin in purple. (b) *Operando* X-ray diffraction patterns. (c) *Ex situ* ^{23}Na and (d) ^{119}Sn 60 kHz magic angle spinning nuclear magnetic resonance at the end of process 1 and 1'. Right panel: (a) Structure of $\text{Na}_{5-x}\text{Sn}_2$. (b) Occupancy versus sodium site 3 versus time spent on process 3'. (c) Fit of the pair distribution function corresponding to the first frame in process 3'.

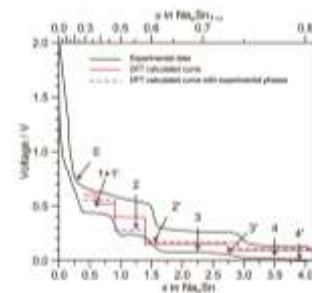


Figure 39. Experimental (black) electrochemistry of a Na-Sn cell cycled at C/20 between 2 and 0.001 V compared to theoretical (red/blue) predictions.

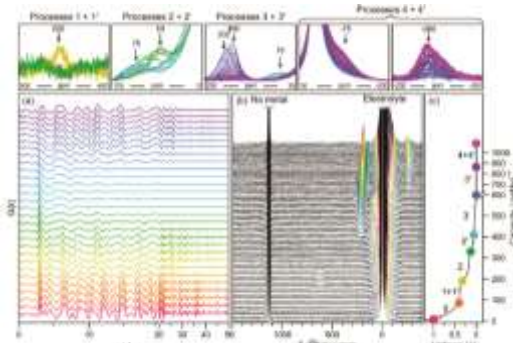


Figure 40. *Operando* (a) pair distribution functions and (b) ^{23}Na nuclear magnetic resonance spectra for Na-Sn cells aligned with corresponding electrochemistry (c).

system. Taken together, this work provides the first evidence for significant solid solution behavior and resulting metastability in the Na-Sn system. These findings have implications beyond the Na-Sn system, highlighting the fact that even in a system under apparent thermodynamic control, the nature of electrochemical alloying means that kinetic considerations remain of primary importance.

Patents/Publications/Presentations

Publication

- Jin, Y., and N.-J. H. Kneusels, P. C. M. M. Magusin, G. Kim, E. Castillo-Martinez, L. E. Marbella, R. N. Kerber, D. J. Howe, S. Paul, T. Liu, and C. P. Grey. “Identifying the Structural Basis for the Increased Stability of the Solid Electrolyte Interphase Formed on Silicon with the Additive Fluoroethylene Carbonate.” *J. Am. Chem. Soc.* (2017). Accepted. doi: 10.1021/jacs.7b06834.

Presentations

- Experimental NMR Conference, Monterey, California (March 2017).
- ACS Meeting, San Francisco, California (April 2017).
- 21st International Conference on Solid State Ionics, Padua, Italy (June 2017).
- Iupac Meeting, Sao Paolo (July 2017).
- ISE Meeting, Providence, Rhode Island (September 2017).
- Alpine NMR meeting, Chamonix-Mont Blanc, France (September 2017).
- 232nd ECS Meeting, National Harbor, Maryland (October 2017).

Task 5.5 – Advanced Microscopy and Spectroscopy for Probing and Optimizing Electrode-Electrolyte Interphases in High-Energy Lithium Batteries (Shirley Meng, University of California – San Diego)

Project Objective. The proposed research aims to develop advanced microscopy and spectroscopy tools to probe, understand, and optimize the anion activities that govern the performance limitations such as capacity and voltage stabilities in high-energy Li-excess TM (such as nickel, cobalt, manganese) oxides cathode materials. The approach uniquely combines atomic resolution STEM, EELS, *operando* Bragg Coherent Diffraction Imaging (BCDI), and first principles computation to probe anion redox and oxygen evolutions in Li-excess NMC materials. Furthermore, the project will track the lithium and oxygen dynamics under electrochemical testing via *operando* neutron diffraction, which will enhance understanding of the overall structural changes due to anion activities. Ultimately, this will hone in on the synthesis efforts to produce the modified materials with optimum bulk compositions and surface characteristics at large scale for consistently good performance. The above-mentioned characterization tools will be extended to diagnose various anode types, such as Li-metal anode.

Project Impact. If successful, this research will enable *operando* imaging at the single particle level by advanced microscopy imaging and high energy resolution O K-edge EELS. This work will provide an in-depth understanding of anion activities in high-voltage electrode materials, which can lead to significant improvement in stabilizing operation voltage and electrode-electrolyte interface for future generation high-energy-density electrodes.

Approach. This unique approach combines STEM/EELS, *operando* BCDI, and *ab initio* computation as diagnostic tools for probing anion redox and oxygen evolutions in Li-excess NMC materials. This allows for pinning down the atomistic/molecular mechanism of anion oxidation and determining the speciation compositions and surface characteristics for enabling high rate and long life in the proposed materials. Neutron enables the characterization of bulk material properties to enhance and further optimize high-energy electrode materials.

Out-Year Goals. The goal is to probe and control oxygen activity in the high-energy composite cathodes and to characterize electrode/electrolyte interface in lithium anodes so that their cycle life and efficiency can be significantly enhanced.

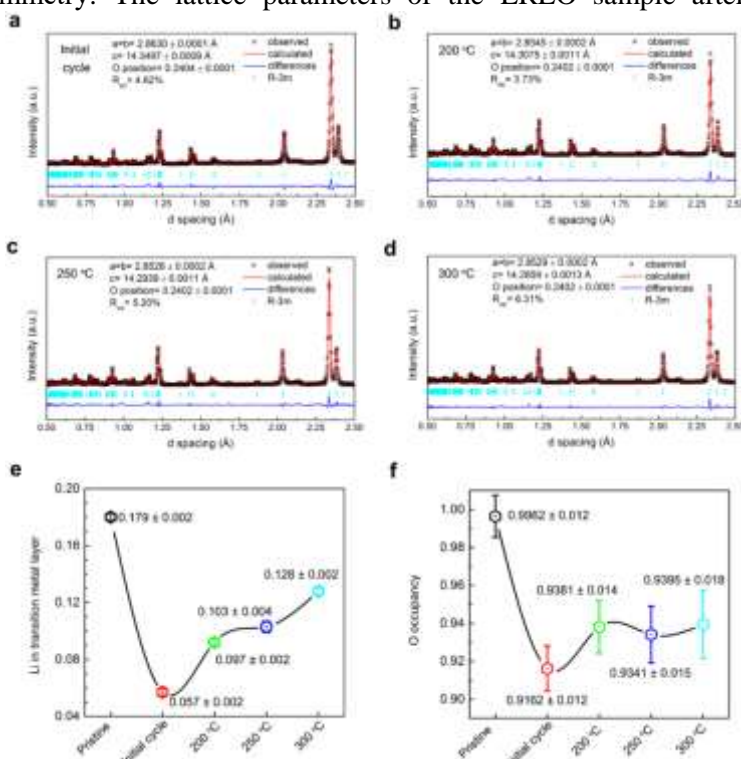
Collaborations. This work funds collaborations on EELS (Miaofang Chi, ORNL); neutron diffraction (Ken An, ORNL); and soft XAS (Marca Doeff, LBNL). It supports collaborative work with Zhaoping Liu and Yonggao Xia at Ningbo Institute of Materials Technology and Engineering in China. It also supports collaboration with Battery500 consortium.

Milestones

1. Neutron diffraction characterization of Li-rich layered oxide for structure recovery. (Completed September 2017).
2. BCDI characterization on single particle of Li-rich layered oxide after cycling. (December 2017 – On track)
3. Chemical composition and structure of electrochemically deposited lithium metal at nano scale. (December 2017 – On track)

Progress Report

Investigation of Structure Recovery in Li-Rich Layered Oxide (LRLO) by Neutron Diffraction. Last quarter, the project demonstrated that bulk structure and working voltage of the cycled LRLO electrode can be recovered through high-temperature annealing ($> 150^\circ\text{C}$). After heat treatment, the superstructure ordering is recovered, which is decisive in restoring the original voltage output of LRLO cathode. Neutron diffraction (ND), a technique with high sensitivity for detecting light elements, was applied to investigate structure transformation of the cycled electrode after heat treatment. Figure 42a-d shows the as-collected TOF ND patterns with ‘Rietveld’ refinement for LRLO cycled electrodes before and after heat treatment. All patterns can be refined well with a layered structure of ‘ $R-3m$ ’ symmetry. The lattice parameters of the LRLO sample after initial cycle are $a = 2.8630(1) \text{ \AA}$, and $c = 14.3497(9) \text{ \AA}$. In comparison, both a and c lattice parameters are reduced after annealing under different temperature. This trend counteracts common effect of material thermal expansion, which indicates structure transformation occurs with strain decrease. To illustrate local structure changes in terms of atomic migration induced by heat treatment, lithium occupancy in TM layer and oxygen occupancy are also shown in Figure 42. After initial cycle, lithium from the TM layer is largely irreversible, with only 32% of lithium reinsertion. Oxygen vacancies are also observed in the cycled sample, which results in a large fraction of under-coordinated TM ions. These unstable TM ions can potentially migrate to fully coordinated octahedral sites nearby. Irreversible lithium insertion together with TM ions migration dramatically alters cation ordering in the TM layer, and thus leads to structure disorder. Surprisingly, lithium occupancy in the TM layer and oxygen occupancy increases for the cycled sample after heat treatment, which is a strong indication of structure ordering recovery. The influence of lithium and oxygen migration during heat treatment on cation ordering in the TM layer will be studied in detail based on nudged elastic band method from *ab initio* computation.



LRLO electrode after the initial cycle. (b-d) Refined ND patterns of the initially cycled electrode after heat treatment under 200, 250, and 300 °C, respectively. (e) Lithium occupancy in transition metal layer and (f) oxygen occupancy for different samples.

BCDI Characterization on Single Particle of LRLO after Cycling. The project has demonstrated 3D dislocation network formation by BCDI in LRLO during the initial charging process under *operando* conditions. It has also revealed the link between this crystalline defect and voltage decay in this material. To further investigate the dislocation evolution during cycling, BCDI measurement was performed on LRLO electrode after the first cycle and the fiftieth cycle (see Figure 43a-b). The truncation rod in the diffraction speckle pattern is less symmetric for the sample after 50 cycles compared with that of the sample after only 1 cycle, which typically indicates strain builds up in LRLO material during electrochemical cycling. The project will focus on quantitative analysis to reconstruct 3D displacement field as well as strain distribution in the single particle to illustrate crystalline defects influence on cycling performance of LRLO material.

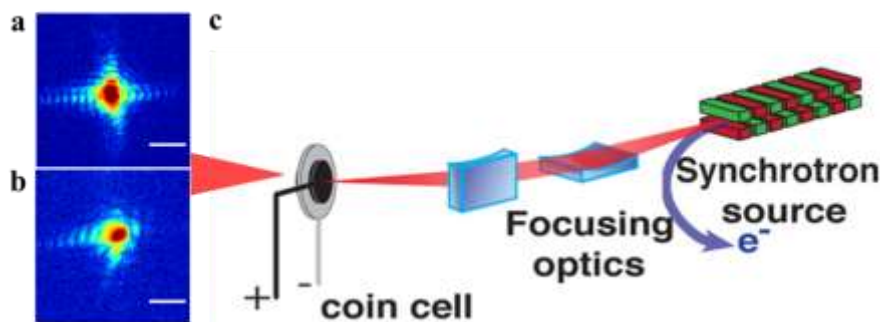


Figure 43. Diffraction data collected for Li-rich layered oxide electrode after the (a) first cycle and (b) fiftieth cycle. (c) Experimental schematic of the *in situ* Bragg Coherent Diffraction Imaging setup. Scale bar is $1e-8$ $1/\text{\AA}$.

Structure and Chemical Composition of Electrochemically Deposited Lithium Metal at Nano Scale

Inspired from the biology community, the project has demonstrated the feasibility of the Cryo TEM to characterize the electrochemically deposited lithium metal (EDLi), especially at the nano scale. The nanostructure of the EDLi is shown in Figure 44a. The identical contrast in the bulk demonstrates the uniformity of the EDLi. Along the edges of the EDLi, an uneven SEI is present with a maximum thickness of ~ 7 nm. Figure 44 surprisingly displays lattice fringes present on the surface rather than the bulk, suggesting that the EDLi metal is amorphous, while part of the SEI is crystalline. The above results were validated by the area FFT patterns. The absence of characteristic bright rings/spots in the bulk area (red square) shows clearly that the EDLi is amorphous (Figure 44b). Conversely, two obvious characteristic bright spots appear at the SEI surface (blue square). The ~ 0.2 -nm lattice spacing is consistent with the lattice plane distance of the LiF (200) and cannot be ascribed to any plane distance of the metallic lithium, further validating the partially crystallized SEI.

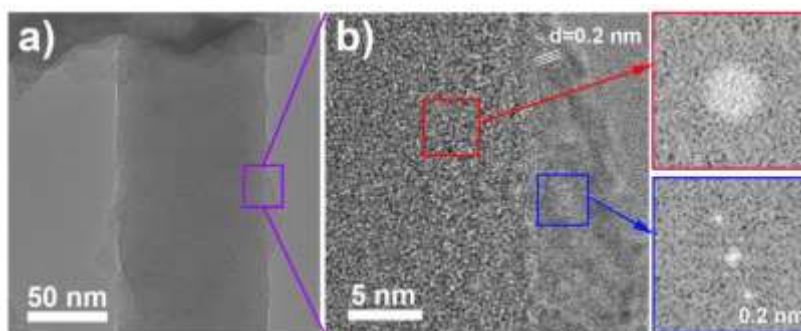


Figure 44. Cryo-transmission electron microscopy (a) image and (b) its regional zoomed-in image with the bulk and surface fast Fourier transformation results of the electrochemically deposited lithium metal using conventional carbonate electrolyte.

Patents/Publications/Presentations

Patent

- Zhang, M., and B. Qiu, and Y. S. Meng. “Structural and Voltage Recovery in Li-rich Layered Oxides.” Provisional U.S. Patent, in application.

Publication

- Wang, X., and M. Zhang, J. Alvarado, S. Wang, M. Sina, B. Lu, J. Bouwer, W. Xu, J. Xiao, J.-G. Zhang, J. Liu, and Y. S. Meng. “New Insights on the Structure of Electrochemically Deposited Lithium Metal and Its Solid Electrolyte Interphases via Cryogenic TEM.” *Nano Letters* (2017). Accepted.

Task 5.6 – *In Situ* Diagnostics of Coupled Electrochemical-Mechanical Properties of Solid Electrolyte Interphases on Lithium Metal Rechargeable Batteries
(Xingcheng Xiao, General Motors; Brian W. Sheldon, Brown University; Yue Qi, Michigan State University; and Y. T. Cheng, University of Kentucky)

Project Objective. The project objective is to develop a comprehensive set of *in situ* diagnostic techniques combined with atomic/continuum modeling schemes to investigate and understand the coupled mechanical/chemical degradation of the SEI layer/lithium system during lithium cycling. The goal of this understanding is to develop a new coating design strategy to achieve high cycle efficiency/dendrite free and extend the cycle life of high-energy-density batteries with lithium as the anode for EV application.

Project Impact. The fundamental understanding of the coupled mechanical/chemical degradation of the SEI layer during lithium cycling will enable the project to identify the desirable mechanical properties on SEI/lithium as a system and the specific transport properties that enable the homogenous lithium stripping/plating while avoiding the mossy structure. Furthermore, it will allow the project to develop a highly impactful strategy to protect lithium metal and achieve dendrite-free high cycle efficiency, which can dramatically increase the energy density of lithium batteries for EV applications.

Approach. Different *in situ* techniques, including AFM, nano-indentor, dilatometer, and stress-sensor, will be developed to investigate the mechanical compatibility between SEI and soft lithium and the relationship between surface morphology and current density distribution that results in an inhomogeneous lithium plating/stripping process. Multiple strategies will be developed to tailor the mechanical and transport properties of SEI and to properly engineer the protective coating/lithium interface.

Out-Year Goals. The project will first develop a lithium film model-system with well-controlled thickness, roughness, and textures for different *in situ* diagnostic tools and cycle performance tests. Then, a comprehensive set of *in situ* diagnostic tools will be adapted from the previous work to characterize the mechanical behavior of both SEI and lithium electrodes. In parallel, the advanced electrochemical characterization and postmortem analysis will be used to characterize the electrochemical performance, composition, and microstructure of the SEI and lithium.

Collaborations. Prof. Huajian Gao (Brown University) and Dr. Qinglin Zhang (GM) will be the key researchers involved in continuum simulation and postmortem analysis. Dr. Chongmin Wang (PNNL), Dr. Wangli Yang (LBNL), and Dr. Jie Xiao will be collaborators on advanced *in situ* analysis and electrolyte additives.

Milestones

1. Li-film electrodes with controlled thickness and roughness developed. (Q1 – Completed December 2016)
2. Composition map of representative SEI as a function of current density and capacity established. (Q2 – Completed March 2017)
3. The results from different tools correlated with SEI microstructure, transport properties, and cycle performance. (Q3 – Completed June 2017)
4. *Go/No-Go*: Decision based on information obtained from *in situ* and *ex situ* experiments demonstrated to be complementary and coherent. (Q4 – Completed September 2017; *Go*)

Progress Report

Investigated the Impact of Surface Coating and Electrolyte on Initial Stages of Lithium Plating and Stripping. The surface condition of Li-metal electrode plays a critical role in lithium plating and stripping. Figure 45 compares the surface morphologies of lithium electrodes after one plating and stripping cycle in a symmetric cell. In carbonate-based electrode, more moss structure and lithium dendrites form on lithium surface, leading to large amount of SEI formed and low cycle efficiency. On the other side, lithium shows the pitting corrosion behavior, where lithium is preferentially stripped away locally from lithium electrode. In contrast, in ether-based electrode (Figure 45b), the plated lithium shows much denser structure and no dendrite forms. However, lithium still shows pitting corrosion although slightly more uniform. Figure 45c shows a 50-nm aluminum film was deposited on Li-metal surface to make current distribution more uniform. As a result, the pitting corrosion behavior was suppressed, but the film promoted dendrite formation. The next step is to further optimize the coating process and select desirable electrolytes to suppress dendrite growth and pitting corrosion.

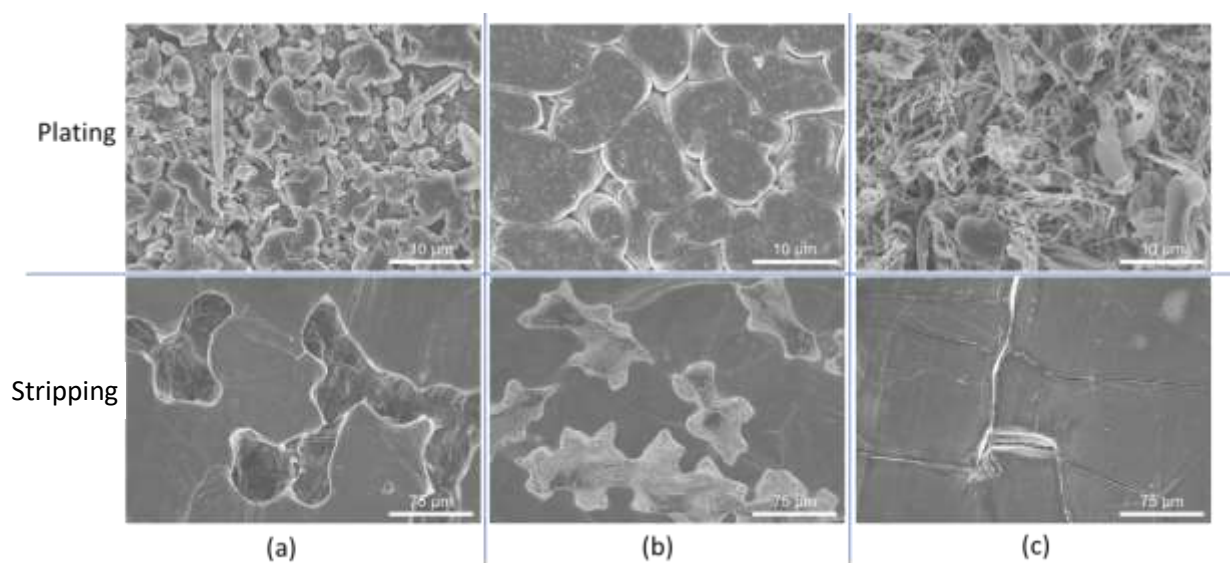


Figure 45. The surface morphology of Li-metal electrode after first plating and stripping cycle. Current density $1\text{mA}/\text{cm}^2$, and lithium capacity $4\text{mAh}/\text{cm}^2$. (a) Lithium electrode in carbonate-based electrolyte. (b) Lithium electrode in ether-based electrolyte. (c) Aluminum film coated lithium electrode in carbonate-based electrolyte.

Investigated the Impact of Morphology Evolution of Lithium Plating and Stripping on Mechanical Stress. An *in situ* stress sensor has been developed to investigate mechanical behavior. The moss structure formed in carbonate-based electrode incorporates more SEI as well as dead lithium in the electrode, leading to slightly higher compressive stress (Figure 46a). In addition, the moss structure also causes more complicated mechanical response since lithium could be plated and stripped in different locations, including lithium bulk metal base and mossy lithium metal on the top. The fracture of SEI layer could also lead to significant stress response. However, the plating and stripping are more uniform, and no dendrite was formed in ether-based electrolyte. As indicated by lower overpotential for lithium plating and stripping, less SEI and dead lithium is incorporated into electrode, which generates lower compressive stress (Figure 46b). Further analysis would be conducted to understand if such compressive stress could lead to the plastic flow in lithium electrode under the SEI layer and its impact on the mechanical integrity of the electrode for long-term cycle stability.

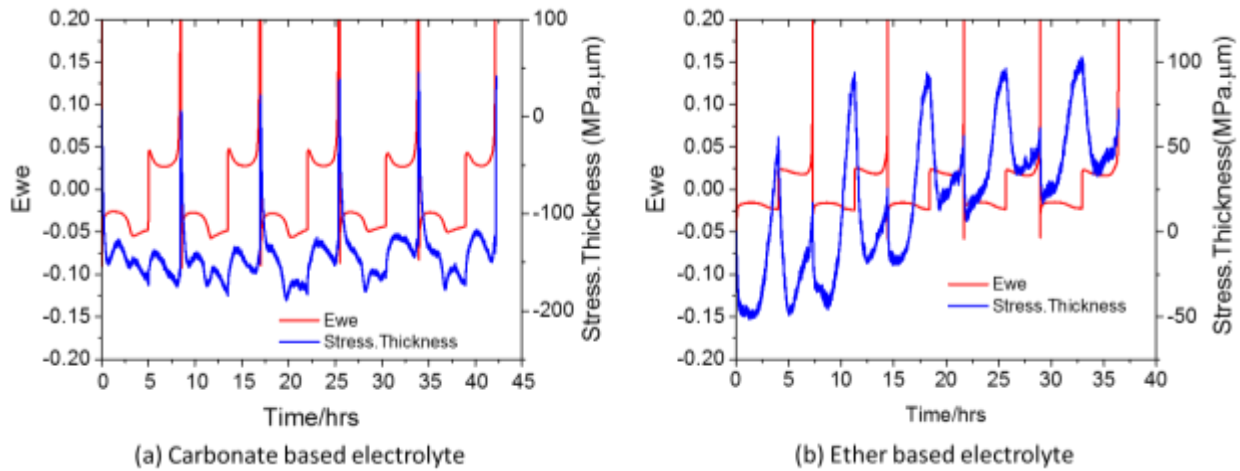


Figure 46. Stress evolution of Li-metal electrodes in different electrolytes.

The Coupled Electrochemical-Mechanical Properties of the SEI on Lithium Metal for Rechargeable Batteries were Investigated. For two typical SEI components, LiF and Li₂O, the bandgaps and band structures were calculated under different loading conditions with density functional theory (DFT) – generalized gradient approximation (GGA) and hybrid (HSE06) functionals. LiF has direct band gap, while Li₂O has indirect band gap. It was found that the band gap decreases under tension and increases under compression. As the primary loading directions are along the Li-F bonds, a structure parameter, h , characterizing the average distances between anions, unifies the variation of band gap with strain under different loading conditions into a single linear function of η for LiF (Figure 47). The structure of Li₂O is quite different from LiF, as the lithium sits in oxygen tetrahedral and oxygen coordinates with 8 lithium neighbors. This causes some s-p hybridization on lithium. More importantly, both the bond distance and bond angle change under uniaxial and biaxial load conditions. The changes in bond angles (some increasing and some decreasing) cause additional small and random variations in band gap. However, all the band gaps can be bounded by the hydrostatic loading condition, which does not cause any bond angle change and, therefore, can be fitted as a linear function of η (dash lines for Li₂O in Figure 47).

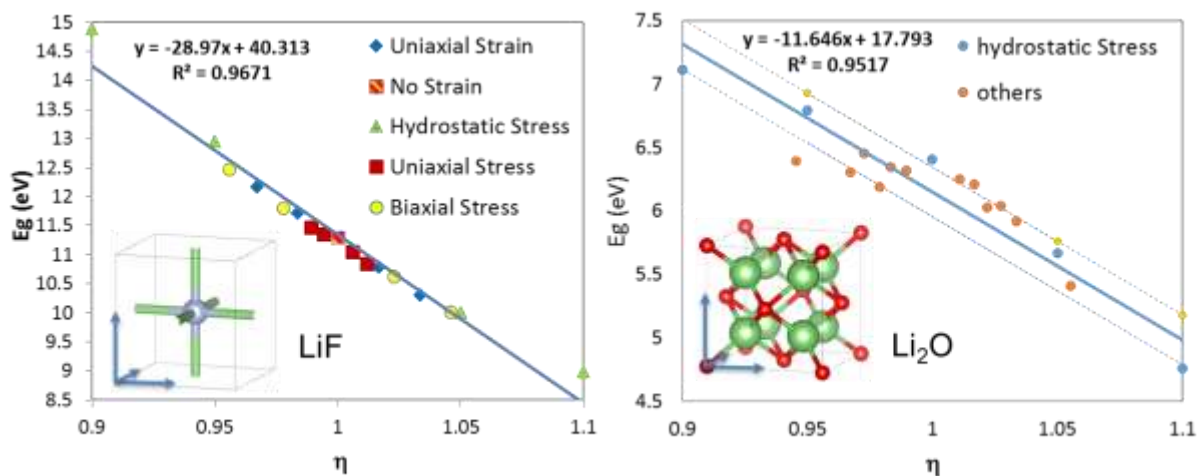


Figure 47. The band gap (HSE06) changes as a function of average anion distance, η .

Patents/Publications/Presentations

Patent

- Xiao, X. “Method of Applying Self-Forming Artificial Solid Electrolyte Interface (SEI) Layer to Stabilize Cycle Stability of Electrode in Lithium Batteries.” United States patent application P042557 (8540R-505), August 2017.

Presentations

- 232nd ECS Meeting, National Harbor, Maryland (October 4, 2017): “Towards High Cycle Efficiency of High Energy Density Lithium Ion Batteries”; X. Xiao. Invited Talk.
- 254th ACS National Meeting, Washington, D. C. (August 2017): “Computational Insights to Charge Transfer Reactions at the Complex Electrode/SEI/Electrolyte Interface”; Yue Qi. Invited talk.
- 54th Annual Technical Meeting of the Society of Engineering Science (SES), Boston, Massachusetts (July 27, 2017): “Ratcheting Induced Deformation and Failure in Li-ion Batteries”; Kai Guo.
- 68th Annual Meeting of the ISE, Providence, Rhode Island (August 28, 2017): “Electrochemically Driven Deformation and Fracture in Solid State Batteries”; Kai Guo.
- 21st International Conference on Solid State Ionics, Padua, Italy (June 18, 2017): “Electrochemically Induced Stress and Fracture in Ceramic Electrolytes”; Brian W. Sheldon. Invited talk.
- SES Annual Meeting, Boston, Massachusetts (July 27, 2017): “Electrochemically Induced Stress and Fracture in Ceramic Electrolytes”; Brian W. Sheldon. Invited talk.
- Annual Meeting of ISE, Providence, Rhode Island (September 1, 2017): “Mechanical Degradation and Optimization of Solid Electrolyte Interphases in Li Ion Batteries”; Ravi Kumar, Jung Hwi Cho, Anton Tokranov, Xingcheng Xiao, and Brian W. Sheldon.

Task 5.7 – Microscopy Investigation on the Fading Mechanism of Electrode Materials (Chongmin Wang, Pacific Northwest National Laboratory)

Project Objective. The objective will be using a combination of *ex situ*, *in situ*, and *operando* HRTEM and spectroscopy to probe the fading mechanism of layer structured cathode under high-voltage operating condition. To complement the HRTEM study, *in situ* liquid cell SIMS and atom probe tomography (APT) will also be used to gain structural and chemical evolution of electrodes and correlate the structural and chemical evolution with battery performance.

Project Impact. The proposed characterization work focused on atomic level structural and chemical analysis and direct correlation with battery fading properties. The work can be directly used to guide the designing of electrode materials with tailored microstructure and chemistry for enhanced properties of increasing the energy density of Li-ion batteries and to accelerate market acceptance of EV, especially for PHEV required by the EV Everywhere Grand Challenge.

Approach. This project will use the unique *ex situ* and *in situ* TEM methods to probe the structure of Li-ion batteries, especially a biasing liquid electrochemical cell that uses a real electrolyte in a nano-battery configuration. It will also use various microscopic techniques, including *ex situ*, *in situ*, and especially the *operando* TEM system, to study the fading mechanism of electrode materials in batteries. This project will be closely integrated with other R&D efforts on high-capacity cathode and anode projects in the BMR Program to: (1) discover the origins of voltage and capacity fading in high-capacity layered cathodes, and (2) provide guidance for overcoming barriers to long cycle stability of electrode materials.

Out-Year-Goals. This project has the following out-year goals:

- Multi-scale (ranging from atomic-scale to meso-scale) *ex situ/in situ* and *operando* TEM investigation of failure mechanisms for energy-storage materials and devices. Atomic-level *in situ* TEM and STEM imaging to help develop fundamental understanding of electrochemical energy-storage processes and kinetics of electrodes.
- Extend the *in situ* TEM capability for energy storage technology beyond lithium ions, such as Li-S, Li-air, Li-metal, sodium ions, and multi-valence ions.

Collaborations. This project collaborates with Michael M. Thackeray and Jason Croy (ANL); Guoying Chen (LBNL); Jagjit Nanda (ORNL); Chunmei Ban (NREL); Khalil Amine (ANL); Donghai Wang (Pennsylvania State University); Arumugam Manthiram (UT Austin); Wei Tong (LBNL); Gao Liu (LBNL); Yi Cui (Stanford University); Jason Zhang (PNNL); Jun Liu (PNNL); Xingcheng Xiao (GM); Shirley Meng (UCSD); and Stan Whittingham (SUNY – Binghamton).

Milestones

1. Void formation mechanism and its correlation with ionic mobility in the lattice upon high-voltage cycling; exploring lattice stability with dopant such as tin, silicon, and phosphorous. (Q2 – Completed March 2017)
2. Atomic-level identification of behavior of nickel, manganese, cobalt, and aluminum in the NCM and NCA when cycled at high voltage; correlate with fading mechanism. (Q3 – Completed June 2017)
3. Environmental TEM (ETEM) studies of the nickel segregation characteristics, and correlation with materials processing temperature. (Q4 – Completed September 2017)

Progress Report

Layered lithium transition metal oxides (LTMO) are promising cathode materials for next generation high-energy-density Li-ion batteries. The challenge for using this category of cathode is the capacity and voltage fading. One factor that contributes to battery fading is the solid-liquid electrolyte interfacial reaction. The side reactions will not only decompose the electrolyte, but also introduce a thick SEI layer on the cathode surface, which is believed to accelerate battery degradation. Therefore, a deep understanding of the chemical and physical processes occurring at the interface between the solid electrode and the liquid electrolyte is crucial for stable operation of batteries. The overwhelming effort on SEI investigations focused on the anode side during past decades. Very limited effort has been made to investigate the SEI formed on the cathode side. However, to achieve high energy density for the next-generation Li-ion batteries, cathodes operating at a higher working voltage (> 4.5 V versus Li/Li^+), such as layered and spinel lithium TM oxides, will be used, which significantly enhance the side reactions between cathode and electrolyte. Previous work has shown that SEI layer is mainly composed of an amorphous organic layer, Li_2CO_3 and LiF . However, the most basic chemical composition and spatial distribution of each component of the SEI and their dependence on the battery operating conditions are still unclear.

STEM coupled with high-sensitivity EDS has been used to investigate the chemical composition and elemental spatial distribution, with high resolution, of the SEI layer formed on the very surface of cathodes that were cycled at a high cutoff voltage (4.7 V) in a typical electrolyte used in Li-ion batteries.

It was found that a significant amount of phosphorus appears in the cathode SEI layer, in addition to other well-known elements, such as carbon, oxygen, and fluorine (Figure 48). Such a P-rich SEI layer presents direct evidence of side reactions between cathodes and LiPF_6 -containing electrolytes. Further studies show that these side reactions can be significantly aggravated at elevated temperature (60°C), but reduced by cycling within a low cutoff voltage (4.2 V versus Li/Li^+) window. Based on the phosphorus content observed on the SEI layers formed in the six cathodes, the electrolyte experiences decreasing stability in the following order: $\text{LiMn}_{1.5}\text{Ni}_{0.5}\text{O}_4 > \text{LiNi}_{0.4}\text{Co}_{0.2}\text{Mn}_{0.4}\text{O}_2$ (NCM424) $> \text{LiNi}_{0.8}\text{Co}_{0.15}\text{Al}_{0.05}\text{O}_2$ (NCA) $> \text{Li}_{1.2}\text{Ni}_{0.13}\text{Co}_{0.13}\text{Mn}_{0.54}\text{O}_2$ (NC-LMR) $\approx \text{Li}_{1.2}\text{Ni}_{0.2}\text{Mn}_{0.6}\text{O}_2$ (20N-LMR) $> \text{Li}_2\text{MnO}_3$. The results indicate that side reactions between electrolyte and cathodes are strongly dependent on cathode structure and chemical composition. In other words, some cathode materials (such as Li_2MnO_3 and LMR cathodes) have strong catalytic effects that promote electrolyte decompositions and, thus, accelerate battery degradation.

The present systematical investigations indicate that such a cathode/Li-salt side reaction shows strong dependence on the structure of the cathode materials, the operating voltage, and the temperature, indicating the feasibility of SEI engineering. These findings provide valuable insights on the interaction between the high-voltage cathode and the electrolyte, as well as the interface evolution upon battery cycling.

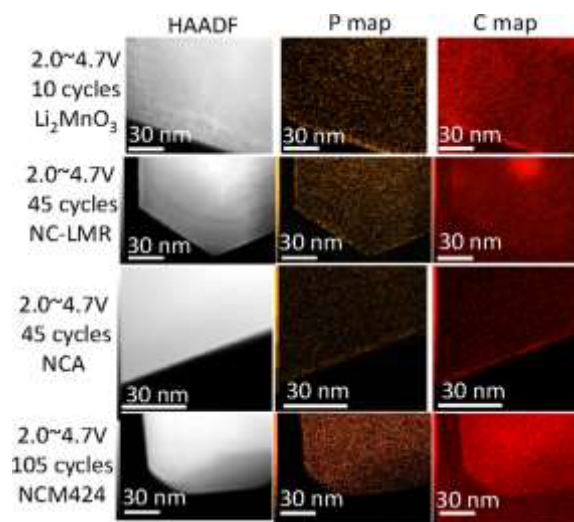


Figure 48. Scanning transmission electron microscopy – energy dispersive spectroscopy map showing the segregation of P and C on the surface of cathode particle of different composition following battery cycling. P and C are typical components from the electrolyte. This observation provides direct evidence on the reaction of cathode with the electrolyte.

Patents/Publications/Presentations

Publication

- Lu, Xiaotang, and Yang He, Scott X. Mao, Chongmin Wang, and Brian A. Korgel. “Size Dependent Pore Formation in Germanium Nanowires Undergoing Reversible Delithiation Observed by *In Situ* TEM.” *J. Phys. Chem. C* 120 (2016): 28825–28831.

Presentation

- Minnesota Microscopy Society Annual Meeting, Minneapolis, Minnesota (September 21–22, 2017): “Probing the Fading Mechanism of Batteries Materials by *In Situ* Transmission Electron Microscopy and Spectroscopy”; Chongmin Wang. Key Note Talk.

Task 5.8 – Characterization and Computational Modeling of Structurally Integrated Electrodes (Michael M. Thackeray and Jason R. Croy, Argonne National Laboratory)

Project Objective. The primary project objective is to explore the fundamental, atomic-scale processes that are most relevant to the challenges of next-generation, energy-storage technologies, in particular, high-capacity, structurally integrated electrode materials. A deeper understanding of these materials relies on novel and challenging experiments that are only possible through unique facilities and resources. The goal is to capitalize on a broad range of facilities to advance the field through cutting-edge science, collaborations, and multi-disciplinary efforts to characterize and model structurally integrated electrode systems, notably those with both layered and spinel character.

Project Impact. This project capitalizes on and exploits DOE user facilities and other accessible national and international facilities (including skilled and trained personnel) to produce knowledge to advance Li-ion battery materials. Specifically, furthering the understanding of structure-electrochemical property relationships and degradation mechanisms will contribute significantly to meeting the near- to long-term goals of PHEV and EV battery technologies.

Approach. A wide array of characterization techniques including X-ray and neutron diffraction, X-ray absorption, emission and scattering, HRTEM, Raman spectroscopy, and theory will be brought together to focus on challenging experimental problems. Combined, these resources promise an unparalleled look into the structural, electrochemical, and chemical mechanisms at play in novel, complex electrode/electrolyte systems being explored at ANL.

Out-Year Goals. The out-year goals are as follows:

- Gain new, fundamental insights into complex structures and degradation mechanisms of high-capacity composite cathode materials from novel, probing experiments carried out at DOE’s user facilities and beyond.
- Investigate structure-property relationships that will provide insight into the design of new or improved cathode materials.
- Use knowledge and understanding gained from this project to develop and scale up advanced cathode materials in practical Li-ion prototype cells.

Collaborators. This project collaborates with the following: Jason R. Croy, Eungje Lee, Arturo Gutierrez, Roy Benedek, and Meinan He of ANL; and Soo Kim and Chris Wolverton of Northwestern University.

Milestones

1. Characterize bulk and surface properties of structurally integrated electrode materials using the DOE User Facilities at ANL, including the APS, Electron Microscopy Center, and Argonne Leadership Computing Facility (ALCF), along with facilities elsewhere (for example, Spallation Neutron Source at ORNL), EMSL at PNNL, and the Northwestern University’s Atomic and Nanoscale Characterization Experimental Center (NUANCE). (Q4 – In progress, September 2017; see text)
2. Use complementary theoretical approaches to further the understanding of structural and electrochemical properties of LS electrodes and protective surface layers. (Q4 – In progress, September 2017)
3. Analysis, interpretation, and dissemination of collected data for publication and presentation. (Q4 – In progress, September 2017)

Progress Report

Lithiated-spinel, LiCoO_2 materials are of interest as potential stabilizing agents to be incorporated in LLS composite cathodes.^[1] Previous experiments have shown that nickel substitution effectively stabilizes the lithiated spinel structure, enhancing electrochemistry. However, manganese substitution results in impurity phases such as Li_2MnO_3 , $\text{Li}_4\text{Mn}_5\text{O}_{12}$, and Co_3O_4 . To obtain better understanding of different effects of manganese and nickel substitution on phase stability, an atomistic simulation of substituted, LiCoO_2 -based, lithiated-spinels was conducted.

The substitution of manganese or nickel on the cobalt site of both spinel (Fd-3m) and layered (R-3m) LiCoO_2 structures was examined via DFT calculations. Possible symmetrically-distinct mixing configurations for $\text{Li}_{16}\text{Co}_{16-x}\text{M}_x\text{O}_{32}$ (up to 64 total atoms; $\text{M} = \text{Mn}$ or Ni ; $0 \leq x \leq 16$) were generated using the Enum package.^[2] Figure 49a displays the calculated ground state DFT formation energy (ΔH_f) of $\text{LiCo}_x\text{M}_{1-x}\text{O}_2$ ($\text{M} = \text{Mn}$ or Ni ; and $0 \leq x \leq 1$) sampled uniformly through the composition space. Here, the DFT formation energy of a generic LiMO_2 compound is defined as $\Delta H_f(\text{LiCo}_x\text{M}_{1-x}\text{O}_2) = E_0(\text{LiCo}_x\text{M}_{1-x}\text{O}_2) - \mu_{\text{Li}} - x\mu_{\text{Co}} - (1-x)\mu_{\text{M}} - 2\mu_{\text{O}}$, where $E_0(\text{LiCo}_x\text{M}_{1-x}\text{O}_2)$ is the calculated DFT total energy of $\text{LiCo}_x\text{M}_{1-x}\text{O}_2$, and μ_i ($i = \text{Li}, \text{Co}, \text{M}, \text{O}$) is the chemical potential of component i . Note that the energy difference between Fd-3m and R-3m structures at each composition is almost negligible, as previously reported.^[3] Furthermore, the calculated ΔH_f of $\text{LiCo}_x\text{M}_{1-x}\text{O}_2$ varies almost linearly between the end-members, LiCoO_2 and LiMO_2 ($\text{M} = \text{Mn}$ or Ni), in Figure 49a.

The mixing tendency of two cathode components, LiCoO_2 and LiMO_2 ($\text{M} = \text{Mn}$ or Ni), can be obtained using: $\Delta E_{\text{mix}} = E_0(\text{LiCo}_x\text{M}_{1-x}\text{O}_2) - \{xE_0(\text{LiCoO}_2) + (1-x)E_0(\text{LiMO}_2)\}$, where $E_0(\text{LiCo}_x\text{M}_{1-x}\text{O}_2)$, $E_0(\text{LiCoO}_2)$, and $E_0(\text{LiMO}_2)$ are the calculated DFT total energies of either Fd-3m or R-3m $\text{LiCo}_x\text{M}_{1-x}\text{O}_2$, LiCoO_2 , and LiMO_2 ($\text{M} = \text{Mn}$ or Ni), respectively. A significantly negative ΔE_{mix} (that is, < -25 meV/site) usually leads to the formation of an ordered compound, while a significantly positive ΔE_{mix} (that is, > 25 meV/site) usually results in a two-phase miscibility gap. In contrast, a slightly negative or positive ΔE_{mix} (that is, -25 to 25 meV/site) indicates a weak preference for ordering or phase separation, respectively, which could be overcome by configurational entropy at elevated temperatures to form a solid-solution. From Figure 49b, it can be observed that manganese substitution in either Fd-3m or R-3m $\text{LiCo}_x\text{Mn}_{1-x}\text{O}_2$ is only favorable at dilute concentrations of Mn ($x > 0.9$). In fact, the mixing of manganese and cobalt on the cobalt sublattice in the LCO structure becomes increasingly unfavorable toward equiatomic compositions of manganese and cobalt. On the other hand, as seen in Figure 49c, the mixing of nickel and cobalt on the cobalt sublattice is generally favorable at all compositions. The energy of mixing becomes increasingly negative (up to ~ -100 meV/site) toward equiatomic compositions of nickel and cobalt; hence, compositions close to $\text{LiCo}_{0.5}\text{Ni}_{0.5}\text{O}_2$ are likely to form ordered compounds. These simulation data are in line with previous experimental results, and corroborate the effectiveness of nickel substitution on stabilizing lithiated spinel structure and improving its electrochemistry.

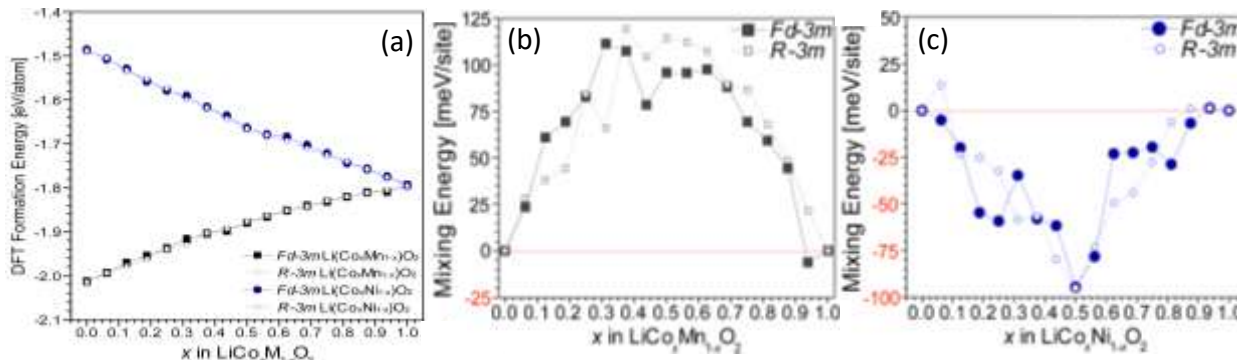


Figure 49. (a) Calculated density functional theory formation energies of $\text{LiCo}_x\text{M}_{1-x}\text{O}_2$ ($\text{M} = \text{Mn}$ or Ni ; $0 \leq x \leq 1$) in both lithiated spinel (Fd-3m) and layered (R-3m) structures. The mixing energies of (b) $\text{LiCo}_x\text{Mn}_{1-x}\text{O}_2$ and (c) $\text{LiCo}_x\text{Ni}_{1-x}\text{O}_2$.

- [1] Lee, E., and J. Blauwkamp, F. C. Castro, J. Wu, V. P. Dravid, P. Yan, C. Wang, S. Kim, C. Wolverton, R. Benedek, F. Dogan, J. S. Park, J. R. Croy, and M. M. Thackeray. “Exploring Lithium-Cobalt-Nickel Oxide Spinel Electrodes for ≥ 3.5 V Li-Ion Cells.” *ACS Appl. Mater. Interfaces* 8 (2016): 27720.
- [2] Hart, G. L. W., and R. W. Forcade. “Algorithm for Generating Derivative Structures.” *Phys. Rev. B* 77 (2008): 224115.
- [3] Wolverton, C., and A. Zunger. “Cation and Vacancy Ordering in Li_xCoO_2 .” *Phys. Rev. B* 57, no. 4 (1998): 2242.

Patents/Publications/Presentations

Publication

- Benedek, Roy. “Role of Disproportionation in the Dissolution of Mn from Lithium Manganate Spinel.” *J. Phys. Chem. C.* (2017). doi:10.1021/acs.jpcc.7b05940.

TASK 6 – MODELING ADVANCED ELECTRODE MATERIALS

Summary and Highlights

Achieving the performance, life, and cost targets outlined in the EV Everywhere Grand Challenge will require moving to next generation chemistries, such as higher capacity Li-ion intercalation cathodes, silicon and other alloy-based anodes, Li-metal anode, and sulfur cathodes. However, numerous problems plague development of these systems, from material-level challenges in ensuring reversibility to electrode-level issues in accommodating volume changes, to cell-level challenges in preventing cross talk between the electrodes. In this task, a mathematical perspective is applied to these challenges to provide an understanding of the underlying phenomenon and to suggest solutions that can be implemented by the material synthesis and electrode architecture groups.

The effort spans multiple length scales from *ab initio* methods to continuum-scale techniques. Models are combined with experiments, and extensive collaborations are established with experimental groups to ensure that the predictions match reality. Efforts are also focused on obtaining the parameters needed for the models, either from lower-length scale methods or from experiments. Projects also emphasize pushing the boundaries of the modeling techniques used to ensure that the task stays at the cutting edge.

In the area of intercalation cathodes, the effort is focused on understanding the working principles of the high nickel layered materials with an aim of understanding structural changes and the associated changes in transport properties. Coatings, an effective strategy for high-voltage operation, are being explored with the aim of providing a rational design approach for new coating materials. In addition, focus is paid to the assembling of porous electrodes with particles to predict the conduction behavior and developing tools to measure electronic conduction.

In the area of silicon anodes, the effort is in trying to understand the interfacial instability and suggest ways to improve the cyclability of the system.

In the area of Li-metal anodes, the focus is on understanding how materials can be designed to prevent dendrite growth using continuum modeling approaches, combined with calculations on mobility in solid conductors. The results are used to guide materials development by providing the properties needed to prevent dendrites while also achieving the energy and power goals. Models are also starting to examine the role of the SEI on the morphology of the dendrite and to describe the mechanical-electrochemical coupled effects that are critical for dendrite formation.

Task 6.1 – Predicting and Understanding Novel Electrode Materials from First Principles (Kristin Persson, Lawrence Berkeley National Laboratory)

Project Objective. This project supports VTO programmatic goals by developing next-generation, high-energy cathode materials and enabling stable cathode operation at high voltages through target particle morphology design, functional coatings, and rational design of electrolytes. The end-of-project goals include: (1) novel disordered, high-rate Li-excess cathodes, (2) new fundamental understanding of the cathode/electrolyte interface and the factors that control the interfacial chemistry and interfacial impedance, (3) critical surface and coating design and optimization strategies that will improve cycling of Li-ion battery cathodes, and finally (4) understanding of the factors that govern stability in nonaqueous electrolytes for Li-ion and Li-S systems.

Project Impact. To enhance the performance of Li-ion systems, improvements on the cathode and the electrolyte side are needed. This project is aimed to result in an improved understanding of the atomistic mechanisms underlying the surface behavior and performance of the Li-ion cathode materials with the ultimate goal being to suggest strategies, such as coatings, surface protection, and particle morphology design. Furthermore, fundamental studies of electrolyte stability, as a function of solvent and salt concentrations, and components will be conducted.

Out-Year Goals. Stable interfaces will be determined by focusing initially on degradation mechanisms related to the release of surface oxygen at high charge. Tuning particle morphology and coating materials—both of crystalline as well as amorphous structure—will be explored using the Materials Project. For the electrolyte development, work will be aimed toward understanding the atomistic interactions underlying the performance of lithium electrolytes specifically elucidating the solvation structure (as a function of salt concentration) and its impact on the stability of different liquid constituent species.

Collaborations. This project is highly collaborative between BMR PIs G. Chen (LBNL), G. Ceder (LBNL) and V. Srinivasan (ANL). Cathode design and synthesis will be performed by Chen and Ceder, surface design by Persson, and electrolyte design and testing by Persson and Srinivasan.

Milestones

1. Provide matrix of surface candidate dopants based on literature search and practical considerations. (December 2016 – Complete)
2. Benchmark calculations of amorphous coating materials, that is, $\text{Al}_2\text{O}_3/\text{SiO}_2$. (March 2017 – Complete)
3. Present first screening of surface dopants. (May 2017 – In progress)
4. *Go/No-Go*: New strategies are identified. Stop this approach if facet stabilization cannot be achieved. (May 2017 – In progress)
5. Evaluate two electrolyte benchmark formulations for Li-S and Li-ion for stability and diffusion. (September 2017 – In progress)

Progress Report

This project is aimed toward the study of dopant oxygen-retaining, surface stabilization strategies of the Li-excess layered oxide materials using first-principles calculations. Targeting Li_xMnO_3 as a ‘worst-case’ representative of the Li-excess, Mn-rich cathodes, the project applied a 3-tier computational screening for possible oxygen-retaining, surface doping strategies spanning 39 doping elements on five stable surfaces. First, the team screened for dopants that preferentially segregate toward the surface, comparing defect formation energies between the surfaces and bulk. The computation showed that 30 out of 38 elements prefer the surface. In Tier 2, the project ordered the 38 elements by the absolute dopant formation energy, to eliminate dopants with a strong driving force to form secondary impurity phases instead of residing within the cathode material. The top 10 candidate dopants selected through Tiers 1 and 2 are as follows: Os, Sb, Ti, Ru, Ir, Fe, Ta, Nb, Cr, and Al.

In the final Tier 3, the project calculates the oxygen evolution energy difference between the doped surface and the pristine surface. It defines the relative oxygen release energy as;

$$\Delta\tilde{E}_O = \tilde{E}_O^{\text{doping}} - \tilde{E}_O^{\text{pristine}}$$

Figure 50 shows $\Delta\tilde{E}_O$ of the top 10 candidate dopants obtained from the two first selection criteria. Here, $\Delta\tilde{E}_O$ is provided for the (001) and (010) surfaces as the two dominant surfaces of Li_xMnO_3 . The oxygen evolution energy of the pristine surface $\tilde{E}_O^{\text{pristine}}$ was defined in previous work using the slab vacuum mode. Each color in Figure 50 represents the relative oxygen evolution energy as compared to the pristine surface; therefore, yellow/purple colors indicate a stronger/decreased oxygen retention relative to the pristine surfaces. The underlying atomistic reason for the improved oxygen retention can be understood by elucidating the influence of the dopant on the local electronic structure at the specific surface facet. The project found that a strong hybridization between the oxygen p-orbitals on the surface and the surface defect d-orbitals. In Figure 50, yellow colored elements exhibit strong electron energy hybridization.

In summary, the 3-tier screening has identified optimal candidate dopants (Os, Sb, Ru, Ir, and Ta) to be added during synthesis of Li-excess, Mn-rich cathode materials for improved surface oxygen retention. It should be noted that the higher concentration of the dopant at the surface, the better oxygen retention is expected. Collaboration with co-PI Chen has resulted in the first Ta-doped disordered Li-excess cathode showing promising results.

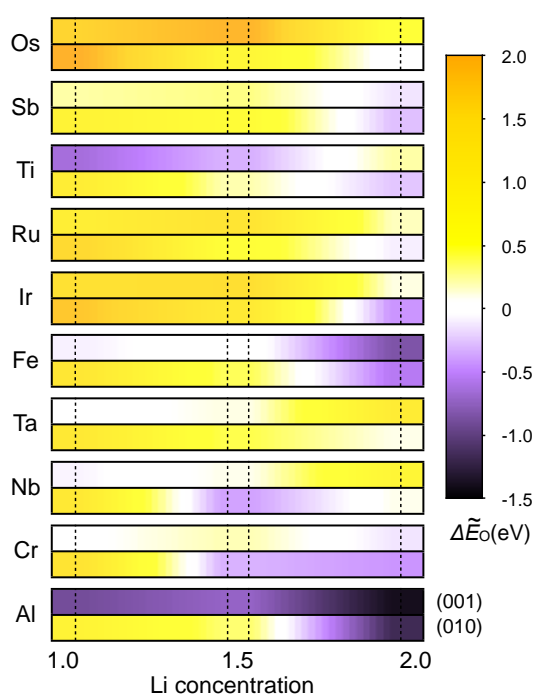


Figure 50. The relative surface oxygen release energy for the top 10 candidate dopants as compared to the pristine systems shown for representative (001) and (010) surface facets. A dark yellow color indicates stronger oxygen retention, while a purple color indicates less protection against oxygen release as compared to the pristine, undoped surface.

Task 6.2 – Addressing Heterogeneity in Electrode Fabrication Processes (Dean Wheeler and Brian Mazzeo, Brigham Young University)

Project Objective. The project goal is to better understand connections between fabrication conditions and undesired heterogeneity of thin-film electrodes by means of new nondestructive inspection techniques and computer models. Two nondestructive inspection techniques will be developed or improved to characterize electrochemical and mechanical uniformity of the electrodes. The first tool will be a flexible contact probe on a polymer substrate for rapidly measuring local electrical conductivity across electrodes of any geometry. The second tool will be a new acoustic probe that measures local elasticity and density of the composite film. These two prototyping efforts will be tied together by a particle-based microstructure model that allows prediction and correlation of electrode conductive and mechanical properties with fabrication conditions.

Project Impact. This work will result in new diagnostic and modeling tools for rapidly and conveniently interrogating how well homogeneity has been maintained in electrodes during fabrication and in subsequent cycling. Real-time measurement of heterogeneity will enable manufacturer quality control improvements. The measurement and modeling tools will further enable researchers to compare different electrodes, improve formulations and processes, and anticipate cell performance of new designs.

Out-Year Goals. This project was initiated October 2016 and concludes September 2018. Overall goals by fiscal year are as follows:

- **2017.** Fabricate first-generation flexible conductivity probe and proof-of-concept of acoustic probe; and improve microstructure model to match experiment.
- **2018.** Integrate flex probe with test fixtures suitable for assessment of large or continuous samples; and demonstrate measurement of localized ionic conductivity.

Collaborations. Ram Subbaraman (Bosch), Daniel Abraham (ANL), Steve Harris (LBNL), Bryant Polzin (ANL), and Karim Zaghbi (HQ) have provided battery materials for analysis. Other collaborations and the transfer of this technology to interested parties are being pursued.

Milestones

1. Complete flex probe prototype and demonstrate that measurements match those for the previous rigid probe. (Q1 – Complete)
2. Integrate the flex probe with existing high-precision positioning system, and make measurements on 3 different electrode materials. (Q2 – Complete)
3. Demonstrate that the dynamic particle packing (DPP) model can predict effective conductivities that match experiment for three different electrode materials. (Q3 – Complete)
4. Complete prototype of localized acoustic probe and associated model. *Go/No-Go:* Determine whether to continue developing the acoustic method by assessing sensitivity to film stiffness. (Q4 – Complete; *Go* decision)

Progress Report

Milestone 4 was completed, and based on a successful outcome, the decision was made to continue developing the acoustic method of interrogating battery electrode films. The ultimate purpose of this type of test is to rapidly determine if there are mechanical variations in an electrode that would lead to poor electrochemical performance. This will allow improvement of the manufacturing process.

There are multiple means of using sound waves to analyze mechanical behavior of thin films. One method was to examine resonance frequencies. Figure 51 depicts that the resonances of three cathodes with a 20- μm aluminum current collector are seen to occur at different fundamental frequencies. Each of the cathodes had coating layers of different thicknesses (42- μm , 38- μm , and 26- μm coatings on top of the current collector) and densities. The purple line labeled “laser off” is a baseline reading to ensure that the peaks seen by the probe are not due to room noise. The tendency of the resonance frequency shown in Figure 51 demonstrates that the battery film acted more like a membrane, with $\sqrt{1/h}$ dependence, where h is the film thickness. The results were also confirmed by comparing the resonance frequencies obtained from a scanning laser doppler vibrometer (SLDV).

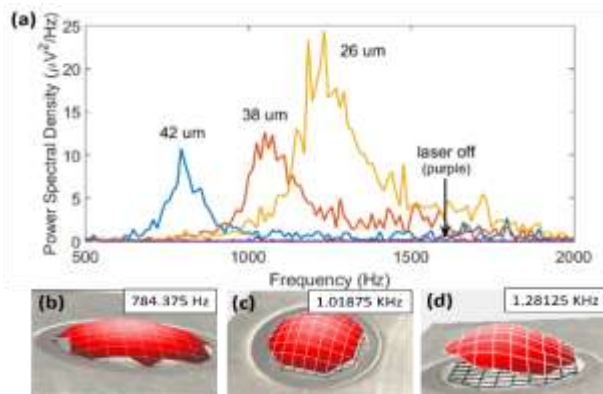


Figure 51. (a) Power spectral density for various battery films. Scanning laser doppler vibrometer results of various battery films with thicknesses of (b) 42 μm , (c) 38 μm , and (d) 26 μm .

Table 6. Measured and calculated properties of coated layer of battery films.

Coating	h (μm)	ρ (g/cm^3)	E (GPa), SLDV	E (GPa), peaks	ν
1	42	2.760	0.344	0.412	0.3
2	38	3.055	1.71	2.01	0.3
3	26	2.479	5.04	4.13	0.3

By fitting the acoustic measurements to the results of a numerical model, the Young’s modulus was found in Table 6. The thickness is the reported value from the manufacturer (of the coating only, not including the 20- μm -thick aluminum current collector), and the Young’s modulus values are obtained from a combination of simulated experimental results.

Based on these results, the acoustic method exhibits enough sensitivity to distinguish different values of Young’s modulus from different coating layers. It is anticipated that refinement of the method is required to give more accurate results and to enable more robust sampling in an industrial environment.

Patents/Publications/Presentations

Publication

- No publications were made, though one publication is in press and three manuscripts are in preparation (expected to be done in the first quarter of FY 2018).

Presentations

- Review of Progress in Quantitative Nondestructive Evaluation (QNDE), Provo, Utah (2017): “Determination of Mechanical Properties of Battery Films from Acoustic Resonances”; K. L. Dallon, J. Yao, D. R. Wheeler, and B. A. Mazzeo.
- QNDE, Provo, Utah (2017): “Flexible Probe for Measuring Local Conductivity Variations in Li-Ion Electrode Films”; E. Hardy, D. Clement, J. Vogel, D. R. Wheeler, and B. A. Mazzeo.

Task 6.3 – Understanding and Strategies for Controlled Interfacial Phenomena in Lithium-Ion Batteries and Beyond (Perla Balbuena, Jorge Seminario, and Partha Mukherjee, Texas A&M University)

Project Objective. The project objective is to evaluate and characterize interfacial phenomena in lithiated silicon and Li-metal anodes and to develop guidelines for potential solutions leading to controlled reactivity at electrode/electrolyte interfaces of rechargeable batteries using advanced modeling techniques based on first-principles.

Project Impact. Understanding SEI growth on constantly evolving silicon surfaces and on highly reactive Li-metal surfaces is expected to define the electrolyte properties required in high-performance cells. Strategies to control the silicon anode instability and pulverization issues and the well-known safety and short effective lifetimes of Li-metal anodes will be developed by tuning the electrolyte composition, structure, dynamic, and stability, as well as that of the electrode morphology and interactions with the electrolyte, based on multiple characterizations of interfacial phenomena.

Approach. A comprehensive multiscale modeling approach including first-principles *ab initio* static and dynamics, classical molecular dynamics, and coarse-grained mesoscopic models will focus on the roles of the electrolyte chemical, structural, and dynamical properties and of the electrode micro- and nanostructure on the formation and evolution of the SEI layer and associated electrochemical performance on silicon and on Li-metal anodes.

Out-Year Goals. Work will progress toward characterizing lithiation and SEI formation at silicon surfaces as well as the subsequent cracking and reforming events under the most realistic modeling conditions. Similarly, the project will investigate electrolyte effects on reactivity and dendrite formation in Li-metal surfaces. The project aims to capture how the chemistry of the various components of the electrolyte (mainly liquids, but also solid polymers and gels) affects the main issues that influence the electrode performance.

Collaborations. This project funds work at Texas A&M University (TAMU). Dr. Chunmei Ban (NREL), Dr. Xiaolin Li (PNNL), and Dr. Kevin Leung (Sandia National Laboratories, SNL) may also contribute.

Milestones

1. Characterize SEI nucleation and modes of cracking as functions of SEI composition on lithiated silicon nanoparticles. (Q1 – Completed December 2016)
2. Identify and quantify Li-ion transport mechanisms through SEI blocks. (Q2 – Completed March 2017)
3. Evaluate and quantify the relative influence of mechanical and chemical degradation interplay in silicon active particles. (Q3 – Completed June 2017)
4. Characterize SEI growth as a function of SEI composition. Compare the SEI rate growth with experimental trends in the literature and from collaborators; if there is any disagreement, revise respective modeling approach. (Q4)

Progress Report

Multiscale Model of SEI Film Growth. Li-ion transport through the SEI layer influences the negative electrode reactions, including lithium reduction and intercalation into active material, as well as the SEI formation. In reality, there is a multiphase SEI growing on the electrode surface. Diffusion kinetics in the

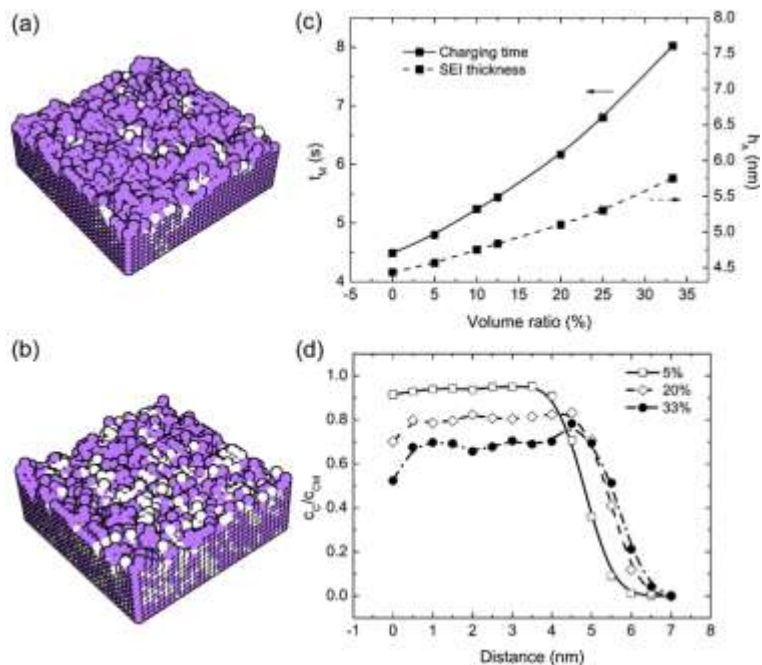


Figure 52. SEI of two components with different activation barriers for lithium diffusion: purple (A, $E_a = 46.1$ KJ/mol) and white (B, $E_a = 65.3$ KJ/mol). SEI morphologies at B volume fractions of 5% in (a) and 33% in (b). (c) Total charging time and SEI thickness for the first charge with varying B volume fraction. (d) Concentration of active lithium traveling through the SEI interstitials (cc) with respect to the theoretical maximum (cM) for various B volume fractions.

SEI layer along with multiphase SEI growth is modeled to understand the underlying physics. As shown in Figure 52, two components: A (purple) and B (white) are considered. Here, Li-ion transport in component B is assumed much slower compared to that in A. The activation energies of Li-ion diffusion in SEI are 46.1 KJ/mol for A and 65.3 KJ/mol for B, which means that the diffusion rate in A is over 2200 times that in B, and the activation energy for solvent diffusion within the SEI is fixed at 67.2 KJ/mol. The values of the activation energies fall within DFT ranges calculated for Li^+ in Li_2CO_3 . The model assumes that the solvent diffuses through the porous SEI and is reduced at the surface of the electrode. The effects of the volume fraction of B are depicted in Figure 52c. As the volume fraction of B increases, the total charging time increases, leading to a thicker SEI film for the first charging cycle. It is worth pointing out that the total charging time and SEI growth have nonlinear relationships with the volume fraction of B. Figure 52a-b illustrates the SEI film configurations, with volume fractions of 5% and 33%. Increasing the B volume fraction could induce nucleation of B, hindering the fast transport pathways in component A. Figure 52d shows that the content of active lithium inside the SEI varies up-and-down along the SEI's depth, and the fluctuation becomes larger increasing the B volume fraction. In contrast, for the 1-component SEI, it exhibits a predominantly linear Li-ion content trend near the electrode-SEI interface. The non-uniform distribution of component B largely accounts for the fluctuation in Li-ion content. Compared to the fast Li-ion diffusion in component A, Li-ions seem to be trapped after they enter the component B. Therefore, this “trapping effect”, along with the non-uniform distribution of B, induces the results in Figure 52d. Moreover, Li-ion diffusion in SEI could become the rate-determining step to govern the overall electrode reactions when the volume fraction of B is large enough.

Delithiation of a Lithiated Silicon Particle. In continuation of previous work, where the project studied cracking mechanisms and effects, it is developing a model using molecular dynamics atomistic simulations to study the delithiation of a silicon nanoparticle anode covered with a LiF model SEI. The initial structure of the model is a fully lithiated silicon nanoparticle, $\text{Li}_{3.5}\text{Si}$, covered by a model SEI showing some cracking and/or amorphization due to the volume expansion during charge. The new simulations will be used to study the diffusion of Li-ions through the many planes of the LiF SEI, to identify how the crackings and amorphization modify the Li-ion transport.

Patents/Publications/Presentations

Publications

- Gomez-Ballesteros, Jose L., and Perla B. Balbuena. “Reduction of Electrolyte Components on a Coated Si Anode of Lithium-Ion Batteries.” *J. Phys. Chem. Lett.* 8 (2017): 3404-3408.
- Horowitz, Yonatan, and Hui-Ling Han, Fernando A. Soto, Walter T. Ralston, Perla B. Balbuena, and Gabor A. Somorjai. “Key to High Performance Silicon Anodes: Fluorine as a Directing Agent for Stable Solid Electrolyte Interphase Formation.” Submitted.
- Hao, Feng, and Zhixiao Liu, Perla B. Balbuena, and Partha Mukherjee. “Mesoscale Elucidation of Solid Electrolyte Interphase Layer Formation in Li-ion Battery Anode.” Submitted.
- Foroozan, Tara, and Fernando A. Soto, Vitaliy Yurkiv, Soroosh Sharifi-Asl, Ramasubramonian Deivanayagam, Zhennan Huang, Ramin Rojaee, Farzad Mashayek, Perla B. Balbuena, and Reza Shahbazian-Yassar. “Synergistic Effect of Graphene Oxide for Impeding the Dendritic Plating of Li.” Submitted.
- Camacho-Forero, Luis E., and Perla B. Balbuena. “Elucidating Electrolyte Decomposition under Electron-Rich Environments at the Lithium-Metal Anode.” Submitted.
- Verma, A., and P. P. Mukherjee. “Mechanistic Analysis of Mechano-Electrochemical Interaction in Silicon Electrodes with Surface Film.” Submitted.

Presentations

- 254th ACS National Meeting, Washington, D. C. (August 22, 2017): “Characterization of Solvation and Reaction Effects at the Li-Metal/Electrolyte Interface”; Perla B. Balbuena.
- NGenE, University of Illinois, Chicago, Illinois (June 27, 2017): “Solid/Liquid and Solid/Solid Electrochemical Interfacial Phenomena”; Perla B. Balbuena.

Task 6.4 – Electrode Materials Design and Failure Prediction (Venkat Srinivasan, Argonne National Laboratory)

Project Objective. The project goal is to develop a continuum-based mathematical model to (1) investigate the impact of mechanical stress on growth of dendritic protrusions and (2) elucidate competition between transport and mechanical means for preventing dendrite growth. Effectiveness of protective layers in preventing growth of dendritic protrusions will also be studied. The focus will be to develop a microscale model that can capture the mechanical stresses and transport processes within lithium metal and adjacent electrolyte/protective layer. Impact of surface energy on growth of dendrites will be investigated. Possibility of plastic deformation within lithium metal and/or solid electrolyte material will also be elucidated along with its effect on propagation of dendrites. Propensity of fracture within the SEI layer (or the protective layer) and its impact on dendrite growth will be explored.

Project Impact. The next-generation Li-ion batteries are expected to use Li-metal based anodes, which offer low reduction potential and superior specific capacity. The biggest drawback preventing widespread usage of Li-metal anodes is formation of dendrites over multiple cycles during operation at higher current densities. Insight gained from this project will provide guidance in designing solid polymer electrolytes (or protective layers) that prevent growth of dendrites on lithium metal.

Out-Year Goals. At the end of this project, a mathematical model will be developed that can capture the mechanical stress field, concentration, and potential profiles around a dendritic protrusion. This model will allow estimation of the propensity for growth of such a protrusion and provide guidance in design of solid polymer electrolytes (or protective layers) for prevention of lithium dendrites.

Milestones

1. Develop mathematical model to understand the proper stress state that exists within lithium metal and adjacent electrolyte during electrochemical deposition of lithium. (Q1 – Complete)
2. Develop mathematical models to investigate and capture possibility of plastic deformation within lithium metal. Impact of plasticity on effective exchange current density will also be explored. (Q2 – Complete)
3. Combine the impact of elasto-plastic stress evolution with transport of lithium within the electrode-electrolyte system. If unsuccessful in combining both elastic and plastic deformation with the transport process, consider only elastic deformation of lithium and electrolyte. (Q3 – In progress)
4. Report on the electrolyte shear modulus required for successful prevention of dendrites. The coupled mechanics and transport framework will be used to analyze the Li-electrolyte system. (Q4 – In progress)

Progress Report

Report on the Electrolyte Shear Modulus Required for Successful Prevention of Dendrites. The coupled mechanics and transport framework will be used to analyze the Li-electrolyte system. Growth of dendritic protrusions is the largest factor preventing widespread commercialization of Li-metal anodes. It has been argued that increasing the electrolyte modulus has the potential to prevent growth of dendritic protrusions [Monroe and Newman, *JES* (2005): A396]. This quarter, the project investigated the impact of electrolyte modulus on dendrite growth by incorporating elastic-plastic deformation of both metallic lithium and polymer electrolyte. A modified version of the Butler-Volmer equation has been adopted from existing literature that takes into

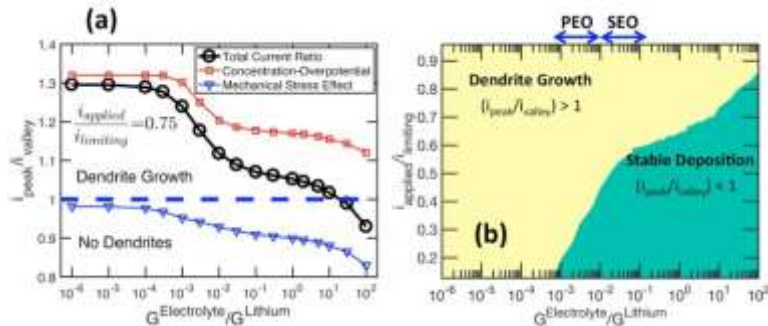


Figure 53. (a) Impact of stress factor and current-distribution factor on the overall reaction current density. Electrolytes with shear modulus 20 times larger than that of lithium may prevent dendrite growth. (b) Phase map demonstrating the correlation between applied current density and electrolyte shear modulus on stabilization of lithium deposition.

account the impact of mechanical deformation induced strain energy. This expression has been used to determine the reaction current at the lithium/electrolyte interface. The two components of the Butler-Volmer equation are as follows: (1) The “mechanical stress factor” that takes into account the impact of strain energy and surface curvature effects, and (2) The “current distribution factor” that takes into account the effect of concentration and potential distribution within the electrolyte.

Figure 53a compares the impact of mechanical stress induced component and the current distribution induced component of the Butler Volmer equation on the ratio of total reaction currents between the protrusion peak and the valley. Mechanical stress always tries to prevent the dendrites, whereas the current distribution helps in growth of the dendritic protrusion. The combined effect clearly indicates that electrolytes with shear modulus 20 times larger than that of lithium may be able to prevent the growth of dendritic protrusions. Figure 53b shows a phase map between applied current density and electrolyte shear modulus, where the domain of stable lithium deposition has been clearly pointed out.

Impact of elastic-plastic deformation experienced by both lithium metal and polymer electrolyte on the suppression of dendritic protrusion has been demonstrated in Figure 54b. For intermediate modulus electrolytes, plastic flow of lithium occurs along with elastic deformation of the electrolyte, which provides the maximum suppression of dendritic protrusion. Following this realization, if the project can improve the yield strength of the present-day polymers by approximately three times, prevention of dendritic protrusion may be possible (see Figure 54b). Determination of a critical electrolyte shear modulus and yield strength that can suppress lithium dendritic protrusions completes the fourth and final milestone of this project.

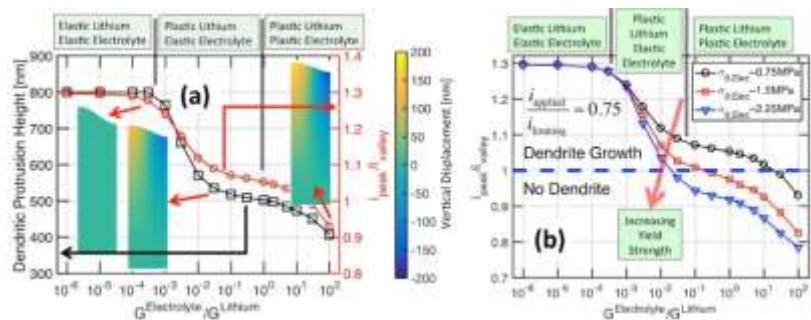


Figure 54. (a) Effect of elastic-plastic deformation of both lithium metal and electrolyte on the overall suppression of the dendritic protrusion. (b) Increasing yield strength of the electrolyte may help to prevent dendrite growth even with present-day polymer electrolytes.

Task 6.5 – First Principles Calculations of Existing and Novel Electrode Materials (Gerbrand Ceder, Lawrence Berkeley National Laboratory)

Project Objective. The main project objectives are as follows: (1) develop very high-capacity, layered cathodes with high structural stability (> 250 mAh/g) and high surface stability; (2) clarify the role that Li-excess and cation disorder play in capacity and structural stability; (3) develop predictive modeling of oxygen charge transfer and oxygen loss, and find ways to make oxygen redox beneficial in terms of increase capacity; and (4) develop materials with engineered surface passivation that does not lead to impedance increase.

Project Impact. The project will lead to insight in how Li-excess materials work and ultimately to higher capacity cathode materials for Li-ion batteries. The project will help in the design of high-capacity cathode materials that are tolerant to TM migration.

Out-Year Goals. Future goals include the following: (1) develop higher capacity Li-ion cathode materials, and novel chemistries for higher energy density storage devices, and (2) guide the field in the search for higher energy density Li-ion materials.

Collaborations. This project collaborates with K. Persson (LBNL), C. Grey (Cambridge), V. Srinivasan (ANL), and G. Chen (LBNL).

Milestones

1. Computational approach to predict cation disorder and synthesis temperature. (Q1 – Complete)
2. Comparison of electronic structure modeling with experimental spectra (for example, XAS, XPS, or EELS). (Q2 – Complete)
3. Use modeling to come up with a new cation-disordered material. (Q3 – On target)
4. Demonstrate reduced surface oxygen loss by surface modification of a disordered cathode material using DEMS or TEM. (Q4 – On target)

Progress Report

Recent project work has shown that Li-excess disordered (rock salt) TM oxides (LEX-RS) are promising candidates for high-capacity cathode materials [Lee et al., *Science* 343 (2014): 519–522]. For this class of materials, however, good lithium percolation requires lithium excess; also, the high capacity observed generally relies on oxygen redox processes that can cause oxygen loss near the surface of the cathode particles. This results in the creation of high impedance surface layers and large polarization of the voltage profile, leading to poor cycling performance.

The project's comparative study of the disordered oxides $\text{Li}_{1.15}\text{Ni}_{0.375}\text{Ti}_{0.375}\text{Mo}_{0.1}\text{O}_2$ (LN15) and $\text{Li}_{1.2}\text{Ni}_{0.333}\text{Ti}_{0.333}\text{Mo}_{0.133}\text{O}_2$ (LN20), with fluorine-substituted $\text{Li}_{1.15}\text{Ni}_{0.45}\text{Ti}_{0.3}\text{Mo}_{0.1}\text{O}_{1.85}\text{F}_{0.15}$ (LNF15) [Lee et al., *Nat. Commun.*, in print] showed that, since fluorine substitution allows for more Ni^{2+} in the as-prepared material, it increases the metal-based redox reservoir of the cathode; this reduces oxygen redox and, therefore, oxygen loss from the lattice on charge, leading to significant improvements in electrochemical performance.



Figure 55. Energy dispersive spectroscopy mapping on one area of a LNF15 particle. Scale bars, red: 100 nm, blue: 25 nm.

The project performed TEM-EDS to prove that fluorine is substituted in the bulk disordered lattice instead of forming secondary phases at the surface of the particles. As shown in Figure 55, EDS mapping reveals a uniform distribution of fluorine in the LNF15 particle.

The project also carried out ^{19}F solid-state nuclear magnetic resonance spectroscopy (ssNMR) to confirm that the fluorine distribution observed with TEM-EDS is not due to LiF on the surface of the particles. The ^{19}F NMR data presented in Figure 56 show the presence of multiple broad fluorine local environments in LNF15, in contrast to the single fluorine site observed for LiF, which confirms that fluorine is doped into the bulk Li–Ni–Ti–Mo oxide lattice.

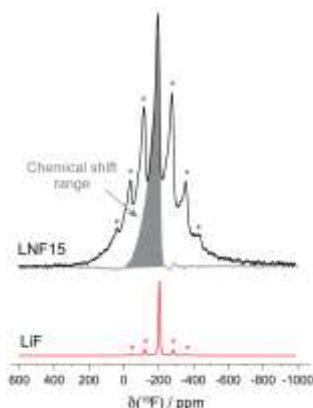


Figure 56. ^{19}F spin echo nuclear magnetic resonance spectra obtained at 30 kHz magic angle spinning for LNF15 and LiF.

DEMS results indicate that LNF15 has less oxygen loss than LN15 and LN20. The produced amount of O_2 gas was reduced from 0.26 and $0.40 \mu\text{mol mg}^{-1}$ for LN15 and LN20, respectively, to $0.07 \mu\text{mol mg}^{-1}$ for LNF15 (see Figure 57).

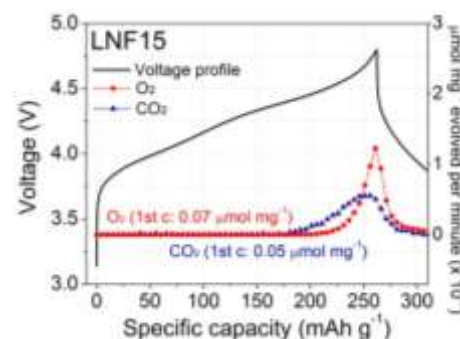


Figure 57. Differential electrochemical mass spectrometry (DEMS) study of LNF15 when charged to 4.8 V and discharged to 1.5 V at 20 mA g^{-1} , along with the DEMS results on O_2 (red circle) and CO_2 (blue triangle).

Task 6.6 – Dendrite Growth Morphology Modeling in Liquid and Solid Electrolytes (Yue Qi, Michigan State University)

Project Objective. The ultimate goal of this project is to develop a validated model to predict lithium dendrite morphology evolution in both liquid and solid electrolytes during electrodeposition and stripping, in order to accelerate the adoption of Li-metal electrodes in current and emerging battery technologies. To achieve this goal, the project has four objects: (1) formulate a general framework that captures the electrochemical-mechanical driving forces for lithium morphology evolution; (2) consider the role of the nm-thin SEI in liquid-electrolytes as well as the microstructures of mm-thick solid-electrolytes for lithium morphology evolution; (3) connect micron-scale phase-field models and atomic-scale DFT-based simulations via parameter- and relationship-passing to predict lithium dendrite nucleation and growth kinetics and morphology; and (4) validate the key input parameters and main conclusions of the multi-scale model as new capabilities being developed step-by-step.

Project Impact. This atomically informed, fully coupled, electrochemical-mechanical dendrite morphology evolution model will allow the project to design the desired properties of artificial SEI coatings, the microstructure of solid electrolyte materials, and the corresponding battery operating conditions, so as to avoid dendrite growth during cycling. It will accelerate design of durable and safe lithium anodes for Li-S, Li-air, and all-solid Li-ion batteries. Thus, it directly impacts emerging technologies, such as Li-S, Li-air, and all-solid Li-ion batteries, which aim to meet the DOE target of the high-energy-density battery cells ($> 350 \text{ Wh/kg}$) for EV applications and to push the cost below $\$100/\text{kWh}_{\text{use}}$.

Out-Year Goals. The goal this year is to illuminate the role of SEI kinetics on lithium dendrite growth in liquid electrolytes. To achieve this goal, a phase-field model will be developed to capture the electrochemical driven dendrite morphology evolution in a liquid electrolyte. The role of SEI will be modeled both implicitly and explicitly. The kinetic properties, as well as lithium diffusion coefficient along the Li/SEI interface will first be computed from DFT- and DFT binding (DFTB)- based atomic simulations. The validation of the model will come from experiments to correlate the distinctively different transport properties of artificial SEI layers with their impact on lithium dendrite morphology.

Collaborations. This project collaborates with UMD, SNL–Albuquerque, PNNL, and the University of Arkansas.

Milestones

1. Computational approach to predict cation disorder and synthesis temperature. (Q1 – Complete)
2. Comparison of electronic structure modeling with experimental spectra (for example, XAS, XPS, or EELS). (Q2 – Complete)
3. Use modeling to come up with a new cation-disordered material. (Q3 – On target)
4. Demonstrate reduced surface oxygen loss by surface modification of a disordered cathode material using DEMS or TEM. (Q4 – On target)

Progress Report

Liquid Electrolyte. The implicitly lithium morphology model was used to investigate the impact of four major SEI properties, namely interfacial energy, anisotropy, diffusion coefficient, and reaction rate constant. The nonlinear phase-field model simulation of the lithium electrodeposition process revealed that higher Li/SEI interface energy, faster Li-ion diffusion in SEI, and slower reaction rate constants favor less branched lithium morphology (as shown in Figure 58), leading to higher CE compared to more branched morphology.

For the atomic simulations of the Li/Li₂CO₃/EC interface, the experimentally defined zero voltage of Li⁺/Li⁰ was calibrated with DFTB and DFT calculations. It was found that at zero voltage, the SEI-covered Li-metal surface is negatively charged with an electron density of $\sim 1e/nm^2$. When the electron density is larger than this (more negative potential), lithium plating occurs; while when the electron density is lower than this (more positive potential), lithium stripping occurs. The excess electrons on lithium surface will trigger more electrolyte decomposition when SEI fractures.

Solid Electrolyte. A general nonlinear phase-field model for lithium dendrite growth in solid electrolyte (for example, LLZO, LLZTO, etc.) has been formulated and implemented in phase field model. DFT calculations were performed to address the nucleation mechanism of metallic lithium inside LLZO. Both tetragonal and cubic phases LLZO were investigated. It was found the excess electrons in LLZO can be trapped to the lanthanum at/near the surface in LLZO. Figure 59 shows the localized electrons clouds on lanthanum. Thermodynamics calculations confirmed that metallic lanthanum can be more stable than metallic lithium with the excess electrons, providing the nucleation mechanism of metallic-Li phase in LLZO. This mechanism is being investigated for LLZO grain boundaries as well.

This mechanism was introduced as a non-uniform, structure-dependent electron activity ($a_e(r)$) in the phase field model. An intergranular lithium dendrite growth has been simulated in 2D microstructures. The results showed that the lithium-dendrite growth rate was higher inside wider grain boundaries or pores than inside the narrow ones, indicating larger growth resistance at narrower grain boundaries or pores.

The explicit SEI model being developed is similar to that used for solid electrolytes.

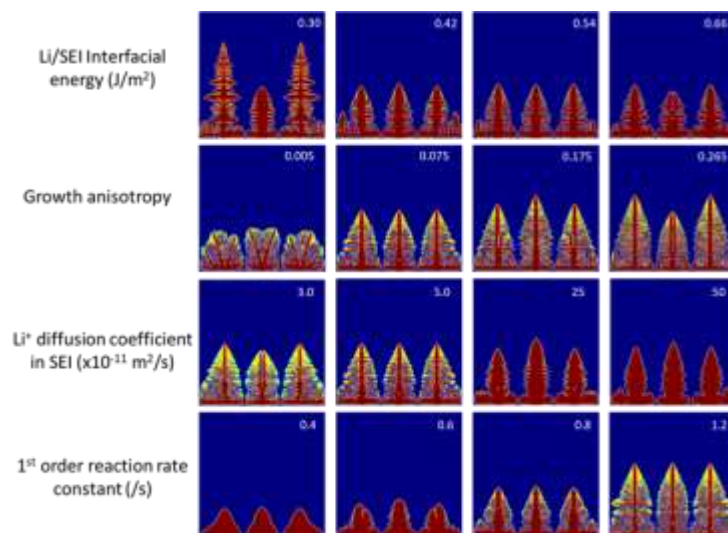


Figure 58. SEI properties – lithium dendrite morphology map from phase field simulation.

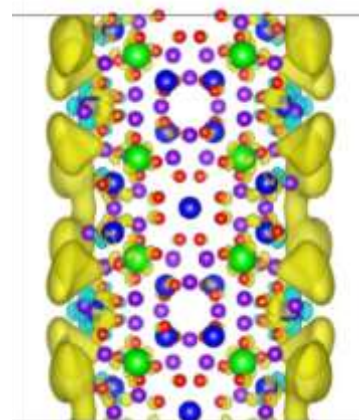


Figure 59. The excess electrons located on lanthanum atoms on LLZO surface.

Patents/Publications/Presentations

Presentations

- 254th ACS National Meeting, Washington, D. C. (August 2017): “Computational Insights to Charge Transfer Reactions at the Complex Electrode/SEI/Electrolyte Interface”; Yue Qi and Yunsong Li. Invited.
- 232nd ECS Meeting, National Harbor, Maryland (October 4, 2017): “Towards High Cycle Efficiency of High Energy Density Lithium Ion Batteries”; X. Xiao. Invited.

Task 6.7 – First Principles Modeling and Design of Solid-State Interfaces for the Protection and Use of Li-Metal Anodes (Gerbrand Ceder, UC Berkeley)

Project Objective. The project objective is to determine the design principles that control the solid electrolyte/lithium electrode interfaces by determining the reaction products stemming from pairing solid electrolytes and lithium metal. The project will conduct rigorous analysis based on computing electrolyte phase-diagrams closed and open to lithium. Li-ion transport properties in bulk electrolytes and interfacial products will be assessed through AIMD and nudged elastic band calculations. Simultaneously, a robust framework will be developed to identify factors controlling Li-dendrite propagation within solid electrolytes and interfacial products by accounting for irregularities, defects, and grain boundaries, through a model that includes elements of fracture mechanics, thermodynamics, and electrochemistry.

Project Impact. The project will lead to understanding of the complex evolution of lithium metal/SEI during electrochemical cycling. The understanding of this process is necessary to determine design principles to develop reliable all solid-state batteries.

Out-Year Goals. The out-year goals include the following: (1) obtain design criteria for solid electrolytes that can resist unstable lithium propagation by computing elastic properties surface energies and decohesion energies, and (2) adapt fracture mechanics models describing crack propagation to lithium dendrite propagation in different scenarios.

Milestones

1. Chemistry selection of solid electrolytes through large-scale material recognition based on the Inorganic Crystal Structure Database (ICSD) and materials prediction. (Q1/Q2 – In Progress)
2. Stability screening of solid electrolyte materials using phase diagrams to assess chemical and electrochemical stability. (Q3/Q4 – On target)

Progress Report

Determining Solid Electrolyte Materials Stable against Li-Metal Anode. Using a framework previously developed [Richards et al., *Chem. Mater.* 28 (2016): 266–273] to assess the stability of electrode/electrolyte interfaces, the project has investigated potential solid electrolyte materials (such as oxides, nitrides, phosphates, and borates) and selected materials that are stable when in contact with a Li-metal anode. Figure 60 shows the strategy that has been implemented to screen for promising solid electrolyte candidate materials that are stable against a Li-metal anode.

Studying of the Mechanisms of Dendrite Growth. As illustrated in Figure 61, lithium dendrite formation and propagation through solid electrolyte materials may be understood as a combination of multiple physical phenomena, including mechanical effects (such as nonlinear elastic and plastic deformation) and electrochemical effects (such as chemical diffusion and the migration of charged species through the electrode and electrolyte materials subject to a constant electrostatic potential, as well as electrochemical reactions taking place at the solid electrolyte/electrode interface). Dendrite growth is also strongly related to crack propagation in brittle materials. Therefore, a framework combining (electro) chemistry, thermodynamics (interface energy), and fracture mechanics is being established.

To construct the overall framework, the project has been addressing several fundamental questions related to dendrite formation and propagation.

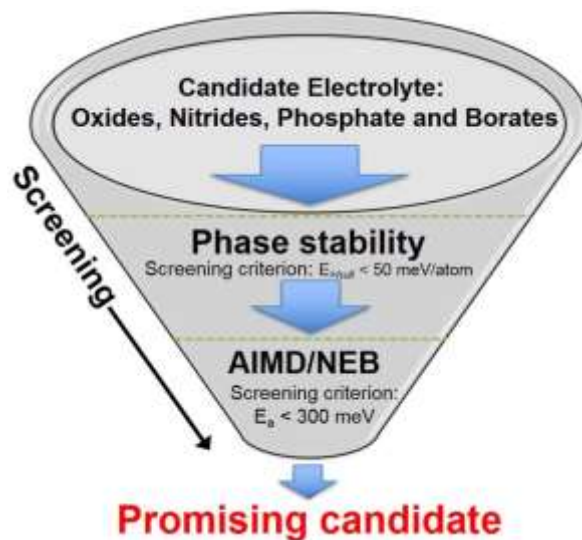


Figure 60. Method adopted here to screen for promising electrolyte materials.

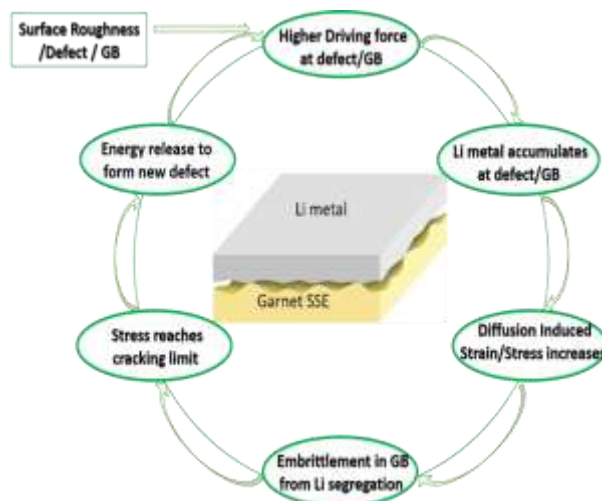


Figure 61. Scheme of the formation and propagation of lithium dendrites during electrochemical cycling of a solid-state battery.

TASK 7 – METALLIC LITHIUM AND SOLID ELECTROLYTES

Summary and Highlights

The use of a metallic lithium anode is required for advanced battery chemistries like Li-air and Li-S to realize dramatic improvements in energy density, vehicle range, cost requirements, and safety. However, the use of metallic lithium with liquid and polymer electrolytes has so far been limited due to parasitic SEI reactions and dendrite formation. Adding excess lithium to compensate for such losses effectively negates the high-energy density for lithium in the first place. For a long lifetime and safe anode, it is essential that no lithium capacity is lost either (1) to physical isolation from roughening, dendrites, or delamination processes, or (2) to chemical isolation from side reactions. The key risk and current limitation for this technology is the gradual loss of lithium over the cycle life of the battery.

To date there are no examples of battery materials and architectures that realize such highly efficient cycling of metallic lithium anodes for a lifetime of 1000 cycles due to degradation of the Li-electrolyte interface. A much deeper analysis of the degradation processes is needed, so that materials can be engineered to fulfill the target level of performance for EV, namely 1000 cycles and a 15-year lifetime, with adequate pulse power. When projecting the performance required in terms of just the lithium anode, this necessitates a high rate of lithium deposition and stripping reactions, specifically about 40 μm of lithium per cycle, with pulse rates up to 10 and 20 nm/s (15mA/cm²) charge and discharge, respectively. This is a conservative estimate, yet daunting in the total mass and rate of material transport. While such cycling has been achieved for state-of-the-art batteries using *molten* sodium in Na-S and zebra cells, solid sodium and lithium anodes are proving more difficult.

The efficient and safe use of metallic lithium for rechargeable batteries is then a great challenge, and one that has eluded R&D efforts for years. This Task takes a broad look at this challenge for both solid-state batteries and batteries continuing to use liquid electrolytes. For the liquid electrolyte batteries, PNNL researchers are examining the use of dual lithium salts and organic additives to the typical organic carbonate electrolytes to impede lithium corrosion and dendrite formation at both the lithium and graphite anodes. If successful, this is the simplest approach to implement. At Stanford, novel coatings and 3D structures are applied to the lithium surface and appear to suppress roughening and lengthen cycle life. A relatively new family of solid electrolytes with a garnet crystal structure shows super-ionic conductivity and good electrochemical stability. Four programs chose this family of solid electrolytes for investigation. Aspects of processing this ceramic garnet electrolyte are addressed at UMD and at the University of Michigan, with attention to effect of flaws and the critical current density (CCD). Computational models will complement their experiments to better understand interfaces and guide reduction of the lithium and cathode area specific resistance (ASR). At ORNL, composite electrolytes composed of ceramic and polymer phases are being investigated, anticipating that the mixed phase structures may provide additional means to adjust the mechanical and transport properties. The last project takes on the challenge to use nano-indentation methods to measure the mechanical properties of the solid electrolyte, the Li-metal anode, and the interface of an active electrode. Each of these projects involves a collaborative team of experts with the skills to address the challenging materials studies of this dynamic electrochemical system.

Highlights. The highlights for this quarter are summarized below.

Development of Solid and Hybrid Batteries

- As observed from nano-indentation tests, the local defect structure in lithium films determines the stress when dislocations mediate the plastic flow. The stress can greatly exceed the nominal yield strength reported for bulk polycrystalline lithium indicating that the Li/solid electrolyte interface cannot be accurately modeled based on the bulk values.
- For cells composed of Li/LLZO/Li, the CCD reached the program target of exceeding 1mA/cm². This represents a 20-fold improvement over the current that led to dendritic shorts at the program's start.

- The spray-coated composite polymer electrolyte containing 50 v% Ohara ceramic powder was cast directly to an NMC cathode. When the cathode current collector was an expanded metal foil, this allowed the liquid electrode to saturate the cathode for a hybrid battery with good performance.
- Performance of batteries with LLZO solid electrolytes composed of dense and porous layers was summarized for Li//NMC and Li//S chemistry. Stable cycling with high efficiency was demonstrated for 200 and 50 cycles, respectively. The NMC was laminated to the LLZO, and pores were filled by a liquid electrolyte. The other electrodes were infiltrated into the LLZO pores.
- A new battery concept based on copper versus lithium electrodes is being tested. The copper is partially dissolved into the LiTFSI containing PVDF-HFP gel, but blocked from the lithium by a bare gel membrane.
- Lithium reactivity with SrTiO₃ was calculated by DFT, indicating the binding energy and sites for different crystallographic faces of the STO. Experimentally, by XPS, lithium is found to reduce Nb⁵⁺ for Nb-doped LLZO, whereas the lithium reduces Zr⁴⁺ for the tantalum-doped LLZO.
- A 3D lithium anode was constructed using Li-rGO as the host, with a flowable interphase coating. This provided a structure that maintains conformal and continuous lithium contact to the solid electrolyte separator through extended cycling.

Liquid Electrolyte Batteries

- The LiAsF₆+VC additives have synergistic effects to form a flexible and robust SEI in the electrolyte of 1 M LiPF₆/PC on lithium. The LiAsF₆ is reduced to Li₃As alloy and LiF, which act as nano-sized seeds for lithium growth on the copper foil. The addition of vinylene carbonate (VC) or FEC enables the uniform distribution of Li₃As seeds and forms polymeric components in the SEI.
- Using high-porosity copper foams as the lithium metal current collector, a CE of ~ 90% was achieved for lithium deposition within the pores; however, with time, the lithium deposited on the surface, which proved much less efficient.
- The morphology of thick lithium deposits on copper (3mAh/cm²) differs when fluorine-containing additives are included in the standard LiPF₆ (EC/dimethyl carbonate, or DMC) electrolyte; with fluorine, the lithium deposited is denser with larger scale, but tortuous, morphology.

Task 7.1 – Mechanical Properties at the Protected Lithium Interface

(Nancy Dudney, Oak Ridge National Laboratory; Erik Herbert, Michigan Technological University; Jeff Sakamoto, University of Michigan)

Project Objective. This project will develop understanding of the Li-metal SEI through state-of-the-art mechanical nano-indentation methods coupled with solid electrolyte fabrication and electrochemical cycling. The goal is to provide the critical information that will enable transformative insights into the complex coupling between the microstructure, its defects, and the mechanical behavior of Li-metal anodes.

Project Impact. Instability and/or high resistance at the interface of lithium metal with various solid electrolytes limit the use of the metallic anode for high-energy-density batteries, such as Li-air and Li-S. The critical impact of this endeavor will be a much deeper analysis of the degradation so that materials can be engineered to fulfill the target level of performance for EV batteries, namely 1000 cycles and 15-year lifetime, with adequate pulse power.

Approach. Mechanical properties studies through state-of-the-art nano-indentation techniques will be used to probe the surface properties of the solid electrolyte and the changes to the lithium that result from prolonged electrodeposition and dissolution at the interface. An understanding of the degradation processes will guide future electrolyte and anode designs for robust performance. In the first year, the team will address the two critical and poorly understood aspects of the protected Li-metal anode assembly: (1) the mechanical properties of the solid electrolyte, and (2) the morphology of the cycled lithium metal.

Out-Year Goals. Work will progress toward study of the electrode assembly during electrochemical cycling of the anode. The project hopes to capture the formation and annealing of vacancies and other defects in the lithium and correlate this with the properties of the solid electrolyte and the interface.

Collaborations. This project funds work at ORNL, Michigan Technological University (MTU), and University of Michigan. Steve Hackney (MTU) has contributed greatly to analysis of the creep mechanisms active for thin-film lithium. Asma Sharafi and Michael Wang (University of Michigan Ph. D. students) and Dr. Robert Schmidt (ORNL) also contribute to the project. Steve Visco (PolyPlus) will serve as a technical advisor.

Milestones

1. Characterize *in situ* changes in lithium anode from a single stripping and plating half cycle. (Q2, March 2017 – On going)
2. Measure the Li-LLZO interface strength as a function of surface treatment using the Instron and EIS capability. (Q3 – Completed June 2017)
3. Examine lithium anode *in situ* during extended electrochemical plating, stripping, and relaxation to assess defect formation and annealing. (Q4 – Completed March 2017)
4. Determine the physical properties of electrolyte failures, the nature of material reduction or lithium incursion/pileup, using indentation and X-ray tomography. Obtain samples from other Task 7 projects. (Q4, September 2017 – X-ray, tomography completed August 2017; insufficient resolution)

Progress Report

Lithium Indentation Studies. A very large data set of indentation tests with vapor-deposited Li-metal films, as detailed in recent reports, has been analyzed and modeled. These are some of the trends and conclusions.

The transition from diffusion to dislocation-mediated plastic flow in vapor-deposited lithium films is found to occur at average mean pressures of approximately 40-100 MPa, depending on the strain rate. These stresses are roughly 80 to 200 times larger than the nominal yield strength of polycrystalline lithium at 298 K. Grain boundaries in lithium are found to act as dislocation sources, as the stress level required to initiate the transition to dislocation-mediated flow is discernably less in close proximity to a boundary. A mechanistic rationalization of the transition to dislocation-mediated plastic flow is provided by the activation of a Frank-Read source. The important implication is that the local defect structure and diffusion controlled $H-h$ pathways determine the stress at the transition. Moreover, the transition is not uniquely triggered by a threshold stress, but a combination of stress and a sufficient length scale over which the dislocation mechanism can physically operate. These observations of the yield stress are generally consistent with the micro compression experiments recently performed by Xu, et al.^[1]

Collectively, these observations demonstrate that the Li/SE interface cannot be accurately modeled based on the bulk plastic properties of polycrystalline lithium. Moreover, in any small-scale defects at the Li/SE interface, the strength of lithium will depend dramatically on the local defect structure, the temperature, and strain rate, which presumably correlates directly with the current density. To fully enable the development of safe and efficient cycling of lithium over many cycles, more information is needed to better understand how defects formed in the lithium during electrochemical cycling migrate, agglomerate, or anneal with further cycling, time and temperature. Ultimately, there is a need to understand how these changes affect lithium's ability to alleviate stress. This knowledge will serve as a cornerstone in understanding the failure mechanism(s) of solid electrolytes.

Li/LLZO Interface Studies. Using the project's precision Instron, housed in an inert atmosphere, the interface resistances of Li-LLZO-Li cells were recorded while cycling the compressive stress (stack pressure) applied to the cell. The project team believes a critical stack pressure is needed to maintain a flux of lithium to the interface in order to maintain contact and avoid formation of pits due to the Kirkendall effect. Li-LLZO-Li cells were fabricated using the best cell assembly protocol, established in Task 7.3, to achieve low and consistent interface resistance. While varying the stack pressure, the project monitored the potential to maintain a current well below the CCD (Figure 62b), and in separate tests, the *in situ* cell impedance (Figure 62c-d). Clearly, there was a noticeable correlation between cell polarization and stack pressure.

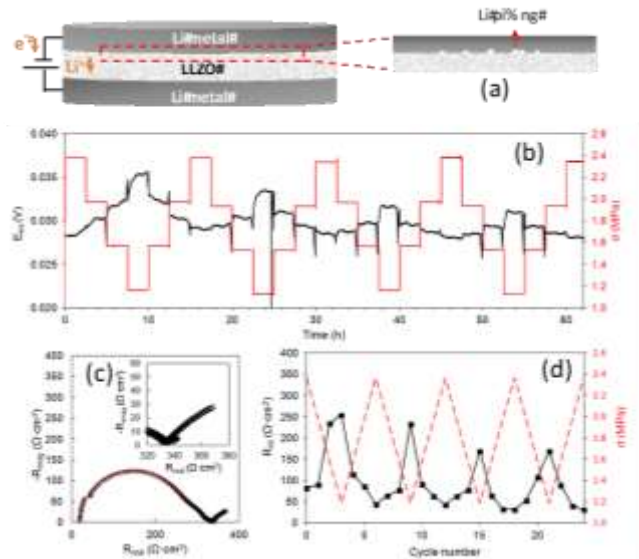


Figure 62. (a) Cell layup and proposed Kirkendall effect. (b) Potential response to a constant 0.1 mA/cm² under a cyclic loading. (c) Representative impedance spectra at 2.4 and 1.2 MPa. (d) Measured interface impedance at each stack pressure during cycling loading.

[1] Xu, Chen, et al., and Julia R. Greer. "Enhanced Strength and Temperature Dependence of Mechanical Properties of Lithium at Small Scales and Its Implications for Li Metal Anodes." *Proceedings of the National Academy of Sciences* 114, no. 1 (2017): 57–61.

Task 7.2 – Solid Electrolytes for Solid-State and Lithium–Sulfur Batteries (Jeff Sakamoto, University of Michigan)

Project Objective. *Enable Advanced Li-Ion Solid-State and Lithium-Sulfur EV Batteries Using LLZO Solid-Electrolyte Membrane Technology.* Owing to its combination of fast ion conductivity, stability, and high elastic modulus, LLZO exhibits promise as an advanced SSE. To demonstrate relevance in EV battery technology, several objectives must be met. First, LLZO membranes must withstand current densities approaching $\sim 1 \text{ mA/cm}^2$ (commensurate with EV battery charging and discharging rates). Second, low ASR between lithium and LLZO must be achieved to obtain cell impedance comparable to conventional Li-ion technology ($\sim 10 \text{ Ohms/cm}^2$). Third, low ASR and stability between LLZO and sulfur cathodes must be demonstrated.

Project Impact. The expected outcomes will: (1) enable Li-metal protection, (2) augment DOE access to fast ion conductors and/or hybrid electrolytes, (3) mitigate Li-polysulfide dissolution and deleterious passivation of Li-metal anodes, and (4) prevent dendrite formation. Demonstrating these aspects could enable Li-S batteries with unprecedented end-of-life, cell-level performance: $> 500 \text{ Wh/kg}$, $> 1080 \text{ Wh/l}$, > 1000 cycles, and lasting > 15 years.

Approach. This effort will focus on the promising new electrolyte known as LLZO ($\text{Li}_7\text{La}_3\text{Zr}_2\text{O}_{12}$). LLZO is the first bulk-scale ceramic electrolyte to simultaneously exhibit the favorable combination of high conductivity ($\sim 1 \text{ mS/cm}$ at 298 K), high shear modulus (61 GPa) to suppress lithium dendrite penetration, and apparent electrochemical stability (0-6 V versus Li/Li⁺). While these attributes are encouraging, additional R&D is needed to demonstrate that LLZO can tolerate current densities exceeding 1 mA/cm^2 , thereby establishing its relevance for PHEV/EV applications. This project hypothesizes that defects and the polycrystalline nature of realistic LLZO membranes can limit the CCD. However, the relative importance of the many possible defect types (porosity, grain boundaries, interfaces, and surface and bulk impurities), and the mechanisms by which they impact current density, have not been identified. Using experience with the synthesis and processing of LLZO (Sakamoto and Wolfenstine), combined with sophisticated materials characterization (Nanda), this project will precisely control atomic and microstructural defects and correlate their concentration with the CCD. These data will inform multi-scale computation models (Siegel and Monroe), which will isolate and quantify the role(s) that each defect plays in controlling the current density. By bridging the knowledge gap between composition, structure, and performance, this project will determine if LLZO can achieve the current densities required for vehicle applications.

Milestones

1. Establish a process to control the microstructural defect that governs the CCD to achieve $> 1 \text{ mA/cm}^2$. (Q1 – Completed December 2016)
2. Establish a process to control the atomic-scale defect that governs the CCD to achieve $> 1 \text{ mA/cm}^2$. (Q1 – Completed December 2016)
3. Design, fabricate, and test beginning of life performance of hybrid Li-LLZO-liquid-S+carbon cells. (Q2 – Completed March 2017)
4. Design, fabricate, and test beginning of life performance of Li-LLZO-liquid-SOA Li-ion cathode cells. (Q3 – Completed June 30, 2017)
5. Experimentally evaluate the CCD, based on the dominant defects (atomic and or microstructural) identified in years 1 and 2, as a function of Q, temp, and pressure. Characterize the CE. (Q4 – Completed September 30, 2017)

6. Design, fabricate, and test beginning of life performance of Li-LLZO-liquid-SOA Li-ion cathode cells. (Q4) (Completed September 30, 2017).
7. Fabricate and test ten Li-LLZO-Sulfur+Carbon cells capable of cycling at $> 1\text{mA/cm}^2$ current density. (Q1 2018 – Starting October 1).

Progress Report

Highlights. Milestone 1.8: After identifying and quantifying the effect of each defect, engineering solutions were developed, optimized, and integrated into all solid-state cells to demonstrate lithium plating/stripping at $\geq 1\text{ mA/cm}^2$ (Figure 63).

Milestone 2.3: Successfully designed, optimized, and integrated LLZO membrane technology into Li-S cells that cycled for ≥ 50 cycles. Li-metal passivation from lithium polysulfides was mitigated.

Milestone Details. Eleven quarters of experimental and theoretical collaboration culminated in the deep fundamental understanding of the factors that govern the stability and kinetics of the Li-LLZO interface. The knowledge gained translated into engineering solutions to increase the maximum tolerable lithium plating/stripping current density (CCD). The goal of the project was to achieve a $\text{CCD} \geq 1\text{ mA/cm}^2$. In Milestone 1.8, $\geq 1\text{ mA/cm}^2$ was demonstrated in all solid-state Li-LLZO-Li cells (Figure 63). The steady voltage response to each current density up to 1.4 mA/cm^2 demonstrates Ohmic behavior and that short-circuiting did not occur (the voltage/current data highlighted in the blue box met and exceeded the project goal). At $> 1.4\text{ mA/cm}^2$, the voltage response is erratic and drops to $\sim 0\text{ V}$, indicating short-circuiting occurred. Nevertheless, $\geq 1\text{ mA/cm}^2$ was clearly demonstrated.

Extended cycling at $\pm 1.0\text{ mA/cm}^2$ at $\pm 3.0\text{ mAh/cm}^2$ charge passed per cycle is underway. EIS and postmortem material characterization also confirms short-circuiting does not occur when cycling below the CCD. Next quarter, Li-LLZO-Li cell technology will be extended to Li-LLZO-cathode hybrid cells.

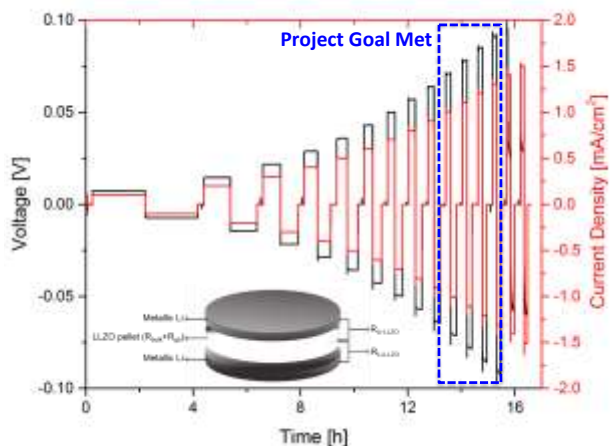


Figure 63. The critical current density of an all solid-state Li-LLZO-Li cell exceeded 1 mA/cm^2 . Red: current density; black: voltage.

Patents/Publications/Presentations

Patent

- Sakamoto, Jeff, and Asma Sharafi. “System and Method for Treating the Surface of Solid Electrolytes.” U. S. Utility Patent Application Serial Number 62/480,080 (2017).

Publications

- Sharafi, Asma, and Eric Kazyak, Andrew L. Davis, Seungho Yu, Travis Thompson, Donald J. Siegel, Neil P. Dasgupta, and Jeff Sakamoto. “Surface Chemistry Mechanism of Ultra-Low Interfacial Resistance in the Solid-State Electrolyte $\text{Li}_7\text{La}_3\text{Zr}_2\text{O}_{12}$.” *Chemistry of Materials*. 2017.
- Sharafi, Asma, and Catherine Haslam, D. Robert Kerns, Jeff Wolfenstine, Jeff Sakamoto, Seungho Yu, Travis Thompson, Donald J. Siegel, and Neil P. Dasgupta. “Controlling and Correlating the Effect of Grain Size with the Mechanical and Electrochemical Properties of $\text{Li}_7\text{La}_3\text{Zr}_2\text{O}_{12}$ Solid-State Electrolyte.” *Journal of Materials Chemistry A* (2017).

Presentation

- Materials Research Society of Japan (MRS-J) 2017, Kyoto, Japan (September 2, 2017): “Solid Electrolytes for Solid-State and Lithium-Sulfur Batteries”; Jeff Sakamoto. Invited.

Task 7.3 – Composite Electrolytes to Stabilize Metallic Lithium Anodes (Nancy Dudney and Frank Delnick, Oak Ridge National Laboratory)

Project Objective. Prepare composites of representative polymer and ceramic electrolyte materials to achieve thin membranes that have the unique combination of electrochemical and mechanical properties required to stabilize the metallic lithium anode while providing for good power performance and long cycle life. Understand the Li-ion transport at the interface between polymer and ceramic solid electrolytes, which is critical to effective conductivity of the composite membrane. Identify key features of composite composition, architecture, and fabrication that optimize performance. Using practical and scaleable processing, fabricate thin electrolyte membranes to use with a thin metallic lithium anode to provide good power performance and long cycle life.

Project Impact. A stable lithium anode is critical to achieve high energy density with excellent safety, lifetime, and cycling efficiency. This study will identify key design strategies that should be used to prepare composite electrolytes to meet the challenging combination of physical, chemical, and manufacturing requirements to protect and stabilize the Li-metal anode for advanced batteries. By utilizing well characterized and controlled component phases, the design rules developed for composite structures will be generally applicable toward substitution of alternative and improved solid electrolyte component phases as they become available. Success in this project will enable these DOE technical targets: 500-700 Wh/kg, 3000-5000 deep discharge cycles, and robust operation.

Approach. This project seeks to develop practical solid electrolytes that will provide stable and long-lived protection for the Li-metal anode. Current electrolytes have serious challenges when used alone: oxide ceramics are brittle, sulfide ceramics are air sensitive, polymers are too resistive and soft, and many electrolytes react with lithium. Composites provide a clear route to address these issues. This project does not seek discovery of new electrolytes; rather, the goal is to study combinations of current well-known electrolytes. The project emphasizes investigation of polymer-ceramic interfaces formed as bilayers and as simple composite mixtures where the effects of the interface properties can be readily isolated. In general, the ceramic phase is several orders of magnitude more conductive than the polymer electrolyte, and interfaces can contribute an additional source of resistance. Using finite element simulations as a guide, composites with promising compositions and architectures are fabricated and evaluated for Li-transport properties using AC impedance and DC cycling with lithium in symmetric or half cells. General design rules will be determined that can be widely applied to other combinations of solid electrolytes.

Out-Year Goal. The out-year goal is to use advanced manufacturing processes where the architecture of the composite membrane can be developed and tailored to maximize performance and cost-effective manufacturing.

Collaborations. Work is conducted by Dr. A. Samuthira Pandian and Dr. Xi Chen. Dr. Jihua Chen (ORNL) assisted with electron microscopic characterization and Dr. Rose Ruther (ORNL) with Raman spectroscopy. Electrolyte powders are obtained from Ohara Corporation and Prof. Sakamoto (University of Michigan). Dr. Sergiy Kalnaus has provided finite element simulations.

Milestones

1. For spray-coated composites with high ceramic loading, vary the salt, plasticizer, and ceramic content to achieve facile ion transport across phase boundaries and 10^{-5} S/cm. (Q2 – Completed March 2017; still shy of 10^{-5} S/cm)
2. Assess lithium/electrolyte interface resistance. Adjust composition or add barrier coating to reduce ASR and passivate interface. (Q3 – Completed June 2017)
3. Fabricate full battery using aqueous spray coating for both the composite electrolyte and cathode incorporating a protected Li-metal anode. Demonstrate lithium cyclability. (Q4 – Stretch goal; nearly completed, September 2017)

Progress Report

A polymer-ceramic-polymer electrolyte (trilayer) cell was constructed to study the interfacial resistance between the polymer and ceramic electrolyte. Sintered ceramic plate (LICGC) from Ohara Corporation was sandwiched between two layers of polymer electrolyte of the same thickness, obtained by spray coating aqueous PEO+LiTf solution. The EIS results of single-layer ceramic plate, single-layer PEO + LiTF, and trilayer are shown in Figure 64a-c. The resistance of the trilayer is at least one order of magnitude larger than the two single layers combined. A SEM of the cross-section of the trilayer (Figure 64c, inset) shows uniform coating and smooth interfaces. The project calculated the interface resistance from the data of the single layers and the trilayer, shown in Figure 64d. At 30°C, the interface resistance is 10000 Ohm. As an effort to decrease the interface resistance, the project tried plasticized polymer electrolyte. Using the same protocol (Figure 64d), the plasticizer, TEGDME, enhances the ionic conductivity of the polymer electrolyte but does not facilitate ion transport across the polymer-ceramic interface. The project will continue this effort by using different plasticizers and surface treatments in the first quarter of FY 2018.

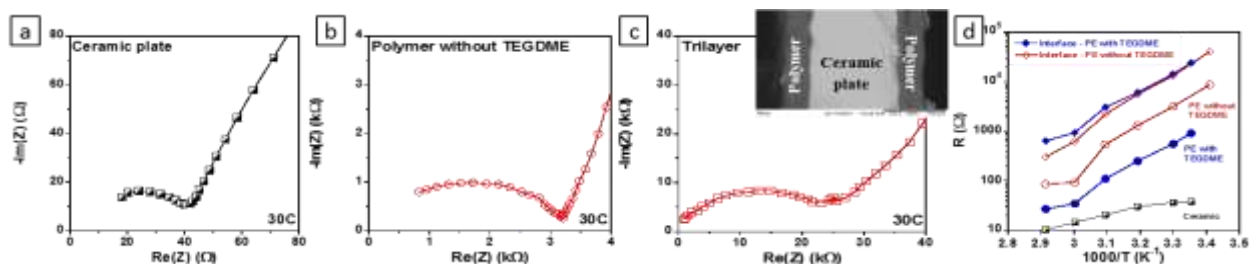


Figure 64. Results for trilayer cell polymer/ceramic/polymer electrolyte. (a-c) Electrochemical impedance spectroscopy (EIS) responses of ceramic plate, polymer electrolytes, and trilayer cells. All EIS responses are measured at 30°C. (Inset of c) Scanning electron microscopy of trilayer cell. (d) Arrhenius plot of interfacial resistance calculated from the trilayer cell data.

The project compared the ion conductivity of a polymer composite containing Ohara powder with that containing Li₇La₃Zr₂O₁₂ (LLZO), as shown in Figure 65. At temperatures above 30°C, composite containing 55 vol% Ohara showed higher conductivity than composite containing the same volume fraction of LLZO. Similar to Ohara composites, LLZO-PEO composite showed lower ion conductivity than both the polymer electrolyte and LLZO.

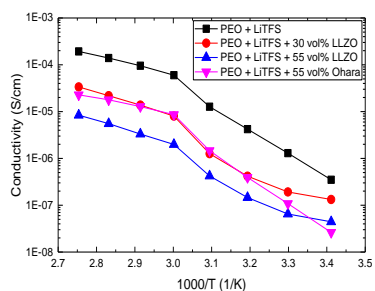


Figure 65. Arrhenius plot of composite containing LLZO, compared to that containing Ohara.

As a stretch goal for demonstrating lithium cyclability, the project fabricated a full cell using a two-layer electrolyte design. The composite electrolyte with a thickness of 10 μm was spray coated on NMC cathode. A layer of Celgard filled with EC:DMC/LiPF₆ was applied, and the cell was cycled against lithium metal. Cycling performance is shown in Figure 66. The composite does not reduce cyclability of NMC electrode (Figure 66) when cycled using an expanded metal current collector, as this allows easy access for electrolyte.

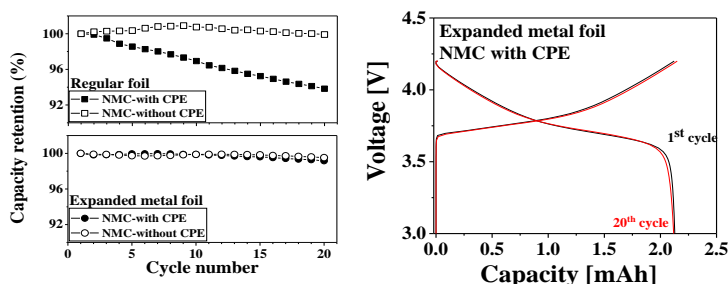


Figure 66. (left) Cycling data of NMC cathode/composite electrolyte/lithium cell on regular and expanded metal foils. (right) Galvanostatic cycling data showing the cycle stability between the 1st and 20th cycle.

Task 7.4 – Overcoming Interfacial Impedance in Solid-State Batteries (Eric Wachsman, Liangbing Hu, and Yifei Mo, University of Maryland College Park)

Project Objective. The project objective is to develop a multifaceted and integrated (experimental and computational) approach to solve the key issue in solid-state, Li-ion batteries (SSLiBs), interfacial impedance, with a focus on garnet-based SSEs, the knowledge of which can be applied to other SSE chemistries. The focus is to develop methods to decrease impedance across interfaces with the solid electrolyte, and ultimately demonstrate a high power/energy density battery employing the best of these methods.

Project Impact. Garnet electrolytes have shown great promise for intrinsically safer batteries with high energy density. The success of the proposed research can lead to dramatic progress on development of SSLiBs based on garnet electrolytes. The methodology of combining computational and experimental methods can lead to an understanding of the thermodynamics, kinetics, and structural stability of SSLiBs with garnet electrolytes. Garnet electrolyte particles are naturally brittle and hard due to their ceramic nature, and thus typically have poor contact between electrolyte particles and with electrode materials. A fundamental understanding of the particle interfaces at the nanoscale and through computational methods, especially with interface layers, can guide improvements to the SSE and battery design and eventually lead to commercial use of SSLiB technology.

Approach. Electrode/electrolyte interfaces in SSLiBs are typically planar, resulting in high impedance due to low specific surface area. Attempts to make high surface area 3D interfaces (for example, porous structure) can also result in high impedance due to poor contact at the electrode-electrolyte interface that hinders ion transport or degrades due to expansion/contraction with voltage cycling. This project will experimentally and computationally determine the interfacial structure-impedance relationship in SSLiBs to obtain fundamental insight into design parameters to overcome this issue. Furthermore, it will investigate interfacial modification (layers between SSE and electrode) to extend these structure-property relationships to demonstrate higher performance SSLiBs.

Collaborations. This project collaborates with Dr. Venkataraman Thangadurai on garnet synthesis. It will collaborate with Dr. Leonid A. Bendersky (Leader, Materials for Energy Storage Program at NIST) and use neutron scattering to investigate the lithium profile across the bilayer interface with different charge-discharge rates. The project is in collaboration with Dr. Kang Xu, ARL, with preparation of perfluoropolyether (PFPE) electrolyte.

Milestones

1. Fabricate and test SSLiBs with Li-NMC Chemistry. (Q1 – Completed December 2016)
2. Fabricate and test SSLiBs with Li-S Chemistry. (Q2 – Completed March 2017)
3. Develop models to investigate interfacial transport for Li-S and Li-NMC SSLiBs. (Q3 – Completed June 2017)
4. Achieve full cell (Li-S or Li-NMC) performance of 350-450 Wh/kg and 200 cycles. (Q4 – Completed September 2017)

Progress Report

Full Cell Performance of Li-NMC Battery

Solid-state batteries consisting of Li-metal anode, NMC cathode, and garnet-type $\text{Li}_7\text{La}_3\text{Zr}_2\text{O}_{12}$ (LLZO) solid electrolyte were fabricated. The LLZO solid electrolyte has a bi-layer dense-porous structure with thickness of 20 μm and 50 μm , respectively. Li-metal anode is hosted in the porous layer; NMC cathode is laminated on the dense layer. A controlled amount of liquid electrolyte is applied to the cathode.

Cycling performances of Li/NMC cells with NMC mass loadings of 13.5 and 32 mg/cm^2 are shown in Figure 67. Figure 67a is the voltage profile of a cell with 13.5 mg/cm^2 NMC loading cycled at 0.1 C rate (1 C = 170 mA/g). Figure 67b shows the capacity and CE of this cell. The capacity is stable at 175 mAh/g for 30 cycles. The energy density of the cell is calculated to be 232 Wh/kg. Capacities and CE of high rate cycling are in Figure 67c. The CE is over 99% during the 200 cycles, and the battery shows 80% capacity retention after 200 cycles at different rates up to 0.5 C. Figure 67d shows the voltage profiles of a cell with a higher NMC mass-loading (32 mg/cm^2) cathode. The cell is cycled at 0.05 C rate in 2 ~ 4.6 V voltage window. The capacity is 175 mAh/g, and the battery energy density is 357 Wh/kg, calculated based on masses of all battery components.

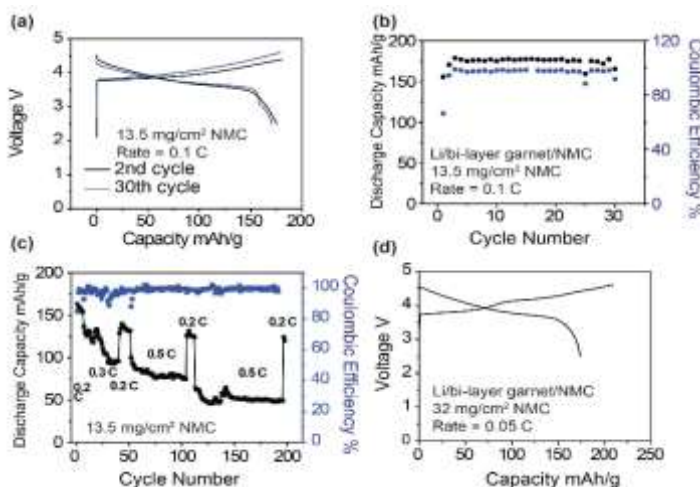


Figure 67. Cycling performances of Li/NMC cells with garnet electrolytes. (a-b) Voltage profiles and cycling performance of Li/NMC cell with 13.5 mg/cm^2 cathode at 0.1 C rate. Stable capacity at 175 mAh/g was achieved. (c) Cycling performance of Li/NMC cell with 13.5 mg/cm^2 cathode at various rates. High Coulombic efficiency and capacity retention were achieved during 200 cycles. (d) Voltage profiles of Li/NMC cell with 32 mg/cm^2 cathode at 0.05 C rate.

Full Cell Performance of Li-S Battery

The project also demonstrated Li-S batteries based on tri-layer garnet solid electrolyte. The tri-layer solid electrolyte is composed of a porous-dense-porous structure. The thickness of each porous layer is 70 μm , and the thickness of the dense layer is 30 μm . Lithium metal is infiltrated in one porous layer (anode), and sulfur is infiltrated in the other porous layer (cathode). Mass loadings of lithium and sulfur are 4.3 mg/cm^2 and 5.4 mg/cm^2 , respectively. The voltage profiles in Figure 68a show a typical Li-S two-plateau behavior with a high capacity of ~ 1200 mAh/g at 50 mA/g current density. The cell shows high capacity retention and nearly 100% CE during 50 cycles (Figure 68b). The total energy density of the tested cell is 272 Wh/kg, as calculated from the integrated cycling curve, based on the total weight of sulfur, carbon, garnet electrolyte, and Li-metal anode.

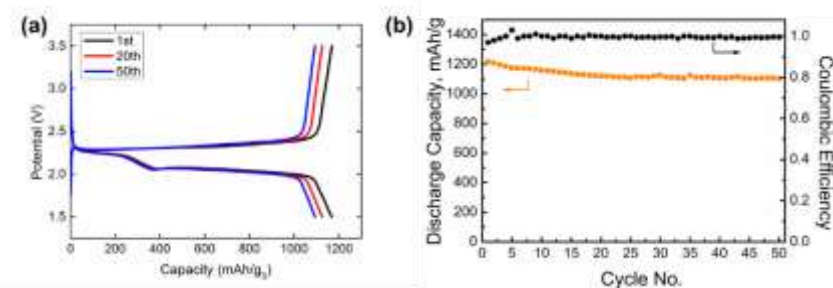


Figure 68. Cycling performances of Li/sulfur cell with garnet electrolytes. (a) Voltage profiles of the 1st, 5th, and 20th cycles of the solid-state Li-S cell at 50 mA/g current density. 1200 mAh/g capacity and low capacity loss were achieved. (b) Cycling results of the solid-state Li-S cell. High capacity retention was achieved with near 100% Coulombic efficiency.

Patents/Publications/Presentations/Presentations

Publications

- Fu, K., and Y. Gong, Y. Li, S. Xu, Y. Wen, L. Zhang, C. Wang, G. Pastel, J. Dai, B. Liu, H. Xie, Y. Yao, G. Hitz, D. McOwen, E. D. Wachsman, and L. Hu. “Three-Dimensional Bilayer Garnet Solid Electrolyte Based High Energy Density Lithium Metal-Sulfur Batteries.” *Energy & Environmental Science* (2017). doi: 10.1039/c7ee01004d.
- Liu, B., and Y. Gong, Y. Zhu, K. Fu, X. Han, Y. Yao, G. Pastel, C. Yang, H. Xie, E. D. Wachsman, and L. Hu. “Garnet Solid Electrolyte Protected Li Metal Batteries.” *ACS Applied Materials & Interfaces* 9 (2017): 18809–188815. doi: 10.1021/acsami.7b03887.
- Lui, W., and Y. Gong, Y. Zhu, Y. Li, Y. Yao, Y. Zhang, K. Fu, G. Pastel, C-F. Lin, Y. Mo, E. D. Wachsman, and L. Hu. “Reducing Interfacial Resistance between Garnet-Structured Solid-State Electrolyte and Li Metal Anode by a Germanium Layer.” *Advanced Materials* 29 (2017). doi: 10.1002/adma.201606042.

Presentations

- International Workshop on Piezoelectric Materials and Applications, 12th Energy Harvesting Workshop and 1st Annual Energy Harvesting Society Meeting, Falls Church, Virginia (September 11–14, 2017): “Ion Conducting Oxides for Electrochemical Energy Conversion and Storage”; Eric Wachsman. Invited.
- 254th ACS National Meeting & Exposition – Journey to Mars, Washington, D. C. (August 20–24, 2017): “Solid-State Electrochemical Energy Conversion and Storage for Exploration of Mars”; Eric Wachsman. Invited.

Task 7.5 – Nanoscale Interfacial Engineering for Stable Lithium-Metal Anodes (Yi Cui, Stanford University)

Project Objective. This study aims to render Li-metal anode with high capacity and reliability by developing chemically and mechanically stable interfacial layers between lithium metal and electrolytes, which is essential to couple with sulfur cathode for high-energy, Li-S batteries. With the nanoscale interfacial engineering approach, various kinds of advanced thin films will be introduced to overcome issues related to dendritic growth, reactive surface, and virtually “infinite” volume expansion of Li-metal anode.

Project Impact. Cycling life and stability of Li-metal anode will be dramatically increased. The success of this project, together with breakthroughs of sulfur cathode, will significantly increase the specific capacity of lithium batteries and also decrease cost, thereby stimulating the popularity of EVs.

Out-Year Goals. Along with suppressing dendrite growth, the cycle life, CE, and current density of Li-metal anode will be greatly improved (that is, no dendrite growth for current density up to 3.0 mA/cm², with CE greater than 99.5%) by choosing the appropriate interfacial nanomaterial along with rational electrode material design.

Milestones

1. Rational design of composite artificial SEI for the stabilization of 3D nano-porous Li-metal anode. (Q1 – Completed December 2016)
2. Explore novel materials and their properties as artificial SEI layer on lithium metal. (Q2 – Completed March 2017)
3. Explore surface coating techniques and materials for Li-metal stabilization. (Q3 – Completed June 2017)
4. Stabilizing 3D Li-metal anode with solid electrolytes. (Q4 – Completion in October 2017)

Progress Report

To address the challenges and make Li-metal anode a viable technology, an attractive strategy is to replace the volatile liquid electrolytes with nonflammable solid counterparts that are electrochemically stable against lithium and are mechanically robust to suppress dendrite growth. Although a wide variety of solid electrolytes for lithium batteries has been developed throughout the years, the same critical challenge, which is the interfacial detachment between solid electrolytes and electrodes, remains to be solved for all the systems.

Unlike liquid electrolytes, solid electrolytes barely have any fluidity to form a continuous contact with active materials inside the electrodes. Therefore, the electrochemical process can be severely limited by the contact area, leading to great interfacial resistance and low utilization of electrode capacity. The issue is even more pronounced for the Li-metal anode,

whose interfacial fluctuation in practical applications can be as large as tens of micrometers, making it difficult to cycle the solid-state lithium batteries at high capacity and current density. Here, the project presents a paradigm shift on the structural design of solid-state lithium batteries. Unlike the previous studies where solid-state cells were constructed using planar lithium foil, this work has adopted 3D lithium anode with high electroactive surface area for the first time. The challenge of creating a

conformal and continuous ionic contact between the 3D lithium anode and the bulk solid electrolyte was successfully addressed via a flowable ion-conducting interphase (Figure 69). This structural design has several major advantages. First, the adoption of a 3D lithium anode significantly increases the electrode-electrolyte contact area, dissipating the current density to facilitate charge transfer and offering opportunities to high-power operation. Second, by dividing bulk lithium into small domains, the interfacial fluctuation during cycling can be reduced to the submicrometer scale, enabling the cells to be cycled at a much higher capacity. More

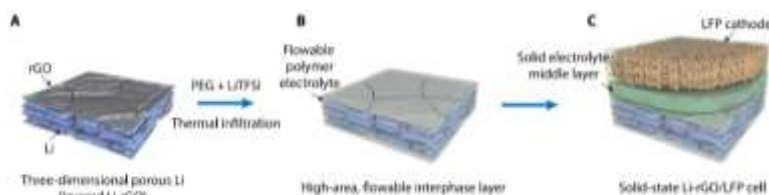


Figure 69. Schematics illustrating the fabrication process of the 3D lithium anode with flowable interphase for solid-state lithium battery. (A) 3D Li-rGO composite anode was first fabricated. (B) A flowable interphase for the 3D Li-rGO anode was created via thermal infiltration of liquid-like PEG-LiTFSI at a temperature of 150°C. (C) A composite polymer electrolyte (CPE) layer consisting of PEO, LiTFSI, and fumed silica or an LLZTO ceramic membrane was used as the middle layer; high-mass loading LFP cathode with the CPE as the binder was overlaid to construct the solid-state Li-LFP full cell.

importantly, incorporation of a flowable interfacial layer can accommodate the varying morphology at the 3D lithium-anode surface during cycling, which is desirable for maintaining a continuous electrode-electrolyte contact. Finally, the 3D lithium-anode design can be adopted as a general approach in solid-state lithium batteries, which is compatible with both solid polymer and inorganic ceramic electrolytes.

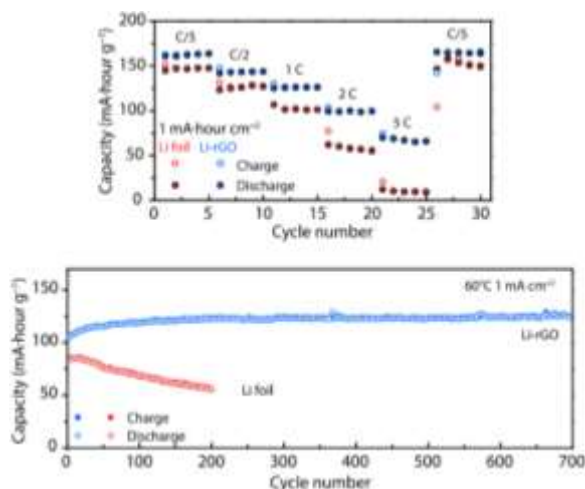


Figure 70. Electrochemical performance of solid-state Li-LFP batteries.

The electrochemical performance was tested pairing with LiFePO_4 (LFP) cathode. Notably—different from many studies on solid lithium batteries, where the cathode mass loading was kept low to minimize the interfacial delamination—a relatively high-capacity cathode ($\sim 1 \text{ mAh cm}^{-2}$) was used here to highlight the effectiveness of the design strategy toward improving interfacial contact. As can be seen from Figure 70, significantly improved rate performance and cycling stability can be achieved.

Patents/Publications/Presentations

Publication

- Liu, Y., and D. Lin, Y. Jin, K. Liu, X. Tao, Q. Zhang, X. Zhang, and Y. Cui. “Transforming from Planar to Three-Dimensional Lithium with Flowable Interphase for Solid Lithium Metal Batteries.” *Science Advances* 3, no. 10 (2017): eaao0713.

Task 7.6 – Lithium Dendrite Prevention for Lithium-Ion Batteries (Wu Xu and Ji-Guang Zhang, Pacific Northwest National Laboratory)

Project Objective. The project objective is to enable lithium metal to be used as an effective anode in rechargeable Li-metal batteries for long cycle life at a reasonably high current density. The investigation will focus on effects of various lithium salts, additives, and carbonate-based electrolyte formulations on Li-anode morphology, lithium CE, and battery performances in terms of long-term cycling stability at room temperature and elevated temperatures and at various current density conditions, rate capability, and low-temperature discharge behavior. The surface layers on lithium anode and cathode will be systematically analyzed. The properties of solvates of cation-solvent molecules will also be calculated to help explain obtained battery performances.

Project Impact. Lithium metal is an ideal anode material for rechargeable batteries. Unfortunately, dendritic lithium growth and limited CE during lithium deposition/stripping inherent in these batteries have prevented practical applications. This work will explore new electrolyte additives that can lead to dendrite-free lithium deposition with high CE. The success of this work will increase energy density of Li-metal batteries and accelerate market acceptance of EVs, especially for PHEVs required by the EV Everywhere Grand Challenge.

Out-Year Goals. The long-term goal of the proposed work is to enable lithium and Li-ion batteries with > 120 Wh/kg (for PHEVs), 1000 deep-discharge cycles, 10-year calendar life, improved abuse tolerance, and less than 20% capacity fade over a 10-year period.

Collaborations. This project collaborates with the following: Bryant Polzin (ANL) on NMC electrodes, Chongmin Wang (PNNL) on characterization by TEM/SEM, and Zihua Zhu (PNNL) on TOF-SIMS.

Milestones

1. Verify formation of a transient high Li⁺-concentration electrolyte layer during fast discharging by direct microscopic observation. (Q1 – Completed December 2016)
2. Identify effects of dual-salt electrolytes on Li-metal protection during fast charging. (Q2, March 31, 2017 – Complete)
3. Identify new electrolytes that are stable with both lithium and high-voltage cathode. (Q3, June 20, 2017 – Completed)
4. Increase the CE of lithium cycling in the new electrolyte to be more than 99%. (Q4, September 30, 2017 – In progress)

Progress Report

This quarter, the synergistic effects of additives $\text{LiAsF}_6 + \text{VC}$ in the electrolyte of 1 M LiPF_6/PC on lithium deposition and the long-term cycling performance of $\text{Li}||\text{NMC-333}$ cells were investigated. It is revealed for the first time that LiAsF_6 can be reduced to Li_3As alloy phase and LiF , which can act as nano-sized seeds for lithium growth and form a robust SEI layer (see Figure 71). The addition of VC or FEC not only enables the uniform distribution of Li_3As seeds because of the initial surface passivation of the copper substrate, but also improves the SEI layer flexibility due to the formation of polymeric components in the SEI.

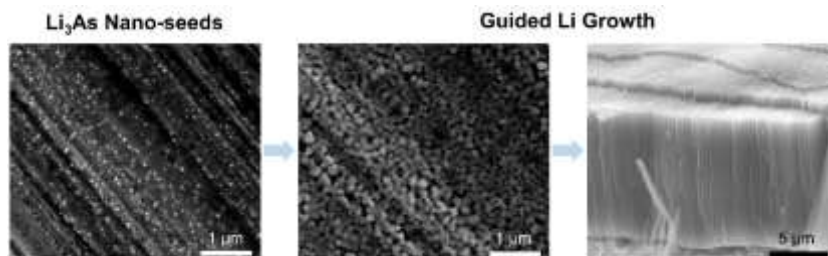


Figure 71. Scanning electron microscopy images of nano-seeds formed on copper substrate after linear sweep voltammetry to 0 V and held at 0 V for 1 min (left), after lithium deposition for 10 min (middle), and after lithium deposition for 15 h (right). The electrolyte is 1 M LiPF_6 in PC, with 2% LiAsF_6 and 2% VC. The current density is 0.1 mA cm^{-2} .

The effects of lithium imide and lithium orthoborate dual-salt electrolytes of different salt chemistries in carbonate solvents on the cycling stability of lithium metal batteries were systematically and comparatively investigated. Two imide salts (LiTFSI and LiFSI) and two orthoborate salts (LiBOB and LiDFOB) were chosen for this study and compared with the conventional LiPF_6 salt. DFT calculations indicate that the chemical and electrochemical stabilities follow the order of $\text{LiTFSI-LiBOB} > \text{LiTFSI-LiDFOB} > \text{LiFSI-LiBOB} > \text{LiFSI-LiDFOB}$. The experimental cycling stability of the Li-metal cells with the electrolytes follows the order from good to poor as $\text{LiTFSI-LiBOB} > \text{LiTFSI-LiDFOB} > \text{LiPF}_6 > \text{LiFSI-LiBOB}$, indicating that LiTFSI behaves better than LiFSI and LiBOB over LiDFOB in these dual-salt mixtures. The LiTFSI-LiBOB can effectively protect the aluminum substrate and form a more robust surface film on Li-metal anode, while the LiFSI-LiBOB results in serious corrosion to the stainless-steel cell case and a thicker and looser surface film on lithium anode.

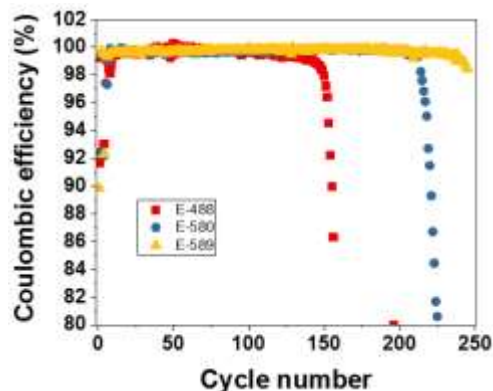


Figure 72. Cycling stability of Coulombic efficiency of $\text{Li}||\text{NMC-333}$ cells using three electrolytes of 1 M LiTFSI-LiBOB plus 0.05 M LiPF_6 in EC-EMC with different solvent compositions and/or other additives (VC and FEC). The current density is 2.0 mA cm^{-2} . E-488 and E-580 have EC-EMC 4:6 by weight, while E-589 has EC-EMC 7:3 by weight. E-580 and E-589 also contain VC and FEC.

The CE of lithium cycling was also studied by optimizing solvent compositions and adding combinational additives in dual-salt electrolytes of LiTFSI-LiBOB in EC-EMC. The increase of EC content in the solvent mixture will slightly improve the average lithium CE from 87.4% for EC-EMC (4:6 wt) to about 91.6% for EC-EMC (7:3, 8:2, and 9:1 wt). The addition of additives (LiPF_6 , VC, and FEC, in single or combination) will largely increase the average lithium CE. For the additive combination of 0.05 M $\text{LiPF}_6 + 2\% \text{ VC} + 2\% \text{ FEC}$ in the dual-salt electrolyte with EC-EMC (7:3 wt) (that is, E-589), the average lithium CE can be further increased to 98.1%. This electrolyte also shows excellent stability with Li-metal anode by the stable and low potential in $\text{Li}||\text{Li}$ symmetric cells for at least 800 h at a current density of 0.5 mA cm^{-2} , and exhibits about 99.7% CE of lithium cycling in $\text{Li}||\text{NMC333}$ cells between 2.7 and 4.3 V at 2.0 mA cm^{-2} , as shown by the yellow data in Figure 72. More performance testing and characterization are under way.

Patents/Publications/Presentations

Publications

- Jiao, S., and J. Zheng, Q. Li, X. Li, M. H. Engelhard, R. Cao, J.-G. Zhang, and W. Xu. “Behavior of Lithium Metal Anode under Various Capacity Utilization and High Current Density in Lithium Metal Batteries.” *Joule*. Accepted.
- Ren, X., and Y. Zhang, M. H. Engelhard, Q. Li, J.-G. Zhang, and W. Xu. “Guided Lithium Metal Deposition and Improved Lithium Coulombic Efficiency through Synergistic Effects of LiAsF₆ and Cyclic Carbonate Additives.” Submitted.
- Li, X., and J. Zheng, M. H. Engelhard, D. Mei, Q. Li, S. Jiao, N. Liu, W. Zhao, J.-G. Zhang, and W. Xu. “Effects of Imide-Orthoborate Dual-Salt Mixtures in Organic Carbonate Electrolytes on the Stability of Lithium Metal Batteries.” Submitted.

Task 7.7 – Lithium Batteries with Higher Capacity and Voltage (John B. Goodenough, University of Texas – Austin)

Project Objective. The project objective is to develop an electrochemically stable alkali-metal anode that can avoid the SEI layer formation and the alkali-metal dendrites during charge/discharge. To achieve the goal, a thin and elastic solid electrolyte membrane with a Fermi energy above that of metallic lithium and an ionic conductivity $\sigma > 10^{-4} \text{ S cm}^{-1}$ will be tested in contact with alkali-metal surface. The interface between the alkali-metal and the electrolyte membrane should be free from liquid electrolyte, have a low impedance for alkali-metal transport and plating, and keep a good mechanical contact during electrochemical reactions.

Project Impact. An alkali-metal anode (lithium or sodium) would increase the energy density for a given cathode by providing a higher cell voltage. However, lithium is not used as the anode in today's commercial Li-ion batteries because electrochemical dendrite formation can induce a cell short-circuit and critical safety hazards. This project aims to find a way to avoid the formation of alkali-metal dendrites and to develop an electrochemical cell with dendrite-free alkali-metal anode. Therefore, once realized, the project will have a significant impact through an energy-density increase and battery safety; it will enable a commercial Li-metal rechargeable battery of increased cycle life.

Approach. The project will design, make, and test cells. The key approach is to introduce a solid-solid contact between an alkali metal and a solid electrolyte membrane. Where SEI formation occurs, the creation of new anode surface at dendrites with each cycle causes capacity fade and a shortened cycle life. To avoid the SEI formation, a thin and elastic solid electrolyte membrane would be introduced, or the solid electrolyte should not be reduced by, but should be wet by, a metallic alkali-ion anode.

Out-Year Goals. The out-year goal is to develop coin cells that are safe and low-cost with a long cycle life at a voltage $V > 3.0 \text{ V}$.

Collaborations. This project collaborates with A. Manthiram at UT Austin, and Karim Zaghib at HQ.

Milestones

1. Demonstrate the cycle life and capacity of a Li-S cell. (Q1 – Complete)
2. Demonstrate a high-voltage cell containing the glass electrolyte. (Q2 – In progress)
3. Demonstrate a new battery concept. (Q3 – In progress)
4. Test energy density, cycle life, and rate of charge/discharge of the new battery concept. (Q4 – In progress)

Progress Report

The Cu^+/Cu^0 redox couple in the cathode was tested in a quasi-solid-state lithium battery cell. To collect more reproducible cell data, the project has fabricated a gel polymer electrolyte membrane based on PVDF-HFP instead of the crosslinked polymer membrane that was used last quarter. LiTFSI and poly(ethylene glycol) methyl ether acrylate were added to the PVDF-HFP solution in acetone, and then the clear solution was cast on a Teflon dish. After vacuum drying at 50°C overnight, the membrane was used as a separator in a quasi-solid-state cell. This quarter, the project has investigated several experimental parameters that affect the electrochemical performance of the Cu^+/Cu^0 redox couple.

Electrochemical Feed of Cu^+ Ions into the Separator Membrane and its Effect on the Discharge Capacity.

First, the project has made coin half-cells with copper foil as the cathode and lithium metal as the anode. During the first charge, copper dissolves into the polymer membrane and exhibits a voltage plateau at around 3.4 V. The electrochemical oxidation time was changed (10, 20, and 40 h at $20\ \mu\text{A}$ and 60°C) to control the Cu^+ concentration in the membrane and to check its effect on the discharge capacity (Figure 73). The results suggest that (1) a higher Cu^+ concentration in the membrane is needed to promote Cu^+ conduction and deliver a higher reversible capacity, (2) Cu^+ diffusion away from the cathode interface must be solved to enhance CE, and (3) copper plating at the lithium surface should be prohibited.

Chemical Feed of Cu^{2+} Ions into the Separator Membrane and Its Effect on the Discharge Capacity.

Second, to enhance electrochemical performance, vacuum-dried Cu^{2+} perchlorate was chemically incorporated into the polymer composite during the membrane fabrication. Cu^{2+} concentration was set to be 1:1 ratio to the Li^+ concentration. The Cu-incorporated membrane could not be solely used as a separator owing to the spontaneous Cu^{2+} reduction reaction at the lithium surface: the bare gel polymer membrane was introduced between the lithium anode and the Cu-incorporated membrane. Figure 74 shows the charge/discharge voltage curves of the coin cell with copper foil as the cathode. The cell was charged first and then discharged at $20\ \mu\text{A}$ and 60°C . Compared to Figure 73, the discharge capacity was greatly improved. Clearly, having sufficient copper ion concentration in the membrane is critical to deliver a higher cell capacity and a higher CE.

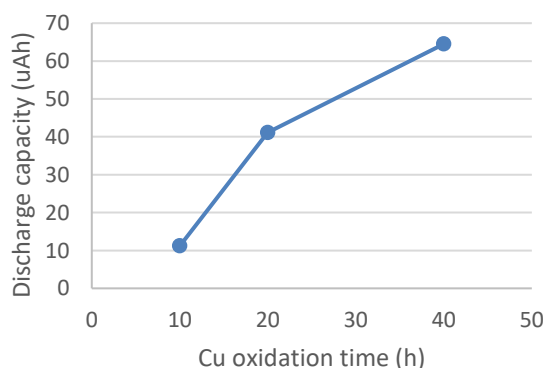


Figure 73. Copper oxidation time and corresponding discharge capacity.

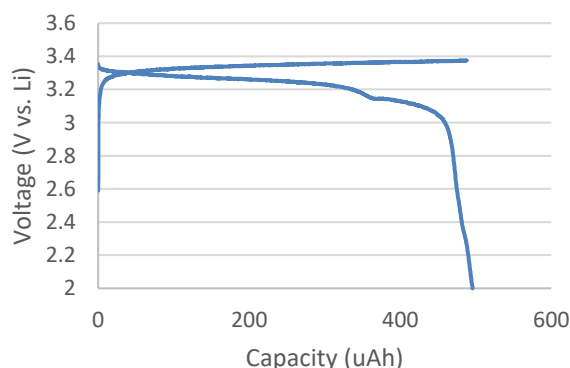


Figure 74. Charge/discharge voltage curves of the copper cathode.

Currently, the project is studying a charged-state cell to quantitatively evaluate the electrochemical performance of the Cu^+/Cu^0 redox couple and to improve the charge/discharge reversibility.

Task 7.8 – Advancing Solid-State Interfaces in Lithium-Ion Batteries (Nenad Markovic and Larry A. Curtiss, Argonne National Laboratory)

Project Objective. The project objectives are multifaceted, including: (1) development of a new mechanically and chemically stable Li-selective solid “membrane” capable of protecting the metal lithium anode during the discharge process in commercially available liquid electrolytes (hereafter denoted as a $S_{Li-SM-EL}$ system); and (2) development of a mechanically/chemically stable and Li-ion conductive ($\geq 2 \times 10^{-4}$ S/cm at 298K) solid electrolyte for a solid-state battery encompassing a metal lithium anode and nonflammable solid electrolyte that can operate at cathode potentials > 5 V (denoted as a $S_{Li-SEL-SC}$ system).

Project Impact. Protective organic and inorganic compounds can enhance stability of interface, improve Li-ion interfacial transport, minimize dendrite formation, and increase safety in Li-ion batteries.

Approach. The project proposes to develop and use interdisciplinary, atomic-/molecular-level insight obtained from integrating both experimental- and computational-based methodologies to define the landscape of parameters that control interfacial properties for a new generation of the Li-ion solid-solid battery systems. The strategy will involve transferring knowledge gained from well-characterized thin-film materials to real-world materials. This strategy forms a closed loop wherein the knowledge gained from model systems is used to design more complex, real-world materials and vice-versa. The work will focus on utilizing existing in-house synthesis and characterization methods to enable rapid transition from fundamental science to realistic cells.

Out-Year Goals. The out-year goals are to use and develop the physical and chemical synthesis methods for design of solid-solid interfaces with unique chemical/mechanical/conductivity properties of $S_{Li-SM-EL}$ and $S_{Li-SEL-SC}$ systems. The proposed work will develop and exploit a variety of *ex situ* and *in situ* experimental optical and surface sensitive techniques and electrochemical methods to explore and explain bulk and interfacial properties of the selected materials. The results will serve to unravel many puzzling bulk and interfacial properties of $S_{Li-SM-EL}$ and $S_{Li-SEL-SC}$ materials.

Collaborations. This project funds work at ANL and University of Illinois at Chicago (Prof. Amin Salehi). It will establish collaboration with Jeff Sakamoto at University of Michigan.

Milestones

1. Development of new synthesis and characterization methods for controlled deposition of lithium on well-defined $SrTiO_3$ single crystals. (Q1 – Initiated November 2016)
2. Use ultra high vacuum (UHV)-based experimental techniques in combination with computational methods to investigate parameters that control interaction of lithium anode with individual components of $Li_{6.5}La_3Zr_{1.5}M_{0.5}O_2$ ($M = Nb, Ta$) and Li_2CO_3 “membrane.” (Q2 – In progress)
3. Design and develop *in situ* evaluation of stability of both Li_2CO_3 “membrane” (ICP-MS) and selected organic electrolytes during charge-discharge processes (DEMS). (Q3)
4. Investigate the CE of, as well as the charge-discharge cyclability for, selected $S_{Li-SM-EL}$ and $S_{Li-SEL-SC}$ systems. (Q4)

Progress Report

Lithium Interfacial Reactivity – Computational Prediction. DFT calculations were performed to rationalize and ultimately understand experimentally observed effects of surface orientation on lithium interactions with SrTiO₃ oxide single crystal surfaces. This is done to gain insight into the structural origins of morphological instabilities. Multiple terminations have been studied for these surfaces, including TiO₂ terminations on the (100) and reconstructed (110) surfaces, as well as O₂ and SrTiO terminations of the (110) surface. Figure 75 (top) shows optimized geometries of lithium atoms on the (100), O₂-(110) and (3x1)-(100) SrTiO₃ surfaces. While lithium binds preferentially to oxygen ions in all cases, the difference between reconstructed (3x1)-(110) and (100) surface is the preference of subsurface positions for lithium on the (110) surface. Calculations of binding energy of lithium (relative to lithium metal) shown in Figure 75 (bottom) indicate that the binding energies correlate with stoichiometry of the surface layer. The results show that the binding of lithium becomes more favorable energetically with increasing oxygen stoichiometry, while oxygen deficiency results in strongly unfavorable interactions between lithium and the surface. These calculations help explain the morphological instabilities observed experimentally. The project's ongoing studies include effects of lithium coverage on the lithium-surface interactions. The next stage of studies is to address lithium interactions with TM oxide surfaces to provide insights into interface properties dependence on the oxide surface orientation and termination.

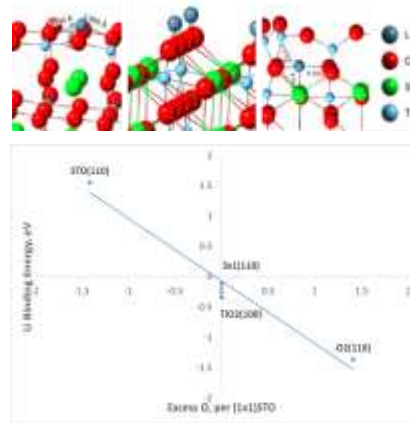


Figure 75. Lithium adsorbed on TiO₂-terminated (100) SrTiO₃ surface, O₂-terminated (110) surface, and (3x1) reconstructed (110) surface. (bottom) Lithium binding energy as a function of oxygen stoichiometry.

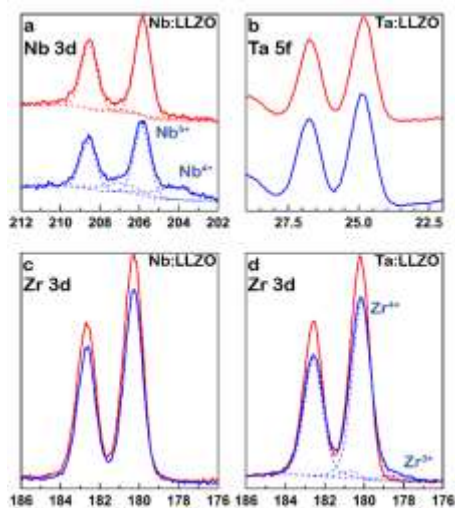


Figure 76. X-ray photoelectron spectroscopy core-level spectra before (red) and after (blue) lithium deposition show (a) reduction of niobium in Nb:LLZO and (d) reduction of zirconium in Ta:LLZO. (b) Tantalum in Ta:LLZO and (c) zirconium in Nb:LLZO are all stable throughout the sputtering.

Lithium Interfacial Reactivity – Experimental Observations.

Experimental studies have been focused on understanding and predicting lithium interaction with niobium and tantalum, two key dopants in LLZO solid electrolyte. Polycrystalline Nb- and Ta-doped LLZO ceramic pellets were synthesized via conventional solid-state route. Given that LLZO can be quickly oxidized in air and form ~ 5- μ m thick Li₂CO₃ at surface, LLZO samples were polished inside argon glove box (O₂ and H₂O < 0.5 ppm) using 1200-grit SiC sandpaper to totally remove Li₂CO₃ surface layer, then immediately loaded into vacuum to prevent further oxidation. As shown in Figure 76, deposition of lithium on Nb:LLZO shows clear evidence of niobium reduction from Nb⁵⁺ to Nb⁴⁺, and no evidence of zirconium reduction. On the contrast, lithium reduced zirconium from Zr⁴⁺ to Zr³⁺ in the Ta:LLZO sample, while tantalum stayed as Ta⁵⁺ before and after sputtering. Considering the molar ratio of doping element (Ta/Nb) to zirconium, the total charge transfer between lithium and the LLZO samples is about the same for these two samples. The methodology minimizes the formation of the oxidation layer at LLZO surface that could block direct interaction between lithium and LLZO, enabling the project to study LLZO stability against lithium for different doping types.

Task 7.9 – Engineering Approaches to Dendrite-Free Lithium Anodes (Prashant Kumta, University of Pittsburgh)

Project Objective. This project will yield Li-metal anodes with specific capacity ≥ 2000 mAh/g (≥ 10 mAh/cm²), ~ 1000 cycles, CE loss $\leq 0.01\%$, and CE $\geq 99.99\%$ with superior rate capability. The goal is to (1) systematically characterize different approaches for generation of dendrite-free Li-metal anodes while also providing understanding of the scientific underpinnings, and (2) evaluate the microstructure and electrochemical performance of dendrite-free Li-metal anodes. Generation of high-performance, dendrite-free Li-metal anodes will successfully demonstrate generation of novel sulfur cathodes, affording fabrication of Li-S batteries meeting the targeted gravimetric energy densities ≥ 350 Wh/kg and ≥ 750 Wh/l with a cost target \$125/kWh and cycle life of at least 1000 cycles for meeting the EV Everywhere Grand Challenge blueprint.

Project Impact. Dendrite formation in electrochemical systems occurs due to inhomogeneous current densities coupled with local diffusion gradients, surface roughness, and kinetic roughening. Lithium dendrite formation and growth are, however, not well understood; adding to the complexity is SEI formation. Control and elimination of Li-metal dendrite formation is a veritable challenge. If overcome, it would render universal adoption of Li-anode batteries for stationary and mobile applications. This project is a scientific study of novel approaches to address dendrite formation in Li-anode batteries, electrolyte decomposition, and associated cell failure. Development of dendrite-free, high-performance lithium anodes will enable the use of Li-free cathodes, opening myriad possibilities to push the envelope in terms of cathode capacity and battery energy density.

Out-Year Goals. This project comprises three major phases to be successfully completed in three years:

- Year 1 – Synthesis, characterization, and scale up of suitable PF (porous foams) for use as current collectors for lithium anodes and Li-ion conductor (LIC) materials to prepare multilayer porous foams (MPF).
- Year 2 – Development of Li-rich structurally isomorphous alloy (SIA) anodes; generation of composite multilayer anodes (CMAs).
- Year 3 – Advanced high-energy-density, high-rate, extremely cyclable cell development.

Collaborations. The project will collaborate with Dr. Moni Kanchan and Dr. Oleg I. Velikokhatnyi Datta (University of Pittsburgh, U Pitt) as co-PIs. It will also collaborate with Dr. D. Krishnan Achary (U Pitt) for solid-state magic angle spinning nuclear magnetic resonance (MAS-NMR) characterization.

Milestones

1. Identify and synthesize materials with high electronic conductivity, electrochemical stability that can be generated as porous architectures. (Q3 – Completed July 2017)
2. Identify and synthesize LIC materials for use as coatings on both PF and use in CMAs with room-temperature ionic conductivity (10^{-3} - 10^{-4} S/cm). (Q3 – Completed July 2017)
3. Synthesize MPF exhibiting: specific capacity ≥ 1000 mAh/g (≥ 4 mAh/cm²), > 400 cycles without cell failure), initial CE: $\leq 95\%$ with $\leq 0.05\%$ loss per cycle. (October 2017 – In progress)
4. Perform first-principles investigations into identifying electronically and ionically conductive materials capable of acting as SIA compositions over a range of lithium compositions. (October 2017 – In progress)
5. Fabricate/characterize suitable thick electrodes for 10-mAh cell configurations. (October 2017 – In progress)
6. Synthesize and test SIA electrodes. (January 2018 – In progress)
7. Optimize MPFs to improve capacity and stability for scaling. (July 2018 – In progress)

Progress Report

Phase 1 of the project is aimed at developing PFs and MPFs of copper using a sacrificial template approach with the primary aim to reduce orthogonal growth of lithium following deposition. Figure 77 shows the SEM image of the Gen-2 PFs after sintering and removal of the sacrificial template. A continuous porous network (porosity $\sim 85\%$) is clearly observed. Figure 78 shows the cycling efficiency of lithium plating and deplating on copper foams at a current density of 1 mA/cm^2 for 1 h with a deplating cutoff voltage of 1 V in 1.8 M LiTFSI, 0.1 M LiNO_3 in DOL:DME (50:50 vol.) electrolyte. The copper foams demonstrate stable cycling to 60 cycles with a CE of $\sim 90\%$, after which they transition into a region of constant fade similar to lithium plating/deplating typically seen on copper foils. This transition from stable cycling to constant fade is attributed to transition of the globular lithium plating morphology within the porous architecture to a columnar morphology forming on the foam surface. Figure 79a shows the cross section of the cycled foam electrodes. Figure 79b-c shows different deposition morphologies in each region attributed to competitive SEI layer formation. Efforts are under way to minimize the SEI growth and improve cycling stability with concomitant increase in the CE.

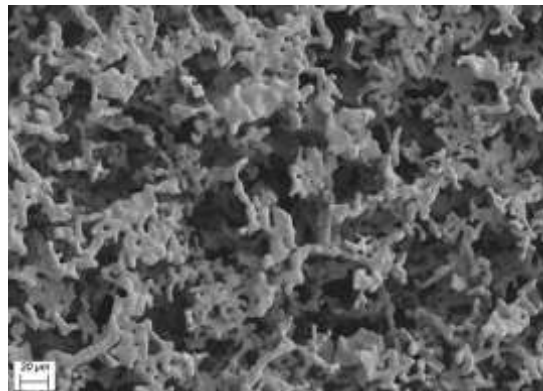


Figure 77. Scanning electron microscopy image of the high porosity ($\sim 85\%$) copper foams after sintering and removal of the sacrificial template.

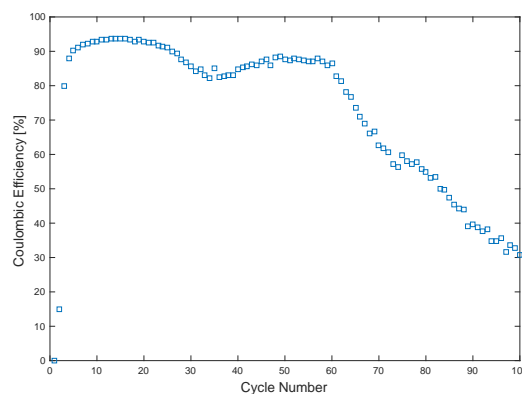


Figure 78. Gen-2 copper foam electrodes demonstrate stable cycling region of 60 cycles at $\sim 90\%$ Coulombic efficiency.

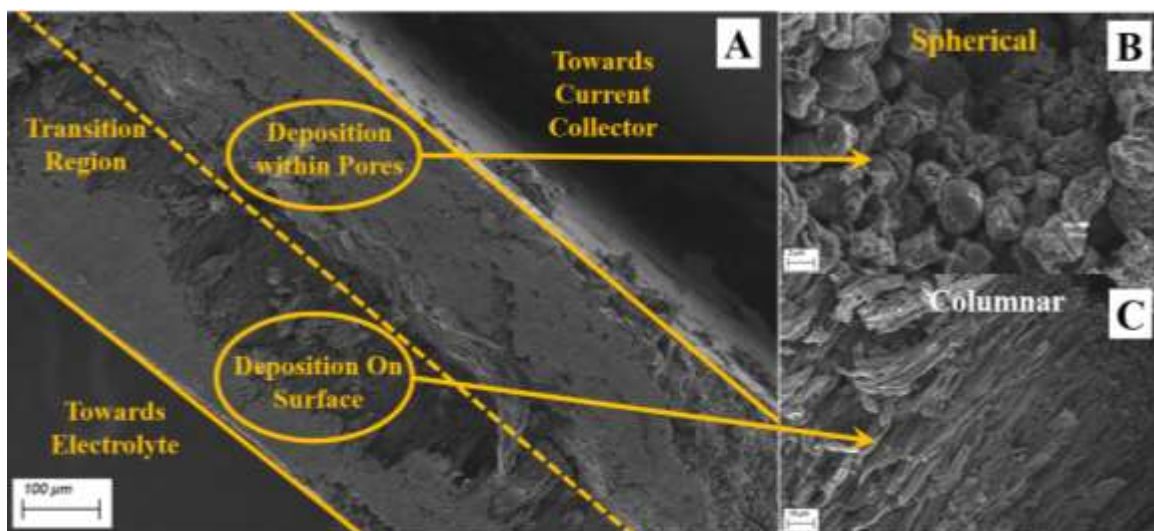


Figure 79. Scanning electron microscopy images of the porous copper foam electrodes after cycling (~ 200 cycles). (a) Cross-section view. (b) Close up of lithium deposited within the foam structure. (c) Close up of lithium deposited on top of the foam surface following pore closure by competitive SEI formation in the foam structure.

Patents/Publications/Presentations

Publication

- Jampani, P.H., and P. M. Shanthi, B. A. Day, B. Gattu, O. I. Velikokhatnyi, M. K. Datta, and P. N. Kumta. “Lithium Metal Anode Based Rechargeable Batteries: Recent Advances and Challenges for the Future.” *Progress in Materials Science* (2017). Under review.

Presentation

- 232nd ECS Meeting, National Harbor, Maryland (October 1–5, 2017): “Engineered Porous Foam Electrodes - New Approaches to Dendrite-Free Anodes for Li-Metal Batteries”; B. A. Day, B. Gattu, P. H. Jampani, P. M. Shanthi, M. K. Datta, and P. N. Kumta. Paper presentation.

Task 7.10 – Self-Assembling and Self-Healing Rechargeable Lithium Batteries (Yet-Ming Chiang, Massachusetts Institute of Technology; Venkat Viswanathan, Carnegie Mellon University)

Project Objective. The project objectives are as follows: (1) investigate formation of lithium halide containing SEI, (2) characterize the structure and composition of the SEI surface film and morphology of the electrochemically deposited lithium, and (3) develop combinations of electrolytes (solvents + salts) and electrolyte additives that produce a highly Li-ion conducting, mechanically robust, and self-healing SEI to suppress lithium dendrite formation and improve CE.

Project Impact. Efforts to achieve practical use of the Li-metal anode in rechargeable lithium batteries have long been plagued by lithium dendrite formation and low CE. Lithium dendrites cause battery short-circuits, leading to serious safety hazards. The low CE of Li-metal anodes demands use of excess lithium to offset the lithium loss during cycling, which lowers the overall energy density of the battery. If successful, this project will enable self-forming and self-healing SEI containing alkali and/or alkaline earth halides that can suppress dendrite formation and improve CE. This will eventually enable high-energy-density (> 400 Wh/kg) and long-cycle-life (> 500 cycles, 80% capacity retention) Li-metal batteries.

Approach. The project approach involves the following: (1) identifying suitable combinations of solvents, Li-electrolyte salts, and halide and other additives that can produce highly Li-ion conducting, mechanically robust, and self-healing SEI, (2) using integrated theory and experiment, and (3) assembling and testing symmetric and asymmetric cells and Li-metal batteries comprising a high areal-capacity cathode (> 3 mAh/cm²) and a capacity-limited Li-metal anode (< 130% lithium excess).

Out-Year Goals. The project will down-select electrolyte compositions, develop designs for prototype full cells of > 10 mAh capacity, and fabricate and deliver cells to DOE-specified laboratories for testing and evaluation.

Collaborations. This project collaborates with 24M Technologies Inc. (18 cm²/80 cm² pouch cell fabrication and tests).

Milestones

1. Complete initial computations and halide solubility studies and construct experimental matrix of halides and solvents. (Q2 – Completed April 30, 2017)
2. Demonstrate cell designs and electrochemical testing parameters that allow clear differentiation of dendritic and non-dendritic behavior of lithium electrodes. (Q3 – Completed June 30, 2017)
3. Deliver characterization results for morphological evolution of Li-metal surface showing that halide additives diminish lithium dendrite formation. (Q4 – Completed September 30, 2017)
4. Demonstrate Li-Li symmetric cell using halide additives that outperforms additive-free cell according to criteria in Q2 and Q3. (Q5 – *Go/No-Go* milestone; In progress)

Progress Report

Results this quarter: halide additives change the morphology of the deposited lithium and diminish the lithium dendrite formation.

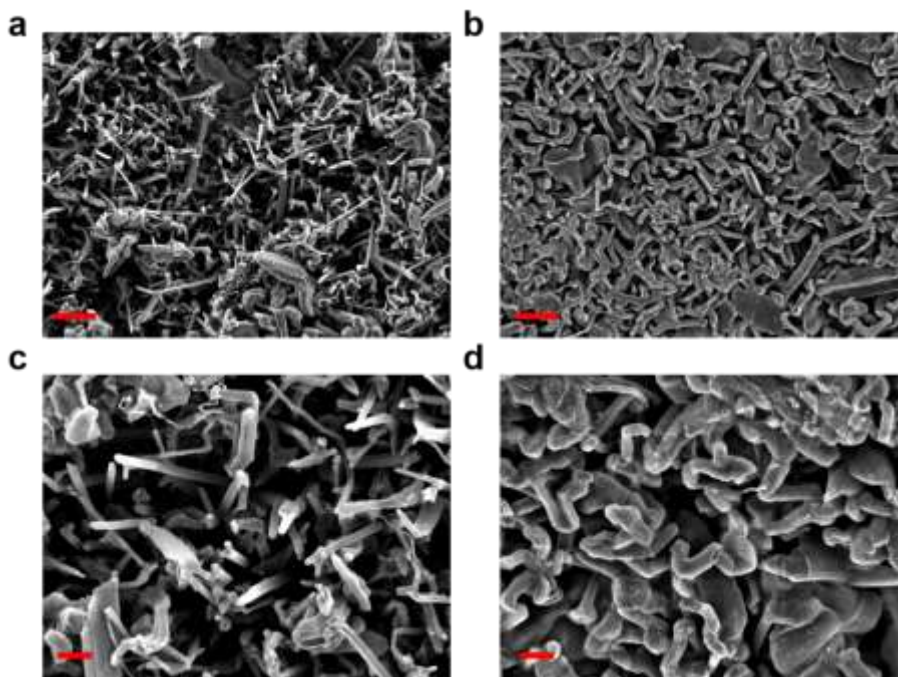


Figure 80. Scanning electron microscopy (SEM) characterization of the morphology of the deposited lithium. (a/c) Top-view SEM images of lithium deposited in 1 M LiPF₆ EC-DMC electrolyte. (b/d) Top-view SEM images of lithium deposited in 1 M LiPF₆-based electrolyte with a fluorine-containing additive. The scale bars in (a/b) are 5 μm . The scale bars in (c/d) are 2 μm . 3 mAh cm^{-2} of lithium is deposited at a current density of 0.6 mA cm^{-2} .

Lithium has been electrochemically deposited onto copper substrates and its morphology examined using SEM. The deposited lithium areal capacity is 3 mAh cm^{-2} , and the current density is 0.6 mA cm^{-2} . The deposited lithium is washed with DMC several times and dried under vacuum before being transferred into the SEM chamber for observation. Figure 80a/c shows the deposited lithium in the electrochemical cell using a standard 1 M LiPF₆ EC-DMC electrolyte without additives. The deposited lithium film is porous and consists of straight, fiber-like deposits. Figure 80b/d shows the deposited lithium in the electrochemical cell using 1 M LiPF₆ based electrolytes with a fluorine-containing additive. The deposited lithium film is much denser compared to the case without the fluorine-containing additive. The morphology of the deposited lithium is also different, being larger and more tortuous. These results have met the fourth-quarter milestone, “Deliver characterization results for morphological evolution of lithium metal surface showing that halide additives diminish lithium dendrite formation.” Concurrently with these observations, the cycling performance of the additive-containing electrolyte has been found to be improved over the additive-free electrolyte, as will be reported next quarter.

Patents/Publications/Presentations

Publication

- Ahmad, Zeeshan, and Venkatasubramanian Viswanathan. “Stability of Electrodeposition at Solid-Solid Interfaces and Implications for Metal Anodes.” *Phys. Rev. Lett.* 119 (2017): 056003.

TASK 8 – LITHIUM–SULFUR BATTERIES

Summary and Highlights

Advances in Li-ion technology have been stymied by challenges involved in developing high reversible capacity cathodes and stable anodes. Hence, there is a critical need for development of alternate battery technologies with superior energy densities and cycling capabilities. In this regard, Li-S batteries have been identified as the next flagship technology, holding much promise due to the attractive theoretical specific energy densities of 2,567 Wh/kg. In addition, realization of the high theoretical specific capacity of 1,675 mAh/g corresponding to formation of Li_2S using earth-abundant sulfur renders the system highly promising compared to other available cathode systems. Thus, the research focus has shifted to developing Li-S batteries. This system, however, suffers from major drawbacks, as elucidated below:

- Limited inherent electronic conductivity of sulfur-based and sulfur-compound-based cathodes;
- Volumetric expansion and contraction of both the sulfur cathode and lithium anode;
- Soluble polysulfide formation/dissolution and sluggish kinetics of subsequent conversion of polysulfides to Li_2S , resulting in poor cycling life;
- Particle fracture and delamination resulting from the repeated volumetric expansion and contraction;
- Irreversible loss of lithium at the sulfur cathode, resulting in poor CE; and
- High diffusivity of polysulfides in the electrolyte, resulting in plating at the anode and consequent loss of driving force for lithium diffusion (that is, drop in cell voltage).

These major issues cause sulfur loss from the cathode, leading to mechanical disintegration. Additionally, surface passivation of anode and cathode systems results in a decrease in the overall specific capacity and CE upon cycling. Consequently, the battery becomes inactive within the first few charge-discharge cycles. Achievement of stable high capacity in Li-S batteries requires execution of fundamental studies to understand the degradation mechanisms in conjunction with devising engineered solutions.

This Task addresses both aspects with execution of esoteric, fundamental *in situ* XAS and *in situ* electron paramagnetic resonance (EPR) studies juxtaposed with conducting innovative applied research comprising use of suitable additives, coatings, and exploration of composite morphologies as well as appropriate engineered strategies. Both ANL and LBNL use X-ray based techniques to study phase evolution and loss of CE in S-based and S-Se-based electrodes, primarily by the former during lithiation/delithiation while understanding polysulfide formation in sulfur and oligomeric PEO solvent by the latter, respectively. Work from PNNL, U Pitt, and Stanford demonstrates high areal capacity electrodes exceeding 4 mAh/cm². Following loading studies reported this quarter, PNNL performed *in situ* EPR to study reaction pathways mediated by sulfur radical formation. Coating/encapsulation approaches adopted by U Pitt and Stanford comprise flexible sulfur wire (FSW) electrodes coated with LIC by U Pitt, and TiS_2 encapsulation of Li_2S in the latter, both ensuring polysulfide retention at sulfur cathodes. BNL work, on the other hand, has focused on benchmarking of pouch cell testing by optimization of the voltage window and study of additives such as LiI and LiNO_3 . *Ab initio* studies at Stanford and U Pitt involve calculation of binding energies, diffusion coefficients, ionic conductivities, and reaction pathways determination, augmenting the experimental results. Similarly, AIMD simulations performed at TAMU reveal multiple details regarding electrolyte decomposition reactions and the role of soluble polysulfides on such reactions. Using kinetic Monte Carlo (KMC) simulations, electrode morphology evolution and mesostructured transport interaction studies were also executed. Studies over the last quarter at PNNL suggest that proper control of electrode porosity/thickness is essential for obtaining high-energy Li-S batteries. Porosity shows strong dependence on calendering pressure because of low tap densities of electrode components such as sulfur and carbon. Increasing the calendering-pressure from 0.2 to 1.5 ton (T) leads to rapid decrease of electrode porosity, resulting in improvement of electrode volumetric energy density.

Measured electrode volumetric energy density increased from 650 Wh L⁻¹ for as-cast electrode (120- μ m thick) to 1300 Wh L⁻¹ for electrode compressed to 60 μ m. Additionally, Pennsylvania State University has shown use of dimethyl disulfide as a functional co-solvent, demonstrating its ability to show an alternate electrochemical reaction pathway for sulfur cathodes by formation of dimethyl polysulfides and lithium organosulfides as intermediates and reduction products. Further, University of Wisconsin has conducted high-performance liquid chromatography (HPLC)-MS studies and has determined the distribution of polysulfides at various discharge and recharge reactions. UT Austin, at the same time, has shown that by integrating polysulfide-filter-coated separators fabricated with CNF, the cells retain 50% of the initial capacity after storing for one year and exhibit a low self-discharge rate of only 0.14% per day.

Each of these projects has a collaborative team of experts with the required skill set needed to address the EV Everywhere Grand Challenge of 350 Wh/kg and 750 Wh/l and cycle life of at least 1000 cycles.

Highlights. This Task reports the following project highlights for this quarter:

- A novel individual solvent (named ANL-2) reported by Dr. Khalil Amine of ANL for Li/Se-S batteries, demonstrates a stable capacity of, approximately, 800 mAh/g for 65 cycles with CE very close to 100%.
- Dr. Arumugam Manthiram (UT Austin) has developed a layer-by-layer carbon nanotube (CNT) coated separator (LBL CNT#3) that exhibits a peak discharge capacity of 1,087 mA h g⁻¹ with superior long-term cyclability with an even higher sulfur loading of 7.5 mg cm⁻² for 200 cycles.
- Use of polysulfide trapping agent (PTA) coated directly doped sulfur architecture (DDSA) electrodes developed by Prof. Prashant Kumta (University of Pittsburgh) showed a capacity of 1112 mAh/g with low fade rate of 0.0017% when cycled over 200 cycles at 0.2C rate.

Task 8.1 – New Lamination and Doping Concepts for Enhanced Lithium-Sulfur Battery Performance (Prashant N. Kumta, University of Pittsburgh)

Project Objective. The project objective is to successfully demonstrate generation of novel sulfur cathodes for Li-S batteries meeting targeted gravimetric energy densities ≥ 350 Wh/kg and ≥ 750 Wh/l with a cost target of \$125/kWh and cycle life of at least 1000 cycles for meeting the EV Everywhere Grand Challenge blueprint. The proposed approach will yield sulfur cathodes with specific capacity ≥ 1400 mAh/g, at ≥ 2.2 V, generating ~ 460 Wh/kg energy density higher than the target. Full cells meeting required deliverables will also be made.

Project Impact. Identifying new laminated S-cathode-based systems displaying higher gravimetric and volumetric energy densities than conventional Li-ion batteries will likely result in new commercial battery systems that are more robust, capable of delivering better energy and power densities, and more lightweight than current Li-ion battery packs. Strategies and configurations based on new LIC-coated sulfur cathodes will also lead to more compact battery designs for the same energy and power density specifications as current Li-ion systems. Commercialization of these new S-cathode-based Li-ion battery packs will represent, fundamentally, a major hallmark contribution of the DOE VTO and battery community.

Out-Year Goals. This multi-year project comprises three phases to be successfully completed in three years:

- Phase 1 (year 1) – Synthesis, characterization, and scale up of suitable LIC matrix materials and multilayer composite sulfur cathodes. (Complete)
- Phase 2 (year 2) – Development of LIC-coated sulfur nanoparticles, scale up of high-capacity engineered LIC-coated multilayer composite electrodes, and doping strategies to improve electronic conductivity of sulfur.
- Phase 3 (year 3) – Advanced high-energy-density, high-rate, extremely cyclable cell development.

Collaborations. The project collaborates with the following members: Dr. Spandan Maiti (U Pitt) for mechanical stability and multi-scale modeling; Dr. A. Manivannan (NETL) for XPS for surface characterization; and Dr. D. Krishnan Achary (U Pitt) for solid-state MAS-NMR characterization.

Milestones

1. Application of ceramic filler incorporated composite polymer electrolytes (CPEs) to improve the specific capacity of commercial sulfur to ~ 812 mAh/g for over 100 cycles. (Q1 – Completed October 2016)
2. Engineering of high-capacity LIC-coated sulfur nanoparticle. (Q2 – Completed January 2017)
3. Synthesis of vertically aligned carbon nanotube (VACNT) and LIC-coated composite materials. (Q3 – Completed April 2017)
4. Optimize doping composition and thickness to maximize capacity, rate capability, and cycling stability. (Q4 – Completed)
5. Cost analysis of the LIC-coated electrodes, electrolytes, separators, binders, and related processes and prismatic/pouch-type full cell assembly of I.E. with optimum thickness. (In progress)

Progress Report

Work this quarter involved conducting fundamental chemical and electrochemical study of the PTA-coated DDSA electrodes reported last quarter. PTA-coated DDSA electrodes developed then showed exceptionally low fade rate of 0.0017% when cycled over 200 cycles (Figure 81) at 0.2C rate (~ 18 mg/cm² S loading). UV-Vis spectroscopic analysis was performed on the electrolyte (1.8 M LiTFSI, 0.1 M LiNO₃ in DOL: DME (1:1)) of slurry coated commercial sulfur (SCCS) electrodes and PTA-coated DDSA electrodes after cycling at 0.2C rate for 200 cycles. The UV-Vis spectrum of PTA-DDSA (Figure 82a) showed considerable decrease in the intensities of peaks corresponding to higher and lower order polysulfides as opposed to the SCCS electrode suggesting adsorption of the polysulfide by the PTA via physical/chemical binding. XPS study of the electrodes after 200 electrochemical charge – discharge cycles (Figure 82b) shows the absence of polysulfide peaks. Also a weak, electrochemically reversible chemical binding of polysulfide onto the PTA was observed (data not shown), thus confirming the UV-Vis spectroscopy results. Work this quarter also involved conducting manufacturing cost analysis of various electrode materials [sulfur hosted composite framework materials (CFM), PTA-coated DDSA, and the LIC-coated sulfur nanoparticles], separators [nanofiller incorporated CPE, CFM added gel polymer electrolyte (GPE), and all solid LIC] and electrolytes developed during the project to assess scalability of all laboratory derived materials. Prismatic pouch cells (4-mAh full cell) are being assembled and tested using Phase-3 optimized systems.

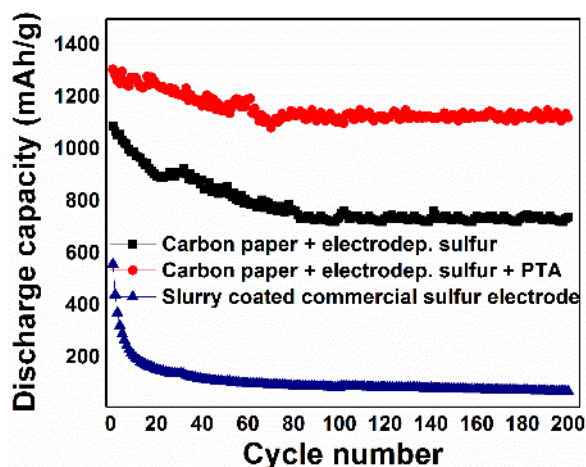


Figure 81. Electrochemical cycling performance of the polysulfide-trapping-agent-coated directly doped sulfur architectures compared with commercial sulfur.

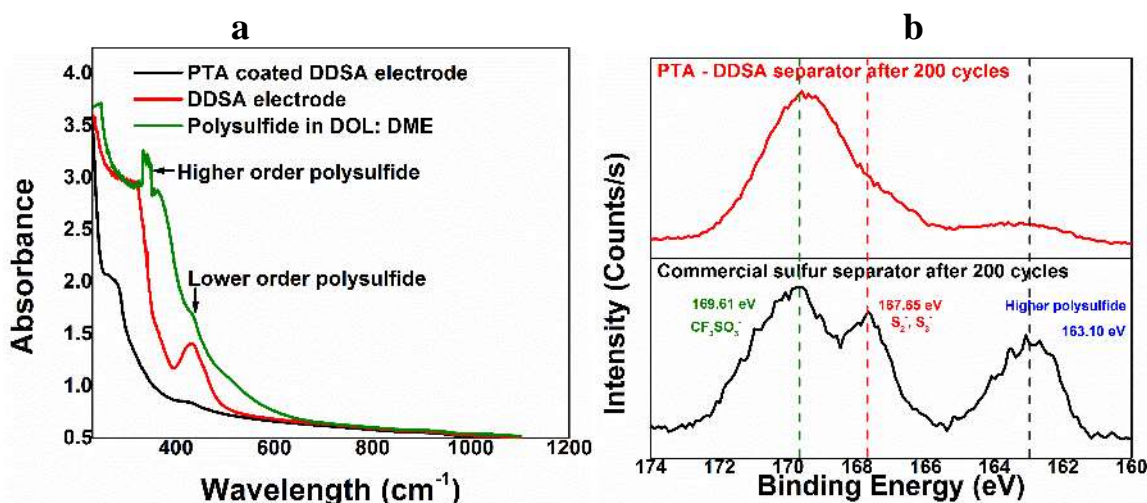


Figure 82. (a) UV – visible spectroscopy of polysulfide trapping agent (PTA)-coated directly doped sulfur architectures (DDSA) electrodes showing absence of polysulfide absorbance. (b) Comparison of X-ray photoelectron spectroscopy patterns of commercial sulfur and PTA - DDSA separators after 200 cycles.

Patents/Publications/Presentations

Patents

- Shanthi, P. M, and P. H. Jampani, B. Gattu, M. K. Datta, O. I. Velikokhatnyi, and P. N. Kumta. “Electrospinning of PVdF-HFP: Novel Composite Polymer Electrolytes (CPEs) with Enhanced Ionic Conductivities for Lithium-Sulfur Batteries.” U. S. Provisional Appln. Serial Number 62/529,638 (2017).
- Jampani, P. H., and P. M. Shanthi, B. Gattu, M. K. Datta, O. I. Velikokhatnyi, and P. N. Kumta. “High Capacity, Air-Stable, Structurally Isomorphous Lithium Alloy (SIA), Multilayer Porous Foams (MPFs) and Composite Multilayer Anodes (CMAs) for Dendrite-Free Lithium Metal Anodes for Li-ion Batteries.” U. S. Provisional Patent Appln. Serial Number 62/529,588, 2017.

Publications

- Shanthi, P. M., and P. H. Jampani, B. Gattu, T. Albuquerque, M. K. Datta, and P. N. Kumta. “Novel Electrospun PVdF – HFP Composite Polymer Electrolytes (CPEs) with Enhanced Ionic Conductivities for Lithium – Sulfur Batteries.” *ACS Applied Materials and Interfaces* (2017), under review.
- Shanthi, P. M., and P. H. Jampani, B. Gattu, M. K. Datta, O. I. Velikokhatnyi, and P. N. Kumta. “The Effect of Mg, Ca, and F Doping on the Ionic Conductivity of Li_4SiO_4 : Experimental and First Principles Investigation.” *Solid State Ionics* (2017), under review.

Presentation

- ECS 232nd Meeting, National Harbor, Maryland (October 1–5, 2017): “Polysulfide Trapping Agent (PTA) Coated Directly Doped Sulfur Architectures (DDSA) – New Platforms for High Capacity Li-S Batteries”; P. M. Shanthi, P. H. Jampani, B. Gattu, M. K. Datta, and P. N. Kumta.

Task 8.2 – Simulations and X-Ray Spectroscopy of Lithium-Sulfur Chemistry (Nitash Balsara, Lawrence Berkeley National Laboratory)

Project Objective. Li-S cells are attractive targets for energy storage applications, as their theoretical specific energy of 2600 Wh/kg is much greater than the theoretical specific energy of current Li-ion batteries. Unfortunately, the cycle-life of Li-S cells is limited due to migration of species generated at the sulfur cathode. These species, collectively known as polysulfides, can transform spontaneously, depending on the environment, and it has thus proven difficult to determine the nature of redox reactions that occur at the sulfur electrode. The project objective is to use XAS to track species formation and consumption during charge-discharge reactions in a Li-S cell. Molecular simulations will be used to obtain X-ray spectroscopy signatures of different polysulfide species, and to determine reaction pathways and diffusion in the sulfur cathode. The long-term objective is to use mechanistic information to build high specific energy lithium-sulfur cells.

Project Impact. Enabling rechargeable Li-S cells has potential to change the landscape of rechargeable batteries for large-scale applications beyond personal electronics due to: (1) high specific energy, (2) simplicity and low cost of cathode (the most expensive component of Li-ion batteries), and (3) earth abundance of sulfur. The proposed diagnostic approach also has significant potential impact, as it represents a new path for determining the species that form during charge-discharge reactions in a battery electrode.

Out-Year Goals. The out-year goals are as follows:

- **Year 1.** Simulations of sulfur and PSL in oligomeric PEO solvent. Prediction of X-ray spectroscopy signatures of PSL/PEO mixtures. Measurement of X-ray spectroscopy signatures of PSL/PEO mixtures.
- **Year 2.** Use comparisons between theory and experiment to refine simulation parameters. Determine speciation in PSL/PEO mixtures without resorting to *ad hoc* assumptions.
- **Year 3.** Build an all-solid lithium-sulfur cell that enables measurement of X-ray spectra *in situ*. Conduct simulations of reduction of sulfur cathode.
- **Year 4.** Use comparisons between theory and experiment to determine the mechanism of sulfur reduction and Li₂S oxidation in all-solid Li-S cell. Use this information to build Li-S cells with improved life-time.

Collaborations. This project collaborates with Tsu-Chien Weng, Dimosthenis Sokaras, and Dennis Nordlund at SSRL, SLAC National Accelerator Laboratory in Stanford, California.

Milestones

1. Continue *in situ* XAS and other spectroscopies to determine reaction products as a function of charge/discharge rate. (Q1 – Completed December 1, 2016)
2. Theoretical prediction of polysulfide solution composition based on thermodynamic calculations of polysulfide and disproportionation reaction Gibbs free energy. (Q2 – Completed February 15, 2017)
3. Employ carbon confinement strategies, and demonstrate improved cycle life relative to all solid Li-S cells with unconfined sulfur. (Q3 – Completed June 10, 2017)
4. Perform *in situ* XAS on Li-S cells containing perfluoropolyether electrolytes; determine reaction products in absence of polysulfide dissolution. (Q4 – Planned for completion on October 23, 2017; Beamtime for XAS was not available before October)

Progress Report

The project has used two techniques to study the chemistry of lithium-sulfur cells: X-ray microtomography (XMT) and XAS. The XMT results are shown in Figure 83a. This figure shows cycling data and corresponding tomograms before cycling and after the second cycle. There are additional data at several time points. The tomography shows that the cathodes in the cells remained intact upon cycling, suggesting that the strategy for confining polysulfides worked. However, what was unprotected in the process was the lithium anode; there was severe delamination of the electrolyte-lithium interface after only two cycles. Finding strategies to simultaneously protect both lithium and sulfur electrodes seems challenging. The work on XAS is described in Figure 83b, which shows the first discharge characteristics of an *in situ* cell with severe polysulfide dissolution issues. These data were published in Wjucik et al. (doi: 10.1149/2.1441614jes). Data obtained from improved XAS cells (Figure 83b) show a radical improvement in first-cycle capacity. The project will study the species formed in the newly designed cells and compare them to previously published data to quantify the effect of polysulfide dissolution on chemistry.

The synchrotron facilities at ALS and SSRL have provided beamtime from October 20–23, 2017. The project was unable to secure beamtime in 2016–2017. The project will close after completion of these experiments.

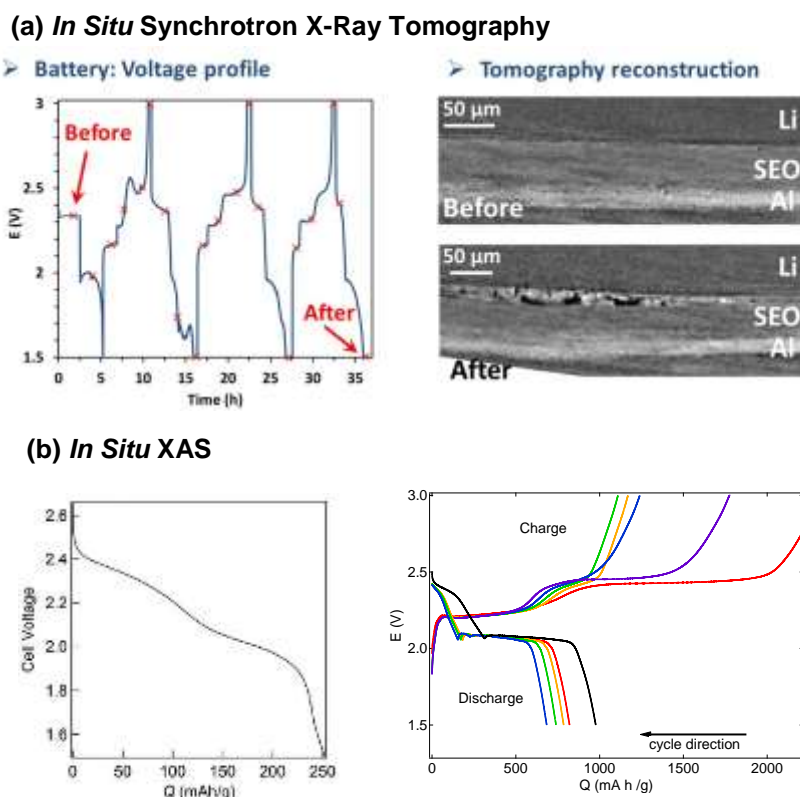


Figure 83. *In situ* experiments on Li-S experiments. (a) X-ray tomography. (b) X-ray absorption spectroscopy: (left) early data with polysulfide dissolution and (right) new data with significantly less polysulfide dissolution.

Task 8.3 – Novel Chemistry: Lithium Selenium and Selenium Sulfur Couple (Khalil Amine, Argonne National Laboratory)

Project Objective. The project objective is to develop a novel S_xSe_y cathode material for rechargeable lithium batteries with high energy density and long life, as well as low cost and high safety.

Project Impact. Development of a new battery chemistry is promising to support the goal of PHEV and EV applications.

Approach. The dissolution of lithium polysulfides in nonaqueous electrolytes has been the major contribution to the low energy efficiency and short life of Li/S batteries. In addition, the insulating characteristics of both end members during charge/discharge (S and Li_2S) limit their rate capacity. To overcome this problem, sulfur or Li_2S are generally impregnated in a carbon-conducting matrix for better electronic conductivity. However, this makes it difficult to increase the loading density of practical electrodes. It is proposed here to solve the above barriers using the following approaches: (1) partially replace S with Se, (2) nano-confine the S_xSe_y in a nano-porous conductive matrix and (3) explore advanced electrolytes with suppressed shuttle effect.

Out-Year Goals. This new cathode will be optimized with the following goals:

- A cell with nominal voltage of 2 V and energy density of 600 Wh/kg.
- A battery capable of operating for 500 cycles with low capacity fade.

Collaborations. This project engages in collaboration with the following: Professor Chunsheng Wang of UMD, Dr. Yang Ren and Dr. Chengjun Sun of APS at ANL, and Dr. Luis Estevez at PNNL.

Milestones

1. Investigating the impact of fluorinated solvents for Se-S systems. (Q1 – Completed December 2016)
2. Investigating the effect of the pore volume of carbon matrix on high-loading Se-S systems. (Q1 – Complete)
3. Investigating the effect of the pore size and specific surface area of carbon matrix on high-loading Se-S systems. (Q2 – Complete)
4. Development of Se-S/carbon composites with high loading and high performance. (Q3 – Complete)
5. Exploration of novel electrolytes for high-loading Se-S systems. (Q4 – In progress)

Progress Report

In FY 2017, the project mainly focused on tuning the interfacial chemistry of Li/Se-S batteries through optimizing electrolytes to mitigate the dissolution issue of polysulfides/polyselenides, and extended the optimal sulfur confinement pore size to large porous carbon that has long been considered an inferior sulfur host material. This interesting finding led to continuous work on manipulating the electrode/electrolyte interfaces to further suppress shuttle effect and stabilize reversible capacity.

This quarter, the project explored a novel individual solvent (named ANL-2) for Li/Se-S batteries. This solvent has a high solubility for LiTFSI; therefore, the project prepared a LiTFSI/ANL-2 electrolyte without any other solvent such as DOL and DME that has high solubility for polysulfides/polyselenides. In addition, no additive such as LiNO_3 was used. Figure 84 shows the charge/discharge curve of a Li/Se-S battery with 45 wt% Se-S loading in the composite configuration with carbon at C/10. As clearly shown, only a single discharge voltage plateau is observed, with an initial discharge capacity of 1400 mAh/g corresponding to a high Se-S utilization of ca. 84%. The initial charge capacity is about 1147 mAh/g, corresponding to a CE of about 120%. The voltage profile in LiTFSI/ANL-2 electrolyte is similar to that for carbonate-based electrolyte, indicating a solid-state (de)lithiation process. This result confirms the previous finding that shows that the electrochemical reaction mechanism of Li/Se-S battery can be tailored by controlling the interfaces. The project will conduct more details by using *operando* Se K-edge XANES to unravel its electrochemistry during the first or second quarter of 2018, depending on the beamtime situation.

Figure 85 shows the corresponding cycle performance. As shown, a stable capacity of around 800 mAh/g can be still maintained up to 65 cycles with the CE also close to 100%, indicating that the polysulfides/polyselenides shuttle has been well mitigated. However, there is a large capacity drop in the initial three cycles. The reason is unknown, but likely could be related to the relatively large voltage polarization and cathode structural defects. The project is working to optimize the electrolyte formula to address this problem and further improve electrochemical performance.

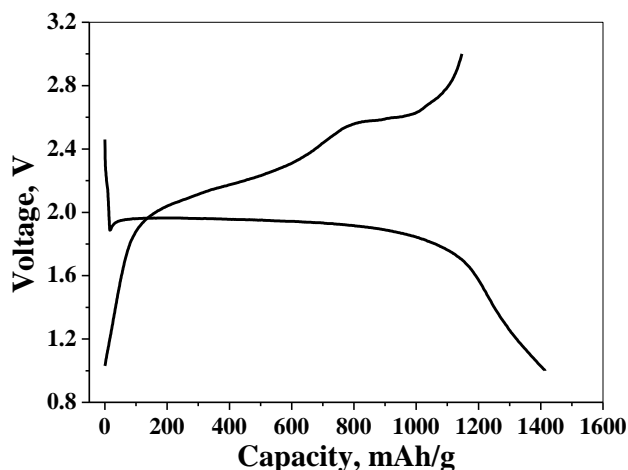


Figure 84. Charge/discharge curve of Li/Se-S battery with 45 wt% Se-S loading in the composite at C/10 in LiTFSI/ANL-2.

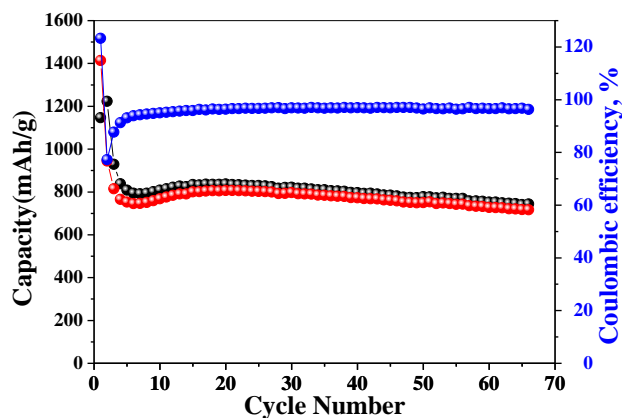


Figure 85. Cycle performance of Li/Se-S battery with 45 wt% Se-S loading in the composite at C/10 in LiTFSI/ANL-2.

Patents/Publications/Presentations

Publication

- Xu, Gui-Liang, and Hui Sun, Luis Estevez, Chao Luo, Tianyuan Ma, Jianzhao Liu, Rachid Amine, Xiaoyi Zhang, Cheng-Jun Sun, Yuzi Liu, Yang Ren, Steve M. Heald, Chun-Sheng Wang, Zonghai Chen, and Khalil Amine. “Enabling High Performance Lithium-Sulfur Batteries by Manipulating Interfacial Chemistry.” *Energy & Environmental Science*, under review.

Task 8.4 – Multi-Functional Cathode Additives for Lithium-Sulfur Battery Technology (Hong Gan, Brookhaven National Laboratory; and Co-PI Esther Takeuchi, Brookhaven National Laboratory and Stony Brook University)

Project Objective. Develop a low-cost battery technology for PEV application utilizing Li-S electrochemical system by incorporating multi-functional cathode additives (MFCA), consistent with the long-term goals of the DOE EV Everywhere Grand Challenge.

Project Impact. The Li-S battery system has gained significant interest due to its low material cost potential (35% cathode cost reduction over Li-ion) and its attractive 2.8x (volumetric) to 6.4x (gravimetric) higher theoretical energy density compared to conventional Li-ion benchmark systems. Commercialization of this technology requires overcoming several technical challenges. This effort will focus on improving cathode energy density, power capability, and cycling stability by introducing MFCA. The primary deliverable is to identify and characterize the best MFCA for Li-S cell technology development.

Approach. TM sulfides are evaluated as cathode additives in sulfur cathode due to their high electronic conductivity. Electrochemically active additives are also selected for this investigation to further improve energy density of the sulfur cell system. In the first year, the project established individual baseline sulfur and TM sulfide coin cell performances and demonstrated strong interactions between sulfur and various MFCA within the hybrid electrode. During the second year, the project identified TiS_2 as the best MFCA candidate and demonstrated the particle size/BET surface area effect on Li-S cell electrochemical performance. In addition, sulfur electrode binder and carbon additives were optimized to achieve high sulfur loading up to 10 mg/cm^2 with good mechanical integrity. This year, the project targets to achieve optimized Li-S cell electrochemical performance by incorporating TiS_2 additive into the cathode formulation with new binder and new carbon additive. Electrode preparation process conditions and cell design factors will also be examined. The cell activation and cycling conditions will be defined, and 4-mAh sample cells will be built for DOE evaluation.

Out-Year Goals. This is a multi-year project comprised of two major phases to be completed in three years. Phase 1 was successfully completed during year 2, with selection of TiS_2 as the leading MFCA. In Phase 2, the project has completed binder and carbon selection. In the third year, tasks include cathode formulation optimization, process optimization, cell design optimization, cell activation, and testing optimization. At the end, the project will build 4-mAh sample cells for DOE testing. The mechanistic studies of MFCA and sulfur interaction will continue throughout the year to advance fundamental understanding of the system.

Collaborations. This project collaborates with Dong Su, Xiao Tong, and Yu-Chen Karen Chen-Wiegart at BNL and with Amy Marschilok and Kenneth Takeuchi at Stony Brook University.

Milestones

1. Cathode formulation and process optimization with TiS_2 . (Q1 – Completed December 2017)
2. Cathode loading/density effect and power optimization. (Q2 – Completed March 2017)
3. Cell design and cell activation procedure development. (Q3 – Completed June 2017)
4. 4-mAh cell samples preparation and confirmation study. (Q4 – Completed September 2017)

Progress Report

All improvements from previous findings are integrated into the final 2032 coin cell design, targeting > 4 mAh deliverable capacity for cycling. Coin cell performance is characterized under several testing conditions. With the same key design parameters, a pouch cell was also tested.

Coin Cell Cycle Life. Excellent cell cycle life up to 150 cycles is achieved with > 3.1 mAh/cm² delivered. The 2032 Li-S coin cells at 1 mA/cm² charging/discharging rate for 150 cycles are shown in Figure 86. After initial 10 cycles, cell capacity stabilized at ~ 5 mAh.

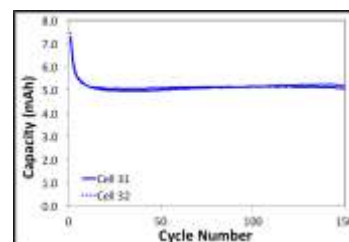


Figure 86. Cycle life test.

Temperature Effect on Discharge Efficiency. Discharge temperature has significant impact on cell voltage profiles and delivered capacity. The cell voltage is severely polarized below 0°C. Higher test temperature led to lower cell voltage polarization and more efficient sulfur utilization (Figure 87). Up to 7.35 mAh (~ 4.6 mAh/cm²) is deliverable at 60°C at 1 mA/cm² rate. The sulfur utilization improvement is dominated by Li₂S₂/Li₂S discharge region.

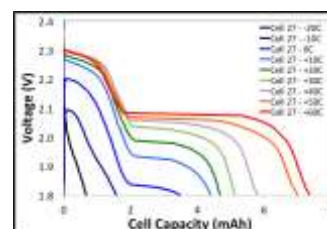


Figure 87. Discharge temperature effect.

Coin Cell Shelf Life. The shelf life study is executed by storing the coin cells for 30 days at 0°C, 20°C, and 50°C, respectively, before cycle testing either at the freshly built state or the fully discharged state. Lower storage temperature is beneficial to cell cycle life and capacity retention. Storage at 50°C causes permanent damage to fully discharged cells in terms of significant loss in cell capacity and poor cycle life (Figure 88). No damage to cell cycling performance was shown at room-temperature or low-temperature storage.

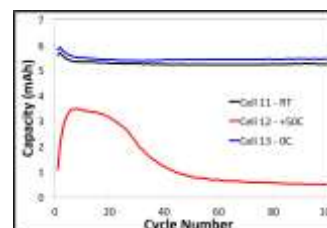


Figure 88. Shelf-life; fully discharged.

Coin Cell Self-Discharge. The coin cell self-discharge is determined for cells stored at fully charged state for 1, 7, 14, 21, and 28 days, respectively (Figure 89) after the stabilization cycles. The cell self-discharge primarily happens at the soluble polysulfide discharge region. With the consumption of polysulfides, the self-discharge levels off at storage time longer than 14 days. Almost all capacity from the second voltage plateau is still delivered after four weeks of storage.

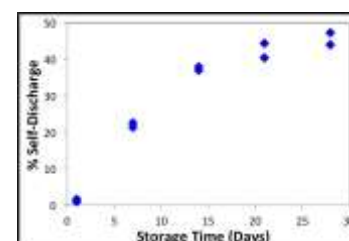


Figure 89. Self-discharge rate.

Pouch Cell Validation. To validate the integrated Li-S cell performance, a single layer pouch cell with 20-cm² cathode area was built and tested, as shown in Figure 90, at various discharge rates. The rate capability of the pouch cell is comparable to that of the coin cells, which confirms the scalability of the sulfur cell technology developed in the project laboratory.

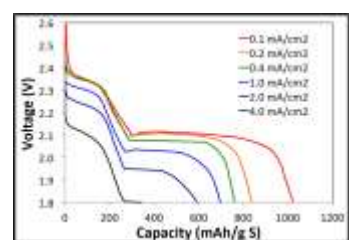


Figure 90. Pouch cell rate capability.

Summary. The project has successfully achieved all milestones, with the proof-of-concept MFCA demonstration and identification of TiS₂ as the leading candidate. In addition, it has achieved high sulfur loading (up to 10 mg/cm²) by optimizing cathode components/formulation and cathode preparation processes. With integration of multiple cell design parameters, the 2032 coin cells with ≥ 4 mAh are demonstrated with excellent cycle life. Pouch cell is also constructed, demonstrating technology scalability. With this performance as the new benchmark, additional research at material, electrode, and cell system levels will continue to further improve Li-S battery technology performance.

Patents/Publications/Presentations

Publication

- Sun, Ke, and Chonghang Zhao, Cheng-Hung Lin, Eli Stavitski, Garth Williams, Jianming Bai, Eric Dooryhee, Klaus Attenkofer, Juergen Thieme, Yu-chen Karen Chen-Wiegart, and Hong Gan. “Operando Multi-modal Synchrotron Investigation for Structural and Chemical Evolution of Cupric Sulfide (CuS) Additive in Li-S Battery.” *Scientific Reports* 7 (2017): 12976. doi:10.1038/s41598-017-12738-0.

Task 8.5 – Development of High-Energy Lithium-Sulfur Batteries (Jun Liu and Dongping Lu, Pacific Northwest National Laboratory)

Project Objective. The project objective is to develop high-energy, low-cost Li-S batteries with long lifespan. All proposed work will employ thick sulfur cathode ($\geq 2 \text{ mAh/cm}^2$ of sulfur) at a relevant scale for practical applications. The diffusion process of soluble polysulfide out of thick cathode will be revisited to investigate cell failure mechanism at different cycling. Alternative anode will be explored to address the lithium anode issue. The fundamental reaction mechanism of polysulfide under the electrical field will be explored by applying advanced characterization techniques to accelerate development of Li-S battery technology.

Project Impact. The theoretical specific energy of Li-S batteries is $\sim 2300 \text{ Wh/kg}$, which is almost three times higher than that of state-of-the-art Li-ion batteries. The major challenge for Li-S batteries is polysulfide shuttle reactions, which initiate a series of chain reactions that significantly shorten battery life. The proposed work will design novel approaches to enable Li-S battery technology and accelerate market acceptance of long-range EVs required by the EV Everywhere Grand Challenge.

Out-Year Goals. This project has the following out-year goals:

- Fabricate Li-S pouch cells with thick electrodes to understand sulfur chemistry/electrochemistry in the environments similar to real application.
- Leverage the Li-metal protection project funded by the DOE and PNNL advanced characterization facilities to accelerate development of Li-S battery technology.
- Develop Li-S batteries with a specific energy of 400 Wh/kg at cell level, 1000 deep-discharge cycles, improved abuse tolerance, and less than 20% capacity fade over a 10-year period to accelerate commercialization of electrical vehicles.

Collaborations. This project engages in collaboration with the following:

- Dr. Xiao-Qing Yang (LBNL) – *In situ* characterization,
- Dr. Deyang Qu (University of Wisconsin at Milwaukee) – Electrolyte analysis,
- Dr. Xingcheng Xiao (GM) – Materials testing, and
- Dr. Jim De Yoreo (PNNL) – *In situ* characterization.

Milestones

1. Study thick sulfur electrode ($\geq 4 \text{ mg/cm}^2$) with controlled porosity/thickness; demonstrate 80% capacity retention for 200 cycles. (Q1 – Completed December 31, 2016)
2. Investigate electrolyte and additive degradation mechanism with thick sulfur electrode. (Q2 – Completed March 31, 2017)
3. Identify approaches to minimize quick capacity drop and efficiency fluctuation occurring in thick sulfur electrode during initial cycles. (Q3 – Completed June 30, 2017)
4. Complete pouch cell assembly and testing by using optimized high energy cathode and electrolyte/additives. (Q4 – Completed September 30, 2017)

Progress Report

Large size pouch cells were used as testing platform this quarter to advance the research and understanding of Li-S battery technology at practical conditions. This is a natural extension of the project's work on addressing the key challenges of high loading sulfur cathode: rational electrode architecture design and performance improvement. Electrode wetting and low sulfur utilization issues associated with high loading sulfur electrodes have been solved by using novel electrode additives and new binder. Low CE is another significant problem for high loading sulfur cathodes, which is caused by unstable lithium anode and quick degradation of electrolyte additive, particularly with low additive/sulfur ratio.



Figure 91. (a) Component weight distribution of Li-S battery with energy density of 300 Wh/kg. (b) Photo image of single-layer pouch cell used in present study (electrode working area 19.4 cm², and sulfur mass loading 5.7 mg/cm²). (c) Dependence of first discharge areal capacity and specific capacity on electrolyte/sulfur ratio (black symbol: pouch cell using pristine separator; red symbol: pouch cell using modified separator).

This quarter, key parameters for preparation of pouch cells are high loading sulfur cathodes with controlled porosity, limited lithium anode, and controlled electrolyte amount. The project investigated effects of cathode additive, electrode porosity, lithium excess amount (anode/cathode capacity ratio), and electrolyte amount on the performance of high loading sulfur electrodes. Using cathodes with sulfur loading about 4.5 mg/cm², the project has demonstrated Li-S pouch cells with total capacity of 1.6 Ah and delivered specific energy density of 247 Wh/kg. To achieve higher cell energy density, not only should areal capacity of sulfur cathodes be improved significantly, but also the parasitic weight of the cell components must be reduced as low as possible; for this, electrolyte amount is a key parameter (as shown in Figure 91a). Based on project research, to reach specific energy over 300 Wh/kg, the areal capacity of sulfur electrodes should be at least 5.0 mAh/cm², while the electrolyte/sulfur ratio should be less than 3 μL/mg, which may vary with change of sulfur utilization rate. Therefore, all pouch cells used this quarter are based on cathodes with sulfur loading ~ 5.7 mg/cm² and electrode porosity below 55%; 50-μm thick lithium anode (~ 10 mAh/cm², anode/cathode capacity ratio < 2); and controlled E/S ratio from 2.7 to 7.2 μL electrolyte/mg sulfur. As part of the results, Figure 91c shows the dependence of electrode areal capacity and sulfur utilization rate on the electrolyte/sulfur ratio. When E/S is higher than 7, deliverable areal capacity is 5.5 mAh/cm² with a high sulfur utilization of 950 mAh/g. Reducing E/S ratio to 4.9, both areal capacity and sulfur utilization rate decline slightly to 5.0 mAh/cm² and 880 mAh/g, respectively. But if the E/S ratio was lowered to 2.8, a significant decrease of areal capacity and sulfur utilization rate is observed, indicating lack of electrolyte for full sulfur conversion. However, if using the project's polymer modified separator (coating < 1 mg/cm²), remarkable improvement is observed. With E/S = 2.7, 5.05 mAh/cm² and 870 mAh/g are achievable, which is comparable to those at E/S = 4.9 with pristine separator. An even lower E/S ratio is predictable in practical multiple-layer pouch cells due to the lower inactive-surface/active-surface ratio. These results indicate that 300 Wh/kg Li-S pouch cell is reasonable and can be achieved based on current electrodes and E/S ratio, which will be experimentally verified by leveraging progress in terms of electrode additives, new binder, electrolyte additive, and modified separator.

Task 8.6 – Nanostructured Design of Sulfur Cathodes for High-Energy Lithium-Sulfur Batteries (Yi Cui, Stanford University)

Project Objective. The charge capacity limitations of conventional TM oxide cathodes are overcome by designing optimized nano-architected sulfur cathodes. This study aims to enable sulfur cathodes with high capacity and long cycle life by developing sulfur cathodes from the perspective of nanostructured materials design, which will be used to combine with Li-metal anodes to generate high-energy Li-S batteries. Novel sulfur nanostructures as well as multi-functional coatings will be designed and fabricated to overcome issues related to volume expansion, polysulfide dissolution, and the insulating nature of sulfur.

Project Impact. The capacity and the cycling stability of sulfur cathode will be dramatically increased. This project's success will make Li-S batteries to power EVs and decrease the high cost of batteries.

Out-Year Goals. The cycle life, capacity retention, and capacity loading of sulfur cathodes will be greatly improved (200 cycles with 80% capacity retention, > 0.3 mAh/cm² capacity loading) by optimizing material design, synthesis, and electrode assembly.

Collaborations. This project engages in collaboration with the following:

- BMR PIs,
- SLAC: *In situ* X-ray, Dr. Michael Toney, and
- Stanford: Professor Nix, mechanics; and Professor Bao, materials.

Milestones

1. Identify the initial activation energy barrier of Li₂S on various metal sulfides. (Q1 – Completed December 2016)
2. Demonstrate the catalytic effect of Li₂S_x species on metal sulfides, enabling good performance of Li-S batteries. (Q3 – Completed April 2017)
3. Establish a standard procedure to quantitatively compare the polysulfide adsorption capability of candidate materials. (Q4 – Completed July 2017)
4. Quantitatively approximate the polysulfide adsorption amount of candidate materials (Completion in October 2017)

Progress Report

Last quarter, the project established a standard procedure to quantitatively compare the polysulfide adsorption capability of various candidate materials. This quarter, ICP-AES is further performed on the supernatant solutions to provide a more accurate quantitative analysis. To quantitatively approximate the polysulfide adsorption capabilities, the Beer-Lambert law can be employed:

$$A = \log_{10} \frac{I_0}{I} = L\epsilon c$$

where A is the absorbance of the sample, I_0 is the initial light intensity, I is the transmitted light intensity, L is the path length, ϵ is the molar absorptivity, and c is the concentration. For the setup, the path length L is constant, and the molar absorptivity ϵ is also constant for any particular wavelength; therefore, the absorbance should vary directly with concentration c of polysulfide species in solution. Consequently, based on the remaining Li_2S_6 concentration in supernatant solution, it is possible to calculate the polysulfide adsorption capability for each candidate material in terms of $\mu\text{mol}/\text{m}^2$ and mg/m^2 . Under the selected standard conditions, an order of magnitude of difference is seen between weak and strong candidate materials, with carbon black and CoS at $1.3 \mu\text{mol}/\text{m}^2$ and $2.6 \mu\text{mol}/\text{m}^2$, respectively, compared to MnO_2 and V_2O_5 at $22.5 \mu\text{mol}/\text{m}^2$ and $23.1 \mu\text{mol}/\text{m}^2$, respectively.

It must be mentioned that while UV-Vis is a useful technique for polysulfide adsorption capability analysis, extreme care is required throughout the procedure, and caution must be applied toward any quantitative data obtained. Lithium polysulfide species such as Li_2S_6 can undergo disproportionation reactions to form other species such as Li_2S_4 and Li_2S_8 , adding complications to the analysis with Li_2S_6 no longer being the sole species present. More importantly, these polysulfide species are not stable in the ambient environment, any slight exposure to air or moisture will quickly result in significant color fading and nullify the validity of any UV-Vis analysis. Samples need to be prepared with adequate sealing and contaminant-free solvents, and the Beer-Lambert law analysis should only be employed as an approximation of numerical values.

ICP-AES can detect the total concentration of lithium and sulfur atoms regardless of their chemical state; therefore, it is much less susceptible to complications brought about by the instability of Li_2S_6 species. Figure 92a shows the linear relationship between ICP-AES lithium intensity and Li_2S_6 concentration. A similar relationship is shown in Figure 92b for sulfur. The only source of lithium introduced to the samples is from the 3mM Li_2S_6 species; therefore, based on the concentration of lithium atoms remaining in supernatant solution, it is possible to determine the amount of lithium adsorbed on the candidate materials. Figure 92c depicts the calculated Li_2S_6 adsorption capability data for candidate materials based on ICP-AES analysis of lithium content. The results match reasonably well with previous UV-Vis approximations and similarly demonstrate one order of magnitude of difference between weak and strong candidate materials, with carbon black and CoS at $1.6 \mu\text{mol}/\text{m}^2$ and $3.5 \mu\text{mol}/\text{m}^2$ respectively, compared to MnO_2 and V_2O_5 at $22.9 \mu\text{mol}/\text{m}^2$ and $22.3 \mu\text{mol}/\text{m}^2$, respectively.

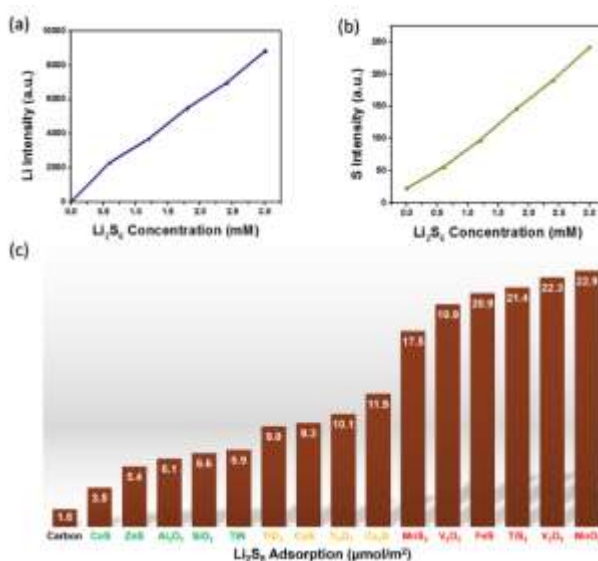


Figure 92. Li_2S_6 polysulfide adsorption test. Inductively coupled plasma atomic emission spectroscopy data of (a) lithium intensity and (b) sulfur intensity with varying Li_2S_6 concentrations without candidate materials, (c) calculated adsorption by candidate materials in 3mM Li_2S_6 solution.

Task 8.7 – Addressing Internal “Shuttle” Effect: Electrolyte Design and Cathode Morphology Evolution in Lithium-Sulfur Batteries (Perla Balbuena, Texas A&M University)

Project Objective. The project objective is to overcome the Li-metal anode deterioration issues through advanced Li-anode protection/stabilization strategies including (1) *in situ* chemical formation of a protective passivation layer and (2) alleviation of the “aggressiveness” of the environment at the anode by minimizing the polysulfide shuttle with advanced cathode structure design.

Project Impact. Through formulation of alternative electrolyte chemistries as well as design, fabrication, and test of improved cathode architectures, it is expected that this project will deliver Li/S cells operating for 500 cycles at efficiency greater than 80%.

Approach. A mesoscale model including different realizations of electrode mesoporous structures generated based on a stochastic reconstruction method will allow virtual screening of the cathode microstructural features and the corresponding effects on electronic/ionic conductivity and morphological evolution. Interfacial reactions at the anode due to the presence of polysulfide species will be characterized with *ab initio* methods. For the cathode interfacial reactions, data and detailed structural and energetic information obtained from atomistic-level studies will be used in a mesoscopic-level analysis. A novel sonochemical fabrication method is expected to generate controlled cathode mesoporous structures that will be tested along with new electrolyte formulations based on the knowledge gained from the mesoscale and atomistic modeling efforts.

Out-Year Goals. By determining reasons for successes or failures of specific electrolyte chemistries, and assessing relative effects of composite cathode microstructure and internal shuttle chemistry versus that of electrolyte chemistry on cell performance, expected results are as follows: (1) develop an improved understanding of the Li/S chemistry and ways to control it, (2) develop electrolyte formulations able to stabilize the lithium anode, (3) develop new composite cathode microstructures with enhanced cathode performance, and (4) develop a Li/S cell operating for 500 cycles at an efficiency greater than 80%.

Collaborations. This is a collaborative work combining first-principles modeling (Perla Balbuena, TAMU), mesoscopic level modeling (Partha Mukherjee, TAMU), and synthesis, fabrication, and test of Li/S materials and cells (Vilas Pol, Purdue University). Balbuena also collaborates with M. Vijayakumar from PNNL.

Milestones

1. Complete electrochemical modeling of cell performance with electrolyte and cathode properties. (Completed December 2016)
2. Complete development of stable electrolytes. (Complete)
3. Produce 3-5 grams of C/S composite material. (Complete)
4. Complete scale-up of cathode composites, cell construction, and testing. (Complete)

Progress Report

Experimental and Theoretical Characterization of Composite Cathode

As shown last quarter, pressurized “autogenic” synthesis routes, studied by Co-PI Vilas Pol at Purdue University, have produced homogeneous carbon-sulfur composites with high sulfur content up to 74 wt%. To further understand the underlying principles of autogenic synthesis, the quality of sulfur and its distribution were explored via electron microscopy and elemental mapping. The overall morphology (that is, of the secondary or aggregate particle) was studied using SEM, and the primary particle morphology was studied using STEM. Elemental mapping was performed using energy dispersive x-ray spectroscopy (EDXS). It was found that carbon-sulfur composites have a secondary particle diameter of $7 \pm 3 \mu\text{m}$. From elemental mapping, sulfur is observed to be distributed uniformly across the carbon particles within a large sample area. After autogenic synthesis, the carbon-sulfur composite particle generally retains the features of the original carbon morphology. The individual primary particle morphology of the carbon-sulfur composite is generally spheroidal and branched like the original carbon precursor. However, the pores in the composite are slightly less easily observable. The overall morphology of the composite is also branched, exhibiting bright signal due to the insulating property of elemental sulfur. Line scans of the carbon-sulfur composite show that sulfur content occurs coincidentally with carbon content. Correspondingly, appreciable sulfur content is not observed beyond the boundaries of carbon signal. Altogether, these observations suggest that sulfur content is generally confined within the substrate carbon phase.

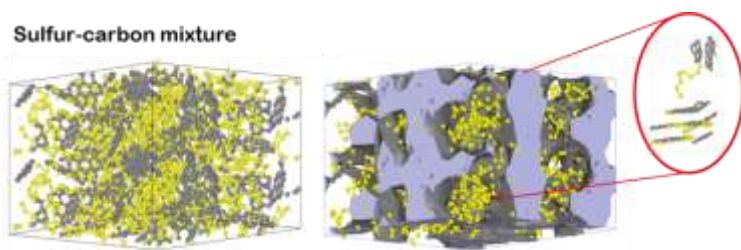


Figure 93. Molecular simulations reveal structural details of C-S composite.

In parallel, Balbuena’s group molecular simulations (detailed last quarter) are advancing the characterization of the microscopic morphology of these composites and their evolution during lithiation. In this way, the project can correlate the cathode morphology with the discharge reaction, and specifically describe the deposition mode of the insoluble products as a function of the cathode structure and porosity.

On the other hand, the electrolytes used in Li-S cells are intriguing compared to traditional electrolytes since their chemical composition evolves during cell operation. These effects were studied with a mesoscopic model in Mukherjee’s group. The electrolyte added at the time of cell fabrication is essentially a lithium salt dissolved in an organic liquid (for example, LiTFSI in EC: DEC). As the cell discharge progresses, solid sulfur dissolves and undergoes successive electrochemical reductions to lower order polysulfides (PS). Thus, at different depths of discharge, the electrolyte accommodates additional species like dissolved sulfur and higher and lower order PS. Depending on the C-rate, these species may co-exist (medium and high rates) or manifest successively (low rates). Toward the end of discharge, a large portion of PS precipitates out. Thus, in addition to changes in species identity, concentrations of various ionic and neutral species also vary significantly during electrochemical speciation of the electrolyte. The presence of more than two species in the solvent leads to mutual interactions such that gradients in one species affect the transport of the other (cross-diffusion terms). At higher concentrations ionic mobility is hindered, which in turn leads to reduced ionic conductivity. The PS concentration is highest around the end of the upper discharge plateau and correspondingly the ionic conductivity is the lowest. This reduced ionic conductivity gives rise to increased polarization. As sulfur loading is increased, the total PS concentration increases, which in turn leads to lower ionic conductivities and more pronounced through connecting the two discharge plateaus. Higher sulfur loading also leads to large microstructural changes and equivalently greater impedance evolution. Thus, through a combination of reduced electrolyte conductivity and higher microstructural resistance, cell capacity decreases at successively higher sulfur loadings.

Patents/Publications/Presentations

Publications

- Chen, C.-F., and A. Mistry, and P. P. Mukherjee. “Probing Impedance and Microstructure Evolution in Lithium-Sulfur Battery Electrodes.” *J. Phys. Chem. C* 121 (2017): 21206.
- Kamphaus, Ethan P., and Perla B. Balbuena. “First Principles Investigation of Lithium Polysulfide Structure and Behavior in Solution.” *J. Phys. Chem. C* 121 (2017): 21105–21117.
- Liu, Zhixiao, and Perla B. Balbuena, and Partha P. Mukherjee. “Hole Polaron Diffusion in the Final Discharge Product of Lithium-Sulfur Batteries.” *J. Phys. Chem. C* 121 (2017): 17169–17175.
- Burgos, Juan Carlos, and Perla B. Balbuena, and Javier Montoya. “Structural Dependence of the Sulfur Reduction Mechanism in Carbon-Based Cathodes for Lithium Sulfur Batteries.” *J. Phys. Chem. C* 121 (2017): 18369–18377.
- Mistry, Aashutosh, and Partha P. Mukherjee. “Precipitation – Microstructure Interaction in Li-S Battery Cathode.” *J. Phys. Chem. C*, under review.
- Liu, Zhixiao, and Aashutosh Mistry, and Partha P. Mukherjee. “Mesoscale Physicochemical Interactions in Lithium-Sulfur Batteries: Progress and Perspective.” *J. Electrochem. Energy Conv. Storage* 15 (2017): 010802.
- Liu, Zhixiao, and Perla B. Balbuena, and Partha P. Mukherjee. “Mesoscale Evaluation of Titanium Silicide Monolayer as a Cathode Host Material in Lithium-Sulfur Batteries.” *J. Minerals, Metals, and Materials Society* 69 (2017): 1532–1536.

Presentations

- 232nd ECS Meeting, National Harbor, Maryland (October 4, 2017): “Microstructural Limitations in Lithium-Sulfur Battery Performance”; A. Mistry and P. P. Mukherjee.
- University of California at Riverside, Riverside, California (September 29, 2017): “Analysis and Design of Materials for Advanced Batteries”; P. B. Balbuena.

Task 8.8 – Investigation of Sulfur Reaction Mechanisms (Deyang Qu, University of Wisconsin Milwaukee; Xiao-Qing Yang, Brookhaven National Laboratory)

Project Objective. With the advantages of the unique analytical assay developed in 2016, the primary objectives are to further conduct focused fundamental research on the mechanism for Li-S batteries, investigate the kinetics for the sulfur redox reaction, develop electrolytes and additives suitable for Li-S chemistry, and optimize the sulfur electrode and cell designs. In these objectives, special attention will be paid to investigation of the redox reaction of sulfur cathode, management for the solubility of polysulfide ions, formation of SEI layer and dead lithium on the surface of lithium anode, rechargeability of lithium anode in the solution containing polysulfide, and exploration of electrode and cell designs. Through such investigations, the Li-S chemistry will be studied systematically, and scientific understanding of the reaction mechanism can be well utilized to guide system engineering design.

Project Impact. The unique *in situ* electrochemical HPLC/MS technique will identify the soluble polysulfides real-time during the charge/discharge of a Li-S battery; thus, the mechanism can be revealed in detail. The project results will guide development of sulfur cathode and Li-S designs.

Approach. This project will use *in situ* electrochemical-MS, electrochemical-HPLC/MS, XPS, SEM, and XRD to study electrochemical reactions associated with sulfur electrodes. Electrochemical techniques such as AC impedance, rotation ring disk electrode, and galvanostat will be used to study the electrode process kinetics. The project is developing an *in situ* electrochemical optical method to investigate the surface of lithium anode during cycling of a Li-S cell.

Out-Year Goals. The out-year goal is to establish tools to investigate the interaction between dissolved sulfur and polysulfide ions with lithium anode, exploring the additives that can migrate such interaction. In addition, the project will gain further understanding of the chemical behaviors of the polysulfide in the electrolyte and propose a valid mechanism for the Li-S reaction.

Collaborations. The PI, Deyang Qu, is the Johnson Control Endowed Chair Professor; thus, the University of Wisconsin at Milwaukee and BNL team have close collaboration with Johnson Controls' scientists and engineers. This collaboration enables the team to validate the outcomes of fundamental research in pilot-scale cells. This team has been closely working with top scientists on new material synthesis at ANL, LBNL, and PNNL, with U.S. industrial collaborators at GM, Duracell, and Johnson Control as well as international collaborators in Japan and South Korea. These collaborations will be strengthened and expanded to give this project a vision on both today's state-of-the-art technology and tomorrow's technology in development, with feedback from the material designer and synthesizers upstream, and from industrial end users downstream.

Milestones

1. Complete design and validation of the *in situ* electrochemical – microscopic cell for *in situ* investigation of lithium anode during cycling. (Q1 – Completed December 31, 2016)
2. Complete study of interaction between dissolved elemental sulfur and polysulfide ions with both the electrolytes and lithium anode. (Q2 – Completed March 31, 2017)
3. Complete investigation of chemical equilibriums among dissolved polysulfide ions during the course of discharge and recharge of Li-S batteries. (Q3 – Completed June 30, 2017)
4. Complete the preliminary engineering design and test for the rechargeable Li-S battery including electrode design and cell design. (Q4 – Completed September 30, 2017)

Progress Report

This quarter, the project continued to utilize the unique HPLC-MS electrochemical technique to investigate the mechanism of sulfur redox reaction and traditional electrochemical method to investigate the electrochemical catalytic reaction of polysulfides on carbon electrodes. The additives that could potentially mitigate the “shuttle-effect” were investigated.

The most widely used inhibition additive in Li-S batteries is LiNO_3 . Many other additives were also reported in the literature; those results, however, were all based on electrochemical studies. Due to the different electrochemical conditions in each work, the inhibition effect of those additives for the reaction between polysulfides and lithium metal was not compared under the same conditions. Based on the unique HPLC/MS method this project has developed, the inhibition effects of 18 additives were compared systematically this quarter. This work also demonstrated that the project’s HPLC method could be an easy, fast platform for screening inhibitors in a future study. The additives tested in the study were tabulated in Table 7.

By directly comparing the chromatographic distributions before and after contact with lithium metal, the inhibition for the additives on the “shuttle effect” in a Li-S battery can be qualitatively and directly investigated. The impacts of the nitrate additives are clearly shown in Figure 94. The chromatographic distributions of dissolved polysulfide ions after being in contact with lithium metal for four days were slightly changed from those of the original electrolytes without exposure to lithium metal. The chromatographic peaks belonging to the long-chain polysulfide species (S_6^{2-} , S_7^{2-}) just slightly decreased, together with a slight increase of the medium-chain polysulfide species (S_4^{2-}). The only notable change in the chromatograms with nitrate additives was the decrease of the chromatographic peak of elemental sulfur after being in contact with lithium metal for four days. The decrease of elemental sulfur after being in contact with lithium metal could be attributed to the lack of passivation of the Li-metal surface during the reaction with

Table 7. Additives tested in the project study using the unique high-performance liquid chromatography mass spectrometry method. (See references listed at the end of this section.)

Additives	Reference
LiNO_3 , KNO_3 , CsNO_3 , NH_4NO_3 , KNO_2 , Nitromethane, etc.	[1]
LiNO_3 , NaNO_3 , KNO_3 , CsNO_3	[2]
CsNO_3	[3]
Five imidazolium salts, including BMPTFSi etc.	[4]
$\text{PYR}_{14}\text{TFSI}$, $\text{NBu}_4\text{SO}_3\text{CF}_3$	[5]
LiClO_4	[6]
P_2S_5	[7]
1,1,2,2-tetrafluoroethyl-2,2,3,3-tetrafluoropropyl ether	[8]
Bis (2,2,2-trifluoroethyl) ether	[9]
CS_2	[10]

elemental sulfur since the reaction products (probably the long-chain polysulfides) between lithium metal and elemental sulfur were highly soluble. For some additives, such as CS_2 and BTFE, although it was reported as shuttle inhibitors, the inhibition effect was hardly observed.

Based on the clear, reliable, and quantitative HPLC results, the inhibition effect for 18 different additives was compared. It was found that P_2S_5 , NaIO_4 , and KBrO_3 were not compatible with polysulfides (react severely); five nitrate additives demonstrated good inhibition effects, while the other ten additives showed limited or no inhibition effect against the shuttle reactions. The influence of the additive concentration and electrolyte concentration on the inhibition effect for shuttle reactions will be studied in future work.

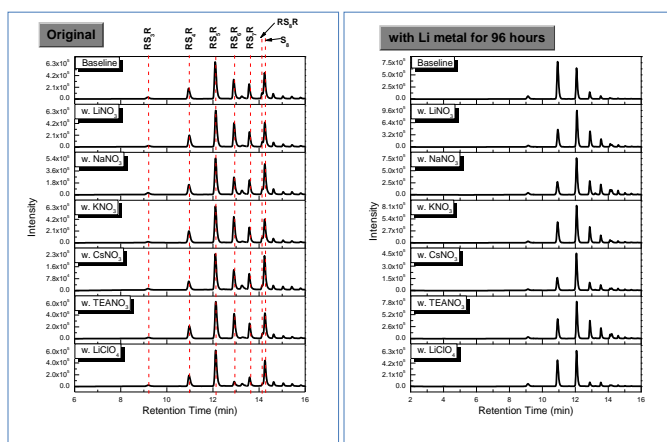


Figure 94. Comparison of inhibition effect for nitrate additives, based on direct comparison of chromatographic distributions before and after contact with lithium metal.

References

- [1] Mikhaylik, Y. V. U. S. Patent 7354680 (2008).
- [2] Kim, J. S., and T. H. Hwang, B. G. Kim, J. Y. Min, and J. W. Choi. *Adv. Funct. Mater.* 24 (2014): 5359.
- [3] Jia, W. S., and C. Fan, L. P. Wang, Q. J. Wang, M. J. Zhao, A. J. Zhou, and J. Z. Li. *ACS Appl. Mater. Interfaces* 8 (2016): 15399.
- [4] Kim, S., and Y. J. Jung, and S. J. Park. *Electrochim. Acta* 52 (2007): 2116.
- [5] Zhang, S. S. *Electrochim. Acta* 97 (2013): 226.
- [6] Kim, H. S., and C. S. Jeong, and Y. T. Kim. *J. Appl. Electrochem.* 42 (2012): 75.
- [7] Lin, Z., and Z. C. Liu, W. J. Fu, N. J. Dudney, and C. D. Liang. *Adv. Funct. Mater.* 23 (2013): 1064.
- [8] Azimi, N., and W. Weng, C. Takoudis, and Z. C. Zhang. *Electrochem. Commun.* 37 (2013): 96.
- [9] Gordin, M. L., and F. Dai, S. R. Chen, T. Xu, J. X. Song, D. H. Tang, N. Azimi, Z. C. Zhang, and D. H. Wang. *ACS Appl. Mater. Interfaces* 6 (2014): 8006.
- [10] Gu, S., and Z. Y. Wen, R. Qian, J. Jin, Q. S. Wang, M. F. Wu, and S. J. Zhuo. *ACS Appl. Mater. Interfaces* 8 (2016): 34379.

Task 8.9 – Statically and Dynamically Stable Lithium-Sulfur Batteries (Arumugam Manthiram, University of Texas – Austin)

Project Objective. The project objective is to develop statically and dynamically stable Li-S batteries by integrating polysulfide-filter-coated separators with a protected Li-metal anode through additives or a modified Li_2S cathode with little or no charge barrier during first charge. The project includes demonstration of electrochemically stable cells with sulfur capacities of $> 1,000 \text{ mA h g}^{-1}$ and cycle life in excess of 500 cycles (dynamic stability) along with positive storage properties (static stability) at $> 70 \text{ wt\%}$ sulfur content and $\sim 5 \text{ mg cm}^{-2}$ loading.

Project Impact. The combination of polysulfide-filter (PS-filter)-coated separator, Li-metal-protection additives, and Li_2S cathode modifications offers a viable approach to overcome the persistent problems of Li-S batteries. This project is systematically integrating the basic science understanding gained in its laboratory of these three aspects to develop the Li-S technology as the next-generation power source for EVs. The project targets demonstrating cells with sulfur capacities of over $1,000 \text{ mA h g}^{-1}$ and cycle life in excess of 500 cycles along with good storage properties at high sulfur content and loading that will make the Li-S technology superior to the present-day Li-ion technology in terms of cost and cell performance.

Approach. Electrochemical stability of the Li-S cells is improved by three complementary approaches. The first approach focuses on establishment of an electrochemically stable cathode environment by employing PS-filter-coated separators. The PS-filter coatings aim to suppress the severe polysulfide diffusion and improve the redox capability of Li-S cells with high-sulfur loadings. The study includes an understanding of materials characteristics, fabrication parameters, electrochemical properties, and battery performance of the PS-filter-coated separators. The second approach focuses on electrode engineering from two aspects. First, investigation of a Li-metal anode with coating- and additive-supporting approaches is aimed at improving the safety of Li-S cells. Second, research on activated- Li_2S cathode with little or no charge-barrier will promote performance and safety of the C- Li_2S cells. Integration of the first two approaches would create statically and dynamically stable Li-S batteries for EVs.

Out-Year Goals. The overall goal is to develop statically and dynamically stable Li-S batteries with custom cathode and stabilized anode active materials. In addition to developing a high-performance battery system, a fundamental understanding of the structure-configuration-performance relationships will be established. Specifically, the optimization of the electrochemical and engineering parameters of PS-filter-coated separators aims at comprehensively investigating different coating materials and their corresponding coating techniques for realizing various high-performance custom separators. The developed PS-filter-coated separators can be coupled with pure sulfur cathodes with high-sulfur loading and content. Multi-functional PS-filter-coated separators, high-loading sulfur cathodes, stabilized-Li-metal anodes, activated- Li_2S cathodes, and novel cell design are anticipated to provide an in-depth understanding of the Li-S battery chemistry and to realize statically and dynamically stable Li-S batteries.

Collaborations. This project collaborates with ORNL.

Milestones

1. Analyze and improve dynamic electrochemical performances of Li-S cells. (Q1 – Completed December 2016)
2. Analyze and improve static electrochemical performances of Li-S cells. (Q2 – Completed March 2017)
3. Increase the sulfur loading of the cells. (Q3 – Completed June 2017)
4. *Go/No-Go*: Fabricate cells with high sulfur content/loading and good electrochemical stability. (Q4 – Completed September 2017)

Progress Report

Three layer-by-layer, nonporous, CNT-coated separators were applied to high-sulfur loading Li-S cells with 5.4 mg cm^{-2} sulfur loading and 70 wt% sulfur content. The three separators are termed as LBL CNT#1 (0.05 mg cm^{-2} CNT coating), LBL CNT#2 (0.10 mg cm^{-2} CNT coating), and LBL CNT#3 (0.15 mg cm^{-2} CNT coating). These cells exhibit peak discharge capacities of, respectively, 1,113, 1200, and 1209 mA h g^{-1} at C/5 rate (Figure 95a). The cell with the LBL CNT#3 separator exhibits a peak discharge capacity of 1087 mA h g^{-1} with superior long-term cyclability with an even higher sulfur loading of 7.5 mg cm^{-2} for 200 cycles, which translates to a high areal capacity and energy density of, respectively, 8 mA h cm^{-2} and 17 mW h cm^{-2} (Figure 95b). Figure 95c reveals that the self-discharge rates of all three cells are lower than the target value of 0.5% per day. Among these three cells, the cell with the LBL CNT#3 separator possesses the lowest self-discharge rate of only 0.16% per day.

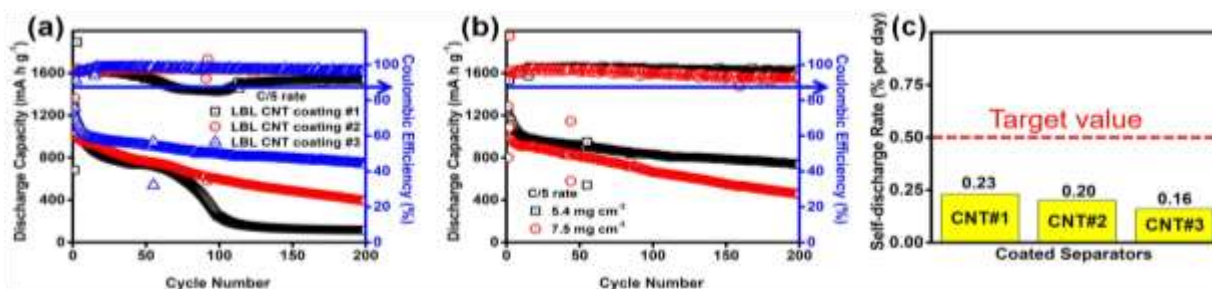


Figure 95. Cycling performances of the cells fabricated with (a) LBL CNT#1, LBL CNT#2, and LBL CNT#3 separators with 5.4 mg cm^{-2} sulfur loading and (b) LBL CNT#3 separator with 5.4 and 7.5 mg cm^{-2} sulfur loadings. (c) Self-discharge rates of the cells fabricated with the three LBL CNT separators after storing for 360 days.

Figure 96 shows an advanced cathode design that was fabricated with a cotton-carbon electrode, in which polysulfide was used as the catholyte. The project's cotton-carbon cathodes with a high sulfur loading (30 mg cm^{-2}) and content (80 wt%) represent the highest sulfur loading/content among the literature reports and are able to smoothly cycle and stably rest at a very low electrolyte/sulfur ratio of only 6.8, which is much lower than the values used in the literature. The cells show good cycle stability with a capacity retention of 70% after 100 cycles, and improved cell-storage stability with a low self-discharge rate of just 0.12% per day after storing for 60 days (Figure 96a-b). Such a well-designed cathode configuration further allowed an ultrahigh sulfur loading of 60 mg cm^{-2} , while the cells retained high electrochemical reversibility and efficiency with a high areal capacity and energy density of, respectively, 56 mA h cm^{-2} and 118 mW h cm^{-2} (Figure 96c). The cell performance metrics are higher than the values obtained with the current commercial Li-ion batteries (4 mA h cm^{-2} and $10.08 \text{ mW h cm}^{-2}$) based on LiCoO_2 .

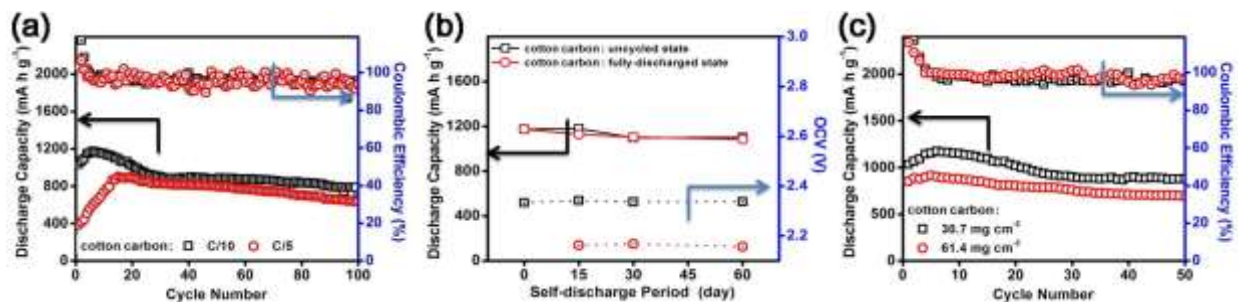


Figure 96. (a) Cycling performance and (b) self-discharge analysis of the cells fabricated with cotton-carbon cathodes with a sulfur loading of 30 mg cm^{-2} . (c) Cycling performance of a cotton-carbon cathode with even a higher sulfur loading of 60 mg cm^{-2} .

Patents/Publications/Presentations

Publications

- Chang, C.-H., and S.-H. Chung, S. Nanda, and A. Manthiram. “A Rationally Designed Polysulfide-Trapping Interface on the Polymeric Separator for High-Energy Li–S Batteries.” *Materials Today Energy* 6 (2017): 72.
- Luo, L., and S.-H. Chung, C.-H. Chang, and A. Manthiram. “A Nickel-Foam@Carbon-Shell with a Pie-Like Architecture as an Efficient Polysulfide Trap for High-Energy Li–S Batteries.” *Journal of Materials Chemistry A* 5 (2017): 15002.
- Luo, L., and A. Manthiram. “Rational Design of High-Loading Sulfur Cathodes with a Poached-Egg-Shaped Architecture for Long-Cycle Lithium–Sulfur Batteries.” *ACS Energy Letters* 2 (2017): 2205.
- Chang, C.-H., and S.-H. Chung, P. Han, and A. Manthiram. “Oligoanilines as a Suppressor of Polysulfide Shuttling in Lithium-Sulfur Batteries.” *Materials Horizons* 4 (2017): 908.

Presentations

- NASA Workshop on Battery Technologies for Future Aerospace Applications, Cleveland, Ohio (August 16–17, 2017): “Next Generation Battery Technologies: Challenges and Opportunities”; A. Manthiram. Invited.
- China University of Hong Kong, Hong Kong (September 29, 2017): “Electrical Energy Storage: Next Generation Battery Technologies”; A. Manthiram. Invited.

Task 8.10 – Electrochemically Responsive, Self-Formed, Lithium-Ion Conductors for High-Performance Lithium-Metal Anodes (Donghai Wang, Pennsylvania State University)

Project Objective. The project objective is to develop and deliver an electrochemically responsive self-formed hybrid Li-ion conductor as a protective layer for Li-metal anodes, enabling Li-metal anodes to cycle with a high efficiency of ~ 99.7% at high electrode capacity ($> 6 \text{ mAh/cm}^2$) and high current density ($> 2 \text{ mA/cm}^2$) for over 500 cycles. The project will also demonstrate prototype ~ 300 mAh Li-S battery cells with energy densities of ~ 200 Wh/kg and ~ 80% capacity retention for ~ 300 cycles at ~ 80% depth of discharge using Li-metal anodes with this protective layer.

Project Impact. This project aims to develop a new hybrid Li-ion conductor that enables safe and high-performance Li-metal anodes. The use of these high-performance Li-metal anodes in turn enables Li-S batteries with high energy density and long cycling life. Such anodes can also lead to a 50% increase in the energy density of conventional Li-ion batteries with Li-metal oxide cathodes. Meeting the technical targets will potentially develop a new high-energy-density lithium battery, promote increased adoption of EVs and PHEVs, and reduce petroleum consumption in the transportation sector by helping battery-powered vehicles become accepted by consumers as a reliable source of transportation.

Approach. The novel multiphase organo- Li_xS_y or organo- $\text{Li}_x\text{P}_y\text{S}_z$ hybrid ion conductors with tunable multi-functional organic components and controlled Li_xS_y and $\text{Li}_x\text{P}_y\text{S}_z$ inorganic components will be designed and prepared, and thus enable safe use of lithium metal with high CE. In the first year, the team will develop the organo- Li_xS_y lithium protection layers with tuned functionality: (1) finding appropriate composition and (2) developing appropriate synthesis and fabrication methods.

Out-Year Goals. Work will progress toward development of organo- Li_xS_y lithium protection layers with tuned functionality. The project will conduct characterization, performance, and compatibility tests on materials and systems. Twelve baseline 300-mAh pouch cells using standard Li-metal anodes and high-performance carbon-sulfur cathodes will be delivered for independent verification.

Collaborations. The project collaborated with Prof. Seong Kim's group at Pennsylvania State University for AFM characterization of the organo- Li_xS_y layer for lithium protection.

Milestones

1. Development of the first-generation of organo- Li_xS_y lithium protection layers with tuned functionality. Conduct characterization and performance tests on the materials. (Q1 – Completed December 2016)
2. Deliver 12 baseline ~ 300 mAh Li-S cells for independent verification. (Q2 – Completed)
3. Optimize organo- Li_xS_y protective layer and demonstrate lithium anodes cycling with ~ 98.5% CE for ~ 200 cycles. (Q3 – Completed)
4. Demonstrate lithium anodes with optimized organo- Li_xS_y protective layer and ~ 99% CE for ~ 200 cycles. (Q4 – Completed)

Progress Report

The composition of SEI layer formed from electrolyte containing sulfur-containing polymer with 90 wt% sulfur (PST-90) was characterized. The SEI layers formed from the control electrolyte, the S-Electrolyte, and SCP-90-Electrolyte are named C-SEI, S-SEI, and PST-90-SEI, respectively. The S 2*p* XPS spectra exhibit major difference among these three SEI layers (Figure 97a). For the S-SEI, the peaks at 160.5 and 161.7 eV reflect composition of Li₂S and Li₂S₂ in the SEI layer, and the small peak at 163.0 eV is also observed, corresponding to the small amount of lithium polysulfides (Li₂S_x, such as Li₂S₃) in the SEI layer. This result demonstrates that the S-SEI layer is mainly composed of inorganic species. For PST-90-SEI layer, besides the peaks at 160.5, 161.7, and 163.0 eV observed in XPS spectra, the additional peak at 162.2 eV corresponding to the S 2*p*_{3/2} from organosulfides is observed, confirming the existence of organosulfides (RS₆Li₆) in the SEI layers. The relatively stronger peak at 163.0 eV corresponds to the lithium polysulfides (Li₂S_x) and organo-polysulfides (RS_xLi₆) that have similar position with lithium polysulfides. In the C 1*s* XPS spectra (Figure 97b), the peak at ~ 292.1 eV can be found

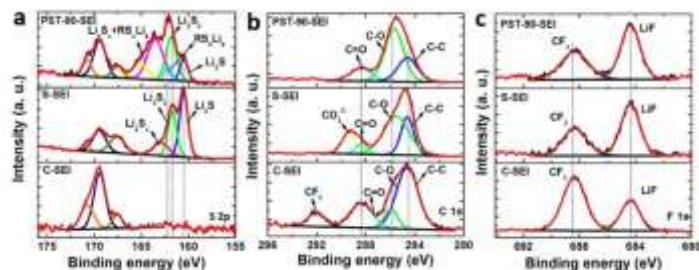


Figure 97. X-ray photoelectron spectroscopy (XPS) spectra of C-SEI layer, S-SEI layer, and SCP-90-SEI layer. (a) S 2*p* XPS spectra. (b) C 1*s* XPS spectra. (c) F 1*s* XPS spectra.

in the C-SEI and corresponds to the C 1*s* from the functional group –CF₃, which may originate from the decomposition of LiTFSI in the control electrolyte. Whereas, this peak disappears when using the PST-90 as the additive in the electrolyte. Moreover, the F 1*s* XPS spectra show two peaks at 684.4 and 688.4 eV assigned to the F 1*s* from the LiF and –CF₃ respectively (Figure 97c), and LiF is also the decomposition product of LiTFSI. The intensity of the peak assigned to LiF becomes stronger than that of –F₃ when using PST-90 as the additive. Both the C 1*s* and F 1*s* spectra illustrate the –CF₃ component is suppressed and comparatively the content of LiF increases when using PST-90 as additive.

FTIR spectra of PST-90-SEI (Figure 98) show a peak at ~ 1170 cm⁻¹, which can be found in the pure PST-90 polymer and is attributed to the vibration of C-N bond. In addition, peaks at 1476 and 838 cm⁻¹ are also observed in both PST-90-SEI and PST-90 polymer, indicating the organosulfide/organopolysulfide in the SEI layers originates from PST-90 polymer.

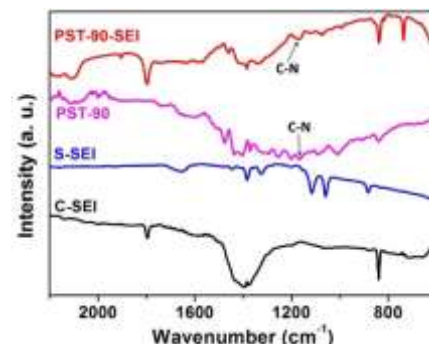


Figure 98. Fourier transform infrared of C-SEI, S-SEI, and PST-90-SEI layer.

Peak force tapping mode of AFM was used to investigate the mechanical properties of different SEI layers. For C-SEI (Figure 99a) and S-SEI (Figure 99b) layers, the slopes of the loading and unloading curves are quite high and overlap each other. This implies that the SEI layers are relatively stiff and viscoelasticity is negligible because these SEI layers are composed of inorganic lithium salts, making them more rigid and brittle. In contrast, the surface of PST-90-SEI (Figure 99c) layer deforms more

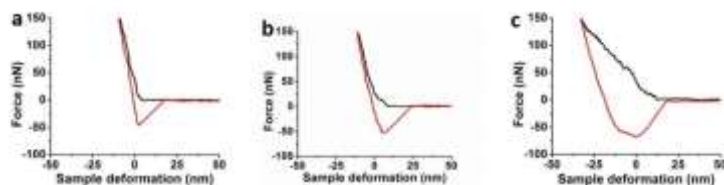


Figure 99. Indentation curves of the C-SEI layer (a), S-SEI layer (b), and PST-90-SEI layer (c).

and shows a large hysteresis between the loading and unloading curves, along with a long pull-off or meniscus before the tip completely returned to the free-standing position. The reduced modulus of the different SEI layers could be estimated by fitting the unloading curves with the Johnson-Kendall-Roberts (JKR) models. The C-SEI and S-SEI layers show the modulus of

903 and 740 MPa from the JKR model fit, respectively. In contrast, PST-90-SEI layer displays a low modulus estimated to be 367 MPa. These results suggest that the organosulfides/organopolysulfides-containing SEI layer (PST-90-SEI) becomes soft and viscoelastic to render it flexible, which is beneficial to withstand the large mechanical deformation originating from the lithium plating/stripping and to both suppress the growth of lithium dendrite and improve cycling CE.

Figure 100 shows the cycling performance of cells using the PST-90-Electrolyte at a current density of 2 mA cm^{-2} and a deposition capacity of 1 mA h cm^{-2} ; the cells deliver an enhanced average CE of 99% over 400 cycles.

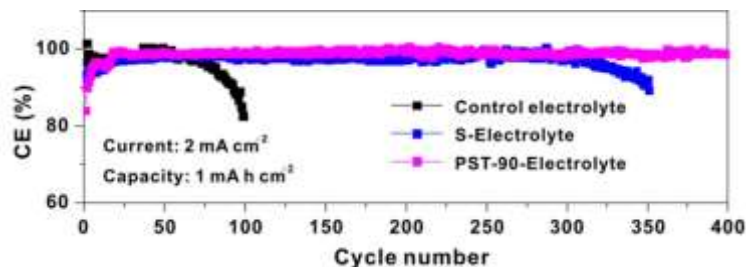


Figure 100. Cycling performances of the cells using different electrolytes at a current density of 2 mA cm^{-2} with a deposition capacity of 1 mA h cm^{-2} .

Patents/Publications/Presentations

Publication

- Li, G. X., and Y. Gao, X. He, Q. Q. Huang, S. R. Chen, S. H. Kim, and D. H. Wang. “Organosulfide-Plasticized Solid-Electrolyte Interphase Layer Enables Stable Lithium Metal Anodes for Long-Cycle Lithium-Sulfur Batteries.” *Nat. Commun.* 8 (2017): 850.

TASK 9 – LITHIUM–AIR BATTERIES

Summary and Highlights

High-density energy storage systems are critical for EVs required by the EV Everywhere Grand Challenge. Conventional Li-ion batteries still cannot fully satisfy the ever-increasing needs because of their limited energy density, high cost, and safety concerns. As an alternative, the rechargeable lithium-oxygen (Li-O₂) battery has the potential to be used for long-range EVs. The practical energy density of a Li-O₂ battery is expected to be ~ 800 Wh kg⁻¹. The advantages of Li-O₂ batteries come from their open structure; that is, they can absorb the active cathode material (oxygen) from the surrounding environment instead of carrying it within the batteries. However, the open structure of Li-O₂ batteries also leads to several disadvantages. The energy density of Li-O₂ batteries will be much lower if oxygen must be provided by an onboard container. Although significant progress has been made in recent years on fundamental properties of Li-O₂ batteries, research in this field is still in an early stage, with many barriers to be overcome before practical applications. These barriers include:

- Instability of electrolytes—The superoxide species generated during discharge or O₂ reduction process is highly reactive with electrolyte and other components in the battery. Electrolyte decomposition during charge or O₂ evolution process is also significant due to high over-potentials.
- Instability of air electrode (dominated by carbonaceous materials) and other battery components (such as separators and binders) during charge/discharge processes in an O-rich environment.
- Limited cyclability of the battery associated with instability of the electrolyte and other battery components.
- Low energy efficiency associated with large over-potential and poor cyclability of Li-O₂ batteries.
- Low power rate capability due to electrode blocking by the reaction products.
- Absence of a low-cost, high-efficiency oxygen supply system (such as oxygen selective membrane).

The main goal of this Task is to provide a better understanding on the fundamental reaction mechanisms of Li-O₂ batteries and identify the required components (especially electrolytes and electrodes) for stable operation of Li-O₂ batteries. PNNL researchers will investigate stable electrolytes and oxygen evolution reaction (OER) catalysts to reduce the charging overvoltage of Li-O₂ batteries and improve their cycling stability. New electrolytes will be combined with stable air electrodes to ensure their stability during Li-O₂ reaction. Considering the difficulties in maintaining the stability of conventional liquid electrolyte, the Liox team will explore use of a nonvolatile, inorganic molten salt comprising nitrate anions and operating Li-O₂ cells at elevated temperature (> 80°C). It is expected that these Li-O₂ cells will have a long cycle life, low over potential, and improved robustness under ambient air compared to current Li-air batteries. At ANL, new cathode materials and electrolytes for Li-air batteries will be developed for Li-O₂ batteries with long cycle life, high capacity, and high efficiency. The state-of-the-art characterization techniques and computational methodologies will be used to understand the charge and discharge chemistries. The University of Massachusetts/BNL team will investigate the root causes of the major obstacles of the air cathode in the Li-air batteries. Special attention will be paid to optimization of high-surface carbon material used in the gas diffusion electrode, catalysts, electrolyte, and additives stable in Li-air system and with capability to dissolve lithium oxide and peroxide. Success of this project will establish a solid foundation for further development of Li-O₂ batteries toward their practical applications for long-range EVs. The fundamental understanding and breakthrough in Li-O₂ batteries may also provide insight on improving performance of Li-S batteries and other energy storage systems based on chemical conversion processes.

Task 9.1 – Rechargeable Lithium-Air Batteries (Ji-Guang Zhang and Wu Xu, Pacific Northwest National Laboratory)

Project Objective. The project objective is to develop rechargeable Li-O₂ batteries with long-term cycling stability. The FY 2017 objective is to stabilize Li-metal anode in Li-O₂ batteries and to investigate the temperature effect on oxygen reduction reaction (ORR) and OER processes of the Li-O₂ chemistry.

Project Impact. Li-air batteries have a theoretical specific energy that is more than five times that of state-of-the-art Li-ion batteries and are potential candidates for use in next-generation, long-range EVs. Unfortunately, the poor cycling stability and low CE of Li-air batteries have prevented their practical application. This work will explore a new electrolyte and electrode that could lead to long cyclability and high CEs in Li-air batteries that can be used in the next-generation EVs required by the EV Everywhere Grand Challenge.

Out-Year-Goals. The long-term goal of the proposed work is to enable rechargeable Li-air batteries with a specific energy of 800 Wh/kg at cell level, 1000 deep-discharge cycles, improved abuse tolerance, and less than 20% capacity fade over a 10-year period to accelerate commercialization of long-range EVs.

Collaborations. This project collaborates with Chongmin Wang of PNNL on characterization of cycled air electrodes by TEM/SEM and with Jinhui Tao of PNNL on characterization of Li-metal anodes by *in situ* AFM.

Milestones

1. Investigate temperature effect on ORR and OER of Li-O₂ batteries. (Q1 – Completed December 2016)
2. Identify factors that affect stability of Li-metal anode in Li-O₂ batteries. (Q2 – Completed March 2017)
3. Develop surface coating or electrolyte additive to stabilize Li-metal anode and improve cycle life of Li-O₂ battery. (Q4 – Completed September 2017)

Progress Report

This quarter, the mechanism on the improved cyclability of Li-O₂ batteries by a facile electrochemical pre-treatment has been further investigated. As shown in Figure 101, the number of stable cycling of the Li-O₂ cells after different pre-treatment conditions is increased when compared to the pristine cell without any pre-treatment. The optimal condition is pre-charging the cell in an inert atmosphere to 4.3 V for 10 min, which leads to a stable cycling for 110 cycles. The variations of cell impedances with cycle time were investigated for pre-treated and pristine Li-O₂ cells, and the corresponding EIS plots at the charged states are shown in Figure 102a-b. The corresponding fitting results of the electrolyte resistance (R₁), the total resistance (R₂) containing the surface film resistance (R_{SEI}) and the charge transfer resistance (R_{ct}) as a function of cycle numbers are also provided in Figure 102c. Figure 102c clearly shows that the pre-treated Li-O₂ cell at the initial stage has a smaller R₁ and R₂ than those with the pristine cells. This is because the Li-metal anode in the pre-charged cell was well protected before O₂ was introduced, so the reactions between lithium, electrolyte, and O₂ are limited. The cell impedances of R₂ decrease from the 1st cycle to the 20th cycle. This can be attributed to both CNTs electrode and Li-metal anode, either pre-treated or untreated, gradually reaching their own well-protected condition with the coverage of the electrolyte decomposition products, thus giving lower cell impedances. After that, the Li-O₂ cell with the optimal pre-treatment shows only slight increase in cell impedance from 20th cycle to 110th cycle, while the cell without pre-treatment shows a rapid increase in cell impedance from the 20th cycle to only 70th cycle. This is because the electrochemical pre-charging process generates protective layers on both CNTs electrode surfaces and Li-metal anode, which suppress the side reactions of reduced oxygen species attacking both CNT electrode and Li-metal anode, as shown in Figure 103.



Figure 103. The schematic of the operation principle of beforehand protections for carbon nanotube air-electrode and Li-metal anode after *in situ* one-step electrochemical process.

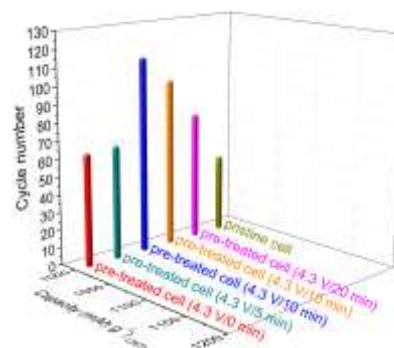


Figure 101. Comparison of cycle life of Li-O₂ cells with and without pre-treatment. The cell cycling was conducted under the 1000 mAh g⁻¹ capacity limited protocol at 0.1 mA cm⁻² between 2.0 V and 4.5 V.

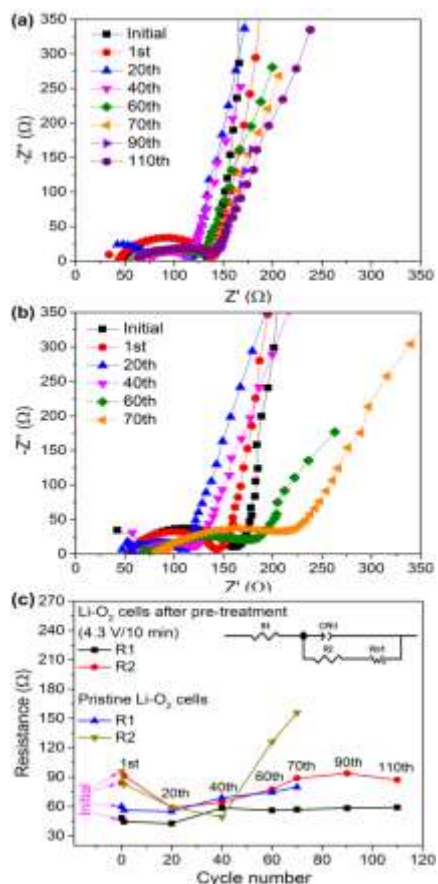


Figure 102. The AC-impedance spectra of the Li-O₂ cells after pre-treatment at 4.3 V/10 min during 110 cycles (a), and pristine Li-O₂ cells during 70 cycles (b). (c) Evolution of fitted resistance values of the above Li-O₂ cells after pre-treatment at 4.3 V/10 min and pristine cells.

Patents/Publications/Presentations

Publications

- Xu, W., and B. Liu, and J.-G. Zhang. “Preformation of Solid Electrolyte Interphase on Electrodes for Rechargeable Lithium Metal Batteries.” PNNL Invention Disclosure Report 31087-E.
- Liu, B., and W. Xu, J. Zheng, P. Yan, E. D. Walter, N. Isern, M. E. Bowden, M. H. Engelhard, S. T. Kim, J. Read, B. D. Adams, X. Li, J. Cho, C. Wang, and J.-G. Zhang. “Temperature Dependence of Oxygen Reduction Mechanism in Nonaqueous Li-O₂ Batteries.” *ACS Energy Lett.* (2017): in press. doi: 10.1021/acseenergylett.7b00845.

Presentation

- 254th ACS National Meeting, Washington, D. C. (August 2017): “Development of Stable Rechargeable Lithium-Oxygen Batteries”; W. Xu, B. Liu, S. Song, and J.-G. Zhang. Invited.

Task 9.2 – Efficient Rechargeable Li/O₂ Batteries Utilizing Stable Inorganic Molten Salt Electrolytes (Vincent Giordani, Liox)

Project Objective. The project objective is to develop high specific energy, rechargeable Li-air batteries having lower overpotential and improved robustness under ambient air compared to current Li-air batteries.

Project Impact. If successful, this project will solve particularly intractable problems relating to air electrode efficiency, stability, and tolerance to the ambient environment. Furthermore, these solutions may translate into reduced complexity in the design of a Li-air stack and system, which in turn may improve prospects for use of Li-air batteries in EVs. Additionally, the project will provide materials and technical concepts relevant for development of other medium temperature molten salt lithium battery systems of high specific energy, which may also have attractive features for EVs.

Approach. The technical approach involves replacing traditional organic and aqueous electrolytes with a nonvolatile, inorganic molten salt comprising nitrate anions and operating the cell at elevated temperature (> 80°C). The research methodology includes powerful *in situ* spectroscopic techniques coupled to electrochemical measurements (for example, electrochemical MS) designed to provide quantitative information about the nature of chemical and electrochemical reactions occurring in the air electrode.

Out-Year-Goals. The long-term goal is to develop Li-air batteries comprising inorganic molten salt electrolytes and protected lithium anodes that demonstrate high (> 500 Wh/kg) specific energy and efficient cyclability in ambient air. By the end of the project, it is anticipated that problems hindering use of both the lithium anode and air electrode will be overcome due to materials advances and strategies enabled within the intermediate (> 80°C) operating temperature range of the system under development.

Collaborations. This project funds work at Liox Power, Inc.; LBNL (Prof. Bryan McCloskey: analysis of air electrode and electrolyte); and California Institute of Technology (Prof. Julia Greer: design of air electrode materials and structures).

Milestones

1. Demonstrate discharge specific energy and energy density ≥ 500 Wh/Kg and ≥ 800 Wh/L, respectively, based on air electrode mass and volume. (Q1 – Completed December 2016)
2. Scale-up downselected cell components for 4-mAh and 10-mAh cells. (Q2 – Completed March 2017)
3. Demonstrate ≥ 10 cycles at $\geq 90\%$ round-trip energy efficiency in laboratory-scale Li-air cells comprising a molten nitrate electrolyte and protected lithium electrode. (Q3 – Completed June 2017)
4. Fabricate and test 4- and 10-mAh cells. (Q4 – Completed September 2017)

Progress Report

This quarter, the project fabricated and tested full Li/nitrate and Li/O₂ cells utilizing a solid electrolyte between the negative and the positive electrode, the latter being constituted of either amorphous carbon black (Li/O₂) or nickel nanoparticles (Li/nitrate); both cathode active materials intimately mixed with the alkali molten nitrate electrolyte. Cells were being tested at 150°C and at a current density of 0.2 mA/cm². The solid electrolyte consisted of a LLZO 1 cm² disc of about 200 microns. The discharge capacity was limited to 4 mAh.

Figure 104 shows the first three discharge/charge cycles of a protected lithium anode cell using an alkali metal nitrate molten salt catholyte. The cell uses a porous nickel cathode (~ 10 mg/cm² nickel loading) and is cycled under argon gas. The typical ~ 2.6 V discharge plateau corresponds to electrochemical reduction of nitrate anion, based on the following reaction: $2\text{Li}^+ + 2\text{e}^- + \text{NO}_3^- \rightarrow \text{Li}_2\text{O} + \text{NO}_2^-$. Lithium oxide fills up the cathode porous structure while nitrite anion dissolves in the melt.

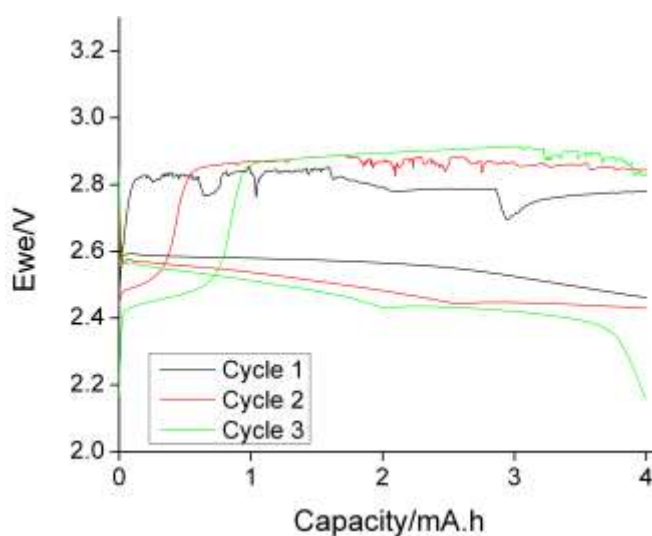


Figure 104. Molten nitrate lithium cell voltage profile at 150°C using nano-porous nickel cathode (Ni:LiNO₃-KNO₃ eutectic 50:50 wt%) at 0.2 mA/cm² current density (mNi = mnitrate = 10 mg) and LLZO-protected Li-metal anode.

Task 9.3 – Lithium–Air Batteries (Khalil Amine and Larry A. Curtiss, Argonne National Laboratory)

Project Objective. This project will develop new cathode materials and electrolytes for Li-air batteries for long cycle life, high capacity, and high efficiency. The goal is to obtain critical insight that will provide information on the charge and discharge processes in Li-air batteries to enable new advances to be made in their performance. This will be done using state-of-the-art characterization techniques combined with state-of-the-art computational methodologies to understand and design new materials and electrolytes for Li-air batteries.

Project Impact. The instability of current nonaqueous electrolytes and degradation of cathode materials limits the performance of Li-air batteries. The project impact will be to develop new electrolytes and cathode materials that are stable and can increase cycle life and improve efficiency of Li-air batteries.

Approach. The project is using a joint theoretical/experimental approach for design and discovery of new cathode and electrolyte materials that act synergistically to reduce charge overpotentials and increase cycle life. Synthesis methods, in combination with design principles developed from computations, are used to make new cathode architectures. Computational studies are used to help understand decomposition mechanisms of electrolytes and how to design electrolytes with improved stability. The new cathodes and electrolytes are tested in Li-O₂ cells. Characterization along with theory is used to understand the performance of the materials used in the cell and make improved materials.

Out-Year Goals. The out-year goals are to find catalysts that promote discharge product morphologies that reduce charge potentials and find electrolytes for long cycle life through testing and design.

Collaborations. This project engages in collaboration with Professor Kah Chun Lau (University of California at Norridge), Professor Amin Salehi (University of Illinois at Chicago), Professor Yang-Kook Sun (Hanyang University), Professor Yiyang Wu (Ohio State University), and Dr. Dengyun Zhai (China).

Milestones

1. Investigation of new architectures for platinum catalysts using hollow nanocarbon cages. (Q1 – Complete)
2. Development of new characterization techniques for determination of the composition and conductivity of discharge products in Li-O₂ batteries. (Q2 – Complete)
3. Design and synthesis of new catalysts for cathode materials based on metal organic frameworks for low charge overpotentials. (Q3 – Complete)
4. Investigation of uniformly synthesized metal clusters as catalysts and nucleation sites for controlling efficiency of Li-O₂ cells. (Q4 – Complete)

Progress Report

In the Li-O₂ battery the oxygen gas and electrolyte often compete for pathways in the conventional cathode based on a porous carbon cathode, which limits the performance of the battery. In this work, the project has used a novel air cathode based on a novel triple-phase structure by using a common textile. The hierarchical networked structure of the textile leads to decoupled pathways for electrolyte and oxygen gas, facilitating the transport of both components NS significantly improving battery performance. The oxygen flows through the woven mesh constructed by the textile fibers, while the electrolyte diffuses along the textile fibers. Due to the facilitated transport, the Li-O₂ battery based on this textile-based cathode shows a high discharge capacity of 8.6 mAh/cm², low over potential of 1.2 V, and stable operation of over 50 cycles. The decoupled transport pathway design has the potential for a flexible Li-O₂ battery design.

The concept of the breathable cathode is based on that of a textile; that is, the surface is a densely coated layer of CNTs. The hierarchical structure of the textile forms the channel for the flow of electrolyte, while the textile material naturally has a good affinity with liquid electrolyte. Therefore, the electrolyte flows underneath the active sites on the CNT layer where the reaction happens. The mesh holes on the textile provide sufficient space for the oxygen to flow through, since it has been shown that the gas flow channel should have a large enough size to facilitate oxygen reduction during discharge. Thus, the liquid electrolyte and the oxygen gas flow on the different sides of the active CNT layer without competing for space. The decoupled pathways for electrolyte and oxygen gas are crucial for the performance of the Li-O₂ battery. All the active sites on the CNT layer always have sufficient electrolyte and oxygen input during the discharge and can be fully utilized. The CNT is decorated with palladium nanoparticles with size of ~ 10 nm as the catalyst. Similar to the active CNT layer, the Pd catalysts in this case are fully exposed to the electrolyte and the oxygen gas.

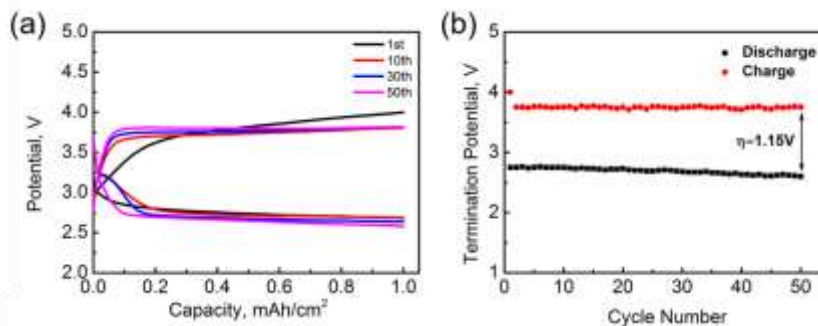


Figure 105. (a) Discharge/charge profile for 50 cycles. (b) The termination voltage of charge/discharge for 50 cycles.

The rechargeability of Li-air battery with the textile-based cathode is very good, as seen in Figure 105. The battery was cycled with a current density of 0.1 mA/cm² and a charge/discharge capacity limit of 1 mAh/cm². Almost no performance drop was observed, even after 50 cycles. The rechargeability of the battery was also studied via the characterization of discharge product. The XRD results indicate the formation of Li₂O₂. Moreover, Raman spectroscopy and XPS were employed to analyze the discharge product. In the Raman spectrum, a distinct peak at 800 cm⁻¹ was observed, which corresponds to amorphous Li₂O₂. In O 1s XPS spectrum after discharge, a peak at 528 eV was detected, which is the characteristic peak of Li₂O₂. Both results indicate that the discharge product is Li₂O₂.

TASK 10 – SODIUM-ION BATTERIES

Summary and Highlights

To meet the challenges of powering the PHEV, the next generation of rechargeable battery systems with higher energy and power density, lower cost, better safety characteristics, and longer calendar and cycle life (beyond Li-ion batteries, which represent today's state-of-the-art technology) must be developed. Recently, Na-ion battery systems have attracted increasing attention due to the more abundant and less expensive nature of the sodium resource. The issue is not insufficient lithium on a global scale, but what fraction can be used in an economically effective manner. Most untapped lithium reserves occur in remote or politically sensitive areas. Scale-up will require a long lead time, involve heavy capital investment in mining, and may require the extraction and processing of lower quality resources, which could drive extraction costs higher. Currently, high costs remain a critical barrier to the widespread scale-up of battery energy storage. Recent computational studies on voltage, stability, and diffusion barriers of Na-ion and Li-ion materials indicate that Na-ion systems can be competitive with Li-ion systems.

The primary barriers and limitations of current state-of-the-art of Na-ion systems are as follows:

- Building a sodium battery requires redesigning battery technology to accommodate the chemical reactivity and larger size of sodium ions.
- Lithium batteries pack more energy than sodium batteries per unit mass. Therefore, for sodium batteries to reach energy densities similar to lithium batteries, the positive electrodes in the sodium battery need to hold more ions.
- Since Na-ion batteries are an emerging technology, new materials to enable sodium electrochemistry and the discovery of new redox couples, along with the diagnostic studies of these new materials and redox couples, are important.
- In sodium electrochemical systems, the greatest technical hurdles to overcome are lack of high-performance electrode and electrolyte materials that are easy to synthesize, safe, and non-toxic, with long calendar and cycling life and low cost.
- Furthermore, fundamental scientific questions need to be elucidated, including (1) the difference in transport and kinetic behaviors between sodium and lithium in analogous electrodes; (2) sodium insertion/extraction mechanism; (3) SEI layer on the electrodes from different electrolyte systems; and (4) charge transfer in the electrolyte–electrode interface and Na⁺ ion transport through the SEI layer.

This task will use synchrotron-based *in situ* X-ray techniques and other diagnostic tools to evaluate new materials and redox couples, to explore fundamental understanding of the mechanisms governing the performance of these materials, and provide guidance for new material developments. This task will also be focused on developing advanced diagnostic characterization techniques to investigate these issues, providing solutions and guidance for the problems. The synchrotron based *in situ* X-ray techniques (XRD and hard and soft XAS) will be combined with other imaging and spectroscopic tools such as HRTEM, MS, and TXM.

Task 10.1 – Exploratory Studies of Novel Sodium-Ion Battery Systems (Xiao-Qing Yang and Seongmin Bak, Brookhaven National Laboratory)

Project Objective. The primary objective is to develop new advanced *in situ* material characterization techniques and to apply these techniques to explore the potentials, challenges, and feasibility of new rechargeable battery systems beyond the Li-ion batteries, namely the Na-ion battery systems for PHEVs. To meet the challenges of powering the PHEV, new rechargeable battery systems with high energy and power density, low cost, good abuse tolerance, and long calendar and cycle life must be developed. This project will use synchrotron-based *in situ* X-ray diagnostic tools developed at BNL to evaluate the new materials and redox couples, exploring the fundamental understanding of the mechanisms governing the performance of these materials.

Project Impact. The VTO Multi-Year Program Plan describes the goals for battery: “Specifically, lower-cost, abuse-tolerant batteries with higher energy density, higher power, better low-temperature operation, and longer lifetimes are needed for development of the next-generation of HEVs, PHEVs, and EVs.” If this project succeeds, the knowledge gained from diagnostic studies and collaborations with U.S. industries and international research institutions will help U.S. industries develop new materials and processes for a new generation of rechargeable battery systems beyond Li-ion batteries, such as Na-ion battery systems, in their efforts to reach these VTO goals.

Approach. This project will use synchrotron-based *in situ* X-ray diagnostic tools developed at BNL to evaluate the new materials and redox couples to enable a fundamental understanding of the mechanisms governing the performance of these materials and to provide guidance for new material and new technology development regarding Na-ion battery systems.

Out-Year Goals. The out-year goals are as follows: (1) Complete the synchrotron based *in situ* XRD and absorption studies of MXene type material V_2C as new cathode material for Na-ion batteries during charge-discharge cycling, and (2) complete the preliminary synchrotron-based X-ray absorption studies of $NaCuMnO_2$ as new cathode material for Na-ion batteries.

Collaborations. The BNL team has been working closely with top scientists on new material synthesis at ANL, LBNL, and PNNL, with U.S. industrial collaborators at GM and Johnson Controls, and with international collaborators.

Milestones

1. Complete the *in situ* XRD studies of one type of MXene material V_2C as new anode material for Na-ion batteries during charge-discharge cycling. (Q1 – Completed December 2016)
2. Complete *in situ* hard X-ray absorption studies at vanadium K-edge of one type of MXene material V_2C as new anode material for Na-ion batteries during charge-discharge cycling. (Q2 – Completed March 2017)
3. Complete soft X-ray absorption studies at vanadium L-edge, carbon, and oxygen K-edge of one type of MXene material V_2C as new anode material for Na-ion batteries at different charge-discharge states. (Q3 – Completed June 2017)
4. Complete the synchrotron-based X-ray absorption at copper and manganese K-edge for a new $NaCuMnO_2$ cathode material for Na-ion batteries during charge-discharge cycling. (Q4 – Completed September 2017)

Progress Report

This quarter, BNL focused on the studies of a new cathode material, Cu-doped β -NaMnO₂ layered material for sodium-ion batteries. *In situ* X-ray absorption near-edge spectroscopy for β -NaCu_{0.2}Mn_{0.8}O₂ was performed to explore the charge transfer mechanism. As shown in Figure 106, the normalized *in situ* XAS data indicate that copper exists as Cu⁺² and that manganese has an oxidation state between Mn⁺³ and Mn⁺⁴. The manganese K-edge spectra shift to higher energy region upon being charged to 4.0 V, nearly overlapping with the K-edge of MnO₂ and suggesting that Mn⁺³ ions are oxidized to Mn⁺⁴ state. For copper, however, the shift is much less significant, indicating that copper is not the major contributor for the charge compensation mechanism. Nevertheless, both manganese and copper XAS spectra feature pronounced shoulder peaks upon charge. This peak is likely due to the ligand-to-metal charge transfer process, which implies a strong covalency between M (copper or manganese) and O upon the charging process.

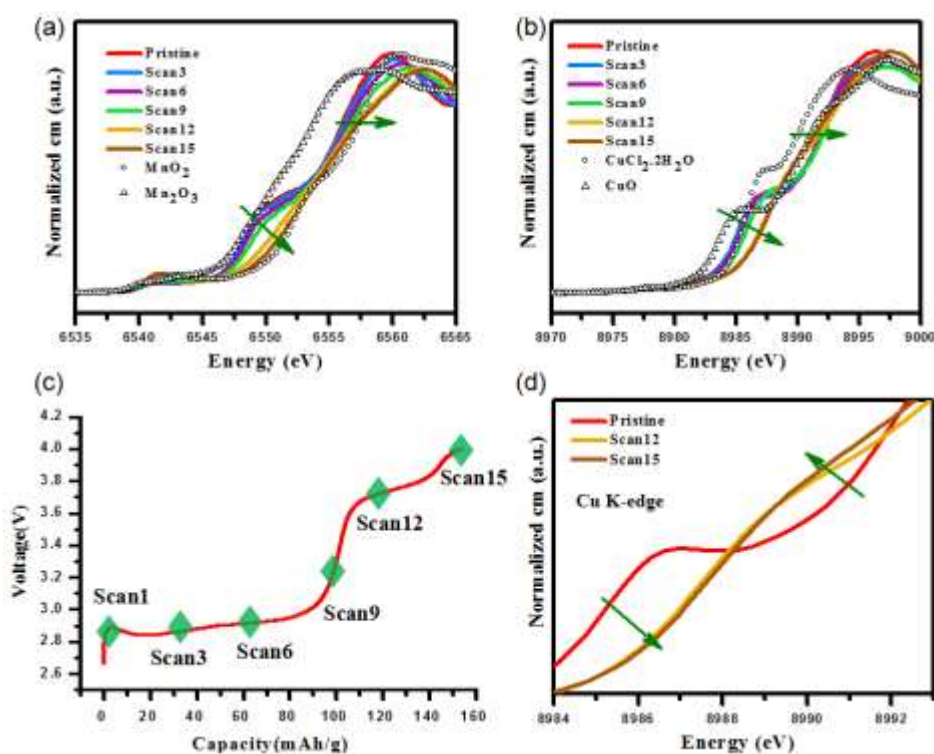


Figure 106. Charge compensation mechanism upon sodium deintercalation/intercalation in β -NaCu_{0.2}Mn_{0.8}O₂. (a) *In situ* X-ray absorption spectroscopy (XAS) spectra at manganese K-edge collected at different charge/discharge states. (b) *In situ* XAS spectra at copper K-edge collected at different charge/discharge states. (c) The load curve of β -NaCu_{0.2}Mn_{0.8}O₂ during the first charge process for *in situ* XAS. (d) The enlarged XAS spectra at copper K-edge.

Patents/Publications/Presentations

Publications

- Yao, Hu-Rong, and Peng-Fei Wang, Yue Gong, Jienan Zhang, Xiqian Yu, Lin Gu, Chuying OuYang, Ya-Xia Yin, Enyuan Hu, Xiao-Qing Yang, Eli Stavitski, Yu-Guo Guo, and Li-Jun Wan. “Designing Air-Stable O₃-Type Cathode Materials by Combined Structure Modulation for Na-Ion Batteries.” *J. Am. Chem. Soc.* 139, no. 25 (2017): 8440–8443. doi: 10.1021/jacs.7b05176.
Wang, Qin-Chao, and Enyuan Hu, Yang Pan, Na Xiao, Fan Hong, Zheng-Wen Fu, Xiao-Jing Wu, Seong-Min Bak, Xiao-Qing Yang, and Yong-Ning Zhou. “Utilizing Co²⁺/Co³⁺ Redox Couple in P2-Layered Na_{0.66}Co_{0.22}Mn_{0.44}Ti_{0.34}O₂ Cathode for Sodium-Ion Batteries.” *Advanced Science* (2017). doi: 10.1002/advs.201700219.
- Shadike, Zulipiya, and Yong-Ning Zhou, Lan-Li Chen, Qu Wu, Ji-Li Yue, Nian Zhang, Xiao-Qing Yang, Lin Gu, Xiao-Song Liu, Si-Qi Shi, and Zheng-Wen Fu. “Antisite Occupation Induced Single Anionic Redox Chemistry and Structural Stabilization of Layered Sodium Chromium Sulfide.” *Nature Communications* (2017). doi: 10.1038/s41467-017-00677-3.